A Study of Human Monoclonal Antibodies to Influenza and Ebola Viruses



Pramila Rijal

Keble College
and
Human Immunology Unit,
Weatherall Institute of Molecular Medicine,
University of Oxford

A thesis submitted for the degree of
Doctor of Philosophy
Michaelmas 2016

Word Count (Main text only): approx. 46, 000

ABSTRACT

A Study of Human Monoclonal Antibodies to Influenza and Ebola Viruses

Pramila Rijal
Keble College

D.Phil.
Michaelmas 2016

This thesis describes an analysis of the B cell repertoire in humans in response to infection or vaccination with Influenza or Ebola. We isolated monoclonal antibodies (mAbs) from individuals using single B cell cloning and PCR technology, and defined their epitopes, binding characteristics and neutralisation properties.

As summarised by Thomas Francis in 1960, we found that the secondary B cell response to Influenza is largely determined by the primary response to the virus that the donor was exposed to in childhood. In some individuals this can lead to focusing of the polyclonal antibody response to a single site on the influenza haemagglutinin. Monoclonal antibodies isolated from such focused responses selected escape mutations *in vitro* that matched actual antigenic drift observed in circulating viruses. Recapitulation of antigenic drift *in vitro* with human mAbs, in parallel with standard analysis with ferret anti-sera, may contribute to improved selection of vaccine strains by the WHO.

A second consequence of preferential selection of B cell responses from memory cells laid down early in life, is the expansion of broadly cross-reactive clones during exposures to viruses that are only distantly related to the original stimulus. We have isolated many protective antibodies to conserved epitopes on both haemagglutinin and neuraminidase from individuals with appropriate exposure histories. One novel antibody binds to the conserved active site of neuraminidase. Antibodies of this type may have therapeutic potential to complement antibodies to the conserved stem of Haemagglutinin.

In contrast to Influenza, the antibody response to the Ebola glycoprotein (GP) in vaccinated humans was essentially primary. The elicited antibodies were closer in sequence to germline than those to Influenza, and contained fewer somatic mutations. The response was more diverse, employing a wide selection of VH/L genes, and was directed at multiple epitopes in at least three distinct regions on the GP. Despite these features, half of the antibodies neutralised an Ebola surrogate virus *in vitro,* and many were therapeutic in a murine infection model. We developed a cocktail of antibodies to three non-overlapping sites for testing as a therapy in a stringent model of Ebola infection in the guinea pig.

Taken together our results fit with a Darwinian model of selection of the fittest B cells in the germinal centre reaction, where memory cells have a selective advantage over naïve B cells.

DECLARATION

I declare that this thesis represents my own work, except where stated below. Contributions made by others have been acknowledged within the text and in the individual figure legends. It has never been submitted for any other degree.

- S-FLU pseudotyped viruses and cells with surface antigen used for screening monoclonal antibodies were developed by Alain Townsend.

Chapter 3

- Isolation of antibodies was done together with Kuan Huang (Taiwan).
- Purification of antibodies was mostly done by Lisa Schimanski.
- Characterisation of antibodies was aided by Alain Townsend and Lisa Schimanski.
- Sequencing of HA and NA genes from escape viruses was done by Rod Daniels.
- Protection of mice by antibodies against virus infection was done by Timothy Powell.

Chapter 4

- Some of the H3 antibodies were isolated by Kuan Huang's lab (Taiwan).
- Sequencing of HA and NA genes from escape viruses was done by Rod Daniels.

Chapter 5

- Isolation of antibodies to N1 neuraminidase was done by Kuan Huang's lab (Taiwan).
- Antibodies to N9 were isolated together with Beibei Wang.
- Antibody characterisation was aided by Alain Townsend.
- Crystal study of N9 antibody with N9 neuraminidase was done by Haihai Jiang and Yi Shi in George Gao's lab (China).

Chapter 6

- Some of the Ebola antibodies analysed were isolated by UCB, Slough and Simon Draper's lab, Jenner Institute
- Yeast peptide display assays were done by Xiao-Ning Xu's lab, Imperial College
- Escape mutant selected by antibody P6 was studied by Peter Halfmann at Yoshihiro Kawaoka's lab, Wisconsin University
- Mice protection data are from Erica Ollmann Saphire's lab, Scripps Research Institute.

Signed,

Pramila Rijal

ACKNOWLEDGEMENTS

This thesis has become a reality through kind support and help of many individuals, and successful collaborations.

Foremost, I would like to express my deepest appreciation to my supervisor Professor Alain Townsend. His guidance, immense knowledge, patience, continuous support and encouragement are divine attitudes that could turn a stone to a gem. This research and thesis would not have been possible without his continuous help and commitment of time and energy on plans, experiments, discussions, thesis writing and proofreading. Not just a great scientist, he is one of the best kind of human. I consider myself fortunate to have him as my supervisor. I find it amazing how he shows enthusiasm for every single piece of data in the lab. This is an inspiring aspect to me. He motivated me with empathy and hope when experiments were not working and motivated me to do more with appreciation for every successful experiment. If I keep writing, I could perhaps write a thesis chapter on how wonderful Alain is as a scientist, a supervisor and a person; I can never thank him enough.

I would also like to thank my Thesis committee members/ Transfer or Confirmation examiners Professor Vincenzo Cerundolo, Professor Andrew McMichael, Professor Paul Klenerman and Professor Tao Dong.

I am indebted to Dr Arthur Huang, my supervisor of the B.Sc. graduation project and a long-term collaborator. My skills in antibody isolation from human PBMC are a gift from him. Thank you for collaborating by sending the influenza specific human monoclonal antibodies to study antigenic drift and to test for therapeutic potential.

I am very thankful to our collaborators on Influenza and Ebola studies without whom this project was not possible. I am grateful to Dr John McCauley, Dr Rod Daniels and members of the Worldwide Influenza Centre, the Crick Institute for sequencing the escape mutants and support for the pursuit of human monoclonal antibodies for studying influenza antigenic drift. I am also thankful to Dr Yi Shi and Professor George Gao for the crystal structure study of our N9 monoclonal antibody. In addition, thanks to Dr Patrick Collins and Dr John Skehel for our ongoing collaboration on the crystal structures studies of antibodies bound to N1 neuraminidase.

My sincere thanks also go to Professor Tao Dong for setting up our collaboration with the Beijing Ditan Hospital for the isolation of antibodies to H7N9 influenza. Thank you for the opportunity to attend the Beijing CDC symposium 2013. I thank Beibei Wang, Linghang Wang and Professor Li at the Ditan Hospital for this successful collaboration.

On the Ebola side, the collaboration with Simon Draper's lab and the Antibody Discovery Unit at the UCB, Celltech have been fruitful. I am immensely thankful to Professor Simon Draper and his group, and other members from the Jenner Institute - Sean Elias,

Catherine Cherry, Simon Mendelsohn, Francesca Donnellan, Genevieve Labbe, Craig Thompson, Matthew Edmans, Teresa Lambe and everyone else involved in the project. Thanks are due to the Antibody Discovery Unit, UCB - Daniel Lightwood, Gillian Burgess, Victoria O'Dowd, Terry Baker, David McMillian, Michael Wright, Laura Newham and Andy Popplewell.

I am grateful to Dr Peter Halfmann and Professor Yoshihiro Kawaoka, Wisconsin University for the escape mutants of Ebola selected with monoclonal antibodies. Similarly, I am thankful to Professor Xiao-Ning at Imperial College and his lab members for identifying epitopes for some of the Ebola antibodies using the yeast display technique.

I am obliged to Professor Erica Ollmann Saphire and Dr Marnie Havert at the Scripps Research Institute for including our Ebola antibodies in the Viral Haemorrhagic Fever Immunotherapeutic Consortium (VIC). Data obtained from the study have been immensely useful for our analysis.

Thanks to Dr Tom Bowden at Strubi Oxford for providing us with recombinant Ebola glycoprotein. I would like to express my gratitude to Professor Antonio Lanzavecchia and Professor Davide Corti at IRB, Bellinzona for generously giving us Ebola control antibodies, and scientific chats. I am thankful also to Professor Ayato Takada, Hokkaido University for the 6D6 control antibody.

I am glad that the antibody project extended to the idea of the lung as factory for antibody production, developed by Tiong Tan, Dr Deborah Gill and Dr Steve Hyde.

Thanks to Philipp, Samara and Helen, who I had the honour to supervise. Some of the data included in my thesis chapters stem from your hard work.

I can't rest without thanking the Townsend lab members. I am grateful to Lisa Schimanski for always being so helpful and friendly, and for proofreading a part of my manuscript. I acknowledge your contributions on the antibody project. Further thanks to Julie Xiao and Tiong Tan for their companionship, and for being kind and helpful. Thanks to Tim Powell and Wenwen for adding data to my chapter and joviality to the lab environment. I would like to mention Dr Elma Tchillian, Pirbright Institute and Professor Willcox for positive inspirations.

I must thank the WIMM FACS facility team - Craig Waugh, Kevin Clark and Paul Sopp for their great help with cell sorting. I acknowledge the friendly and co-operative environment created by the Drakesmith lab, Human Immunology Unit, and WIMM scientists and staffs.

I acknowledge my WIMM peers Kinda, PeiJin and Natasha. Thanks to Kinda for proofreading a thesis chapter.

Special thanks to all my family members. I am indebted to my loving and caring parents (Gunanidhi Sharma and Manarupa Rijal) who raised me, and provided me with an opportunity to have a continuing higher education. Thank you my *daju-bhai* (Gyanendra, Rabindra and Yogesh) and *bhauju haru* (Anita and Ranju), niece (Luna) and nephew (Shashanka) for your concern and cherishing family times. I would like to express my gratitude to my parents-in-law (Vishnu Raj Atreya and Arya Atreya) for their compassion and good wishes. I appreciate the togetherness and openness of *dijju haru* (Alaka, Preeti, Angya and Samata), *daju* Alok, *bhinjau haru*, *chori* and *bhanja-bhanji*. It would be difficult to cope with stress without family holidays and regular chats.

I would also like to thank all my friends in Oxford and outside; because of you I can say I have a social life. This list includes Sonu-Pawan and their little Aura, Deepali, Shrochis, Agya, Bhawana *dd*, Niran *bhinjau*, Prabin, Poojan, Saroj, Leela di, Sradda, Kailash, Uma, Menuka, Avi and the Nepali community in Oxford. Thanks for all the gatherings to refresh, and much-needed support at the time of writing. I thank Diwakar *dai* and Sobha *bhauju* for making us feel, we have guardians in Oxford.

At the end, I would like to express my heartfelt appreciation to my beloved husband Alankar Aryal Atreya. Words cannot express how grateful I am for all the love, care and support you have given to me. I appreciate your patience; thank you for bearing with me through all my tantrums in these last few months and thank you for being a listening ear.

My DPhil was supported by NDM/RDM studentship prize, Clarendon scholarship and de Breyne Keble College scholarship.

To my parents,

Gunanidhi Sharma and Manarupa Rijal

Who believed in educating their children.

And endured to build a strong foundation on which I may grow.

TABLE OF CONTENTS

TABLE OF CONTENTS i

LIST OF ABBREVIATIONS vii

LIST OF FIGURES xi

LIST OF TABLES xvi

LIST OF APPENDICES xviii

CHAPTER 1 Introduction to Influenza and Ebola Viruses 1

IMMUNE RESPONE TO VIRUSES 1

1.1 Cell mediated immunity 1

1.2 B cell immunity 3

INFLUENZA VIRUS 5

1.3 Influenza A virus: Structure and subtypes 5

1.4 Influenza as a global health problem 6

1.5 Life cycle of Influenza 10

1.6 Host specificity and transmission of Influenza 12

1.7 Influenza vaccination 13

1.8 Haemagglutinin and the role of monoclonal antibodies in antigenic analysis 15

1.8.1 Antigenic sites of H1 haemagglutinin 18

1.8.2 Antigenic sites of H3 haemagglutinin 18

1.8.3 Use of monoclonal antibodies to study antigenic drift 20

1.8.4 Broadly neutralising HA antibodies 23

1.8.5 Evolution of influenza virus and original antigenic sin 24

1.8.5.1 OAS and the Germinal Centre Reaction 26

1.8.5.2 OAS may or may not be “sinful” 26

1.9 Neuraminidase 29

1.9.1 Globular catalytic head domain 31

1.9.2 Neuraminidase inhibitors 32

1.9.3 B cell immunity to neuraminidase 33

1.9.4 Monoclonal antibodies to neuraminidase 34

EBOLA VIRUS 36

1.10 Ebola Virus Outbreak 36

1.11 Structure of Ebola Virus 38

1.12 Ebola virus glycoprotein 39

1.12.1 GP transcription 39

1.12.2 GP structure 42

1.13 Cell entry by Ebola virus 46

1.13.1 Macropinocytosis 46

1.13.2 Proteolytic processing of GP in endosomes 46

1.13.3 NPC-1 receptor binding and fusion 47

1.14 Small molecule inhibitors of Ebola entry. 47

1.15 Monoclonal antibodies to Ebola Virus 48

1.15.1 Antibodies to the glycan cap 50

1.15.2 Antibodies to the Receptor Binding Region (RBR) 50

1.15.3 Antibodies to the Base or GP1-GP2 interface 51

1.15.4 ZMapp (Antibody cocktail) Therapy 52

1.16 EBOV Vaccines 53

1.17 Aim of the Ebola Project 54

CHAPTER 2 Materials and Methods 55

2.1 Materials 55

2.2 Growing wild type viruses 56

2.3 Pseudotyped influenza viruses (S-FLU) 56

2.4 Stable expression of neuraminidase on 293T cells 59

2.5 Isolation of human monoclonal antibodies 59

2.5.1 PBMC isolation 59

2.5.2 Staining of antibody secreting cells or plasmablasts 60

2.5.2.1 Staining 60

2.5.2.2 Flow Cytometry 61

2.5.3 PCR and cloning 61

2.5.3.1 PCR 61

2.5.3.2 Digestion 66

2.5.3.3 Ligation 66

2.5.3.4 Transformation and minipreps 66

2.5.3.5 Transfection of 293T cells 67

2.6 Optimization of sorting protocol and antibody cloning 68

2.6.1 Transmembrane domain antibody recombinants and staining with HA 68

2.6.2 Antigen specific sorting of plasmablasts 70

2.6.3 Gibson Cloning and the 96-well system 71

2.7 Expression and Purification of antibodies 73

2.8 Screening and characterising monoclonal antibodies 74

2.9 Immunofluorescence Assay (IFA) 74

2.10 Haemagglutination inhibition (HI) assay 75

2.11 Enzyme Linked Immunosorbent Assay (ELISA) 75

2.12 ELISA based micro-neutralisation (MN) assay using reassortant or wild type influenza viruses 76

2.13 EGFP based micro-neutralisation assay using pseudotyped viruses 77

2.14 Enzyme linked lectin assay (ELLA) 78

2.15 Antibody cross-inhibition binding of the antigen for epitope mapping 80

2.16 Escape mutant virus selection by antibodies for epitope mapping 80

2.17 Thermolysin Digestion of Ebola glycoprotein 81

2.18 Site-directed mutagenesis 82

2.19 *In vivo* protection studies 82

2.20 Data and statistical Analysis 83

2.21 Haemagglutinin sequence numbering 84
2.22 Study approval 84

CHAPTER 3 Monoclonal antibody repertoire to haemagglutinin of H1N1/2009 in a vaccinated individual 85

CHAPTER 3 INTRODUCTION 85
CHAPTER 3 RESULTS 88
3.1 Response to influenza virus after vaccination 88
3.2 Sorting of HA-specific plasmablasts 90
3.3 Antibody repertoire following vaccination in donor H 93
3.4 Antibodies to H1N1 globular head 95
3.4.1 Antibodies specific to H1N1pdm09 viruses 95
3.4.2 Head antibodies cross-reactive to seasonal (pre-2009) H1N1 and H1N1pdm09 viruses 100
3.4.3 Antibodies to the head are focused on K163 101
3.4.4 Effect of somatic mutations on the fine specificity of antibodies for drifted viruses 103
3.4.5 Cross-inhibition by antibodies to pdm09 HA 103
3.4.6 Reactivity with natural antigenic drift variants of H1N1pdm09 with K163 change 106
3.4.7 Cross-reactivity to A/USSR/90/1977 107
3.4.8 The antibody response from donor H is focused 109
3.4.9 Additional donor sera focused to K163 site 111
3.4.10 The rise of clade 6B viruses 111
3.5 Broadly cross-reactive stem antibodies 113
3.6 Therapeutic Potential 114
CHAPTER 3 DISUCSSION 115
FUTURE PLANS 122

CHAPTER 4 The evolution of H3N2 influenza studied by application of human monoclonal antibodies 127

CHAPTER 4 INTRODUCTION 127

CHAPTER 4 RESULTS 131

4.1 The majority of isolated antibodies are head specific and potent binders and neutralisers 131

4.2 Cross-reactivity of H3 antibodies to past H3N2 strains 134

4.3 Reactivity to recent clades 3C.2a and 3C.3a 135

4.4 Human monoclonal antibodies select escape mutants that recapitulate natural antigenic drift. 136

4.5 Antibodies that may predict future antigenic drift. 142

CHAPTER 4 DISCUSSION 146

CHAPTER 5 Broadly cross-reactive human monoclonal antibodies to neuraminidases 151

CHAPTER 5 INTRODUCTION 151

CHAPTER 5 RESULTS 152

5.1 Neuraminidase antibody screening 152

5.2 Broadly-inhibiting N1 mAbs from human individuals 153

5.2.1 N1 mAbs cross-react on pandemic H5N1 neuraminidase 157

5.3 Broadly reactive N2 mAb isolated from a vaccinated individual 158

5.4 Antibodies to N9 isolated from H7N9 infected patients 160

5.4.1 N9 antibodies synergistic effect 160

5.4.2 N9 antibodies may have arisen from memory cells to N1 neuraminidase 162

5.5 Residue K432E is indispensable for antibody Z2B3 inhibition. 163

5.6 Cross-reactive N1 and N2 mAbs protect mice from lethal influenza infection ... 165

CHAPTER 5 DISUCSSION 168

CHAPTER 6 Human monoclonal antibodies to Ebola glycoprotein 177

CHAPTER 6 INTRODUCTION 177

CHAPTER 6 RESULTS 178

6.1 Principle of antigen specific cell sorting 178

6.2 Plasmablast cell sorting and antibody screening 181

6.3 Influenza pseudotyped virus to test antibody neutralisation 185

6.4 Neutralising antibodies 187

6.5 Partially neutralising antibodies 191

6.6 The relationship between neutralisation *in vitro* and protection *in vivo* 192

6.7 Defining antibody epitopes 194

6.7.1 Yeast display library screening 194

6.7.2 Escape mutants generated in vitro 199

6.7.3 Identification of binding sites by Cross-Inhibition 203

6.8 Identification of MLD dependent antibodies 209

6.9 Some antibodies may neutralise by blocking cathepsin digestion 211

6.10 Effect of Combinations of antibodies on virus neutralisation 214

6.11 Effect of trypsin on antibody binding 216

6.12 Cross-reactive antibodies to other Ebola species 219

6.13 Antibody sequence analysis 225

6.13.1 HCDR3 length and somatic mutations 227

CHAPTER 6 DISCUSSION 229

FUTURE PLANS 238

BIBLIOGRAPHY 242

Publication: Huang, K. Y., P. Rijal, L. Schimanski, T. J. Powell, T. Y. Lin, J. W. McCauley, R. S. Daniels, and A. R. Townsend. 2015. 'Focused antibody response to influenza linked to antigenic drift', *J Clin Invest*, 125: 2631-45.

LIST OF ABBREVIATIONS

ADCC	Antibody Dependent Cell -mediated Cytotoxicity
ASC	Antibody Secreting Cells
BSA	Bovine Serum Albumin
CD	Cell Differentiation
CDC	Centres for Disease Control and Prevention
ChAD	Chimpanzee Adeno
CHO	Chinese Hamster Ovary
CMV	Cytomegalovirus
DMEM	Dulbecco's Modified Eagle Medium
DNA	Deoxyribonucleic Acid
EBV	Epstein-Barr Virus
eGFP	Enhanced Green Fluorescence Protein
ELISA	Enzyme-Linked Immunosorbent Assay
ELLA	Enzyme Linked Lectin Assay
FACS	Fluorescence Activated Cell Sorting
FCS	Fetal Calf Serum
FITC	Fluorescein isothiocyanate
FIX	Fixative
FSC	Forward Scatter
GAH	Goat Anti-Human
GC	Germinal Centre
GC	Glycan Cap
GISRS	Global Influenza Surveillance and Response System
GP	Glycoprotein
h	hour(s)

H	Heavy chain
HA	Hemagglutinin
HAI	Hemagglutination Inhibition
HAU	Hemagglutination Unit
HF	High Fidelity
HI	Hemagglutination Inhibition
HM bufffer	HEPES MES buffer
HRP	Horseradish Peroxidase
IFA	Immunofluorescence Assay
IFL	Internal Fusion Loop
Ig	Immunoglobulin
IMGT	International Immunogenetics Information System
J	Junctional region
L	Leader sequence
LAIV	Live Attenuated Influenza Virus
M1	Matrix 1
M2	Matrix 2
mAb	Monoclonal antibody
MBC	Memory B cells
MDCK	Madin Darby Canine Kidney
MN	Micro Neutralization
MVA	Modified Vaccine Ankara
MVA-BN	Modified Vaccine Ankara - Bavarian Nordic
NA	Neuraminidase
NCBI	National Center for Biotechnology Information
NEB	New England Biolabs
NIBSC	National Institute for Biological Standards and Control

NIC	National Influenza Centre
NIMR	National Institute for Medical Research (now the Crick Institute)
NP	Nucleoprotein
NPC	Niemann-Pick
OAS	Original Antigenic Sin
PA	Polymerase Acid protein
PB	Plasmablast
PB1	Polymerase Basic protein 1
PB2	Polymerase Basic protein 2
PBS	Phosphate Buffered Saline
PE	Phycoerythrin
PEI	Polyethylenimine
PHE	Public Heath England
PMBC	Peripheral Mononuclear Blood cells
PR8	A/Puerto Rico/8/34 (H1N1)
RAH	Rabbit Anti-Human
RBC	Red Blood Cells
RBD	Receptor Binding Domain
RBR	Receptor Binding Region
RBS	Receptor Binding Site
rHA	Recombinant Hemagglutinin
RNA	Ribonucleic Acid
RPMI	Roswell Park Memorial Institute
RT	Room Temperature
RT-PCR	Reverse Transcription Polymerase Chain Reaction
S-FLU	Signal deleted flu vaccine (Live attenuated)
SA	Sialic Acid

SHM	Somatic Hyper Mutation
SIAT	Sialyltransferase
SSC	Side Scatter
SV40	Simian virus 40
TCID50	Tissue Culture Infectious Dose at 50%
THL	Thermolysin
TIM	T-cell immunoglobulin and mucin domain
TIV	Trivalent Influenza Vaccine
TMB	3,3', 5,5"-tetramethylbenzidine
TPCK	Tosyl Phenylalanyl Chloromethyl Ketone
V	Variable
VDM	Virus Dilution Medium
VGM	Virus Growth Medium
VSV-G	Vesicular stomatitis virus - Glycoprotein
WHO	World Health Organization
WIC	Worldwide Influenza Centre
κ	Kappa chain
λ	Lambda chain
ϒ	Gamma

LIST OF FIGURES

Figure 1. 1 Antigen presentation by MHC class I molecules to CD8+ T cell.. 2

Figure 1. 2 B cell expansion, selection and maturation in germinal centre…….. 4

Figure 1. 3 Structure and subtypes of influenza virus.. 8

Figure 1. 4 The history and epidemiology of influenza disease 9

Figure 1. 5 The lifecycle of Influenza virus and the role of antibodies 11

Figure 1. 6 Structure of haemagglutinin.....17

Figure 1. 7 Antigenic sites of H1 haemagglutinin.....19

Figure 1. 8 Antigenic sites of H3 haemagglutinin.....20

Figure 1. 9 Structure of neuraminidase. 30

Figure 1. 10 Phylogeny of the Ebola viruses isolated from infected humans during the 2013-2016 outbreak in West African nations 37

Figure 1. 11 Ebola Virus genome and structure. 38

Figure 1. 12 Ebola GP gene transcription 41

Figure 1. 13 Structure and make up of Zaire ebolavirus 44

Figure 1. 14 Ebola virus entry 45

Figure 1. 15 Identified epitopes for numbers of Ebola antibodies published so far.....51

Figure 2. 1 Design and propagation of S-FLU virus. 58

Figure 2. 2 Steps of monoclonal antibody isolation from a single-cell PCR cloning methods 59

Figure 2. 3 Proof of principle for direct staining of plasmablast B cells shown by binding of recombinant HA to transmembrane expressed IgG on 293T cell 69

Figure 2. 4 Micro neutralisation assay.. 78

Figure 2. 5 Enzyme linked lectin assay (ELLA) for measuring neuraminidase activity and inhibition by antibodies 79

Figure 3. 1 The serological neutralisation titres for former seasonal H1, H3, H1pdm09, and H5-pseudotyped influenza viruses in donor H before and after trivalent seasonal influenza vaccination. 89

Figure 3. 2 Day 7 plasmablasts from donor H following 2011-12 influenza vaccination. 91

Figure 3. 3 Antibody response in donor H is polyclonal as shown by VDJ heavy chain gene rearrangement of 157 antibodies 92

Figure 3. 4 The 6 largest VH-related sets of HA-binding antibodies derived from day 7 H1 HA-specific B cells 94

Figure 3. 5. Antibodies of 3 specificities with varying in-vitro neutralisation potency. 96

Figure 3. 6 Mapping of K163E/Q substitutions selected by head-specific T2-6A (V_H 3-7) and head cross-reactive T3-4B (V_H 3-15) antibodies 99

Figure 3. 7 Binding activity of HA head-specific and head cross-reactive antibodies on cells infected with the variant viruses. 100

Figure 3. 8 Competitive binding to purified A/England/195/2009 HA by the various sets of antibodies that are sensitive to K163E/Q 104

Figure 3. 9 Neutralising activities by sera and monoclonal antibodies from vaccinated individuals against the variant viruses 105

Figure 3. 10 Mapping of the HA1 K163 residue in former H1N1 viruses 108

Figure 3. 11 Graphical summary of the finding in this chapter 110

Figure 3. 12 Emergence of clade 6B viruses with characteristic substitution in K163Q. 112

Figure 3. 13 Emergence of clade 6B.1 in 2015/16 with S162N substitution resulting in glycosylation and masking of the residue 163 Sa site 113

Figure 4. 1 The evolution of clade 3C.2a and 3C.3a H3N2 viruses in 2014.....130

Figure 4. 2 Binding and neutralisation by H3 HA antibodies. 133

Figure 4. 3 The amino acid substitutions selected by antibodies to X217 (A/Victoria/361/2011) virus.....140

Figure 4. 4 Evolution of H3N2 viruses with different amino acid changes in the major antigenic sites of the haemagglutinin head 141

Figure 4. 5 Substitutions selected by antibodies that neutralise clade 3C.2a virus….144

Figure 5. 1 Screening for antibody to neuraminidase by different methods. 153

Figure 5. 2 ELLA screening of antibodies for inhibition of various H1N1 viruses from year 1934 to recent 2014 strains 154

Figure 5. 3 ELLA inhibition titres of antibodies to N1 neuraminidases from H1N1 or H5N1 viruses 155

Figure 5. 4 Titration of anti-N1 antibodies on recombinant neuraminidase proteins derived from different H5N1 clades. 158

Figure 5. 5 Inhibition titration of N2 antibody M6B12 to H3N2 viruses 159

Figure 5. 6 Inhibition of N9 neuraminidase enzymatic activity by anti N9 antibodies on enzyme-linked lectin assay 161

Figure 5. 7 Binding synergy of N9 antibodies. 162

Figure 5. 8 Cross-reactivity of N9 antibodies to N1 NA.....163

Figure 5. 9 Antibody Z2B3 complexed with N9 neuraminidase 165

Figure 5. 10 In vivo prophylaxis with N1 antibodies.....166

Figure 5. 11 In vivo prophylaxis treatment with N2 antibody M6B12. 167

Figure 5. 12 Phylogeny of neuraminidases in this chapter.....169
Figure 5. 13 Conservation between N1 (A/California/07/2009) and other N1 and N9 neuraminidases shown on PDB 4B7J. 170

Figure 6. 1 Principle for antigen specific cell sorting using antigen + biotinylated-mAb sandwich technique 180
Figure 6. 2 GP-ELISA and plasmablasts measurement from eight donors from the Ebola vaccine trial.....182
Figure 6. 3 Plasmablast sorting and antibody screening 184
Figure 6. 4 Sorting of plasmablasts and GP-specific plasmablasts from donor 66....185
Figure 6. 5 Total of 82 antibodies were isolated from 11 vaccinated volunteers.....188
Figure 6. 6 Neutralisation of pseudotyped virus E-S-FLU with monoclonal antibodies 190
Figure 6. 7 In vitro neutralising concentration of monoclonal antibodies shown as IC50 and IC90.....191
Figure 6. 8 Yeast Screen Display of mAb 114.....196
Figure 6. 9 Yeast Screen Display of mAb P6.....197
Figure 6. 10 Yeast Screen Display of mAb 66-3-9C. 198
Figure 6. 11 Antibody Binding Sites Identified by Yeast Peptide Display.....199
Figure 6. 12 Plaque reduction neutralisation (PRNT) assay and selection of escape viruses by mAb P6 201
Figure 6. 13 MAb P6 recognises a novel site on glycoprotein.....202
Figure 6. 14 Neutralisation profile of the antibodies to wild-type E-S-FLU and E-S-FLU (GP I260R, S322G, S347P) pseudotyped viruses 203
Figure 6. 15 An example of competition for binding to ebola glycoprotein.....204

Figure 6. 16 Assignment of antibodies to their defined regions based on cross-inhibition assays 209
Figure 6. 18 Identifying antibodies recognising mucin-like domain of the glycoprotein. 210
Figure 6. 19 MAb P6 blocks the thermolysin cleavage. 213
Figure 6. 20 Neutralisation of E-S-FLU pseudotyped virus by antibodies in combination.....215
Figure 6. 21 Antibodies sensitive to trypsin.....218
Figure 6. 22 Antibodies requiring trypsin cleavage of glycoprotein for binding.....219
Figure 6. 23 Amino acid sequence phylogeny of different Ebola species. 220
Figure 6. 24 FACS plots shows the binding of mAbs to MDCK-SIAT1 cells transfected with glycoproteins of Makona, Mayinga, Sudan and Bundibugyo Ebola viruses. 221
Figure 6. 25 Cross-reactive antibodies 222
Figure 6. 26 Binding of antibodies to glycoprotein of Zaire (C15/2014) and Mayinga (1976) strains. The correlation coefficient is 0.96. 223
Figure 6. 27 Overall cross-reactivity of Zaire antibodies to Sudan and Bundibugyo GPs 223
Figure 6. 28 Antibodies cross-reactive to Sudan and Bundibugyo GP 224
Figure 6. 29 Phylogeny of the antibodies based on VDJ amino acid sequences 226
Figure 6. 30 Average HCDR3 length (with standard deviation) and average somatic mutations in the antibodies encoded by different VH genes 228

LIST OF TABLES

Table 1. 1 List of important findings in influenza research into the antibody response in chronological order. 28

Table 1. 2 Drug repurposing to inhibit Ebola virus (Courtesy of Julie Xiao).....48

Table 1. 3 Antibodies against Ebola virus 49

Table 2. 1 List and recipe of commonly used mediums and buffers. 56

Table 2. 2 List of primers for amplification of variable heavy and light chains of IgG. 63

Table 2. 3 Gibson reaction compatible Nested PCR primers 73

Table 2. 4 List of viruses and their dose used in animal experiments. 83

Table 3. 1 Influenza vaccination History of donor H. 88

Table 3. 2 Summary of the antibodies and their VH gene analysis. 91

Table 3. 3 MN of natural variants and in vitro antibody-selected variant viruses 98

Table 4. 1 HI titres (in ng/ml) of H3N2 antibodies against various H3N2 viruses using human and turkey RBC 132

Table 4. 2 Cross reactivity of H3 head and stem antibodies to antigenically drifted viruses from different years. 134

Table 4. 3 Neutralisation reactivity of antibodies to recent clade 3C.2a and 3C.3a viruses. 136

Table 4. 4 Amino acid substitutions in escape mutant viruses selected by the antibodies to X217 (A/Victoria/361/2011) virus. 137

Table 4. 5 Amino acid substitutions selected by human monoclonal antibodies analysed comparing to the past and circulating H3N2 virus strains. 137

Table 4. 6 Substitutions selected by monoclonal antibodies that neutralise clade 3C.2a virus 144

Table 6. 1 Number of antibodies isolated from vaccinated individuals.....188

Table 6. 2 Partial neutralising antibodies and their properties.....192

Table 6. 3 Antibodies tested on yeast display screening assay 195

Table 6. 4 Cross-inhibition of antibodies for mapping epitopes.....205

Table 6. 5 Glycoproteins from different Ebola subtypes with % amino acid identity 220

Table 6. 6 Cross-reactivity of some of the antibodies tested by FACS 221

Table 6. 7 Use of VH gene by different donors 227

Table 6. 8 HCDR3 length of antibodies.....227

LIST OF APPENDICES

Appendix 3. 1 Antigenic analysis of influenza A(H1N1)pdm09 viruses: post-infection ferret antisera and human monoclonal antibodies 124

Appendix 3. 2 Antigenic analysis of influenza A(H1N1)pdm09 viruses: post-infection ferret antisera and human post-vaccination antisera 125

Appendix 3. 3 Protection against influenza challenge with the antibodies described in the text.....126

Appendix 4. 1 Variable Heavy and light genes of the H3N2 antibodies.....150

Appendix 5. 1 V(D)J genes of neuraminidase antibodies with number of somatic mutations and CDR lengths 175

Appendix 5. 2 Structure of antibody NC10 Fab complexed with N9 neuraminidase PDB:1NMB. 176

Appendix 6. 1 Affinity of the selected antibodies to Ebola glycoprotein monomer and trimer.....239

Appendix 6. 2 In vivo protection of mice against Ebola virus by human monoclonal antibodies given at 100 μg dose 2-day post infection.....240

Appendix 6. 3 Combination data including: cross-reactivity, neutralisation, in vivo protection and kinetic analysis for the selected antibodies 241

CHAPTER 1 | Introduction to Influenza and Ebola Viruses

IMMUNE RESPONE TO VIRUSES

In this general introduction, I will cover topics that are relevant to the work described in the thesis with one exception: I have started with a brief description of cell mediated immunity and cytosolic antigen presentation. Although this subject is not central to the work I describe it has played a key role in the history of the Townsend Lab, and is often the starting point for our discussions of viral immunity.

1.1 Cell mediated immunity

T cell mediated immunity is one arm of the adaptive immune response against viruses and other pathogens. Through antigen processing peptides derived from intracellular proteins are exposed at the cell surface in association with class I molecules of the MHC (Townsend, Gotch, and Davey 1985; Townsend and McMichael 1985; Townsend and Bodmer 1989). CD8+ T cells recognise such peptides and limit viral replication by destruction of infected cells and the secretion of cytokines. T cells tend to recognise peptides from the more conserved internal proteins, which creates an opportunity to develop broadly protective immune responses (Figure 1.1). Memory CD8+ T cells are present in naturally infected individuals, which become effective at the time of subsequent infections leading to more rapid clearance of virus and reduced pathology (Townsend and Bodmer 1989; Sridhar et al. 2013). Thus, influenza virus tends to be more frequently fatal in infants as they lack memory T cells, and in the elderly because of waning immunity.

Pre-existing cross-reactive CD4+ T cells also correlated with protection against influenza infection in humans, even in the absence of prior neutralising serum antibodies (Wilkinson et al. 2012). In the case of infection with Ebola virus, high levels of activation of CD4+ and CD8+ T cells was reported in survivors, which was sustained long after resolution of the disease (McElroy et al. 2015).

CD4+ helper T cells (T_H cells) also play an important role in B cell selection and stimulation. They are responsible for the formation and maintenance of germinal centres in lymphoid organs, which are the site of B cell expansion and maturation.

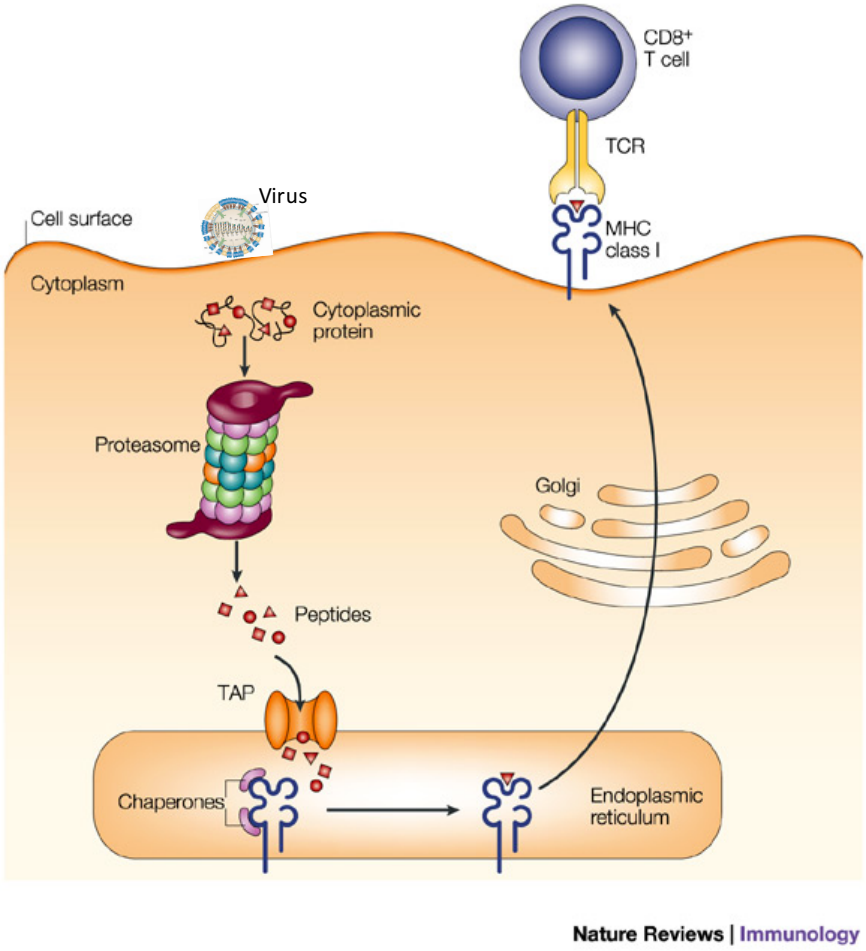

Figure 1. 1 ***Antigen presentation by MHC class I molecules to CD8+ T cell****. Figure adapted from Yewdell et al. (Yewdell, Reits, and Neefjes 2003).*

1.2 B cell immunity

Antibodies are made exclusively by B cells. Naïve B cells, with IgM as the surface immunoglobulin or B cell receptor (BCR), reside in bone marrow. These cells circulate in peripheral lymphoid organs and bind to antigen via BCR by which they are activated, with the aid of cytokine stimulation and with or without T cell help (Murphy 2011).

Following activation by antigen and Th signals, naïve or memory B cells migrate to the dark zone of the germinal centre (GC), where they undergo clonal expansion and somatic hypermutation (Figure 1.2). Afterwards they may migrate to the light zone of the GC, where they acquire antigens from follicular dendritic cells, where they process in endosomes and present the derived peptides bound to class II MHC molecules to the CD4+ helper T (T_{FH}) cells. T_{FH} cells in turn signal B cells to undergo class switching (Crotty 2015), and promote a return to the dark zone for further somatic mutation. B cells may cycle repeatedly through the dark and light zones during affinity maturation. Within the dark zone, B cell receptors go through somatic hypermutation (SHM) mediated by activation-induced deaminase (AID), the mechanism by which the clonal variants of B cells arise with altered antigen affinity and specificity (Pavri and Nussenzweig 2011). In the light zone, B cells undergo selection by T_{FH} cells based on antigen recognition and high affinity. Higher affinity B cells acquire positive signals to go back to dark zone for further SHM and proliferation. This is a Darwinian process of survival of the fittest B cells (Victora and Wilson 2015). Unselected and autoimmune B cells are signalled to apoptosis. Positively selected B cells further differentiate to plasmablasts, memory cells or long lived plasma cells (reviewed in (Victora and Nussenzweig 2012)).

Plasmablasts retain surface immunoglobulins and are the precursors for plasma cells. Plasma cells are matured B cells which can secrete antibodies at astonishingly high rate.

These cells either undergo terminal differentiation or die after several days. Long lived plasma cells survive in bone marrow for months or years and continue to secrete antibodies into the blood. Memory B cells reactivate and go to the germinal centres upon recognition of antigen for further rounds of affinity maturation.

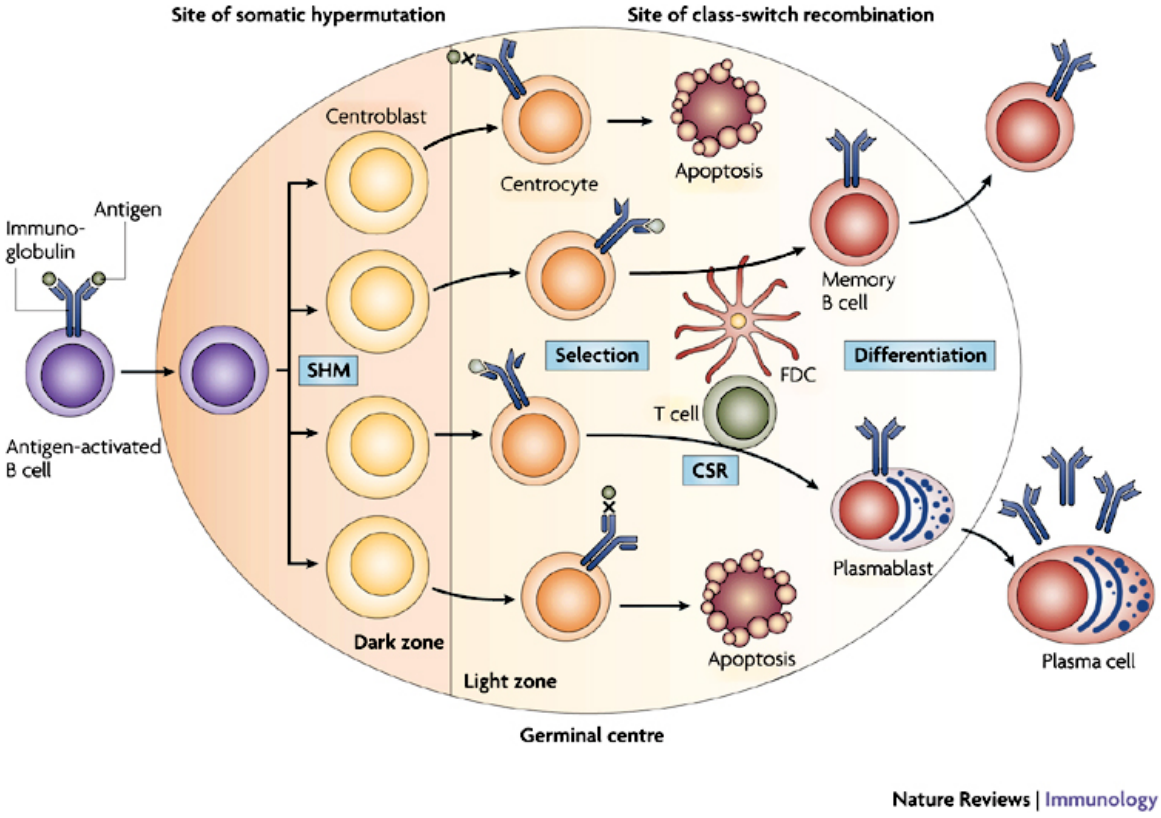

Figure 1. 2 ***B cell expansion, selection and maturation in germinal centre.*** *In the peripheral compartment, B cells present antigens to helper T cell and receive co-stimulatory signals. The selected cells enter dark zone of the germinal centre, where they undergo clonal expansion and somatic hypermutation. Afterwards, the cells migrate to the light zone of the germinal centre within where they are exposed to antigens on the follicular dendritic cells. The low affinity and autoreactive B cells do not receive positive survival signal and undergo apoptosis. High affinity B cells are selected, with the help from T cells, for further proliferation and affinity maturation. They may re-enter the dark*

zone for further maturation. Then, B cells exit germinal centres as memory B cells or plasma cells. Figure taken from (Klein and Dalla-Favera 2008).

INFLUENZA VIRUS

1.3 Influenza A virus: Structure and subtypes

Influenza virus belongs to the *Orthomyxoviridae* family. It is an enveloped RNA virus with a segmented, negative sense, single-stranded RNA genome (Figure 1.3). The influenza virus particle is 80-120 nanometres in diameter and mostly spherical in shape (Lamb and Choppin 1983). The envelope contains two types of glycoprotein spikes of which 80% are haemagglutinin (HA) and the rest are neuraminidase (NA) (Easterday et al. 1969; Webster et al. 1982). The viral core is a genome of about 13 kb in size, composed of eight negative-strand RNA segments which encode 14 different viral proteins. Each RNA segment forms a ribonucleoprotein complex consisting of a nucleocapsid protein (NP) and the viral polymerases PB1, PB2 and PA proteins. These are surrounded by a shell of matrix protein (M1). Further, a tetrameric M2 protein protrudes out from the envelope to form ion channels.

Influenza A viruses are classified into subtypes based on the two surface glycoprotein antigens: haemagglutinin (HA or H) and neuraminidase (NA or N). There are 18 haemagglutinins (H1 to H18) and 11 neuraminidases (N1 to N11) known. Both HA and NA glycoproteins are classified into two major phylogenetic groups, identified as group 1 and group 2. HA group 1 includes H1, H2, H5, H6, H8, H9, H11, H12, H13, H16, H17 and H18, and group 2 - H3, H4, H7, H10, H14, and H15 (Figure 1.3B) (Air 1981; Centers for Disease Control and Prevention 2016b). NA group 1 includes N1, N4, N5 and N8 and group 2 – N2, N3, N6, N7 and N9 (Figure 1.3C).

HA is a trimeric protein responsible for binding to the cell surface of host cells and entry into the cells. Conversely, NA is a tetrameric sialidase enzyme which facilitates the release of viral progeny from infected cells and the spread of the virus from one cell to another by cleaving terminal sialic acid residues from host-membrane bound glycoproteins and glycolipids.

Influenza virus constantly evolves via two mechanisms: antigenic drift and antigenic shift. Random point mutations in the genome occur owing to the non-proofreading RNA polymerase, at a frequency estimated at $2.3x10^{-5}$ per nucleotide per cell infection (Sanjuan et al. 2010). This allows selection of the best adapted viruses, and continual evolution by escape from neutralising antibodies. This is the process of antigenic drift (Medina and Garcia-Sastre 2011). Antigenic shift is caused by gene re-assortment of the 8 vRNA strands from different influenza subtypes during dual infection of a single cell, and is a relatively rare event. When it involves the vRNAs encoding the surface proteins a potentially pandemic virus can emerge for which there is no established neutralising antibody in the human population.

1.4 Influenza as a global health problem

Influenza is an acute viral infection caused by influenza viruses (mainly type A). It is a global public health problem because of pandemics and epidemics leading to high morbidity and mortality. Worldwide, seasonal epidemics result in about 3 to 5 million cases of severe illness and 250,000 to 500,000 deaths annually (WHO 2012) (Figure 1.4C). Influenza pandemics are recorded every 10 to 30 years and each cause thousands to millions of deaths. The worst pandemic on record, the Spanish flu in 1918-1919 took more than 50 million human lives (Figure 1.4A). In addition, H2N2 (1957), H3N2 (1968), H1N1 (1977) and H1N1 (2009) have appeared as pandemics in the recent past (Figure

1.4B). The H2N2 virus was wiped out by the emergence of H3N2. The H3N2 and H1N1 viruses continued evolving as seasonal influenza viruses. The seasonal H1N1from 1977 was replaced by pandemic swine H1N1 after 2009. There have been random incursions into the human population of avian H5N1 (since 1997) and H7N9 (since 2013) infections. To date none of these has resulted in sustained human to human spread. However, in the ferret model of infection relatively few mutations are required to enable an H5N1 virus to transmit by aerosol between ferrets (Herfst et al. 2012). Ferrets are thought to be the best animal model for human infection as the ferret respiratory tract has a similar distribution of α-2,6 sialic acid as the human, and ferrets can be infected with human influenza without adaptation (de Graaf and Fouchier 2014). Emergence of a new pandemic, possibly derived from highly pathogenic avian viruses H5N1, H7N9 or H2N2, therefore seems likely.

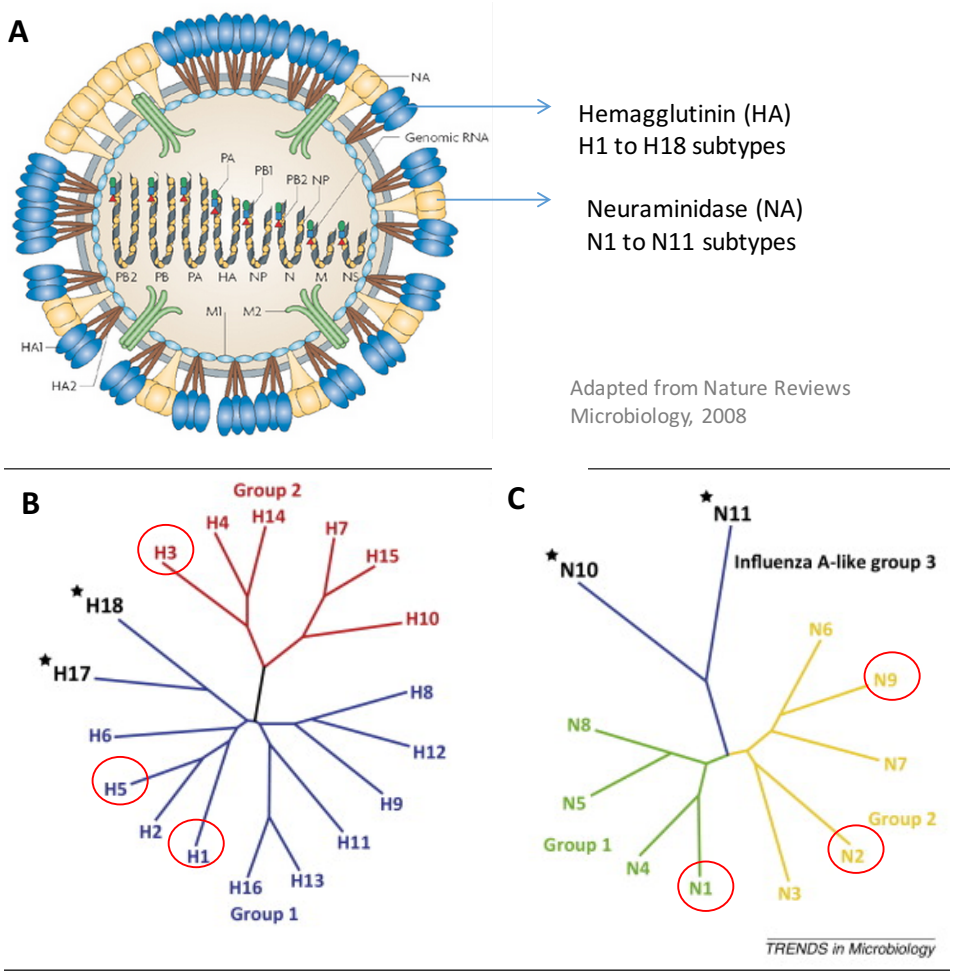

Figure 1. 3 A) ***Structure and subtypes of influenza virus****. The influenza genome is composed of eight single RNA strands. Haemagglutinin and neuraminidase are the two surface glycoproteins that define the influenza subtype. B) Eighteen haemagglutinin and C) eleven neuraminidase are classified into two groups based on their sequence homology. Circled subtypes have caused infection in humans: Seasonal viruses (H1N1, H3N2) and avian viruses (H5N1, H7N9). Figures adapted from: A) (Karlsson Hedestam et al. 2008) and B) (Wu et al. 2014).*

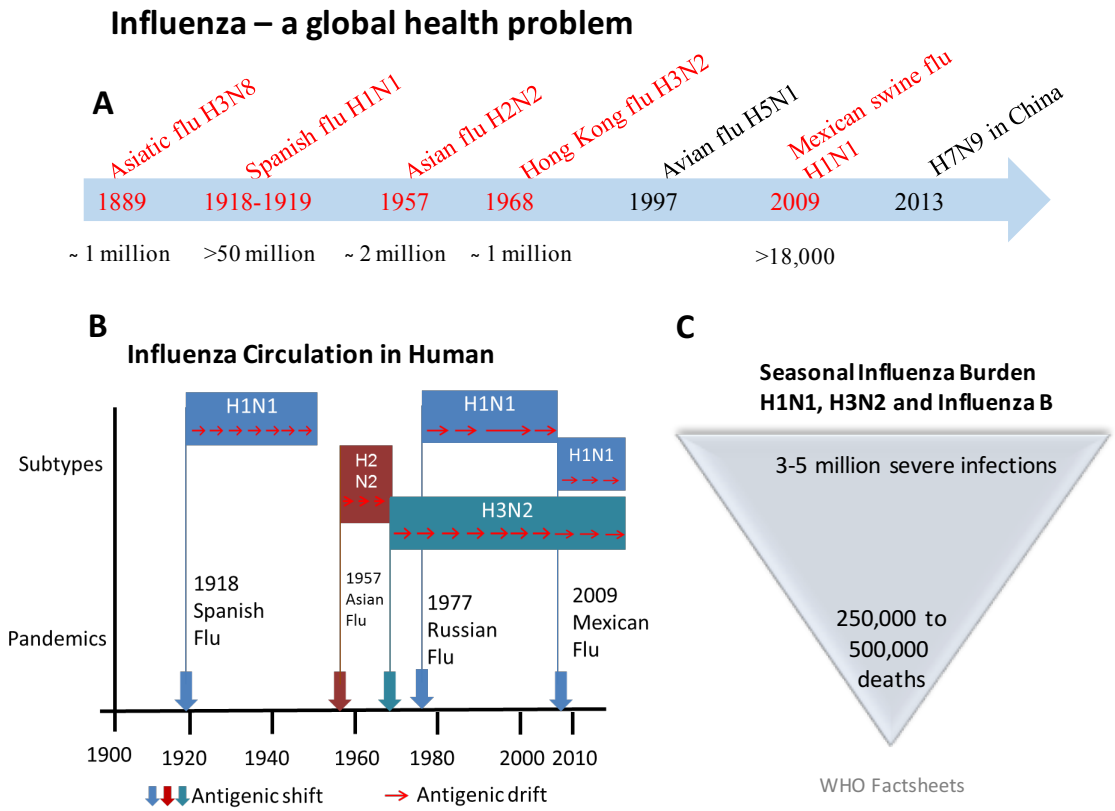

Figure 1. 4 ***The history and epidemiology of influenza disease****. **A)** Emergence of avian and swine influenza viruses in the human population from last century to now. Influenza cases in red are pandemic and in black are potentially pandemic. Numbers below the years are number of deaths from influenza. **B)** Human influenza viruses that emerged from avian or swine source and continued circulating in humans as seasonal influenza. Three incidences of H1N1 pandemics occurred in the last 90 years. The recent seasonal H1N1 is a swine origin H1N1/2009. The H2N2 (1957) continued as seasonal virus until 1968 when the H3N2 appeared. The H3N2 virus is continuing to evolve via antigenic drift. **C)** Influenza virus (H1N1, H3N2 and influenza B) causes 3-5 million severe infections and 250-500 thousand deaths annually.*

Nomenclature of Influenza Virus

The current nomenclature system for influenza A virus is written as follows: Influenza type/host of origin/Geographic source/Isolate number/Year of isolation (HA and NA subtype of the isolate) e.g. A/Swine/Iowa/15/1930 (H1N1) (WHO 1980). However, for the human influenza virus, the host of origin is omitted e.g. A/England/195/2009 (H1N1).

1.5 Life cycle of Influenza

The replication cycle of influenza can be summarized in the following five points (Figure 1.5).

i. **Viral attachment and entry to the cell:** Virus binds to the sialic acid receptors on the epithelial cell surface via its receptor binding site on the head of haemagglutinin. The virus is taken up by receptor mediated endocytosis.

ii. **Fusion/Uncoating:** The endosomal compartment is acidified which induces a conformational change in the cleaved HA. Fusion peptide releases from the HA complex and inserts into the host membrane, resulting in fusion of viral and endosomal membrane, finally leading to the entry of the viral genome into the cytosol (Skehel and Wiley 2000).

iii. **mRNA synthesis and RNA replication:** The negative strand viral RNA transcribes to form positive stranded mRNA and cRNA. The mRNA directs protein expression. cRNA forms the template for production viral RNA for replication of the genome prior to packaging into viral particles.

iv. **Viral assembly:** Cell glycoproteins, accessory proteins and viral ribonucleoproteins assembled in the cell membrane to form a complete viral particle.

v. **Budding and release:** As a final step of lifecycle, virus particle is budded through the host cell membrane and released from the cell surface by the enzymatic activity of neuraminidase.

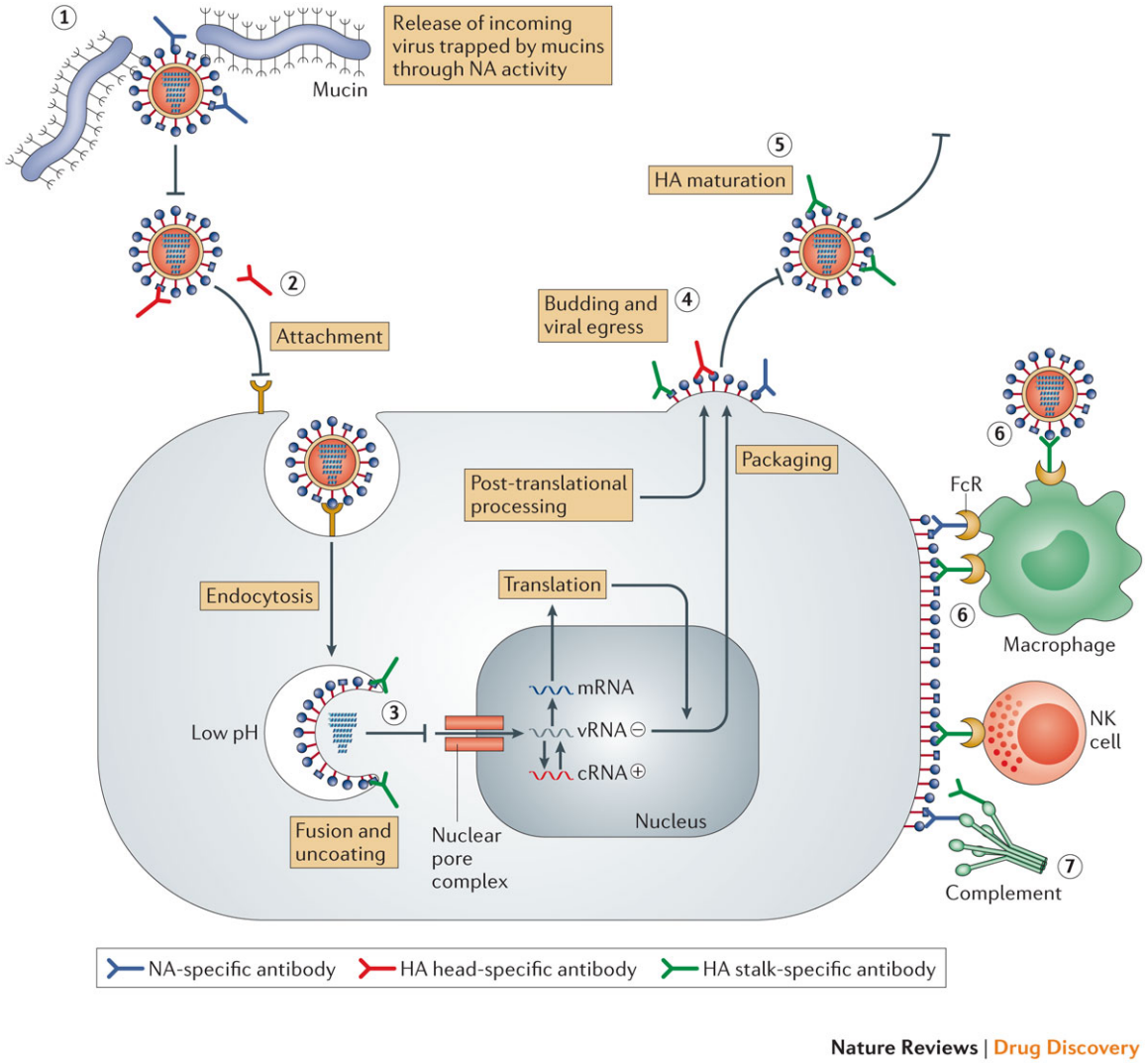

Figure 1. 5 ***The lifecycle of Influenza virus and the role of antibodies****. Antibodies directed against the head (coloured red) and stem (coloured green) of haemagglutinin (HA) and the neuraminidase (coloured blue) inhibits the virus replication via different mechanisms. Virus entry to the lung epithelial cells is facilitated by neuraminidase, that enzymatically pierce through the highly glycosylated mucin layer (Step 1). NA antibodies may inhibit this step. HA head antibodies may block the binding of HA to sialic acid*

receptors on the cell surface which is critical for cell entry by endocytosis (Step 2). Some NA antibodies may also block receptor binding by steric hindrance. Inside endosomes at acidic pH, HA undergoes a conformational change exposing the fusion loop. Stem antibodies block at this step by preventing fusion of viral and endosomal membrane and preventing the uncoating of virus (Step 3). Inside the nucleus, viral RNA transcribes to form mRNA which expresses viral proteins. cRNA is formed from a viral RNA for replication of the genome. Virus components assemble at the cell membrane to form a virus particle and bud out. Virus budding and egress may be prevented by HA head and stalk, and NA antibodies (Step 4). HA stalk antibodies also sterically inhibit HA maturation (Step 5). HA stalk antibodies and possibly NA reactive antibodies also act through antibody dependent cell-mediated cytotoxicity (ADCC) (Step 6) and complement-dependent cytotoxicity (CDC) (Step 7). cRNA, complementary RNA; FcR, Fc receptor; NK, natural killer; vRNA, viral RNA. Figure adapted from (Krammer 2015).

1.6 Host specificity and transmission of Influenza

Wild ducks or waterfowl are the natural reservoir of avian influenza viruses but themselves are resistant to infection. Domestic animals including horses, cats, chickens, ferrets, cattle are known sources for infection with different strains of influenza A viruses. Avian viruses can rarely transmit directly to human handlers, or the pig can be the intermediate host for transmission. Only H1N1, H2N2 and H3N2 have the ability to transmit from human to human. Direct transmission of viruses from birds to human is however rare (example H5N1 and H7N9). One of the reasons for this is the difference in specificity of HA for sialic acids (Neumann and Kawaoka 2015). HA of avian influenza viruses bind to α-2,3 sialic acid, while HA of human influenza viruses bind α-2,6 sialic acid receptors. Because avian influenza viruses lack binding to α-2,6 sialic acid receptors which are prevalent in the upper respiratory tract, human to human transmission of these

viruses is rare (de Graaf and Fouchier 2014). Unlike avian influenza viruses, swine influenza viruses can bind to both types of sialic acid receptors and both α-2,3- and α-2,6-linked sialic acids occur in the trachea of swine. The pig is thus considered a mixing vessel or an intermediate host between avian and human influenza A viruses.

The highly pathogenic avian H5N1 virus needs less than five mutations to be transmissible between ferrets (Enserink 2011). This involves adaptive mutations that increase binding to α-2,6 sialic acid receptors, and additional mutations that stabilise the trimer.

1.7 Influenza vaccination

Each year seasonal influenza is estimated to result in at least 250,000 deaths worldwide, for which nearly 500 million doses of influenza vaccine are distributed to prevent the disease (Palache et al. 2015). Those at most risk of severe disease are adults aged 65 and over, pregnant women and those of any age with underlying medical conditions. Influenza vaccines– both inactivated sub-unit vaccines and live attenuated influenza vaccines are formulated as trivalent and quadrivalent preparations that contain H1N1 antigen, H3N2 antigen and antigen from the B/Victoria lineage or the B/Yamagata lineage of influenza B viruses for trivalent vaccines or from both lineages for quadrivalent vaccines. Vaccination campaigns are conducted in the autumn of each year and the timing of these campaigns are aligned to the distinct timings of the influenza season in Northern and Southern hemispheres. To produce the most effective influenza vaccines, the WHO recommends twice each year viruses that should be included in vaccines for the forthcoming campaigns. The recommendations are based on the characteristics of viruses sampled from around the world through the WHO Global Influenza Surveillance and Response System (GISRS). GISRS consists of 143 WHO

National Influenza Centres (NICs) located in 113 UN member states, four Essential Regulatory Laboratories, 13 WHO H5 Reference Laboratories and six WHO Collaborating Centres (WHO CCs), and stems from an international collaborative network of laboratories first set up in 1947 (Chu, Andrewes, and Gledhill 1950) to examine the evolution of influenza viruses on a global scale. The Francis Crick Worldwide Influenza Centre is one of the six WHO CCs.

The recommendations for vaccines are based primarily on the antigenic properties of influenza viruses, backed up by gene sequence analysis. The primary methods for antigenic analysis have changed little since 1947, although cartographic methods for probing and illustrating the antigenic results have added to the power of these analyses. The primary tool in the analysis of the antigenic properties of circulating viruses remains unchanged: recognition of isolated viruses by antisera prepared from naïve ferrets infected with reference viruses assessed in haemagglutination inhibition (HI) assays or micro-neutralisation (MN) assays. These antigenic analyses with ferret antisera are supplemented through studies with small panels of post- vaccination human antisera and representative viruses. New methods are being developed to predict the antigenic characteristics of influenza viruses from the gene sequences (Neher et al. 2016; Harvey et al. 2016) and methods have been developed to predict which viruses might predominate in future months (Neher et al. 2016; Luksza and Lassig 2014); however, currently, antigenic assessment of circulating viruses done by either the haemagglutination inhibition (HI) assay or the micro-neutralisation (MN) assay is paramount. There is room for improvement: the Cochrane collaboration calculate an average efficacy of the vaccine at ~54% (Demicheli et al. 2014) .

Sub-unit vaccines induce a specific antibody response which can be highly protective if well matched to the viruses circulating at the time. However, the combination of mismatching through antigenic drift, and egg adaptation mutations, can result in the complete loss of efficacy, as happened for the H3N2 component of the vaccine last year (Skowronski, Janjua, et al. 2014). There are several ways that vaccine efficacy could be improved. At the most basic level, matching could be improved by reducing the use of eggs in production, and in our opinion (discussed in chapter 3) introducing human monoclonal antibodies to supplement ferret sera in antigenic analysis of circulating viruses. Standardization of the NA content would add another tranche of improvement (discussed in chapter 5). Finally, developing vaccines that can induce a local cross-protective cell mediated immune response in the lung, in addition to a specific antibody response, would be likely to add another layer of efficacy. The licensed live attenuated influenza vaccine could do all this if given locally to the lung (Baz et al. 2015), but the producers are cautious about applying this in humans as the vaccine virus can still replicate to some level (Loeb et al. 2016).Experimental single cycle influenza viruses such as S-FLU can overcome this potential danger (Powell et al. 2012; Baz et al. 2015) (reviewed in (Nogales and Martinez-Sobrido 2016)).

1.8 Haemagglutinin and the role of monoclonal antibodies in antigenic analysis

The mature HA is a homotrimeric protein of ~ 190 kDa and ~ 560 amino acids in length, each monomer (~ 63 kDa) having a globular head domain (HA1) and stem domain (HA2) (Figure 1.6). The first crystal structures of HA visualized in the 1980s revealed the receptor binding site and other important features of HA (Wiley, Wilson, and Skehel 1981; Wilson, Skehel, and Wiley 1981). The HA0 precursor is cleaved at Arg329 by host proteases into HA1 and HA2 chains, which remain linked by a single disulphide bond

between residue 14 of HA1 and residue 137 of HA2 (Figure 1.7A). HA1 is important for binding and entry into the cell while HA2 is involved in the uncoating of the virus in the cell (Skehel and Wiley 2000). The globular domain is primarily composed of eight antiparallel beta sheets which form a groove for receptor binding. Within the globular domain, the triangular binding depression is formed by the 130-loop, 190-helix and 220-loop (Figure 1.6C). The principal recognition sites for neutralising antibodies are on the globular domain. The fusion peptide of the HA2 domain is buried within the core of the HA trimer. The HA undergoes a conformational change inside the endosomal compartment under acidic conditions, which triggers the fusion peptide to penetrate the vesicle membrane (Figure 1.6 and 1.7). Localized trimeric haemagglutinin mediates the fusion of the viral and host lysosomal membrane and forms a fusion pore through which the viral ribonucleoproteins are eventually released into the cytosol (Figure 1.5, step 3).

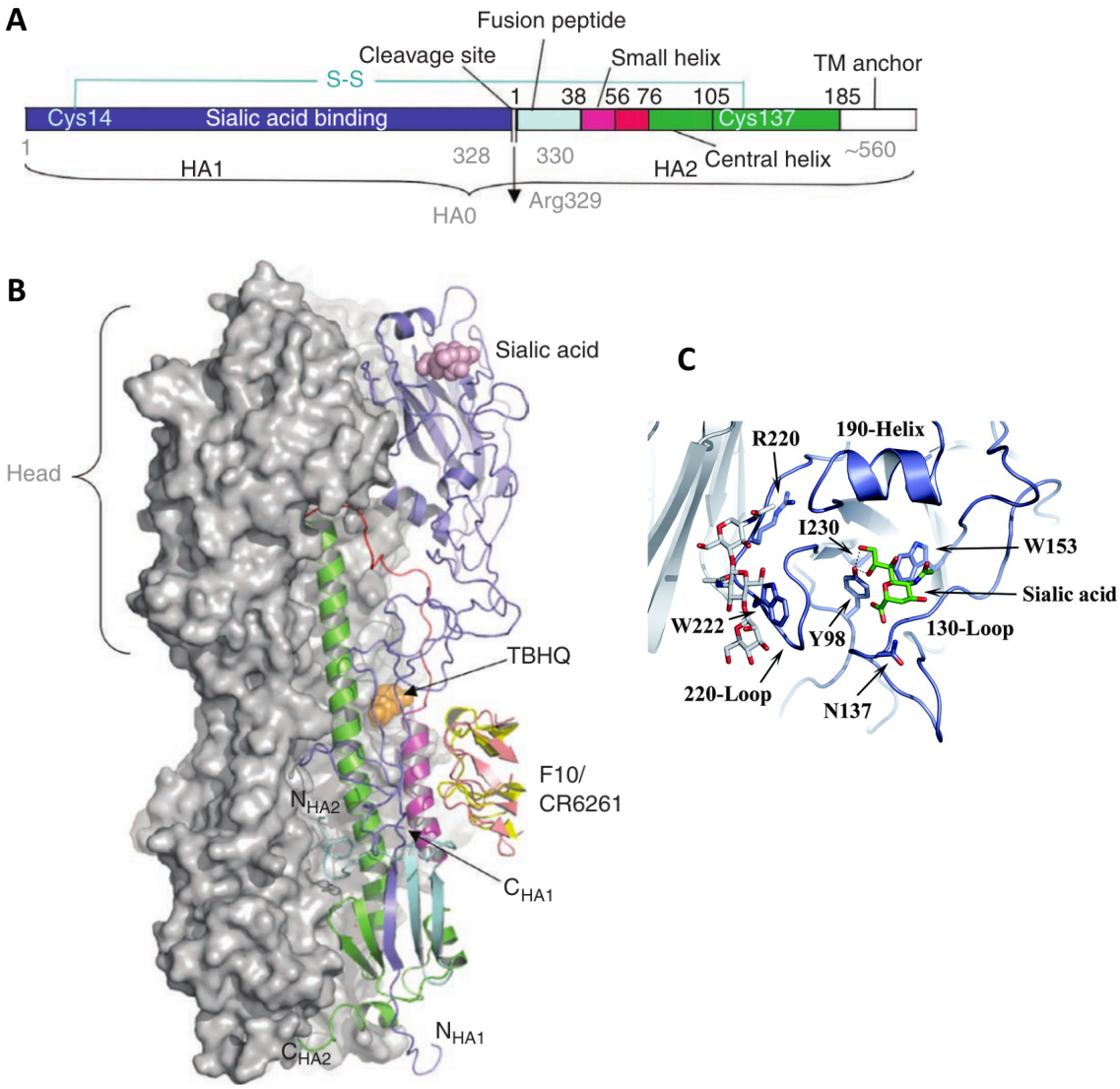

Figure 1. 6 ***Structure of haemagglutinin****. A) HA is composed of two polypeptides HA1 and HA2 which are linked by a disulphide bond. HA1 harbours the sialic acid binding site and HA2 begins with the fusion peptide. B) The HA protein is composed of three monomers, each formed of HA1 and HA2 domains. HA1 domain forms a globular head region and HA2 a stem or stalk region. The former is primarily composed of beta sheets forming a receptor binding groove whereas the latter of alpha helices and a fusion peptide. Broadly cross-reactive antibodies (F10/CR6261) are directed against the conserved stem region (Lingwood et al. 2012). TBHQ (tert-Butylhydroquinone) is a food preservative known to inhibit influenza virus by stabilizing the neutral pH structure and*

preventing fusion (Russell et al. 2008). C) The residues within the receptor binding site (RBS) of HA of A/Aichi/2/1968 (H3 HA) are shown. The triangular depression is formed by 130-loop, 190-helix and 220-loop structure within the outer part of globular domain where the sialic acid (shown in green) binds via hydrogen bonds, facilitating the attachment of a virus to the cell surface. Figures adapted from A,B) (Das et al. 2010). C) (Meisner et al. 2008).

1.8.1 Antigenic sites of H1 haemagglutinin

Antigenic sites for murine monoclonal antibodies were mapped on to the A/PR/8/1934 virus haemagglutinin by Yewdell and Gerhard (Yewdell and Gerhard 1981) (Figure 1.7). The antigenic map comprising five immunodominant antigenic regions namely, Ca1, Ca2, Cb, Sa, and Sb, was constructed based on the single amino acid substitutions selected by ~58 mAbs (Yewdell, Webster, and Gerhard 1979; Gerhard et al. 1981; Caton et al. 1982).

1.8.2 Antigenic sites of H3 haemagglutinin

Similar to H1 HA, the antigenic sites on the head of H3 HA, namely A, B, C, D, and E (Figure 1.8), were mapped by generating escape viruses with murine monoclonal antibodies, and analysing the sites of antigenic drift between 1968-1980 (Webster and Laver 1980; Wiley, Wilson, and Skehel 1981; Skehel et al. 1984). Even though the haemagglutinins of H1 and H3 subtypes differ by >60% in amino acid sequences, their antigenic sites overlap significantly. The sites A, B and D are the approximate equivalents of H1 (PR8) sites Ca2, Sb and C1 respectively (Caton et al. 1982). However, cross-reactivity of mAbs against the head region of H1 and H3 HAs is very rare.

The sites A and B have been shown to be immunodominant in the human population. In mice, sites A and E were shown to be immunodominant (reviewed in (Popova et al. 2012)). Koel et al. revealed that antigenic drift of H3N2 virus from 1968-2003 was driven by just seven key residues in sites A and B surrounding the sialic acid binding groove, which occurred as single residue substitutions at times of major antigenic change (Koel et al. 2013).

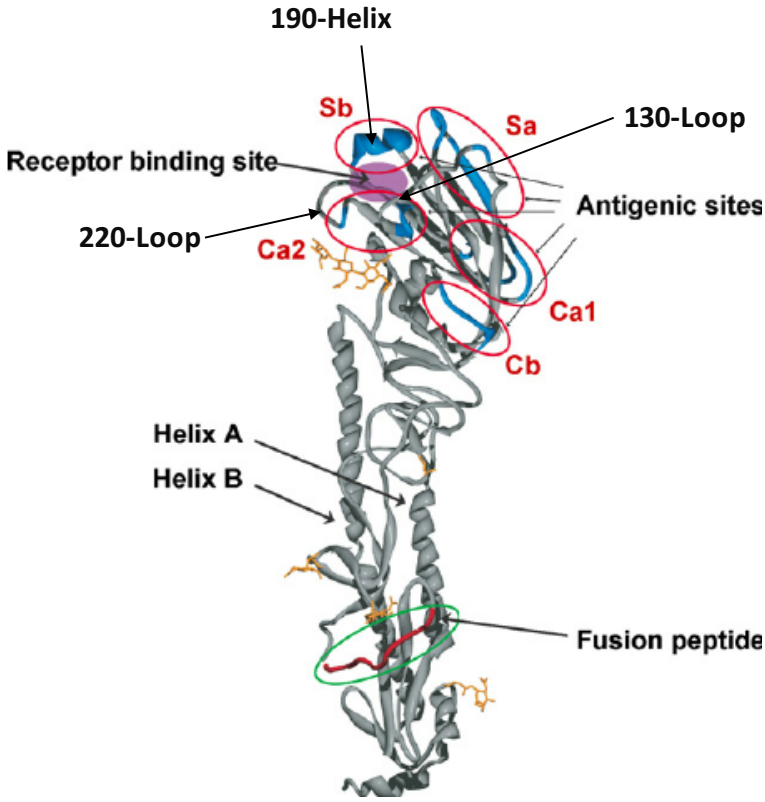

Figure 1. 7 ***Antigenic sites of H1 haemagglutinin****. Five antigenic sites namely, Sa, Sb, Ca1, Ca2 and Cb are mapped on the HA1 surface of H1 haemagglutinin. The receptor binding site is the triangular depression formed by the loop-helix-loop (130-loop, 190-helix and 220-loop) structure within the outer part of globular domain. Figure adapted from (Palese P. 2013).*

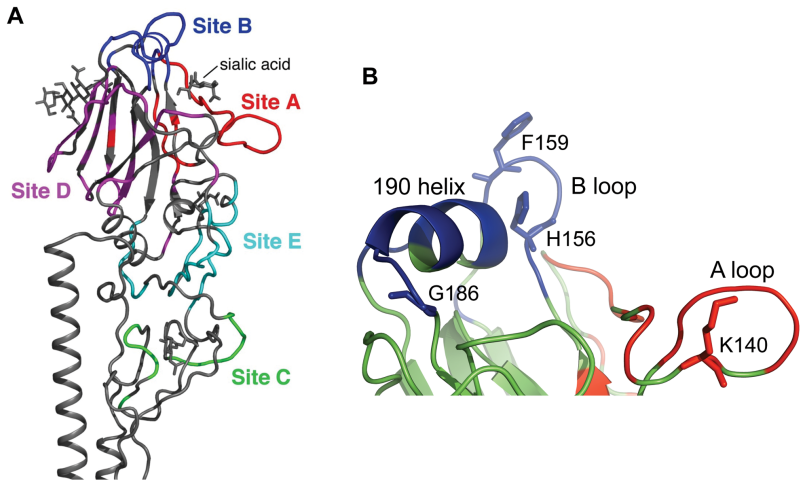

Figure 1. 8 ***Antigenic sites of H3 haemagglutinin. A)*** *Five antigenic sites namely, site A-E are mapped on the surface of H3 haemagglutinin. Site A (coloured red) and Site B (coloured blue) are localized on the top of HA around the sialic acid binding site.* ***B)*** *Site A which includes the A loop and other residues, and site B formed by the B loop and 190-helix are the main (immunodominant) antigenic sites that have caused antigenic drift in the past. The site B residue F159S/Y substitution was the major contributor to the 2013-2014 antigenic change. Antibodies targeting the A and B sites inhibit virus by directly blocking receptor binding and antibodies directed at epitopes farther from the RBS block indirectly by steric hindrance (Knossow et al. 2002). Some broadly cross-reactive stem antibodies inhibit the conformational change required for fusion. Figure adapted from (Popova et al. 2012).*

1.8.3 Use of monoclonal antibodies to study antigenic drift

After the crystal structure of haemagglutinin molecules were solved and antigenic sites were mapped on to the 3D structure by escape virus selection with murine monoclonal antibodies, the use of mAbs was extended, to delineate the antigenic relationships between HAs of different virus strains and subtypes. The mAbs were able to differentiate two antigenically different viruses where polyclonal antisera failed to distinguish these

subtle antigenic differences (Yewdell and Gerhard 1981). However, the use of murine mAbs to predict antigenic drift was not feasible because of the diversity of the antibody response of immunologically naïve mice to stimulation with a single HA antigen. Webster found that the majority of epitopes defined by murine antibodies were not "epidemiologically significant" in the sense that they did not match actual antigenic drift of viruses in the human population (Webster and Laver 1980).

The effect of prior antigen exposure on the selection of memory B cells for expansion in the germinal centre has revealed a profound effect on the specificity of the antibody response (Li et al. 2013; Andrews et al. 2015; Victora and Wilson 2015). Humans, unlike mice, are exposed repeatedly to influenza viruses or vaccines and antibodies that dominate the human response are mainly (but not exclusively) derived from cross-reacting memory B cells induced by earlier exposures (Francis 1960), which undergo somatic hyper-mutation and evolutionary selection by the new strains. This results in each individual developing a unique antibody "landscape" (Fonville et al. 2014). It is these antibodies that are thought to be the important drivers for antigenic drift in seasonal influenza.

Given that several independent sites for neutralisation exist on the HA molecule the question arises as to how many substitutions are required to prevent neutralisation by a polyclonal serum? Das et al. recently studied this issue by testing A/PR/8/1934 viruses for neutralisation by a murine hyperimmune serum after sequential selection by a series of monoclonal antibodies. They found that 12 sequential substitutions were required to escape neutralisation completely (Das et al. 2013). The mutation frequency of influenza A virus has been measured at $2.5x10^{-5}$ per nucleotide per cell infection (Sanjuan et al. 2010). This would predict that $>10^{65}$ cell infections would be required for such a mutant

to arise. The total number of cells in the human lung has been estimated at ~ 4.3 $x10^{11}$ (Bianconi et al. 2013). If humans produced polyclonal antibody responses equivalent to the sera studied by Das et al., some 10^{53} individuals would need to be infected to select a drifted influenza virus, and antigenic drift would not occur.

Antigenic drift is a reality. How then does it occur? One possibility is for some substitutions to have a global effect on antibody binding and neutralisation. Such mutations were postulated by Fazekas de St Groth (Fazekas de St and Webster 1966), and have been demonstrated to occur but are rare *in vitro*. De St Groth suggested such mutations could have a global effect on sera by increasing the binding affinity of the HA for sialic acid and called them "adsorptive" mutations (and later demonstrated by (Yewdell, Caton, and Gerhard 1986)). Hensley et al. have found that, as postulated by St Groth, that adsorptive mutants simultaneously increased receptor avidity and diminished antigenicity (Hensley et al. 2009). These results would predict that if antigenic drift were dominated by adsorptive mutations the binding affinity of the HA for sialic acid would steadily *increase* with time under selection.

However, the exact opposite has been found for the H3N2 viruses which have been under continuous selection since 1968. Lin et al. find that there has been a steady *decrease* in the binding affinity of H3 haemagglutinin for sialic acid since 1968 (Lin et al. 2012). This has become a major problem for monitoring antigenicity of viruses with the HI assay, as more than half of recent H3N2 isolates fail to agglutinate red cells at all, and in many cases the NA is contributing significantly as a sialic acid receptor, and the addition of oseltamivir to the HI assay is required to allow interpretation of the results (The Crick Worldwide Influenza Centre 2016).

The alternative explanation for antigenic drift is that the majority of human sera are much more focused in their specificity than a hyperimmune murine or sheep serum, and can select resistant viruses in a similar manner to monoclonal antibodies. Evidence in favour of this explanation has existed since the discovery of monoclonal antibodies and the selection of the first resistant mutants (reviewed in (Huang et al. 2015)). In the 1980's the observation was made that occasionally mutations in viruses selected with single monoclonal antibodies could abrogate neutralisation by a *specific* serum, suggesting that the majority of the antibodies in the serum were directed at a single site on the HA. With the development of human monoclonal antibody technology, the component antibodies of such sera could be individually isolated and the mutants selected studied to confirm this hypothesis (Popova et al. 2012; Linderman et al. 2014; Huang et al. 2015). This explanation for antigenic drift fits with a deeper understanding of the Darwinian selection of antibodies in the germinal centre during affinity maturation (Victora and Wilson 2015).

Human monoclonal antibody technology has opened the doors to recapitulating antigenic drift *in vitro*, and the possibility of predicting future antigenic drift as described in chapter 3 and 4 of this thesis.

1.8.4 Broadly neutralising HA antibodies

The first cross-reactive mAb (C179) specific to the stalk region was isolated in 1993 from a hyper-immunized mouse and found to neutralise H1, H2 and H5 (but not H3) viruses by blocking fusion (Okuno et al. 1993). Despite the high level of epitope conservation, a single amino acid mutation allowed escape from neutralisation. With the evolution of human monoclonal antibodies techniques, the subject has been resurrected. The appearance of pdmH1N109 in the human population in 2009 elicited otherwise rare broadly neutralising antibodies (bnabs) targeted to the conserved stem domain (reviewed

by (Air 2015) and (Lee and Wilson 2015)). Most of these neutralising antibodies have their epitopes in the alpha helical region of the stem comprised mainly of HA2 sequences of HA, which is highly conserved in many strains and subtypes (Ekiert et al. 2009; Sui et al. 2009).

These antibodies are known to neutralise by blocking fusion (inhibiting HA conformational change), locking HA in its native trimer form, and inhibiting virus egress (reviewed by (Krammer and Palese 2013). They are also shown to protect *in vivo* via additional antibody effector functions, such as ADCC (Jegaskanda et al. 2013; DiLillo et al. 2014). Involvement of complement-mediated cytotoxicity (Terajima et al. 2011) and antibody-dependent cellular phagocytosis (Mullarkey et al. 2016) have been shown for stem antibodies *in vitro*.

The use of broadly reactive antibody to treat human influenza infections has been started (Kallewaard et al. 2016). The antibody developed by Medimmune, MEDI8852 that neutralises all known HA subtypes, was found safe and promising in a Phase II trial (MedImmune 2015).

1.8.5 Evolution of influenza virus and original antigenic sin

Influenza study took a bounce after the 1918 pandemic (NIMR 2014; Taubenberger and Morens 2006). A descendant of this virus was isolated from the pig in 1931 by Shope (Shope 1931). However, it was only in 1933 that the first human influenza virus was isolated by infection of ferrets (Smith W 1933). In the late 1930s, it was found that influenza viruses are antigenically diverse. After Burnet developed methods to propagate influenza virus in eggs (Burnet 1937), the development of the first practical vaccine was possible (experimental immunisation of humans with inactivated virus propagated in murine lung was attempted earlier (NIMR 2014)). Francis and Salk developed the first

vaccine given to US military in the 1940s (Francis et al. 1945) with successful clinical protection but it failed in 1947 (Francis, Salk, and Quilligan 1947). Later, this vaccine failure was attributed to antigenic shift with another H1 (Kilbourne et al. 2002), similar to the situation that occurred in 2009.

In the early 1950s, a group of scientists reported the phenomenon where the primary response to the antigen dominated the secondary response (Davenport, Hennessy, and Francis 1953; Francis, Davenport, and Hennessy 1953). In a population age-cohort sera study against influenza A viruses from different years, Davenport et al. reported, "the antibody response of humans is dominated by the major antigens of the viruses encountered in the primary infections of childhood" (Davenport, Hennessy, and Francis 1953). This phenomenon was termed 'original antigenic sin' (OAS) by Francis (Francis 1960) (reviewed by (Morens, Burke, and Halstead 2010)). This was observed later with other infections (e.g., Dengue, HIV, alphaviruses) as well. OAS was defined as causing an enhanced response to the originally encountered virus and to have the propensity to produce cross-reacting antibody (Destgroth and Webster 1966). The phenomenon of OAS is seen mainly within a subtype and not between different subtypes (Morita, Suto, and Ishida 1972). The mechanism of OAS was later investigated at the cellular level of antibody producing cells (Deutsch and Bussard 1972).

In a vaccination study of 1994, it was found that the antibodies induced by the current vaccine were sourced from the antibodies to the influenza virus circulating during the childhood of vaccinees in each age cohort (Powers and Belshe 1994). The vaccine efficacy in elderly adults was low but this was not related to OAS. The higher antigenic distance between the previously exposed strain and the vaccinating strain may overcome the 'sin' effect of OAS by generating a greater novel response. The effect of OAS wanes

over time. In the elderly population, novel non-cross-reacting antibodies with a lower frequency of somatic mutations are induced in addition to the reactivation of memory B cells. OAS can be overcome by the use of higher antigen dose (Webster et al. 1976), or more frequent exposures, or with adjuvants (Kim et al. 2012; Ndifon 2015).

1.8.5.1 OAS and the Germinal Centre Reaction

At the B-cell level, OAS is thought to influence the response by preferential selection of previously-induced memory B cells to cross-reactive epitopes, rather than recruiting low-affinity naïve B cells (reviewed in (Park et al. 2016; Victora and Wilson 2015). Because of the low affinity of the BCR on the naïve B cell, even though it may be against the specific dominant epitope it is outcompeted by the memory B cells to more conserved epitopes, during the selection in the germinal centre reaction for further somatic hypermutation and expansion.

Further, early and easy availability of cross-reactive memory T cells and presentation of cross-reactive epitopes by APCs rather than naïve T cell activation may further favour the stimulation of memory B cells via T cell-dependent activation.

1.8.5.2 OAS may or may not be "sinful"

From the above discussion of OAS and the germinal centre reaction, OAS can be seen simply as the expected memory response. A relatively recent change in the meaning of the term OAS refers to the induction of "sinful antibodies" that retain a high affinity and neutralising capacity for the original stimulus, but through antigenic drift are now non-neutralising to the most recent viruses. Occasionally such antibodies can dominate the response and render an individual more susceptible to recent strains; A/PR/8/34 and A/FM/1/1947 as a pair show this effect (Kilbourne et al. 2002; Skountzou et al. 2010)

This type of OAS is regarded as a problem that can arise after repeated vaccination (Ohmit et al. 2014).

The cross-reactive antibodies induced by the mechanism of OAS may be fully neutralising and useful (Fazekas and Webster 1966, reviewed by (Adalja and Henderson 2010) (Khurana 2012). This was seen with H1N1/2009 pandemic, where elderly adults initially had a lower mortality rate than children and younger adults (Falagas et al. 2011) owing to the presence of cross-reacting immunity (McCullers et al. 2010; Xu et al. 2010) from earlier exposures. I describe an example of this in detail in chapter 3.

Table 1. 1 List of important findings in influenza research into the antibody response in chronological order.

Year	Findings and development	Subject	Literature
1924	Ferrets infected with distemper as a model for influenza (NIMR)		NIMR 2014
1933	Human influenza virus isolated first time, by propagation in ferrets		
1936	Recognised that influenza viruses are antigenically diverse		
1937	Influenza virus grown in eggs		Burnet 1937, JEP
1938	First inactivated influenza vaccine given to humans, which stopped working in 1947	Vaccine	Francis 1945, JCI
1953	Studies involving the antibodies to primary exposure dominating the secondary response (Human seroarcheology study)	OAS	Davenport 1953, JEM
1955	Francis coined the term 'Original antigenic sin'	OAS	
1956	Studied OAS in human sera and in ferret model using absorption with influenza antigens	OAS	Jensen 1956, JEM
1960	Original antigenic sin described: The imprint established by the original virus infections governs the antibody repsonse thereafter	OAS	Francis, 1960, APS
1966	OAS defined as: a partial anamnestic response, caused by a related antigen stimulating that sector only of the originally primed cells which is destined to produce cross-reacting antibody	OAS	Fazekas 1966, JEM
1972	Found that OAS is seen only within, and and not between, HA subtypes	OAS	Morita 1972, JID
1972	OAS is observed at the cellular level (antibody-forming spleen cells of hapten immunised mice)	OAS	Deutsch 1972, EJI
1973	WHO issued annual recommendations for the compositions of influenza vaccine based on surveillance results of circulating strains	Vaccine	
1976	OAS can be overcome by increasing vaccine dosage of the second antigen	OAS	Webster 1976, JID
1978	The first trivalent vaccine including two influenza A and one influenza B strains	Vaccine	
1979	Murine monoclonal antibodies mapped to hypervariable region of H1 HA head, which frequenctly mutate to undergo antigenic drift.	Antigenic sites	Yewdell 1981, Nature
1980	Antigenic sites on to H3 HA identified	Antigenic sites	Webster 1980, Virology; Skehel 1984, PNAS
1981	Three-dimensional crystal structures of haemagglutinins identified	Structure	Wiley 1981, Nature; Wilson 1981, Nature
1993	First broadly neutralizing stem antibody isolated	Epitopes	Okuno 1993, JV
1994	OAS not related to decreased vaccine efficacy in elederly adults	OAS	Powers 1994, JID
2011	Isolation of first human stem antibody binding to all HA subtypes	Human mAb	Corti 2011, Science
2016	First stem broadly neutralizing antibody approved for use in humans in a fast track Phase III trial	Human mAb	Kallewaard 2016, Cell

1.9 Neuraminidase

Neuraminidase (NA) is a mushroom shaped homotetrameric type II membrane protein formed by four identical polypeptides, each of 469-470 amino acids and ~ 60kDa molecular mass (Figure 1.9). Unlike HA, there is no proteolytic cleavage of NA. The NA protein contains four domains: N-terminal cytoplasmic tail, hydrophobic transmembrane region, variable stalk and globular head with catalytic site (reviewed by (Colman 1994; Air 2012)) (Figure 1.9A).

- The cytoplasmic tail is a single chain of six conserved amino acids (MNPNQK), which is nearly 100% conserved in all influenza A NA subtypes.
- NA is anchored to the membrane by a single hydrophobic helix of 7-29 amino acids that varies among different NA subtypes.
- Transmembrane and head domains are connected by a short stalk domain. The stalk domain varies among different NA subtypes and contains canonical glycosylation sites (N-X-S/T) but its structure is not known. The stalk is made up of about 50 amino acids but some N1 and N2 NA have an 18 amino acid deletion (Air 2012) . The stalk domain is important for the formation and stability of the tetramer. The amino acid Y66 in the stalk is critical for NA stability (Zanin et al. 2016).

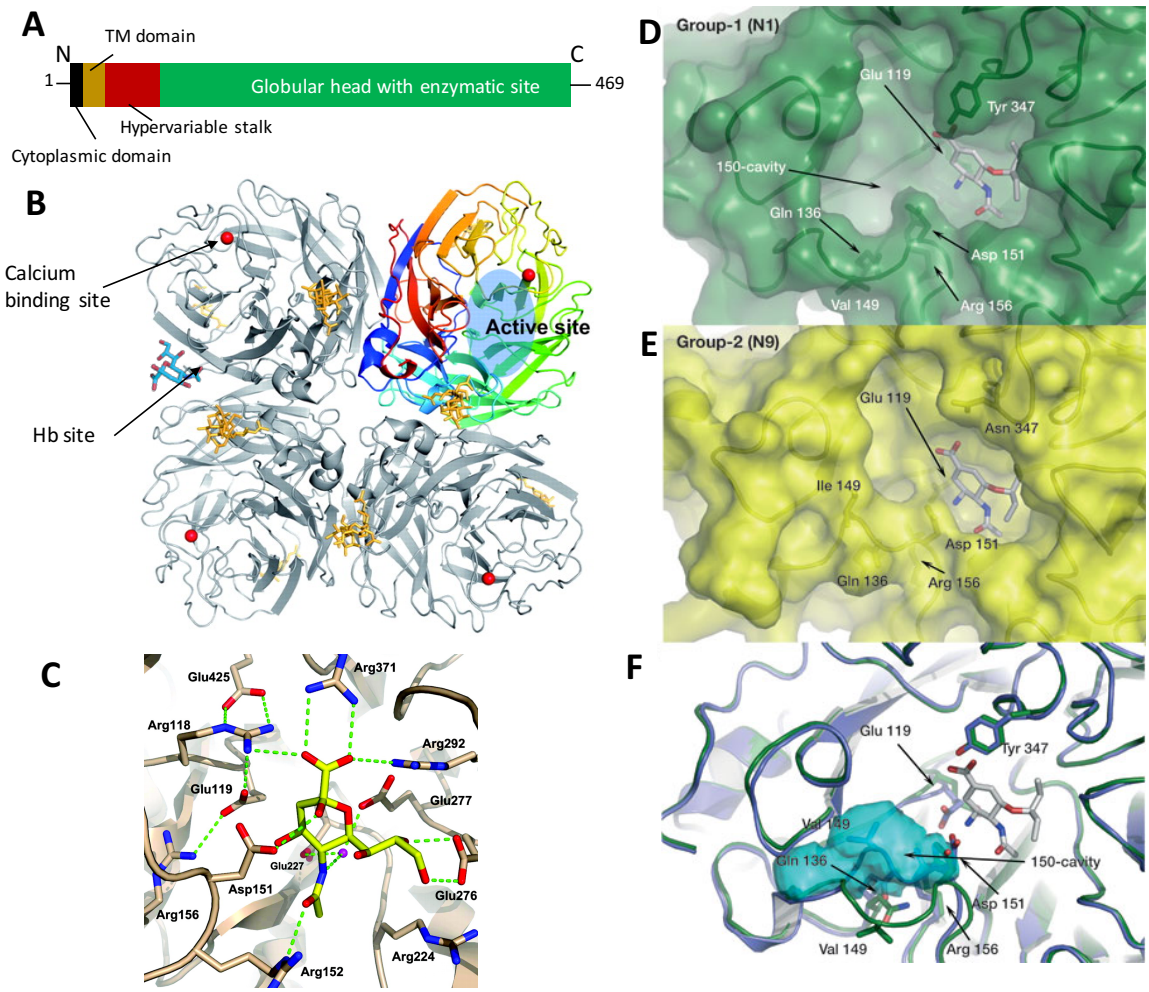

Figure 1. 9 ***Structure of neuraminidase. A)*** *Tetrameric organization of different domains of neuraminidase. It has a N-terminal cytoplasmic domain, short trans-membrane region, hypervariable stalk and a globular head.* ***B)*** *NA monomer is a six-bladed propeller structure. Each globular head of a tetrameric NA contains an active site and a calcium binding site.* ***C)*** *The active site is a sialic acid binding site, where many residues form direct or indirect contacts with the substrate. Residues in the active site pocket are highly conserved in all neuraminidases.* ***D)*** *Sialic acid binding pocket of avian H5N1 neuraminidase. In some neuraminidases (avian N1, 1918 N1, N4, N5, N8) there is an additional pocket called the 150-cavity, in proximity to the active site pocket. Oseltamivir is shown fitted into the active site.* ***E)*** *Active site of N9 neuraminidase.* ***F)*** *Superimposition of N1 (green) and N9 (blue) together with oseltamivir. The 150-cavity is*

also shown and labelled. Hb: haemadsorption. Figures are adapted from: B) (Wang et al. 2011); C) (Yen et al. 2006); D,E,F) (Russell et al. 2006).

1.9.1 Globular catalytic head domain

Four subunits of NA are arranged in a circular symmetry (Figure 1.9B). The three-dimensional structure of neuraminidases show each subunit as a symmetrically folded six-bladed propeller-like structure (reviewed by (Colman 1994; Shtyrya, Mochalova, and Bovin 2009; Air 2012)). Each blade or motif is composed of four twisted antiparallel ß-sheets stabilized and shaped by disulphide bonds and proline residues and connected by loops of different length. These connecting loops, especially between the second and third sheets and between motifs, are important for enzyme function. The loops exposed parallel to the viral membrane contain many important antigenic sites. Central and outer ß-sheets in each blade are arranged respectively as parallel and perpendicular to the propeller axis. The enzyme active site is located at the centre of each subunit as a deep pocket sited over the 6 central ß-strands. The active site is highly conserved in different NA subtypes in sequence as well as spatial properties.

Catalytic active site: Although these four subunits of NA have seemingly independent catalytic sites, the monomeric form has no activity (Bucher and Kilbourne 1972). There are eight catalytic residues (R118, D151, R152, R224, E276, R292, R371, and Y406; N2 numbering) that make contacts with the substrate sialic acid and eleven framework residues (E119, R156, W178, S179, D198 (or N198 in N7 & N9), I222, E227, H274, E277, N294, and E425; N2 numbering) that hold the catalytic residues in place (Yen et al. 2006). These residues are highly conserved in N1-N9 (reviewed in (Li, Sun, et al. 2012))**.** In NAs of group 1, particularly NA of avian virus H5N1, there is a cavity in proximity to the active site, formed by the different orientation of the '150-loop' (residues 147-152)

(Russell et al. 2006). Swine-origin H1N1 A/California/07/2009 NA lack this 150-cavity (Li et al. 2010).

Calcium binding site: Calcium is required for the stability and activity of neuraminidase. Calcium binds to the putative site buried under the active site, formed by residues 293, 347, 111-115 and 139-143 (Colman 1994; Shtyrya, Mochalova, and Bovin 2009; Air 2012)). The Ca^{2+} is coordinated by carbonyl oxygens of D293, G297, G345, and N347 and a carboxyl oxygen of D324 (N2 numbering). NA has optimal pH range of 5.5-6.5. Calcium stabilizes the NA tetramer and its active site in the low pH state also.

Second sialic acid binding site (Hb site): The second neuraminic acid binding site, called the haemadsorption site (Hb site), is found in N9 neuraminidase (Varghese et al. 1997) and N9 NA possess haemagglutinating activity (Laver et al. 1984). This site is formed by six amino acids from three loops: S367, S370, S372, N400, W403, and K432, which are conserved in avian neuraminidases. However, avian influenza NAs of other subtypes lack K432 and this does not seem to interfere with haemadsorption activity. Although the role of Hb site is not clear, it is assumed that it may play a part as a surrogate of influenza virus HA for attachment to the host cell. These signature amino acids for Hb binding are not present in human NAs.

1.9.2 Neuraminidase inhibitors

The concept of neuraminidase as a drug target was realised and became feasible in the 1980s, after the structure of the NA active site was known (Laver 1978). NA inhibitors that mimic the sialic acid, such as Oseltamivir and Zanamivir, were developed and licensed in the 1990s which are still the main line of treatment against influenza at the present time (reviewed in (Moscona 2005)). The Cochrane review of these inhibitors highlighted that these drugs have a rather moderate effect on reducing the duration of

symptoms in adults, but not in asthmatic children (Jefferson et al. 2014). Systematic review of neuraminidase inhibitors from Heneghan et al. found a lack of evidence for reduction in mortality (Heneghan et al. 2016).

1.9.3 B cell immunity to neuraminidase

Neuraminidase antibodies have been under the shadow of HA antibodies. NA as an antigen was viewed as less important because NA is present at only 1:4 ratio with HA, and NA antibodies do not interfere with the initiation of virus infection, and are thus non-neutralising.

However, work by Schulman, Webster, Kilbourne and colleagues showed the protective effects of anti-neuraminidase antibodies in mice and ferrets. Mice inoculated with virus or purified neuraminidase protein elicited NA immunity which was protective (Schulman, Khakpour, and Kilbourne 1968; Kilbourne et al. 2004). The NA antibodies were shown to inhibit NA activity *in vitro* and reduce the virus plaque size (Kilbourne et al. 1968). NA immunity protected mice from infection, presumably, by abrogating the release of virus from infected cells. Many groups subsequently elaborated the protective effects of neuraminidase antibodies in animal models (Rockman et al. 2013; Doyle, Hashem, et al. 2013; Wan et al. 2013).

Kilbourne and colleagues later showed that protective anti-neuraminidase antibodies are elicited in humans as well, following natural infection (Kilbourne, Christenson, and Sande 1968; Schild 1969) and exposure to inactivated whole-virus vaccine (Couch et al. 1974). The presence of NA antibodies to N2 corelated with reduced severity of pandemic H3N2 influenza infection (Murphy, Kasel, and Chanock 1972). Individuals who had higher antibodies to H2N2 showed less severe infection against H3N2 virus. This may be important in the context of avian H5N1 infections in human, where N1 antibodies to

seasonal H1N1 may be partially cross-protective (Gillim-Ross and Subbarao 2007). Current challenge studies in humans also confirm the independent protective effect of antibodies to NA (Memoli et al. 2016). Finally, two groups have recently established the NA antibody titre in human sera as a correlate of protection in large clinical trials (Monto et al. 2015; Memoli et al. 2016).

Despite this overwhelming evidence for the protective effect of antibodies to NA, the quality and quantity of NA in vaccines is not regulated, and varies widely between manufacturers (Johansson and Cox 2011).

1.9.4 Monoclonal antibodies to neuraminidase

The majority of the NA monoclonal antibodies published so far are from mouse and rabbits, with specificity limited to a subtype. Among the first monoclonal antibodies to NA from mouse, antibodies NC10 and NC41 specific to N9 NA, were analysed for functional and structural characteristics in the 1980s and 1990s. Although these antibodies have epitopes that largely overlapped, different antigenic residues were found to make critical contacts in NC10- and NC41-NA complexes (Malby et al. 1994; Lee and Air 2002).

The first 3D structures of NA-antibody complexes showed that the antibody can make contacts with 15-30 residues within the NA epitope (Tulip et al. 1991; Tulip et al. 1992; Malby et al. 1994; Venkatramani et al. 2006; Wan et al. 2015). Despite the involvement of a large surface area for binding, only few amino acids are critical for the interaction. Even a single amino acid mutation within the epitope can significantly alter the binding and inhibition by antibody (Webster, Hinshaw, and Laver 1982; Varghese et al. 1988). The amino acids critical for neuraminidase inhibition were also determined by generation

of escape mutants (Air, Laver, and Webster 1990), similar to the methods used to define epitopes bound by antibodies to HA.

Another mouse antibody CD6 which was protective against several N1 subtype viruses including, seasonalH1N1, pandemicH1N1 and avian H5N1, was found to make several contacts at the adjacent NA monomers (Wan et al. 2013; Wan et al. 2015). The NA antibodies mainly act through steric hindrance and blocking access of the active site to sialic acid. Since the antibodies act independently of the active site, drug resistant mutations within the active site should not affect the inhibition by antibody. The only antibody that is known to bind to the active site is HCA-2 (Doyle, Jaentschke, et al. 2013), that was generated from rabbits by injecting a 9-mer conserved peptide from the active site (residues 222-230) (Doyle, Hashem, et al. 2013). This antibody cross-inhibits multiple strains and subtypes from influenza A and B subtypes.

These antibodies are limited. The protective effective of antibody CD6 is subtype specific (Wan et al. 2015) and moreover, it has lost its epitope in recent H1N1 (post 2014) strains. The broadly cross-reactive rabbit antibody HCA-2 offers only partial protection even at the higher antibody dose of 60 mg/kg, and may be affected by mutations in the active site generated by drug resistance (Doyle, Hashem, et al. 2013).

There is scope for potent and broadly reactive human antibodies to NA that could confer better protection. In chapter 4, human monoclonal antibodies to neuraminidase N1, N2 and N9, isolated from vaccinated or infected individuals are discussed. These NA mAbs are broadly inhibiting to multiple strains of a subtype and some cross-reactive to different subtypes.

EBOLA VIRUS

1.10 Ebola Virus Outbreak

The Zaire Ebola virus outbreak in 2013-2016 in West Africa resulted in 28,616 cases and 11,310 deaths (as of June 10, 2016 after which the end of Ebola transmission was declared by WHO) with a case fatality rate of around 50% (WHO 2016). It is suspected that Ebola virus may have caused a significant number of asymptomatic infections (Richardson et al. 2016).

Bats (fruit bats) are thought to be the natural reservoir of Ebola virus (Leroy et al. 2005). Ebola virus causes severe haemorrhagic fever in non-human primates and humans. The case fatality of Ebola virus disease has varied from 25% to 90% in past outbreaks (WHO 2016). The virus transmits via direct contact with contaminated body fluids, has an incubation period of 2 to 21 days and in most cases the patient dies of uncontrolled viral replication, septic shock and multiple organ failure (Chertow et al. 2014). Ebola virus (Zaire subtype or ZEBOV or simply EBOV) was first discovered in 1976 in an isolate from a human infection (Centers for Disease Control and Prevention 2016a), and after that four more species have been discovered: *Bundibugyo* Ebola virus (BDBV), *Sudan* Ebola virus (SUDV), *Tai forest* Ebola virus (or *Cote d'Ivoire)* and *Reston* Ebola virus (RESOV) (Kuhn et al. 2010). Tai forest Ebola virus and REBOV have infected humans but are not fatal and have not caused large outbreaks, unlike the other three (WHO 2016).

Figure 1.10 shows the genetic analysis of viruses from 2014-2016 that caused infections in different regions of West Africa: Guinea (green), Liberia (red) and Sierra Leone (blue) (Bedford 2016). The mutation rate for Ebola virus was reported to be only slightly higher compared to the past outbreaks (Carroll et al. 2015; Holmes et al. 2016) with nucleotide substitution rate average of 1.2 $x10^{-3}$ substitutions per site per year (Hoenen et al. 2015;

Holmes et al. 2016). The evolution of Ebola virus is slower compared to that of influenza virus; where the mean substitution rates of HA and NA genes of H1N1/2009 are 5.34 x 10^{-3}, 5.21 x 10^{-3} nucleotide substitutions per year, respectively (Su et al. 2015).

A significant substitution at A82V in GP1 receptor binding region was found in post-2014 Ebola strains (Gire et al. 2014; Carroll et al. 2015) that may have been responsible for increased infectivity in human cells (Diehl et al. 2016; Urbanowicz et al. 2016).

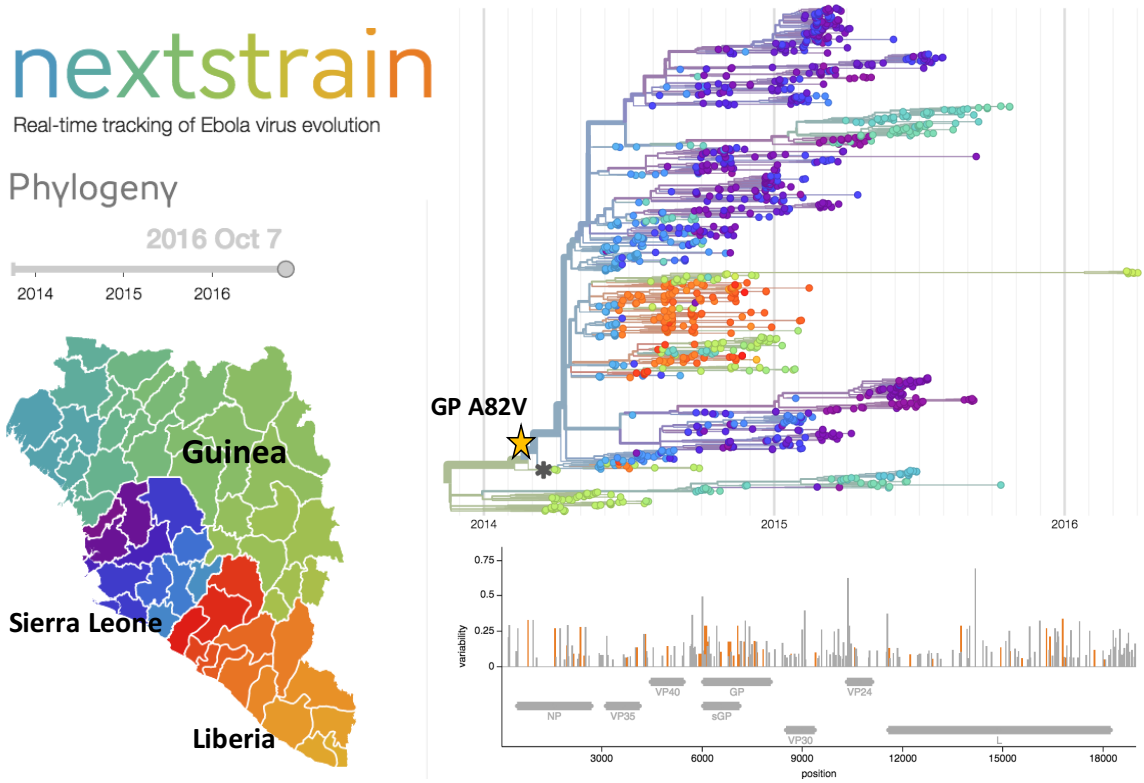

Figure 1. 10 ***Phylogeny of the Ebola viruses isolated from infected humans during the 2013-2016 outbreak in West African nations:*** *Guinea (green), Liberia (red) and Sierra Leone (blue). Asterisk denotes the Zaire virus strain used in our study (Kissidougou-C15). Star denotes the human adaptation mutation A82V in GP. Figure made using nextstrain.org (Bedford 2016).*

1.11 Structure of Ebola Virus

Ebola virus belongs to the Filoviridae family. It is an enveloped, cylindrical/tubular structure about 800 nm long and 80 nm in diameter, carrying a linear, single strand negative-sense RNA genome approximately 19 kb in length (Figure 1.11). The seven genes encode seven structural proteins and one non-structural protein. The seven structural proteins are nucleoprotein (NP), polymerase cofactor (VP35), major matrix protein (VP40), glycoprotein (GP), transcription activator (VP30), minor matrix protein (VP24) and large RNA–dependent RNA polymerase (L). Virion-attached GP encoded by GP gene is the product of a transcriptional shift.

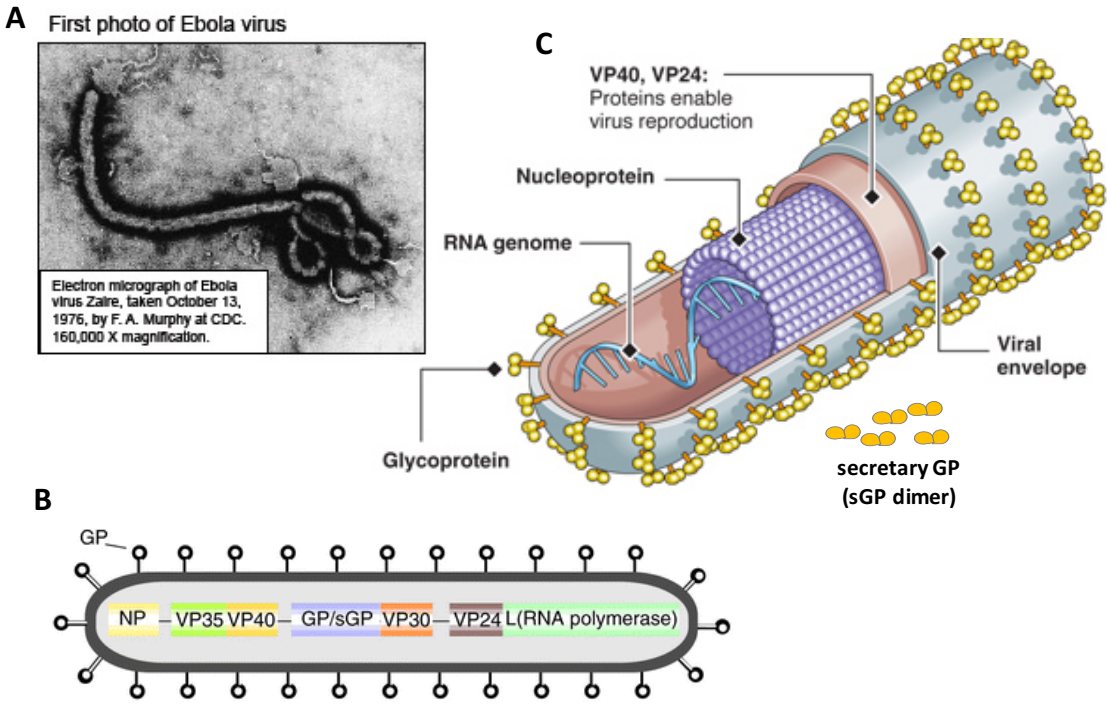

Figure 1. 11 ***Ebola Virus genome and structure. A)*** *First electron micrograph picture of Yambuku strain Ebola Zaire virus isolated in 1976 (Murphy 1976).* ***B)*** *Genome of Ebola virus contains seven genes which encode seven structural (NP, VP35, VP40, GP, VP24, Large RNA polymerase) and one non-structural protein (dimeric sGP). The Glycoprotein (GP) in trimeric form is present on the virion surface and is the target antigen for*

protective antibodies. ***C)*** *Ebola virus is an enveloped, cylindrical structure with a single strand, negative sense RNA genome. Figures B and C adapted from (Lieff 2014).*

1.12 Ebola virus glycoprotein

Glycoprotein is the only surface protein of the Ebola virus and essential for cell entry and receptor binding. It is also the main component of the vaccine for inducing protective antibodies.

1.12.1 GP transcription

The details of GP described here are based on ZEBOV GP. RESOV GP differs from ZEBOV GP in some ways. The GP gene encodes three glycoproteins: ssGP (small secreted GP), sGP (secreted GP) and membrane GP (simply called as GP) via transcriptional stuttering (Figure 1.12) (reviewed in (Lee and Saphire 2009; Cook and Lee 2013)). These three are expressed in abundancy of 5%, 70% and 25% respectively (Mehedi et al. 2011). The primary open reading frame is well conserved among all Ebola subtypes and transcribes to express a 364-residue non-structural protein called secreted GP (sGP). The N-terminal 295 amino acids are identical for sGP, ssGP and GP but they differ at their C terminal. The GP gene contains seven adenosine nucleotides within a predicted hairpin loop around nucleotides GGGAAACU - CCUCACU where the L polymerase stutters and can insert an additional (one or two) adenosine nucleotides (Mehedi et al. 2013). Without an insertion, the reading frame ends at codon 365 and encodes sGP.

A single adenosine insertion results in a frameshift such that translation continues to read for a total of 676 codons to produce full length GP, a type I transmembrane glycoprotein of 676 amino acids.

Both pre-sGP and pre-GP undergo a post-translational proteolytic cleavage by furin to form a mature product. Furin cleavage of pre-sGP results in a mature sGP with five N-glycosylation sites and a small secreted protein called Δ-peptide. Two monomeric sGP are covalently linked by two disulphide bonds to form a 110 kDa homodimeric sGP (Volchkova et al. 1998) which is secreted outside the cell. It may act as decoy for antibodies and play a role in immune evasion.

Five percent of GP transcripts encode ssGP which is transcribed after addition of two, or deletion of one adenosine during stuttering (Figure 1.12), resulting in an alternative frame shift that meets a stop codon at codon 299 and encodes ssGP of 298 amino acids. ssGP forms a homodimer via disulphide linkage towards C-terminus (Mehedi et al. 2011). It is also secreted outside the cell but the function is still unknown.

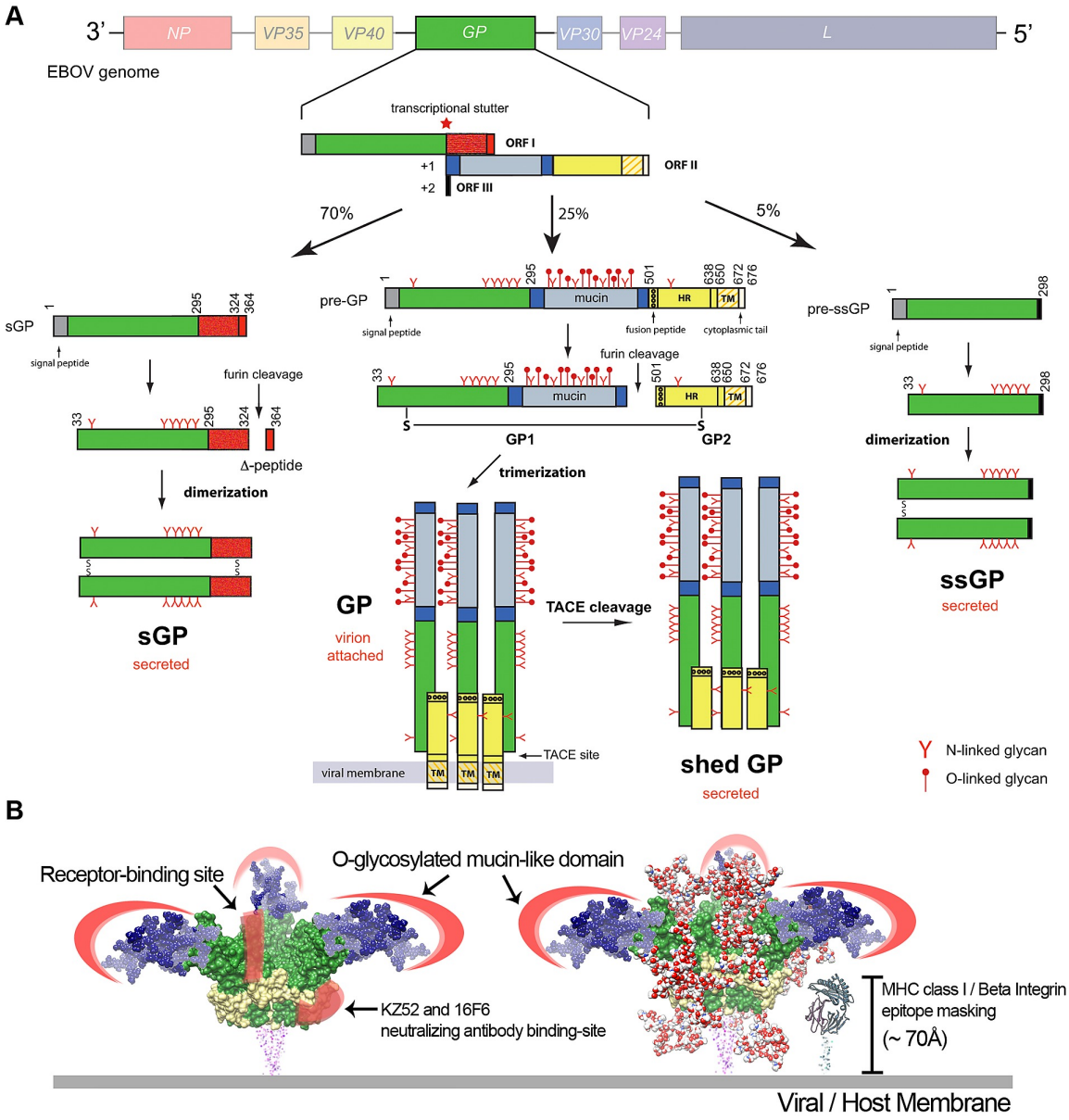

Figure 1. 12 ***Ebola GP gene transcription****. **A)** The primary GP transcript encodes a secreted GP (sGP) of ~110 kDa and 364 residues. Transcriptional stuttering of GP gene results in two other forms of GP: trimeric membrane GP and a dimeric small, secreted GP (ssGP). The N-terminal 295 residues of sGP, membrane GP and ssGP are same **B)** Trimeric membrane GP is the only antigen against which the antibodies are induced. Each monomer consists of GP1 and GP2 domains which remain linked by a disulphide bond. Mucin-like domain (MLD) (shown as blue surface) is heavily covered by O- and N-glycans (~ 80 O-linked glycosylation sites). GP epitopes are masked by 11-18 N-linked*

glycans (shown as red and white spheres. The height of GP is ~150 Å which may block small surface proteins such as MHC-class I molecules and ß-integrins (~70 Å) by steric hindrance. Figure taken from (Cook and Lee 2013).

1.12.2 GP structure

The membrane glycoprotein forms two subunits GP1 and GP2 after furin cleavage which remain linked by a disulphide bond between Cys53 (GP1) and Cys609 (GP2). The final membrane GP is a 450 kDa trimeric structure of three heterodimeric GP monomers. TACE (TNF-α-converting enzyme) can cleave the GP on viral surface at a site proximal to the transmembrane domain.

Lee et al. described the structure of a trimeric, pre-fusion GP based on the crystallization of GP complexed with an Fab fragment from antibody KZ52, which had been isolated from a human survivor from the 1995 epidemic (Lee et al. 2008). Crystallization of whole GP was difficult, so the mucin-like domain (MLD), transmembrane domain and two N-linked glycosylation sites were removed (Lee et al. 2008). The GP molecule is a trimer that forms a chalice and a cradle shaped structure. The chalice is formed by three GP1 subunits, with a glycosylated glycan cap, and projected mucin-like domain and a receptor-binding site (RBS or head) almost enclosed inside the chalice bowl (Figure 1.13). Three GP2 subunits form the base of the chalice that cradle and encircle the GP1. In the crystal structure, mainly three subdomains can be seen: base (GP1-GP2 interface), head (receptor binding site) and glycan cap.

The GP1 subunit is comprised of residues 1 to 501, of molecular weight ~130 kDa. It contains the glycan cap, putative receptor binding region (RBR) and a heavily glycosylated mucin-like domain (MLD). The C-terminal GP2 of molecular weight about 20 kDa contains the hydrophobic internal fusion loop, two heptad repeats (HR1 and

HR2), a disulphide bond motif (CX_6CC), membrane-proximal external region (MPER) and a transmembrane anchor. Heptad repeat is H P P H C P C, where H, P and C mean hydrophobic, polar and charged residues.

Within GP1, there are four discontinuous sections that form a hydrophobic, semi-circular surface within the base (Figure 1.13, green), which interacts with the internal fusion loop and heptad region in GP2. These sections may be required to hold and stabilize the GP2 in its pre-fusion conformation. Four other discontinuous sections (Figure 1.13, blue) form the head which is thought to contain the receptor binding site. The glycan cap is formed by a continuous domain of residues 227-310, which sits on the top of the head domain. There are four predicted N-linked glycosylation sites (Asn228, Asn238, Asn257 and Asn268) on the glycan cap. The mucin-like domain is formed by 150 residues (313 to 464), and is the least conserved domain among EBOV subtypes. It is heavily glycosylated with O- and N-linked oligosaccharides and sits on the tip of the glycan cap.

The internal fusion loop (IFL) of 46 residues (511-556) in GP2 bears more resemblance to the class II or III virus (VSV-G) fusion peptides than class I (influenza HA). EBOV GP lacks a central coiled-coil α-helical structures as in the post fusion conformation of haemagglutinin. Instead it contains a β- sheet ectodomain structure. The IFL wraps around the base of GP.

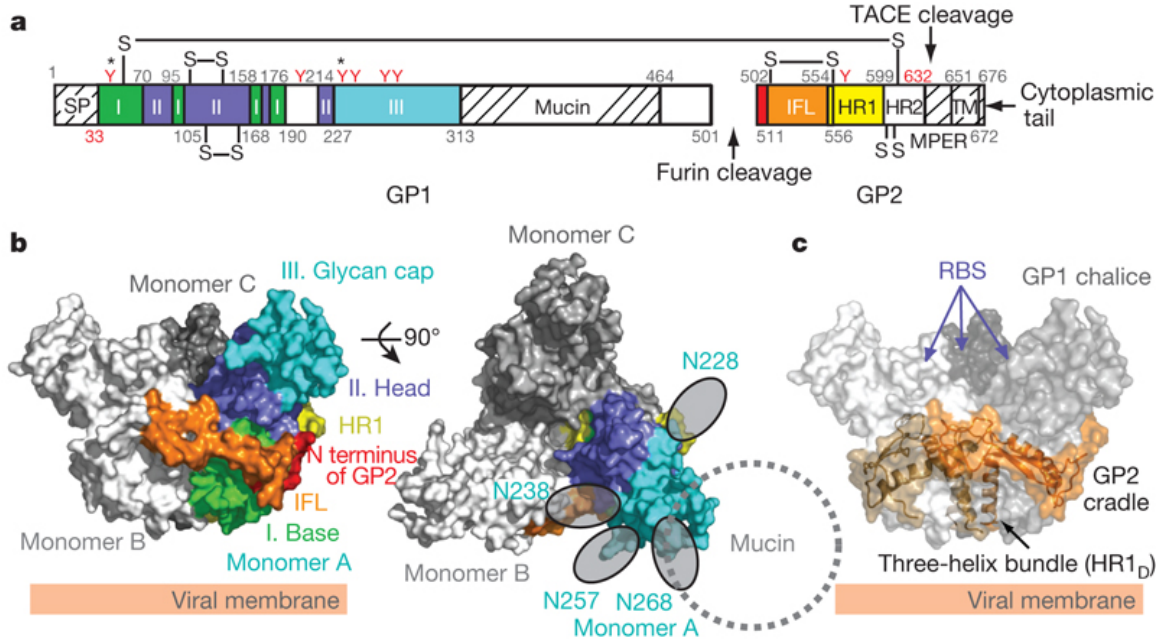

Figure 1. 13 ***Structure and make up of Zaire ebolavirus****. A) Schematic drawing of GP gene. GP1 and GP2, two subunits are linked by a disulphide bridge. B) Trimeric GPΔmucΔtm (GP without the transmembrane and mucin-like domains). Base, head and glycan cap of a monomer are coloured green, blue and cyan respectively. IFL (internal fusion loop) coloured orange wraps around the GP1. In the second figure, the top view of the glycoprotein is shown. N228, N238, N268 and N257 are N-linked glycosylation sites in glycan cap. C) Trimeric GP molecule (GPΔmucΔtm) is shown as a chalice and cradle structure. Three GP1 subunits form the chalice and GP2 subunits form the cradle which wraps around the base of the GP1 chalice. GP: Glycoprotein; HR: Heptad repeat region; IFL: Internal fusion loop; MPER: Membrane-proximal external region; RBS: Receptor-binding site; SP: Signal peptide; TACE: TNF-α-converting enzyme; TM: Transmembrane anchor. Figure taken from (Lee and Saphire 2009).*

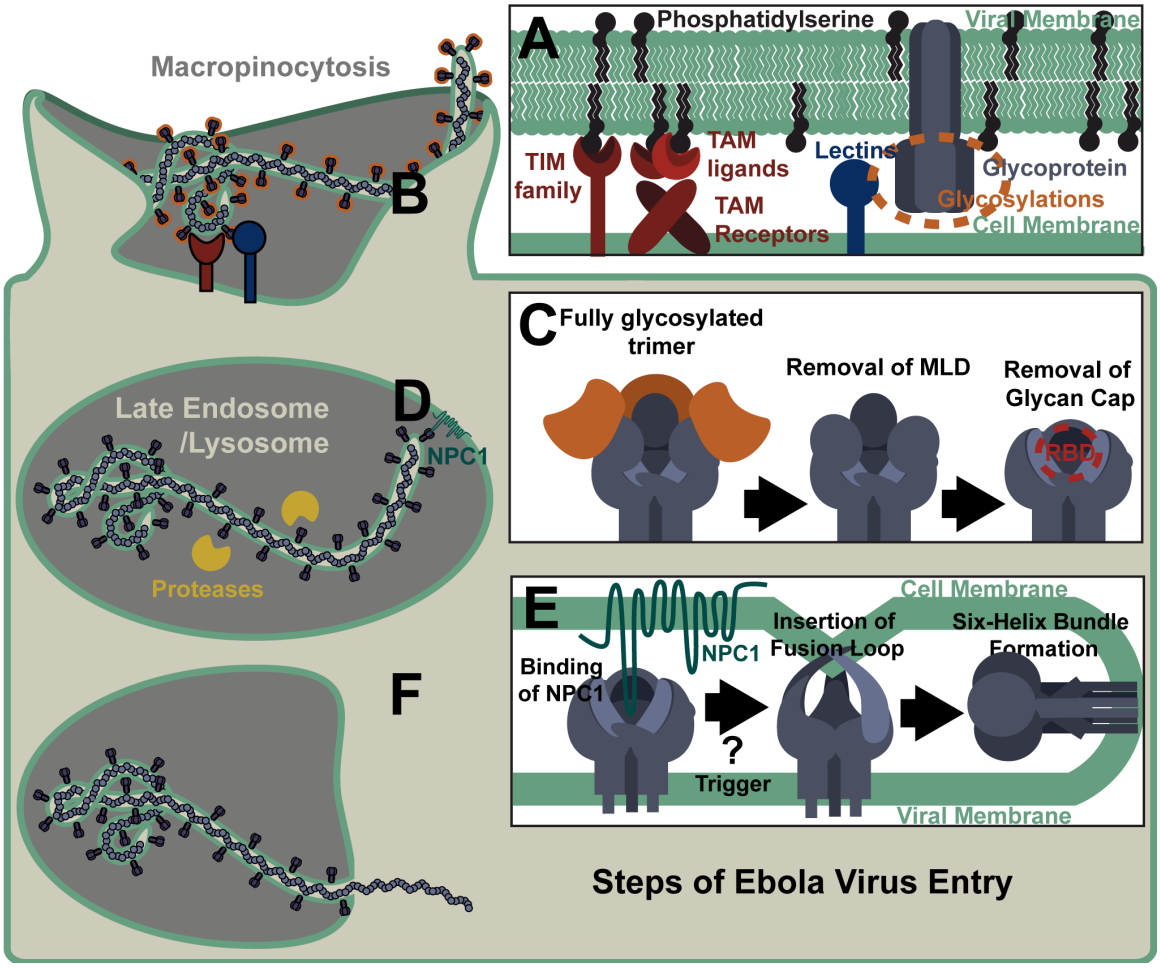

Figure 1. 14 ***Ebola virus entry****. **A)** Ebola virus attachment to host cell membrane is non-specific by the use of glycans on GP to bind to C-type lectins and viral envelope to bind to phosphotadylserine receptors (TIM-1 etc.). **B)** Virus is taken up by macropinocytosis. **C)** Cathepsins B and/or L cleaves off the mucin-like domain and glycan cap and exposes the receptor binding domain completely to bring GP to its fusion-ready state. **D)** GP RBD binds to the C domain of the NPC1 receptor on the late endosome/lysosome membrane. **E)** Following NPC1 binding, fusion is triggered by an unknown factor that releases the fusion loop allowing it to insert into the vesicle membrane. HR1 and HR2 regions of GP2 collapse to form a six-helix bundle bringing the viral and vesicle membrane in proximity leading to the formation of a "hemifusion" stalk and subsequent fusion pore. **F)** Viral*

genome and proteins are released into the cytosol for the process of replication. Figure is taken from (Moller-Tank 2015).

1.13 Cell entry by Ebola virus

1.13.1 Macropinocytosis

Studies are still ongoing to determine the exact mechanisms involved in Ebola virus entry. The studies so far suggest that Ebola virus internalization occurs via macropinocytosis (Saeed et al. 2010) and clathrin-mediated endocytosis (Aleksandrowicz et al. 2011) and this is reviewed by (Lee and Saphire 2009; Rhein and Maury 2015; Moller-Tank 2015).

Virus binds non-specifically to cell receptors: EBOV GP binds to C-type lectins (DC-SIGN, L-SIGN) via N- and O-linked oligosaccharides on GP and the viral envelope binds to phosphatidylserine receptors (TIM-1, TIM-4) (Moller-Tank and Maury 2014). These receptors may enhance the attachment, not necessarily being the primary requirement for virus entry. However, TIM-1 is shown to have critical role in Ebola virus entry (VLPs and pseudotyped viruses) independent of GP (Kondratowicz et al. 2011; Moller-Tank et al. 2013) in some cell lines.

1.13.2 Proteolytic processing of GP in endosomes

After endocytosis of virus, EBOV GP undergoes proteolysis by low-pH dependent cathepsin B and/or L (CatB/L) proteases. This proteolysis removes the glycan cap and mucin-like domains from the GP and is essential for subsequent fusion events and viral replication, although cathepsins are not specifically or exclusively required for infection (Marzi, Reinheckel, and Feldmann 2012). GP1 is cleaved by Cat L from native ~130 kDa

size to a 50 kDa fragment, and further to 17 to 19 kDa sized GP1, exposing the receptor binding site. Cat L cleaved 19 kDa GP1 may be further trimmed by Cat B.

1.13.3 NPC-1 receptor binding and fusion

The exposed RBS of the proteolytically primed GP1 binds to the transmembrane protein NPC1 luminal C-domain (Gong et al. 2016) in a late endo/lysosomal compartment, reviewed by (Hunt, Lennemann, and Maury 2012). Binding to NPC1 is essential for membrane fusion (Carette et al. 2011; Cote et al. 2011). NPC1 protein is known to be involved in cholesterol trafficking and homeostasis but this function plays no role in GP binding and fusion because cells lacking NPC2, a key component for the lipid transport function of NPC1, are efficiently infected (Carette et al. 2011). The HOPS complex, which mediates fusion of endosome and lysosome membranes, is also found to be an important factor in fusion and viral entry (Carette et al. 2011). Kuroda et al. suggest that a TIM-1/NPC-1 interaction may be also important for fusion.

1.14 Small molecule inhibitors of Ebola entry.

In recent drug repurposing screens, an unusually high frequency of small molecules have been identified that can inhibit Ebola virus entry. The exact mechanisms by which these molecules work is still unclear, but it seems likely that each of the entry steps described above can be a target (Figure 1.14). Examples are shown in the table 1.2 (courtesy of Julie Xiao), and include drugs that i) interfere with macropinocytosis, ii) induce an NPC1 like phenotype and presumably interfere with NPC1 structure), iii) block lysosmal calcium channels (that may be involved in the fusion process), iv) inhibit proteases (that may prevent exposure of the receptor binding region of GP), and v) proton ionophores (that may interefere with H+ dependant proteases), vi) drugs like Arbidol are membrane

fusion inhibitors, and finally vii) RNA polymerase inhibitor like favipiravir (Lai, Ng, and Cheng 2014).

Table 1. 2 Drug repurposing to inhibit Ebola virus (Courtesy of Julie Xiao).

Mechanism	Example of Drug
Na/H (Proton) Exchange	Amiloride
Proton Ionophore	Niclosamide
Calpain Cathepsin B inhibitor	MDL 28170
Lysomotropism (pKa/LogP)	Chloroquine, Tricyclics, Tamoxifen, Clomiphene, Amiodarone, Verapamil
Fusion Inhibitors	Arbidol (Russian anti-flu Drug)
RNA polymerase inhibitor	Favipiravir
Nucleoside Analogues/Inhibitors	Gemcitabine, Brequinar, Aminopterin

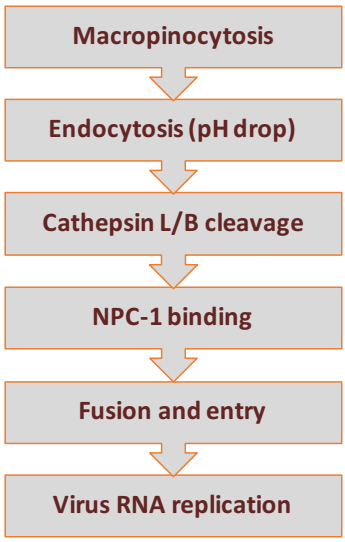

1.15 Monoclonal antibodies to Ebola Virus

Numbers of monoclonal antibodies to EBOV glycoprotein from different species including, human (Maruyama et al. 1999; Flyak et al. 2016; Corti et al. 2016), macaques (Keck et al. 2016) and mice (Furuyama et al. 2016; Marzi et al. 2012; Wilson et al. 2000; Qiu, Audet, et al. 2012; Pettitt et al. 2013; Takada et al. 2007) have been isolated. These antibodies were studied for their *in vitro* neutralisation potency, epitope recognition and protection in different animal models (mice, guinea pigs and macaques) (Table 1.3). Some of these antibodies with respect to their protection and epitope recognition are reviewed by Saphire and Aman (Saphire and Aman 2016) (Figure 1.15).

Table 1. 3 Antibodies against Ebola virus

							In-vivo protection				
Antibody	**Species Origin**	**Ig subtype**	**VH**	**Epitope**	**In vitro neutralization**	**Cross-reactivity**	**Infection model**	**Virus**	**Dose**	**Protection**	**Literature**
KZ52	Human	IgG1		GP1-GP2 Base	Yes		Rhesus Macaques	Zaire	50 mg/kg (1 dbi)	No	Oswald et al, 2007, Plos Pathogens
KZ52	Human	IgG1		GP1-GP2 Base			Guinea Pigs	Zaire	25 mg/kg (6h pi)	No	Parren et al, 2002, JOV
KZ52	Human	IgG1		GP1-GP2 Base			Guinea Pigs	Zaire	25 mg/kg (1h pi)	Partial (80%)	Parren et al, 2002, JOV
m8C4	Mouse			GC	Yes	All	Mice IFN-$\alpha\beta^{-/-}$	Sudan	10 mg/kg (day -1, 1 & 3)	Partial (70%)	Holtsberg et al ,2016, JV
2G4	Mouse			GP1-GP2 Base	Yes		Mice BALB/C	Zaire	5 mg/kg (1 dpi)	Partial (60%)	Qui et al, 2012, PLosNTDS
2G4	Mouse			GP1-GP2 Base			Guinea Pigs	Zaire	~10 mg/kg (1 dpi)	Partial (60%)	Qui et al, 2012, PLosNTDS
4G7	Mouse			GP1-GP2 Base, GP1 459-500	Yes		Mice BALB/C	Zaire	5 mg/kg (1 dpi)	Partial (~70-83%)	Qui et al, 2012, PLosNTDS
4G7	Mouse			GP1-GP2 Base, GP1 459-500	Yes		Guinea Pigs	Zaire	~10 mg/kg (1 dpi)	Partial (60%)	Qui et al, 2012, PLosNTDS
4G7 + 1H3 + 2G4 (Zmab)	Mouse			Base + GC +Base	Yes		Guinea Pigs	Zaire	~10 mg/kg (2 mg+1.5mg+1.5 mg resp) (2 dpi)	Complete	Qui et al, 2012, PLosNTDS
4G7 + 1H3 + 2G4 (Zmab)	Mouse			Base + GC +Base	Yes		Guinea Pigs	Zaire	~ 10 mg/kg (2 mg+1.5mg+1.5 mg resp) (3 dpi)	Partial (67%)	Qui et al, 2012, PLosNTDS
murine 6D8	Mouse	IgG2a		MLD 389-405 (HNTP**VYKLDISEA**TQVE)		Zaire	Mice BALB/C	Zaire	5 mg/kg (2 dpi)	Partial (60%)	Wilson et al, 2000, Science
murine 13C6	Mouse	IgG2a		GC	Yes	Zaire, Sudan	Mice BALB/C	Zaire	5 mg/kg (2 dpi)	Partial (80%)	Wilson et al, 2000, Science
murine 13F6	Mouse	IgG2a		MLD 401-417 (ATQV**EQHHRRTDN**DSTA)		Zaire	Mice BALB/C	Zaire	5 mg/kg (2 dpi)	Partial (30%)	Wilson et al, 2000, Science
h-13F6CHO	Mouse			MLD 401-417			Mice	Zaire	~1.5 mg/kg (dbi)	Partial (60%)	Zeitlin et al, 2011, PNAS
h-13F6 (N. benthamiana)	Mouse			MLD 401-417			Mice	Zaire	~1.5 mg/kg (dbi)	Complete (100%)	Zeitlin et al, 2011, PNAS
MB003 CHO (c13C6, h-13F6, and c6D8)				GC + MLD (401–417) + MLD (389–405)			Rhesus Macaques	EBOV-K	50 mg/kg/mAb (1hpi, 4 & 8 dpi)	Partial (33%)	Olinger et al, 2014, PNAS; Audet et al , 2014, Scientific Reports
MB003 RAMP (c13C6, h-13F6, and c6D8)				GC + MLD (401–417) + MLD (389–405)			Rhesus Macaques	EBOV-K	16.67 mg/kg/mab (2, 6, 8 & 10 dpi)	Partial (70%)	Olinger et al, 2014, PNAS
MB003 (c13C6, c13F6, and c6D8) (N. benthamiana)				GC + MLD (401–417) + MLD (389–405)			Rhesus Macaques	EBOV-K	16.67 mg/kg/mab (? dpi)	Partial (43%)	Pettitt et al, 2013, STM
ZMab (1H3, 2G4, and 4G7)				GC + Base + Base			Cynomolgus Macaques	Zaire	25 mg/kg (1, 4 & 7 dpi)	Complete (100%)	Qiu et al, 2012, STM
ZMab (1H3, 2G4, and 4G7)				GC + Base + Base			Cynomolgus Macaques	Zaire	25 mg/kg (2, 5 & 8dpi)	Partial (50%)	Qiu et al, 2012, STM
ZMapp1 (c13C6 + c2G4 + c4G7)				GC + Base + Base			Guinea Pigs	Zaire	~10 mg/kg (3 dpi)	Partial (67%)	Qiu et al, 2014, Nature
ZMapp1 (c13C6 + c2G4 + c4G7)				GC + Base + Base			Rhesus Macaques	EBOV-K	50 mg/kg (3, 6 & 9 dpi)	Complete (100%)	Qiu et al, 2014, Nature
ZMapp (c13C6 + c2G4 + c4G7)				GC + Base + Base			Rhesus Macaques	EBOV-K	50 mg/kg (5, 8 & 11 dpi)	Complete (100%)	Qiu et al, 2014, Nature
16F6	Mouse			GP1-GP2 Base	Yes	Zaire, Sudan	Mice IFN-$\alpha\beta^{-/-}$	Sudan	25 mg/kg (day -1, 1 & 4)	Partial (90%)	Chen et al, 2014, ACS
F4	Synthetic (16F6, human scaffold)	IgG1	3-23	GP1-GP2 Base	Yes	Zaire, Sudan	Mice IFN-$\alpha\beta^{-/-}$	Sudan	25 mg/kg (day -1, 1 & 4)	Partial (90%)	Chen et al, 2014, ACS
E10	Synthetic (16F6, human scaffold)	IgG1	3-23	GP1-GP2 Base	Yes		Mice IFN-$\alpha\beta^{-/-}$	Sudan	25 mg/kg (day -1, 1 & 4)	Partial (80%)	Chen et al, 2014, ACS
ch226	Mouse			GP1 core (escape mutant at 134)	Yes		Mice	Zaire	5 mg/kg (2 dpi)	Partial (88%)	Takada et al, 2007, Vaccine
ch133	Mouse			GP1-GP2 Base (escape mutant at 549)	Yes		Mice	Zaire	5 mg/kg (2 dpi)	Partial (88%)	Takada et al, 2007, Vaccine
6D6	Mouse	IgG1		Fusion loop (Gly528, Gly529, Leu530)	Yes	All	Mice BALB/C	Zaire	5 mg/kg (1 dpi)	Complete	Furuyama et al 2016, Nature
6D6	Mouse	IgG1		Fusion loop (Gly528, Gly529, Leu530)	Yes	All	Mice IFN-$\alpha\beta^{-/-}$	Zaire	5 mg/kg (1 dpi)	Complete	Furuyama et al 2016, Nature
FVM09	Macaque			GP1 conserved loop GEWAF	No	All	Mice BALB/C	Zaire	25 mg/kg (day 0 & 3)	Partial	Keck et al 2015, JOV
FVM02p	Macaque			Conserved Fusion loop AIGLAWIPY	No		Mice BALB/C	Zaire	25 mg/kg (day 0 & 3)	Partial	Keck et al 2015, JOV
FVM02p + FVM09	Macaque			IFL + GC		All & MARV	Mice BALB/C	Zaire	15 mg/kg total (day 0 & 3)	Complete	Keck et al 2015, JOV
FVM04	Macaque			RBR (Block NPC-1 receptor)	Yes	All & MARV	Mice BALB/C	Zaire	25 mg/kg (day 0 & 3)	Complete	Keck et al 2015, JOV
FVM04	Macaque			RBR (Block NPC-1 receptor)	Yes	All & MARV	Mice BALB/C	Zaire	5 mg/kg (2 dpi)	Complete	Howell et al, 2016, Cell Reports
FVM04	Macaque			RBR (Block NPC-1 receptor)	Yes	All & MARV	Guinea Pigs	Sudan	15 mg/kg (3 dpi)	Complete	Howell et al, 2016, Cell Reports
FVM04	Macaque			RBR (Block NPC-1 receptor)	Yes	All & MARV	Guinea Pigs	Zaire	15 mg/kg (1 dpi)	Partial (40%)	Howell et al, 2016, Cell Reports
FVM04 + c13C6 + c2G4				RBR + GC + Base			Guinea Pigs	Zaire	15 mg/kg (3 dpi)	Partial (70%)	Howell et al, 2016, Cell Reports
114	Human	IgG1	3-13*01	RBR (Block NPC-1 receptor)	Yes		Rhesus Macaques	Zaire	50 mg/kg (5, 6 & 7 dpi)	Complete (100%)	Corti et al, 2016, Science; Misasi et al, 2016, Science
100	Human	IgG3	4-59*01	GP1-GP2 Base	Yes						Corti et al, 2016, Science; Misasi et al, 2016, Science
EBOTAb	Sheep			Polyclonal			Guinea Pigs	Zaire	51 mg/animal (3, 4, 5, 7, 9 & 11 dpi)	Partial (83.3%)	Dowall et al, 2016, Scientific Reports
EBOTAb	Sheep			Polyclonal			Guinea Pigs	Zaire	72 mg/animal (3 dpi) [5 mg/ml EBOV sp. ab.]	Partial (33%)	Dowall et al, 2016, Scientific Reports
ZMapp (c13C6 + c2G4 + c4G7)	Mouse						Guinea Pigs	Zaire	5 mg/animal (3 dpi)	Complete (100%)	Dowall et al, 2016, Scientific Reports
EBOTAb	Sheep			Polyclonal			Guinea Pigs	Zaire	25 mg/animal (day 3-7, 9, 11)	Partial (75%)	Dowall et al, 2016, JID
EBOTAb	Sheep			Polyclonal			Guinea Pigs	Zaire	25 mg/animal (day 2-7, 9, 11)	Complete (100%)	Dowall et al, 2016, JID

GC: Glycan cap; RBR: Receptor binding region; MLD: Mucin-like domain; IFL: Internal fusion loop; dpi: day post-infection; dbi: day before-infection; IFN-αβ: Interferon alpha-beta; c before antibodies mean chimeric (with human IgG1)
RAMP: Nicotiana benthamiana-based rapid antibody manufacturing platform; EBOTAb: an ovine polyclonal antibody-based therapeutic

1.15.1 Antibodies to the glycan cap

The majority of the published antibodies target GP1 glycan cap. This seems to be an immunodominant site although covered by glycans. The glycan cap (GC) shields the NPC-1 receptor binding site, which is exposed after it is cleaved off by cathepsin proteases. Some antibodies targeting the GC are also found to be neutralising and partially protective, which seems counter intuitive. The antibody FVM09 which recognises the filovirus-conserved epitope GEWAF in the glycan cap is also partially protective despite being non-neutralising *in vitro* (Keck et al. 2016). One mechanism of action of these apex antibodies is believed to be via an ADCC dependant mechanism (Saphire and Aman 2016; Schmaljohn and Lewis 2016). For example, antibodies 13C6 and 6D8 offer poor virus neutralisation alone *in vitro* and require complement for their neutralisation (Wilson et al. 2000). A second mechanism for these antibodies may involve the inhibition of proteolysis by blocking access to the cathepsin cleavage site, which I have investigated for our set of GC antibodies in chapter 6.

1.15.2 Antibodies to the Receptor Binding Region (RBR)

Antibodies like 114 (Corti et al. 2016) and FVM04 (Howell et al. 2016; Keck et al. 2016) from human and macaque origin respectively are RBR directed, and are potently neutralising *in vitro* and protective *in vivo* post-exposure. These antibodies act by blocking GP binding to NPC-1, which is essential for fusion and successful infection.

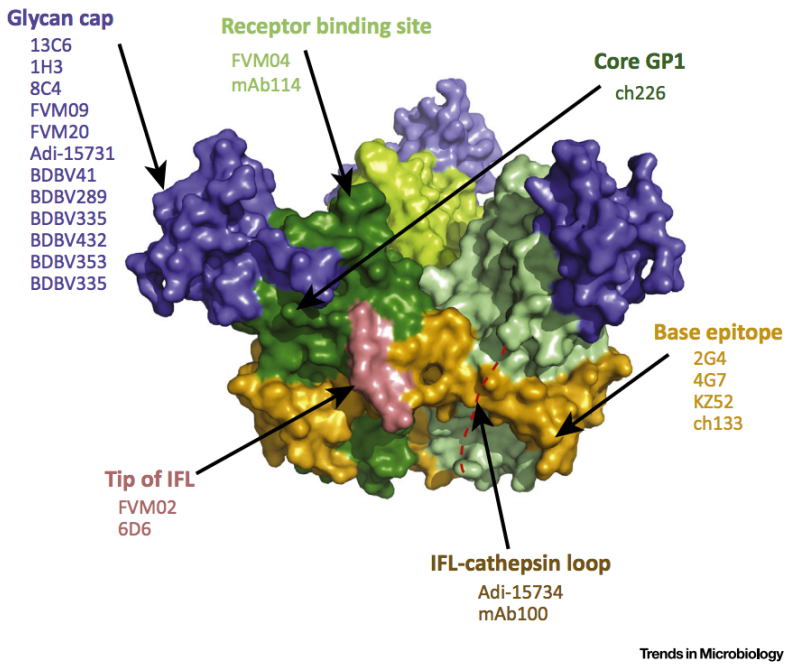

Figure 1. 15 ***Identified epitopes for numbers of Ebola antibodies published so far.*** *There are many epitopes within the glycan cap, receptor-binding region, base and internal fusion loop. Figure taken from (Saphire and Aman 2016).*

1.15.3 Antibodies to the Base or GP1-GP2 interface

The base is a compact structure formed by the GP1-GP2 interface and includes the internal fusion loop and heptad repeats. The majority of antibodies to the base are strong neutralisers and are often protective *in vivo*. The base antibody KZ52 was found to be non-protective in NHPs despite being a potent neutraliser and protective in rodents (Lee et al. 2008; Oswald et al. 2007; Parren et al. 2002). The reason for this lack of protection in the NHP model is not clear. The selection of resistance mutants was ruled out as an explanation (Oswald et al. 2007). Recently two antibodies, FVM02 (Howell et al. 2016) and 6D6 (Furuyama et al. 2016), have been described that are targeted to the conserved internal fusion loop. Both are broadly cross-reactive with other Ebola strains and are

protective. The mechanism of action of these antibodies may be by locking the GP in its pre-fusion conformation, and also blocking cathepsin cleavage (Tran et al. 2016).

1.15.4 ZMapp (Antibody cocktail) Therapy

The ZMapp cocktail of murine chimeric antibodies (c13C6, c2G4 and c4G7), one targeting glycan cap and two to the base, was successful in protecting 100% NHPs as late as 5-day post infection (Qiu et al. 2014). ZMapp antibodies are produced in tobacco plants. This turned out to be important for the full potency of the ZMapp mixture. The plant cell specific glycosylation (absence of fucose on N-glycans attached to Fc domains) was shown to enhance binding of the antibodies to the FcγRIII receptor, and this was associated with improved protection *in vivo* (Zeitlin et al. 2011). The antibodies produced in a standard mammalian CHO cell lines are fucosylated by (α1,6-linked fucose) N-glycans on the Fc domain. Another ZMapp-based cocktail MIL77E, comprising just two antibodies c13C6 and c2G4, developed by a Chinese group in modified CHO cells (that lack the fucosylation function similar to tobacco cells), was at least as protective as ZMapp in NHPs (Qiu et al. 2016). This opens the door to production of fully potent ZMapp in cells, which can give high yields more easily than the plants.

Although the ZMapp cocktail was not proven statistically to be protective in humans because of the small number of participants, there was a trend in the direction of improved survival (p ~0.1) (Prevail Team 2016). Together with the evidence from the NHP trials with ZMapp, this result certainly encourages the development of optimised cocktails of antibodies for use in human disease. ZMapp is not cross-reactive with strains of Ebola other than Zaire. Fully cross-reactive cocktails may be a possibility given the evidence from antibodies like the murine 6D6 (Table 1.3) that neutralises Zaire, Bundibugyo and Sudan strains.

1.16 EBOV Vaccines

Before the 2014-2015 outbreak there were no vaccines or drugs licensed for use against Ebola virus. Candidate vaccines are based on the induction of antibody and T cell responses to the Ebola GP, as in animal models these appear to be the most protective immune responses (Martins et al. 2016). The rVSV-ZEBOV recombinant vaccine was effective in preventing the infections with 70-100% success in a ring-vaccination protocol (Henao-Restrepo et al. 2015; Henao-Restrepo et al. 2017). This was a fully recombinant and replication competent virus, where the Ebola GP sequence replaced the VSV-G receptor to provide a portal of entry. The vaccine virus replicates in the vaccinated individuals to cause a viremia. This is associated with mild symptoms, particularly arthralgia in up to 20% of recipients (Henao-Restrepo et al. 2015).

Other vaccines based on replication incompetent Adeno viruses and Modified Vaccinia Ankara (MVA), have also been developed. Unlike the recombinant VSV vaccine, these viruses are not replication competent, but can express the Ebola GP during a single cycle infection in human cells. As both viruses are antigenically complex, and the GP is just one of many proteins in the vaccine infected cells competing to induce an immune response, it has become common practice to induce a primary response with one vaccine and a secondary response with the other, to try and focus the immune response on the Ebola GP which is common to both. An example is the ChAd3-EBO-Z developed by GSK/NIAID from a chimpanzee adenovirus. An adenovirus of Chimpanzee origin was used to try and avoid natural specific immunity in humans to their own adenoviruses which would prevent infection by the vaccine. GSK have described pre-clinical antibody responses in NHPs and humans (Geisbert and Feldmann 2011), particularly enhanced when boosted with MVA-BN-Filo (an MVA that expresses GP and NP from Ebola) (Ewer et al. 2016; Tapia et al. 2016).

1.17 Aim of the Ebola Project

In this project, described in chapter 6, we have developed monoclonal antibodies from human recipients of ChAd3-EBO-Z and MVA-BN-Filo vaccines in the Jenner Vaccine Trial (Ewer et al. 2016). In humans, this vaccine combination induced a modest but significant neutralising antibody response. We set out to see if vaccinated volunteers could be the source of potent neutralising antibodies that could form the basis of a treatment cocktail. The result is not a forgone conclusion as the antibodies are being generated in naïve recipients and have had little time for affinity maturation, unlike antibodies isolated from individuals who have recovered from the infection, which may be persistent. However, isolation of antibodies from recovered donors is complicated by the risks involved in handling specimens due to viral persistence, and the difficulties of availability of donors and transport of samples. If the principle of isolating effective antibodies from vaccinated donors could be established, then monoclonal antibody isolation should become part of all experimental vaccine trials, as these would represent golden opportunities for the development of novel treatments.

CHAPTER 2 | Materials and Methods

2.1 Materials

Influenza wild type H1N1 and H3N2 seasonal viruses were kindly provided by John McCauley at the Worldwide Influenza Centre, the Crick Institute.

Re-assorted seasonal vaccine viruses and sheep anti-sera to different influenza viruses were bought from NIBSC, UK.

Monoclonal antibodies used as controls were provided by various labs and are described in the text.

Haemagglutinin and Ebola glycoproteins were made by my supervisor Alain Townsend from 293T cells expressing a secreted shortened form of the proteins as described by Powell et al. (Powell et al. 2012). The Ebola glycoprotein used for plasmablast sorting was kindly provided by Tom Bowden, Strubi, University of Oxford.

Influenza and Ebola pseudotpyed S-FLU viruses were designed and made by Alain Townsend, and are described in the text (Baz et al. 2015; Huang et al. 2015; Powell et al. 2012).

The source of commercial antibodies, reagents and instruments used in our studies are described in the relevant sections, and commonly used media and buffers are listed in table 2.1.

Table 2. 1 List and recipe of commonly used mediums and buffers.

Mediums and buffers	Volume	Content
D0	500 ml	DMEM only (Sigma)
D10	500 ml	DMEM + 5 ml Pen/Strep (100 U) + 5 ml Glutamine (2 mM) + 50 ml FCS (Sigma)
Virus growth medium (VGM)	500 ml	DMEM + 5 ml Pen/Strep (100 U) + 5 ml Glutamine (2 mM) + 1.66 ml of 30% BSA (Sigma #A0336) (0.1 %) + filtered 5 ml HEPES (10 mM)
R0	500 ml	RPMI 1640 medium only (Sigma)
R2	500 ml	RPMI+ 5 ml Pen/Strep (100 U) + 5 ml Glutamine (2 mM) + 10 ml FCS (Sigma)
R10	500 ml	RPMI+ 5 ml Pen/Strep (100 U) + 5 ml Glutamine (2 mM) + 50 ml FCS (Sigma)
50 x TAE buffer	1000 ml	242 g Tris base (Mw = 121.1) + 57.1 g glacial acetic acid + 100 ml 0.5 M EDTA; in dH2O
5 M NaCl	500 ml	146.1 g NaCl in dH2O
1 x TBS buffer	500 ml	15 ml of 5 M NaCl (150 mM) + 16.67 ml of 1.5 M Tris.Cl pH 8.6 (20 mM); in dH2O
0.1 M Citric acid buffer	1000 ml	19.21 g anhydrous citric acid (Fw = 192.1) in dH2O
0.1 M Sodium citrate buffer	100 ml	2.94 g sodium citrate (Fw = 294.1) in dH2O
Antibody elution buffer, pH2.5-3	50 ml	3.5 ml of 0.1 M NaCitrate + 46.5 ml of 0.1 M Citric acid
FACS fix buffer	500 ml	PBS + 5 ml FCS (1%) + 500 µl of 20% Na azide (0.02%) + 5 ml of 40% formaldehyde (0.4%)
FACS wash buffer	500 ml	PBS + 5 ml FCS (1%) + 500 µl of 20% Na azide (0.02%)
RT-PCR catch buffer	5 ml	5 ml Rnase free water + 50 µl of 1 M Tris pH 8 + 125 µl Rnasin Rnase inhibitor (Promega)
Protein A sepharose column		0.3 g protein sepharose (Sigma #P3391) in 1 ml TBS buffer. Let settle on the washed column. [1g swells to 4ml]
10% Formalin	50 ml	5 ml formaldehyde (37 wt%, Sigma #F1635) in 45 ml PBS
HEPES MES (HM) buffer	500 ml	1.95 g MES (Sigma) (20 mM) + 10 ml of 1 M HEPES (20 mM) + 13 ml of 5 M NaCl (130 mM) in dH2O. Adjust pH to 7.5

DMEM: Dulbecco's Modified Eagle's Medium, RPMI: Roswell Park Memorial Institute, FCS: Fetal Calf Serum, BSA: Bovine Serum Albumin
TAE: Tris base, Acetic acid and EDTA, TBS: Tris Buffered Saline, PBS: Phosphate Buffered Saline, FACS: Fluorescence-Activated Cell Sorting
HEPES: 4-(2-hydroxyethyl)-1-piperazineethanesulfonic acid, MES: 2-(N-morpholino)ethanesulfonic acid

2.2 Growing wild type viruses

A monolayer of MDCK-SIAT1 cells in a 175cc flask were infected with 10 ml of a seed virus diluted in VGM (virus growth medium) to give a multiple of infection <0.1. After 1 hour, medium was changed to 40 ml VGM/TPCK-trypsin (1 µg/ml) and incubated for 48 hours. Virus was harvested and stored at -80 °C. Virus was titrated by haemagglutination assay, $TCID_{50}$ by limiting dilution, or titration of MDCK-SIAT1 cell infection to find the 50% infectious dose in 96-well plates containing $3x10^4$ cells per well.

2.3 Pseudotyped influenza viruses (S-FLU)

Pseudotyped S-FLU viruses were propagated and grown in MDCK-SIAT1 cell lines (Matrosovich et al. 2003) transduced with disabled Lenti virus to express the surface proteins haemagglutinin or Ebola glycoprotein as described by Powell et al. (Powell et al.

2012). The disabled Lenti virus vector was pHR-SIN (Demaison et al. 2002). Transduced cells were stained with specific monoclonal antibodies and FACS sorted for maximal surface expression. Sorted cell lines maintained stable expression of influenza HA and Ebola GP over at least nine consecutive passages.

S-FLU has been described in detail (Powell et al. 2012). It is a single cycle influenza A/PR/8/1934 virus with the hemagglutinin disabled by inactivation of the signal sequence, and replacement of the coding sequence with eGFP so that infected cells fluoresce green (Figure 2.1). Pseudotyped S-FLU stocks were prepared from cloned virus by passage in the desired transduced MDCK cell lines. Batches of S-FLU coated in Ebola GP (E-S-FLU), or particular HAs, were expanded to 200 ml volumes and frozen in aliquots at -80 ºC. HA pseudotyped virus required trypsin for growth, but GP coated virus did not. Virus stocks were titrated for infection of wild type MDCK-SIAT1 cells. Dilutions of virus that just reached plateau infection (1:4 to 1:32 dilution for most batches) were used in the neutralisation assay (see below) with titrations of monoclonal antibodies.

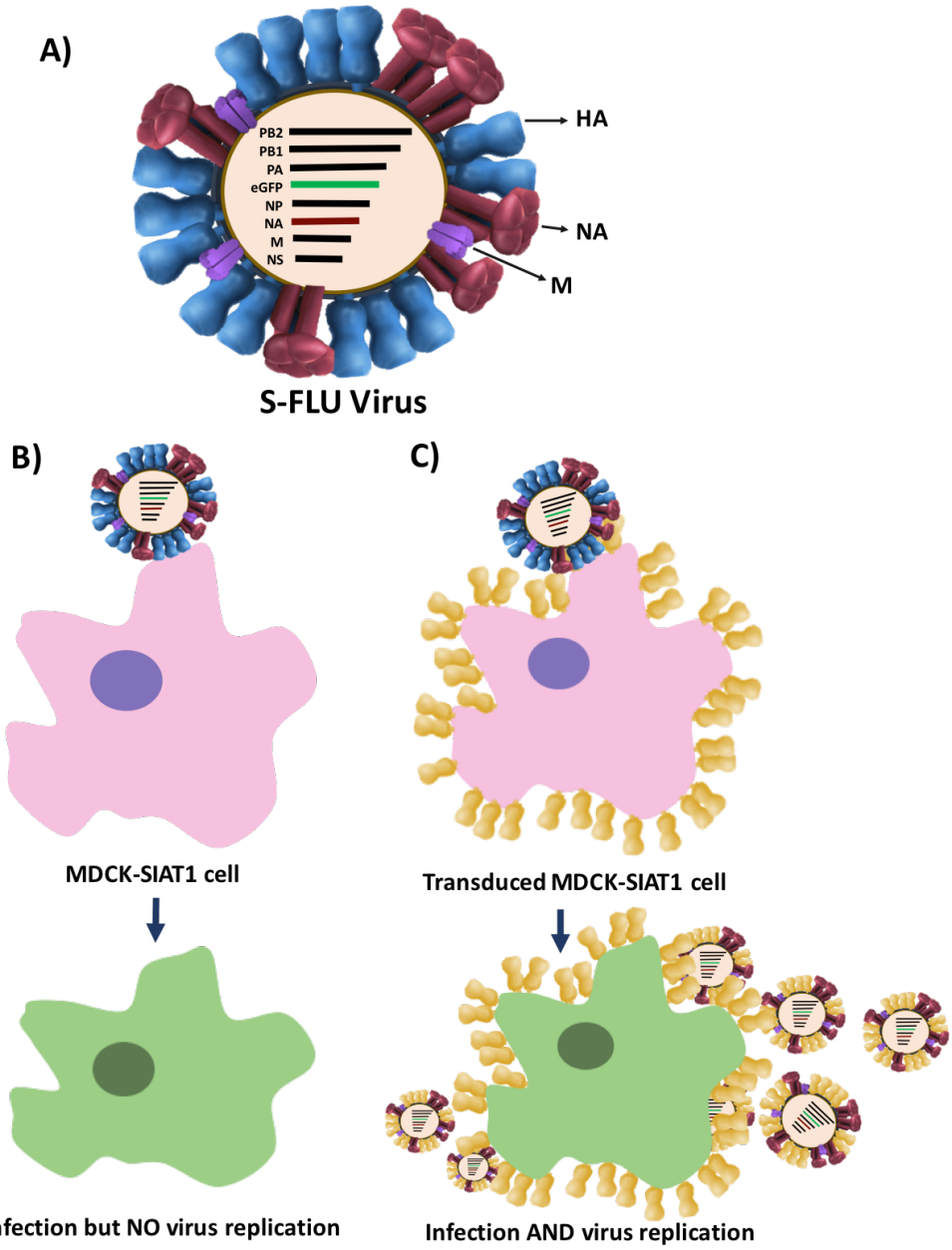

Figure 2. 1 ***Design and propagation of S-FLU virus****. **A)** Virus is attenuated by replacing HA gene with eGFP gene. Neuraminidase and internal genes are derived from PR8 virus.* ***B)*** *S-FLU can infect cells once but can not propagate.* ***C)*** *Propagation of S-FLU virus requires cells expressing surface glycoprotein that can provide binding and fusion activity.*

2.4 Stable expression of neuraminidase on 293T cells

293T cells were transfected with neuraminidase gene in pCMV vector using lipofectamine or PEI transfection reagent. After 2 days, transfected cells were stained with a monoclonal antibody and sorted by FACS. Sorted cells were grown, stored and used for screening for binding of antibody supernatants.

2.5 Isolation of human monoclonal antibodies

The staining of plasmablasts, sorting and PCR cloning of antibody variable regions from single cells was adapted from a protocol by Wrammert et al (Wrammert et al. 2008) and Smith K et al (Smith et al. 2009). A picture outlining the steps involved is shown in figure 2.2

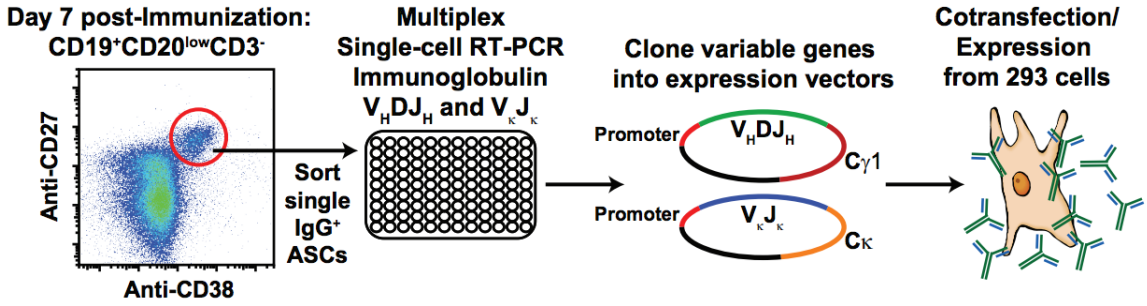

Figure 2. 2 ***Steps of monoclonal antibody isolation from a single-cell PCR cloning methods.*** *Figure adapted from (Wrammert et al. 2008).*

2.5.1 PBMC isolation

Blood was drawn from donors on day 7 post-vaccination, when plasmablast release into the circulation is at its peak (Wrammert et al. 2011). About 15-20 ml fresh heparinised blood was layered over 15 ml of Lymphoprep (Axis Shield) in a 50 ml Leucosep tubes and peripheral blood mononuclear cells (PBMC) were separated from whole blood by

density gradient centrifugation at 800*g*, 20 min at 20 ºC without a brake. PBMC were collected in a different tube and diluted to 45 ml with RPMI medium 1640 (R0, Sigma). Cells were then pelleted by centrifugation at 720*g* for 10 min. Cells were again washed with R2 medium and spun at 320*g* for 10 min. Finally, cells were re-suspended in R10 medium. Cells were sorted on the same day but placed in 37 ºC incubator until ready. PBMC were counted by ABX Pentra 60 cell counter (Horiba Medical).

2.5.2 Staining of antibody secreting cells or plasmablasts

The staining of plasmablasts and antibody PCR and cloning was adapted from a protocol by Wrammert et al. (Wrammert et al. 2008) and Smith et al. (Smith et al. 2009).

2.5.2.1 Staining

Materials

Cold FACS buffer: PBS, 1% FCS (without azide)

CD3 PB (BD Biosciences, cat. 558117)

CD20 APCH7 (BD Biosciences, cat. 641396)

CD19 FITC (BD Biosciences, cat. 55412)

CD38 PECy5 (BD Biosciences, cat. 555461)

CD27 PECy7 (BD Biosciences, cat. 560609)

IgM APC (BD Biosciences, cat. 561010)

IgD APC (BD Biosciences, cat. 561303)

5 ml Polypropylene tubes

Half million and 5-15 million PBMC were used for FACS analysis and sorting respectively. PBMC were washed with FACS wash buffer (PBS/1% FCS), then incubated with antibodies specific for the following cell surface markers: mouse anti human PB

anti-CD3, FITC anti-CD19, APC-H7 anti-CD20, PE-Cy7 anti-CD27, PE-Cy5 anti-CD38, anti-IgG and/or anti-IgM and anti-IgD for 20 min at room temperature with minimal light exposure. After washing, cells were re-suspended in wash buffer and passed through the cell strainer to prevent the clogging of the cytometer.

2.5.2.2 Flow Cytometry

Cell sorting was done with a FACS Aria III (BD Biosciences). Antigen specific plasmablasts were gated as: Lymphocytes/ Singlets/ $CD20^{neg\&low}$/ $CD3^{neg}$/ $CD19^{pos}$/ $CD27^{high}$/ $CD38^{high}$/ IgM,IgD^{neg} or IgG^{pos} cells. Single cells were sorted on a 96-well PCR plate (Row A-D only) containing 10 µl of RNase-inhibiting RT-PCR catch buffer (50 µl of 1 M Tris pH 8.0 buffer (Ambion) and 125 µl RNasin (Promega) in 5 ml RNAse free water). Row H contained only buffer to serve as PCR negative controls. Plates were immediately sealed, spun briefly and placed on dry ice. They were stored at -80 °C until used for PCR. Data were analysed with FlowJo V7 (Tree star Inc., California).

2.5.3 PCR and cloning

2.5.3.1 PCR

One-step RT-PCR kits and Hotstar Taq PCR kits were bought from Qiagen and HPLC purified primers from Eurofins or Sigma (Refer to table 2). Detailed protocols are shown in box 1 and 2 below. The plate was thawed, spun briefly and 15 µl of RT-PCR reaction mix was added in each well. Each reaction of the RT-PCR contained 6.5 µl RNase free water, 1 µl dNTP mix (10 mM each), 5 µl one-step RT-PCR buffer, 1 µl forward primer mix (~ 7 µM), 1 µl reverse primer mix (10 µM) and 0.5 µl one-step RT-PCR enzyme. The forward primer mix was prepared from a dilution of 14 primers (No. 1-4, 6-8 and 10-16, table 2) from stock of 100 µM each. These primers include leader sequence (L) and

variable region sequences of heavy and light chain from different immunoglobulin families. The reverse primers mix contained 3 primers (No. 5, 9 and 17). PCR was run as: reverse transcription of 30 min at 50 ^{o}C followed by 15 min at 95 ^{o}C to deactivate reverse transcriptase and activate thermal *Taq* and then 50 cycles of 94 ^{o}C for 30 s, 58 ^{o}C for 30 s and 72 ^{o}C for 1 min and the final elongation was performed at 72 ^{o}C for 10 min.

Using 3 µl RT-PCR product as template DNA, nested PCR was performed together with 30.25 µl water, 0.5 µl dNTP mix, 4 µl HotStar Taq buffer, 1 µl forward primer mix (10 µM), 1 µl reverse primer mix (10 µM) and 0.25 µl HotStar *Taq* enzyme. Forward primer mix for heavy chain PCR contained 11 primers (No. 18-28), kappa PCR 9 primers (No. 34-42) and lambda 6 primers (No. 47- 52). Reverse primer mix for heavy PCR contained 3 primers (No. 29-31), kappa (No. 43-46) and lambda (No. 53). These primers possess restriction sites for specific enzymes for cloning purposes. PCR was run as: 95 ^{o}C for 15 min for hot start, 50 cycles of 94 ^{o}C for 30 s, 58 ^{o}C for 30 s and 72 ^{o}C for 45 s and at 72 ^{o}C for 10 min. Nested PCR products were run on a 1% agarose gel, 1x TAE buffer. Heavy, kappa and lambda chain products were approximately 380 bp, 350 bp and 500 bp respectively. Nested PCR products were extracted from the gel and purified using QIAquick gel extraction kit.

Table 2. 2 List of primers for amplification of variable heavy and light chains of IgG.

#	Oligo Name	Sequence 5' to 3'
	RT-PCR Primers	
1	5' L VH 1	ACAGGTGCCCACTCCCAGGTGCAG
2	5' L VH 3	AAGGTGTCCAGTGTGARGTGCAG
3	5' L VH 4/6	CCCAGATGGGTCCTGTCCCAGGTGCAG
4	5' L VH 5	CAAGGAGTCTGTTCCGAGGTGCAG
5	3' Cγ CH 1	GGAAGGTGTGCACGCCGCTGGTC
6	5' L Vκ 1/2	ATGAGGSTCCCYGCTCAGCTGCTGG
7	5' L Vκ 3	CTCTTCCTCCTGCTACTCTGGCTCCCAG
8	5' L VK4	ATTTCTCTGTTGCTCTGGATCTCTG
9	3' Cκ 543-566	GTTTCTCGTAGTCTGCTTTGCTCA
10	5' L Vλ 1	GGTCCTGGGCCCAGTCTGTGCTG
11	5' L Vλ 2	GGTCCTGGGCCCAGTCTGCCCTG
12	5' L Vλ 3	GCTCTGTGACCTCCTATGAGCTG
13	5' L Vλ 4/5	GGTCTCTCTCSCAGCYTGTGCTG
14	5' L Vλ 6	GTTCTTGGGCCAATTTTATGCTG
15	5' L Vλ 7	GGTCCAATTCYCAGGCTGTGGTG
16	5' L Vλ 8	GAGTGGATTCTCAGACTGTGGTG
17	3' Cλ	CACCAGTGTGGCCTTGTTGGCTTG
	Variable Heavy PCR	
18	5' AgeI VH 1/5/7	CTGCAACCGGTGTACATTCCGAGGTGCAGCTGGTGCAG
19	5' AgeI VH 3	CTGCAACCGGTGTACATTCTGAGGTGCAGCTGGTGGAG
20	5' AgeI VH 4	CTGCAACCGGTGTACATTCCCAGGTGCAGCTGCAGGAG
21	5' AgeI VH 3-23	CTGCAACCGGTGTACATTCTGAGGTGCAGCTGTTGGAG
22	5' AgeI VH 4-34	CTGCAACCGGTGTACATTCCCAGGTGCAGCTACAGCAGTG
23	5' AgeI VH 1—18	CTGCAACCGGTGTACATTCCCAGGTTCAGCTGGTGCAG
24	5' AgeI VH 1—24	CTGCAACCGGTGTACATTCCCAGGTCCAGCTGGTACAG
25	5' AgeI VH 3—9/30/33	CTGCAACCGGTGTACATTCTGAAGTGCAGCTGGTGGAG
26	5' AgeI VH 6—1	CTGCAACCGGTGTACATTCCCAGGTACAGCTGCAGCAG
27	5′ AgeI VH 4—39	CTGCAACCGGTGTACATTCCCAGCTGCAGCTGCAGGAG
28	5′ AgeI VH 3—33	CTGCAACCGGTGTACATTCTCAGGTGCAGCTGGTGGAG
29	3' SalI JH 1/2/4/5	TGCGAAGTCGACGCTGAGGAGACGGTGACCAG
30	3' SalI JH 3	TGCGAAGTCGACGCTGAAGAGACGGTGACCATTG
31	3' SalI JH 6	TGCGAAGTCGACGCTGAGGAGACGGTGACCGTG
	Variable Kappa PCR	
32	5' Pan Vκ	ATGACCCAGWCTCCABYCWCCCTG
33	3' Cκ 494-516	GTGCTGTCCTTGCTGTCCTGCT
34	5' AgeI Vκ 1-5	CTGCAACCGGTGTACATTCTGACATCCAGATGACCCAGTC
35	5' AgeI Vκ 1-9/1-13	TTGTGCTGCAACCGGTGTACATTCAGACATCCAGTTGACCCAGTCT
36	5' AgeI Vκ 1D-43/1-8	CTGCAACCGGTGTACATTGTGCCATCCGGATGACCCAGTC
37	5' AgeI Vκ 2-24	CTGCAACCGGTGTACATGGGGATATTGTGATGACCCAGAC
38	5' AgeI Vκ 2-28/2-30	CTGCAACCGGTGTACATGGGGATATTGTGATGACTCAGTC
39	5' AgeI Vκ 3-11/3D-11	TTGTGCTGCAACCGGTGTACATTCAGAAATTGTGTTGACACAGTC
40	5' AgeI Vκ 3-15/3D-15	CTGCAACCGGTGTACATTCAGAAATAGTGATGACGCAGTC
41	5' AgeI Vκ 3-20/3D-20	TTGTGCTGCAACCGGTGTACATTCAGAAATTGTGTTGACGCAGTCT
42	5' AgeI Vκ 4-1	CTGCAACCGGTGTACATTCGGACATCGTGATGACCCAGTC
43	3' BsiWI Jκ 1/2/4	GCCACCGTACGTTTGATYTCCACCTTGGTC
44	3' BsiWI Jκ 3	GCCACCGTACGTTTGATATCCACTTTGGTC
45	3' BsiWI Jκ 5	GCCACCGTACGTTTAATCTCCAGTCGTGTC
46	3' BsiWI Jκ 1 50/3	GCCACCGTACGTCTGATTTCCACCTTGGTC
	Variable Lambda PCR	
47	5' AgeI Vλ 1	CTGCTACCGGTTCCTGGGCCCAGTCTGTGCTGACKCAG
48	5' AgeI Vλ 2	CTGCTACCGGTTCCTGGGCCCAGTCTGCCCTGACTCAG
49	5' AgeI Vλ 3	CTGCTACCGGTTCTGTGACCTCCTATGAGCTGACWCAG
50	5' AgeI Vλ 4/5	CTGCTACCGGTTCTCTCTCSCAGCYTGTGCTGACTCA
51	5' AgeI Vλ 6	CTGCTACCGGTTCTTGGGCCAATTTTATGCTGACTCAG
52	5' AgeI Vλ 7/8	CTGCTACCGGTTCCAATTCYCAGRCTGTGGTGACYCAG
53	3' XhoI Cλ	CTCCTCACTCGAGGGYGGGAACAGAGTG
54	5′Ab sense	GCTTCGTTAGAACGCGGCTAC

BOX 1

One-Step RT-PCR

Materials

Filtered tips (20, 200 and 1000 µl)
P20, P200 and P1000 pipettes used only for PCR
Qiagen one-step RT-PCR kit (Cat No. 210212), enough for 204 reactions
Compatible domed caps (we use Biorad TCS1201 caps for Biorad HSP-9641 plates)
Forward primer mix (7 µM each), 14 primers, No. 1-4, 6-8, 10-16
Reverse primer mix (10 µM each), 3 primers, No. 5,9,17

Master mix	1x (in µl)
H2O	6.5
5x One step RT-PCR buffer	5
Forward primer mix	1
Reverse primers mix	1
dNTP mix (10 mM each)	1
One step RT PCR enzyme mix	0.5
	15

1) Perform PCR inside thoroughly cleaned hood. RnaseZap may be used to avoid Rnase contamination
2) Prepare master mix for required number of reactions, with all reagents except enzyme mix
3) Store master mix on ice
4) Take out plate from -80 °C freezer and clean the surface with tissue
5) Quick spin the plate if needed
6) When everything is ready, add enzyme to the master mix and pipete up and down
7) Add 15 µl of master mix to each well using separate tips for each well
8) Quick spin the plate and run PCR program

PCR Program

Step 1	50 °C , 30 min	Reverse transcription
Step 2	95 °C , 15 min	Deactivate reverse transcription and activate thermal Taq
Step 3	94 °C , 30 s	
Step 4	58 °C , 30 s	
Step 5	72 °C , 1 min	
Step 6	Repeat steps 3-6, 49 cycles	
Step 7	72 °C , 10 min	Final elongation
Step 8	Cool to 4 °C	

9) Store the plate after PCR at -20 °C

BOX 2

NESTED PCR

Materials

Filtered tips

Hot Star Taq Polymerase (Qiagen 203203)

Thin walled non-skirted 96-well PCR plate (Starlab)

Heavy chain primers:

Forward primer mix (10 µM each), 11 primers, No. 18-28

Reverse primer mix (10 µM each), 3 primers, No. 29-31

Kappa Chain primers:

Forward primer mix (10 µM each), 9 primers, No. 34-42

Reverse primer mix (10 µM each), 4 primers, No. 43-46

Lambda Chain primers:

Forward primer mix (10 µM each), 6 primers, No. 47-52

Reverse primer mix (10 µM each), 1 primer, No. 53

Perform Heavy chain PCR first, and perform light chain PCR only for those wells which are positive for heavy chain

Prepare master mix for required number of reactions, with all reagents except enzyme mix

Master mix	1x (in µl)
H2O	30.25
10x Hot Star Taq buffer	4
Forward primer mix	1
Reverse primers mix	1
dNTP mix (10 mM each)	0.5
Hot star Taq polymerase	0.25
	37

Prepare master mix and thaw the RT-PCR plate

Add enzyme to the master mix and pipette 37 µl to each well

Transfer 3 µl DNA from RT-PCR plate to the nested PCR mix

Quick spin the plate and run PCR

PCR Program

95 ^{o}C , 15 min	Hot Start
94 ^{o}C , 30 s	
58 ^{o}C , 30 s	
72 ^{o}C , 45 s	
Repeat steps 3-6, 49 cycles	
72 ^{o}C , 10 min	Final elongation
Cool to 4 ^{o}C	

Run 5 µl PCR product on 1% agarose gel, 1x TAE buffer for analysis

Run total product on gel, extract and purify for the paired heavy and light chains

2.5.3.2 Digestion

Heavy chain inserts (30 µl) were digested with AgeI-HF (2.5 U) and SalI-HF (20 U) enzymes (New England Biolabs) in 40 µl final volumes for 3-4 h incubation at 37 ºC. Similarly, kappa and lambda inserts were digested with AgeI-HF (2.5 U) and BSiWI (5 U) and, AgeI-HF (2.5 U) and XhoI (10 U) enzymes respectively. The inserts were then purified using QIAquick PCR purification kit and eluted in 40 µl elution buffer.

2.5.3.3 Ligation

The insert DNA for heavy, kappa and lambda were ligated with the Igγ, Igκ and Igλ expression vectors (NCBI GenBank accession numbers FJ475055, FJ475056 and FJ517647) respectively containing a CMV promoter for transcription, murine Ig signal peptide, respective constant regions, SV40 polyadenylation sequence and ampicillin resistance gene (Smith et al. 2009). The vectors were prepared by digesting with the same restriction enzymes as for the isolation of inserts, and dephosphorylated to avoid self ligation. Insert and vector were ligated in 3:1 molar ratio using 1 µl T4 DNA ligase enzyme (NEB) in a total volume of 20 µl and incubating in RT for 2-3 hours.

2.5.3.4 Transformation and minipreps

Five µl of ligation mix and 200 µl competent MC1061 (*E. Coli* strain, made competent with $CaCl_2$ treatment) cells were incubated together on ice for 40 min followed by heat shock treatment of 2 min at 45 ºC and immediately placed back on ice. Together with 1 ml Luria-Bertani broth (LB) medium transformed bacteria were incubated for 1 hour at 37 ºC in a rotary shaker at 230 rpm. Then, 200 µl was plated on LB-agar plates containing 100 µg/ml ampicillin. The plates were incubated in 37 ºC for 16 hours. For each plasmid, three colonies were picked and grown separately in 13 ml LB medium with

100 µg/ml ampicillin. Cells were pelleted by centrifuging tubes for 40 min at 800*g* at 4 ºC and processed following the protocol outlined in the QIAprep Spin Miniprep Kit (QIAGEN), and resuspended in 50 µl of the kit elution buffer.

For analysis (optional), 2 µl of each miniprep was digested with 10 U each of restriction enzymes HindIII and EcoRI in a total volume of 20 µl. The characteristic insert fragments for heavy, lambda and kappa chain were observed on 0.7% agarose gel at approximately 1446, 744 and 884 bp respectively. The purity and concentration of the miniprep DNA product was assessed using a Nanodrop ND-1000 Spectrophotometer (Wilmington, DE, USA). Concentration was found to be between 200 and 600 ng/µl and purity was acceptable.

2.5.3.5 Transfection of 293T cells

The transfection protocol was optimized by using different ratios of linear Polyethylenimine (PEI, Sigma) and pCDNA3.1/- containing eGFP insert (homemade). Plasmid DNAs encoding heavy chain and light chain in 100 µl each (both prepared in DMEM without additives) were mixed, incubated 15 min at RT with titrated PEI, and then added to 293T cells (5.10^4 /500 µl) which were prepared in a 24-well plate, a day prior to transfection. 293T cells are modified human embryonic kidney (HEK) cells that contain SV40 T-antigen, which allows amplification of transfected plasmids containing SV40 origin of replication. Cells were incubated for 4 days in 37 ºC, 5% CO_2 incubator. The viability of cells and high GFP expression were observed when 30 µg/ml linear PEI with 0.5 µg DNA and 60 µg/ml linear PEI with 0.25 µg DNA were used. No difference was observed in expression when medium was exchanged with Ultra-chicken hamster ovary (CHO) serum free medium on day 1.

Two heavy and two light chains were paired and four transfections were done per antibody clone. One µl of each heavy and light minipreps with 60 µg/ml linear PEI were used per transfection. On day 4, supernatant was collected and stored at 4 ºC and used for antibody analysis. In-house known control monoclonal antibodies were used as positive controls.

2.6 Optimization of sorting protocol and antibody cloning

2.6.1 Transmembrane domain antibody recombinants and staining with HA

Primers were designed spanning the transmembrane region of human IgG1 (GenBank X52847.1) (Kinoshita, Shimizu, and Honjo 1991) with unique restriction sites SmaI and HindIII for cloning into the Abvec heavy chain vector (GenBank accession number FJ475055). This pair of unique enzyme sites allow the accurate insertion of the membrane spanning region of the membrane bound form of human IgG1 into the cDNA encoding the secreted form. IgG stained plasmablasts (20 cells) were bulk sorted and RT PCR was performed using the primers 5'(SmaI/IgG1)GCCCCCATCCCGGGATGAGCTG and 3'(HindIII/TMIgG1)ATGGTCAAGCTTACTAGGCCCCCTGTCCGATCATG (Sigma) and using the protocol described for the nested PCR above. A PCR product of approx. 500 bp was extracted from the gel, purified and digested with SmaI and HindIII enzymes (NEB). The PCR insert was then ligated to the desired antibody heavy chain vector which was also previously digested with same enzymes and phosphatase treated. The resulting vector encoding the authentic transmembrane form of human IgG1 was confirmed by sequencing and will be referred to as "TM-Heavy" vector. 293T cells were co-transfected with recombinant TM-Heavy vector encoding a desired variable sequence and a paired light chain. After 2-3 days incubation, the cells were stained with biotinylated HA (10 -

20 µg/ml) and extravidin-PE (Sigma, #E4011) and detected on flowcytometry. Staining of TM-IgG on cell surface was confirmed with labelled anti-IgG1, and mimics the staining of plasmablasts.

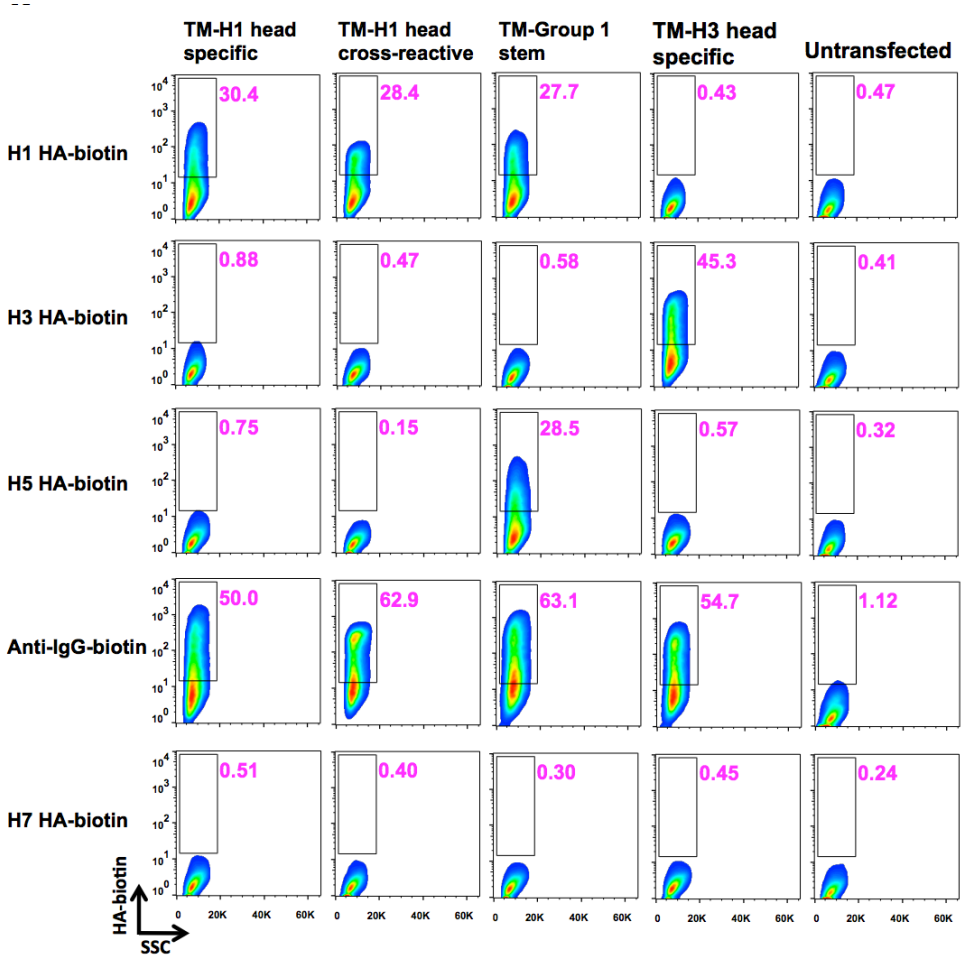

Figure 2. 3 ***Proof of principle for direct staining of plasmablast B cells shown by binding of recombinant HA to transmembrane expressed IgG on 293T cell.*** *Staining of 293T cells transfected with TMIgG1 with soluble HAs. The percentage of positive cells is shown in the pink boxes.TM: Trans-membrane.*

As shown in figure 2.3, all cells expressing antibodies (TMIgG1) on the surface were stained with anti-IgG biotin reagent irrespective of their specificity (row 4). These cells were stained with different biotin conjugated recombinant haemagglutinin (HA) proteins. The proteins used were H1pdm09 (A/England/195/2009), H3 (A/Victoria/361/2011), H5

(A/Vietnam/1203/2004) and H7 (A/Anhui/1/2013). In row 1, recombinant H1 HA stained cells expressing TMIgG1 to epitopes in the H1 HA head and stem but not TMIgG1 to H3 HA head. Similarly, H3 HA specifically stained TM-H3 head IgG expressing cells (row 2). H5 HA only stained TM-stem IgG (cross-reactive) (row 3). None of these antibodies expressed on the cell surface were stained by H7 HA because they are not cross-reactive to this haemagglutinin (row 5). This shows that staining by this method with soluble HA was specific, and suggested that this could be used to stain plasmablasts.

Indirect labelling of cells expressing TMIgG1, by a sandwich method, with a first layer of unlabelled HA protein antigen and then by a specific monoclonal antibody to a different site with a biotin label for detection was also developed. This method was applied to stain plasmablasts with unlabelled antigen protein. This method was applied particularly to staining with the soluble Ebola GP and is described in Chapter 6 figure 6.1.

2.6.2 Antigen specific sorting of plasmablasts

In addition to the staining protocol described in section 2.5.2, cells were pre-stained with biotinylated antigen, for example haemagglutinin H1 or H3 at 20 μg/ml for 1 h to stain B-cell receptors on the surface of plasmablasts. Extravidin-PE (Sigma) was used to detect the biotin.

In case of PBMC from Ebola vaccinated donors, the sandwich method of antigen specific staining was applied (Chapter 6 Figure 6.1). PBMC were stained with a first layer of unlabeled glycoprotein and then with characterised biotinylated GP-specific monoclonal antibody. This method can be applied to any antigen specific sorting where a defined monoclonal antibody is available.

2.6.3 Gibson Cloning and the 96-well system

To improve the efficiency of assembly of antibody cDNAs and increase the numbers of clones that can be processed at one time we developed Gibson cloning in a 96 well platform, instead of the individual assembly reactions described above. Gibson assembly (Gibson et al. 2009) offers digestion free cloning in a one-step isothermal reaction via assembly of DNA sequences overlapping at their end sequences (20-40 nucleotides). This involves three steps of i) exonuclease activity which chews back 5' DNA forming a region of single strand ready to anneal, ii) filling in by DNA polymerase and iii) ligation by DNA ligase. This reaction requires a 20-40 base pair overlap between adjacent DNA fragments. Primers in table 2.3 were designed by Alain Townsend to make primers compatible with Gibson assembly in the vectors described above. Overlapping bases were added on to existing 5' and 3' primers without interfering with the restriction sites, which could be used as a back up. Some of the primers need optimization as they fail to give a product compared to the traditional shorter primers.

PCR reactions were done as described in section 2.5.3.1. PCR products were purified in a Qiagen 96-well system and the inserts were assembled with cut plasmid in the Gibson mix from NEB. Gibson mix can also be made much more cheaply by following the online protocol from Cooper's lab (Cooper-lab 2013). Two µl of assembled product was used to transform 10 µl highly competent DH5α *E Coli* (NEB) in 96-well plates. Three colonies for each heavy and light chain were grown in a 96-well format and purified using Qiagen Turbo 96 miniprep kit with the manufacturer's protocol. Plasmids were eluted using 100 µl TE buffer. Transfection of 293T cells and immunofluorescence screening assays were also performed in a 96-well tissue culture plate.

Transfection in a 96-well plate: Optimal transfection was obtained using 0.5 µg DNA and 120 µg/ml PEI mixed in 25 µl volume of each and added to 200 µl of 293T cells in D10 (seeded as 3.10^4 cells/well a day before). The miniprep concentration of plasmid, from the Qiagen 96 miniprep kit was 50-100 ng/µl. Nine transfections were done for each antibody using three heavy and three light plasmids. Twelve microliter (~600 ng) heavy and light plasmids were diluted in a U-bottomed 96-well plate in 75 µl D0. From the dilutions, 25 µl of heavy and light plasmids (~200 ng each) were mixed in another 96-well plate and 50 µl PEI (pre-diluted to 120 µg/ml in D0) was added slowly. After 15 min incubation at RT on a shaker, a total 100 µl was added to 293T cells. Cells were incubated for 4-5 days after which supernatants were transferred to a U-bottomed 96-well plate and 50 µl aliquots were used for binding screening assays on monolayers of transduced MDCK-SIAT1 cells expressing the HA or GP of interest.

Table 2. 3 Gibson reaction compatible Nested PCR primers

#	Oligo Name	Sequence 5' to 3'
	Variable Heavy PCR	
18	5' AgeI VH 1/5/7 TAP	CCTTTTTCTAGTAGCAACTGCAACCGGTGTACATTCCGAGGTGCAGCTGGTGCAG
19	5' AgeI VH 3 TAP	CCTTTTTCTAGTAGCAACTGCAACCGGTGTACATTCTGAGGTGCAGCTGGTGGAG
20	5' AgeI VH 4 TAP	CCTTTTTCTAGTAGCAACTGCAACCGGTGTACATTCCCAGGTGCAGCTGCAGGAG
21	5' AgeI VH 3-23 TAP	CCTTTTTCTAGTAGCAACTGCAACCGGTGTACATTCTGAGGTGCAGCTGTTGGAG
22	5' AgeI VH 4-34 TAP	CCTTTTTCTAGTAGCAACTGCAACCGGTGTACATTCCCAGGTGCAGCTACAGCAGTG
23	5' AgeI VH 1—18 TAP	CCTTTTTCTAGTAGCAACTGCAACCGGTGTACATTCCCAGGTTCAGCTGGTGCAG
24	5' AgeI VH 1—24 TAP	CCTTTTTCTAGTAGCAACTGCAACCGGTGTACATTCCCAGGTCCAGCTGGTACAG
25	5' AgeI VH 3—9/30/33 TAP	CCTTTTTCTAGTAGCAACTGCAACCGGTGTACATTCTGAAGTGCAGCTGGTGGAG
26	5' AgeI VH 6—1 TAP	CCTTTTTCTAGTAGCAACTGCAACCGGTGTACATTCCCAGGTACAGCTGCAGCAG
27	5′ AgeI VH 4—39 TAP	CCTTTTTCTAGTAGCAACTGCAACCGGTGTACATTCCCAGCTGCAGCTGCAGGAG
28	5′ AgeI VH 3—33 TAP	CCTTTTTCTAGTAGCAACTGCAACCGGTGTACATTCTCAGGTGCAGCTGGTGGAG
29	3' SalI JH 1/2/4/5 TAP	GGGGAAGACCGATGGGCCCTTGGTCGACGCTGAGGAGACGGTGACCAG
30	3' SalI JH 3 TAP	GGGGAAGACCGATGGGCCCTTGGTCGACGCTGAAGAGACGGTGACCATTG
31	3' SalI JH 6 TAP	GGGGAAGACCGATGGGCCCTTGGTCGACGCTGAGGAGACGGTGACCGTG
	Variable Kappa PCR	
34	5' AgeI Vk 1-5 TAP	CCTTTTTCTAGTAGCAACTGCAACCGGTGTACATTCTGACATCCAGATGACCCAGTC
35	5' AgeI Vk 1-9/1-13 TAP	CCTTTTTCTAGTAGCAACTGCAACCGGTGTACATTCAGACATCCAGTTGACCCAGTCT
36	5' AgeI Vk 1D-43/1-8 TAP	CCTTTTTCTAGTAGCAACTGCAACCGGTGTACATTGTGCCATCCGGATGACCCAGTC
37	5' AgeI Vk 2-24 TAP	CCTTTTTCTAGTAGCAACTGCAACCGGTGTACATGGGGATATTGTGATGACCCAGAC
38	5' AgeI Vk 2-28/2-30 TAP	CCTTTTTCTAGTAGCAACTGCAACCGGTGTACATGGGGATATTGTGATGACTCAGTC
39	5' AgeI Vk 3-11/3D-11TAP	CCTTTTTCTAGTAGCAACTGCAACCGGTGTACATTCAGAAATTGTGTTGACACAGTC
40	5' AgeI Vk 3-15/3D-15 TAP	CCTTTTTCTAGTAGCAACTGCAACCGGTGTACATTCAGAAATAGTGATGACGCAGTC
41	5' AgeI Vk 3-20/3D-20 TAP	CCTTTTTCTAGTAGCAACTGCAACCGGTGTACATTCAGAAATTGTGTTGACGCAGTCT
42	5' AgeI Vk 4-1 TAP	CCTTTTTCTAGTAGCAACTGCAACCGGTGTACATTCGGACATCGTGATGACCCAGTC
43	3' BsIW1 Jk 1/2/4 TAP	GATGAAGACAGATGGTGCAGCCACCGTACGTTTGATYTCCACCTTGGTC
44	3' BsIW1 Jk 3 TAP	GATGAAGACAGATGGTGCAGCCACCGTACGTTTGATATCCACTTTGGTC
45	3' BsIW1 Jk 5 TAP	GATGAAGACAGATGGTGCAGCCACCGTACGTTTAATCTCCAGTCGTGTC
46	3' BsIW1 Jk 1 50/3 TAP	GATGAAGACAGATGGTGCAGCCACCGTACGTCTGATTTCCACCTTGGTC
	Variable Lambda PCR	
47	5' AgeIλV1	CCTTTTTCTAGTAGCAACTGCAACCGGTTCCTGGGCCCAGTCTGTGCTGACKCAG
48	5' AgeIλV2	CCTTTTTCTAGTAGCAACTGCAACCGGTCCTGGGCCCAGTCTGCCCTGACTCAG
49	5' AgeIλV3 TAP	CCTTTTTCTAGTAGCAACTGCAACCGGTTCTGTGACCTCCTATGAGCTGACWCAG
50	5' AgeIλV4/5 TAP	CCTTTTTCTAGTAGCAACTGCAACCGGTTCTCTCTCSCAGCYTGTGCTGACTCA
51	5' AgeIλV6 TAP	CCTTTTTCTAGTAGCAACTGCAACCGGTCTTGGGCCAATTTTATGCTGACTCAG
52	5' AgeIλV7/8 TAP	CCTTTTTCTAGTAGCAACTGCAACCGGTTCCAATTCYCAGRCTGTGGTGACYCAG
53	3'Xho CL TAP	CCTTGTTGGCTTGAAGCTCCTCACTCGAGGGYGGGAACAGAGTG

2.7 Expression and Purification of antibodies

Antibodies were expressed by transfection of 293T cells (ten 175 cc flasks). Per flask, 12-25 μg of each heavy and light plasmids in 10 ml medium with 120 μg/ml linear PEI in 10 ml medium, mixed and incubated for 20 min were added to cells in 50 ml D10. Cells were incubated for 3-4 days without medium exchange. Supernatant was harvested, filtered with 0.45 μM filter (Nalgene), pH adjusted to 8 by addition of 1 M Tris pH 8 to 10 mM and passed through the protein A sepharose (Sigma) in Biorad columns. The column was washed with TBS buffer and elution done with pH 2.5-3 citrate buffer (see

Table 2.1 for preparation). Eluted fractions were neutralised by adding 1 M Tris pH 8 and absorbance was read using Nanodrop at 280 nm. Pooled fractions were desalted over desalting sepharose G10 columns (GE Healthcare), filtered and stored at -80 °C. Antibody was found to be stable for 3-4 years even at 4 °C.

We obtained 5-10 mg of antibody from 700 ml culture by using the above mentioned cells and protocol. We are planning to optimise the antibody expression by using ExpiCHO cells and transfection protocols from Life Technologies which are claimed to produce 1 to 3 mg/ml GMP grade human IgG.

2.8 Screening and characterising monoclonal antibodies

Antibody supernatants were screened for binding to the antigen (HA, NA or Ebola GP) by immunofluorescence assays. MDCK-SIAT1 cells with stable surface expression of the relevant protein or transfected 293T cells were used for immunofluorescence assays. After establishing positive binding antibody was tested in functional assays such as micro-neutralisation assays (HA and EBOV GP antibodies), enzyme inhibition assays (NA antibodies) and *in vivo* protection.

2.9 Immunofluorescence Assay (IFA)

Immunofluorescence assay was used to screen the binding of antibodies in culture supernatant to a desired glycoprotein. A 96-well plate was coated overnight with stable transduced Madin-Darbey Canine Kidney-sialyltransferase (MDCK-SIAT1) cells (3.10^4 cells/well) expressing antigen (HA or Ebola-GP) on their surface. Next day, the cell supernatant was removed and 50 µl antibody supernatant was added and incubated for 1-2 hr at 4 ^{o}C. The plate was washed with wash buffer (PBS/0.02% Azide), 50 µl second antibody goat anti human IgG FITC conjugate (1:160) (Life Technologies, #62-8411)

was added, incubated for 1-2 hours at 4 ºC and again washed with cold wash buffer. Finally, the cells were fixed with 100 µl cold FACS FIX (PBS/0.1% BSA/4% formaldehyde) and observed under the fluorescence microscope (Zeiss). Fluorescence was also quantified in a Clariostar platereader (BMG Labtech).

2.10 Haemagglutination inhibition (HI) assay

In a 96-well round bottomed plate , 25 µl of antibody supernatant with desired dilutions were prepared. Then, 25 µl of virus (2-4 HAU) were added and incubated by shaking for 1 hour at room temperature. Meanwhile, human red blood cells (RBCs) were washed in PBS and diluted 1:2 and adjusted to OD_{600} 1.8±0.5 (equivalent to 1% vol/vol). After incubation 50 µl of RBC was added to the wells and incubated in at RT for 1 hour. Virus back titration was performed, principally before doing the HI assay, to confirm the haemagglutination of RBC by virus titre 2-4 HAU.

The plate was tilted to observe the tear drops formed by RBC due to lack of inhibition of haemagglutination by neutralising activity of the antibody. HI titre was determined to be the highest antibody dilution at which there was haemagglutination inhibition defined as loss of tear drop formation.

2.11 Enzyme Linked Immunosorbent Assay (ELISA)

A 96-well plate (Nunc, ELISA plate) was coated with recombinant HA at 20 µg/ml in PBS by incubating for 2 hours in room temperature. Antigen was removed, washed with PBS and the plates were blocked with 300 µl blocking buffer (5% milk/0.02% azide). Blocking was done for 2 hours to overnight at 4 °C. The plate was washed and serial dilutions of antibody in 50 µl were added to the plate. After incubation for 1-2 hours at room temperature, the antibody was removed and plate washed. Rabbit-anti-human HRP

conjugate antibody (Dako, #P0214) (diluted 1:1600) was added in 50 µl/well and incubated for 1-2 hours in room temperature. Antibody was removed and the plate was washed and then developed with 50 µl TMB solution (Roche) for 5-15 min. The reaction was stopped by adding 50 µl of 1M H_2SO_4. Absorbance was read in Clariostar platereader (BMG Labtech) at 450 nm.

2.12 ELISA based micro-neutralisation (MN) assay using reassortant or wild type influenza viruses

The MN assay was based on the technique of Rowe T et al 1999 (Rowe et al. 1999), with the fixation and staining procedure of Matrosovich M et al 2006 (Matrosovich et al. 2006), using the MDCK SIAT-1 cell line described by Matrosovich M et al, 2003 (Matrosovich et al. 2003). The viruses used for cell infection are wild type viruses (Crick Institute), reassortant viruses (NIBSC) or in-house pseudotyped viruses.

Dilutions of antibodies and virus were made in virus growth medium, VGM (DMEM/0.1% BSA/10 mM Hepes). Two-fold dilutions of antibodies or sera was performed in a 96-well plate in 50 µl volume. And 50 µl of virus titrated to give plateau infection (normally 2-4 HAU for influenza viruses) was added to the antibody dilution. The plate was incubated at 37 ^{o}C for 2 hours. Virus only and medium only controls for maximum and minimum signal occupied 8 wells each. After incubation, 3.10^4 /100 µl MDCK-SIAT1 cells diluted in VGM were added per well. These cells highly express α2,6-SA and are superior to conventional MDCK cells in propagating influenza viruses (Oh et al. 2008). The plate was then incubated overnight at 37 ^{o}C, 5% CO_2 incubator.

Next day, the supernatant was removed and the cells were fixed with 100 µl of 10% formalin in PBS by incubating at least for 30 min at 4 ^{o}C. Cells were washed with PBS/

20 mM glycine (to block formalin) and incubated with 50 µl permeabilization buffer (PBS/ 20 mM glycine/ 0.5% Triton) for 20 min at RT. Cells were then washed with PBS and 50 µl mouse anti-nucleoprotein antibody to influenza A (Abcam, clone AA5H, 0.3 µg/ml) was added. After incubation for 1-2 hours at 4 °C, the cells were washed, 50 µl goat anti-mouse (GAM) HRP conjugated antibody (diluted 1:800) (Dako, #P0447) was added and incubated for 1-2 hours at 4°C. After thorough washing, the plate was developed with 50 µl TMB substrate (Roche) for 5 min and absorbance was measured at 450 nm.

Replication based MN assay for some wild type viruses: Some wild type viruses (recent clade 6B H1N1) gave high background NP staining. To overcome this, the method was slightly modified by incubating antibody or sera with 100 $TCID_{50}$ virus and adding them to cell monolayer plated the day before. TPCK-Trypsin (1 µg/ml) (Sigma) was added to allow virus replication. After incubation for 48 hours at 37 °C, nucleoprotein staining was done as described above.

2.13 EGFP based micro-neutralisation assay using pseudotyped viruses

The setup of the assay is similar to the one described above; the only differences being antibody dilution and reading of the assay. Antibody dilution was done in PBS and virus and cells were diluted in VGM. It was found that having 25% PBS increased the infection of the cells by S-FLU pseudotyped viruses by 1.5 – 2 fold. The reason behind this is unclear. Instead of NP-ELISA, eGFP fluorescence was observed under the microscope and read by the Clariostar platereader. Blockade of eGFP expression was used as an indication of neutralisation. A neutralising antibody inhibits the cell infection and thus also the fluorescence. Maximum eGFP fluorescence is seen for the virus only control and the negative controls were uninfected cells.

MN for H3 antibodies using S-FLU pseudotyped viruses is vital since egg based viruses gain spurious egg adaptation mutations that can alter antibody binding sites and thus give misleading results. The H3 protein coating S-FLU is fixed in sequence from the transduced MDCK cells in which the S-FLU is grown, thus avoiding egg and tissue culture adaptation mutations. H3N2 viruses passaged in MDCK-SIAT1 cells are known to have less adaptation mutations compared to egg, VERO or MDCK cells (McWhite, Meyer, and Wilke 2016) . Thus, using MDCK-SIAT1 cells for selection of escape mutants with antibodies (discussed in section 2.16) is also important.

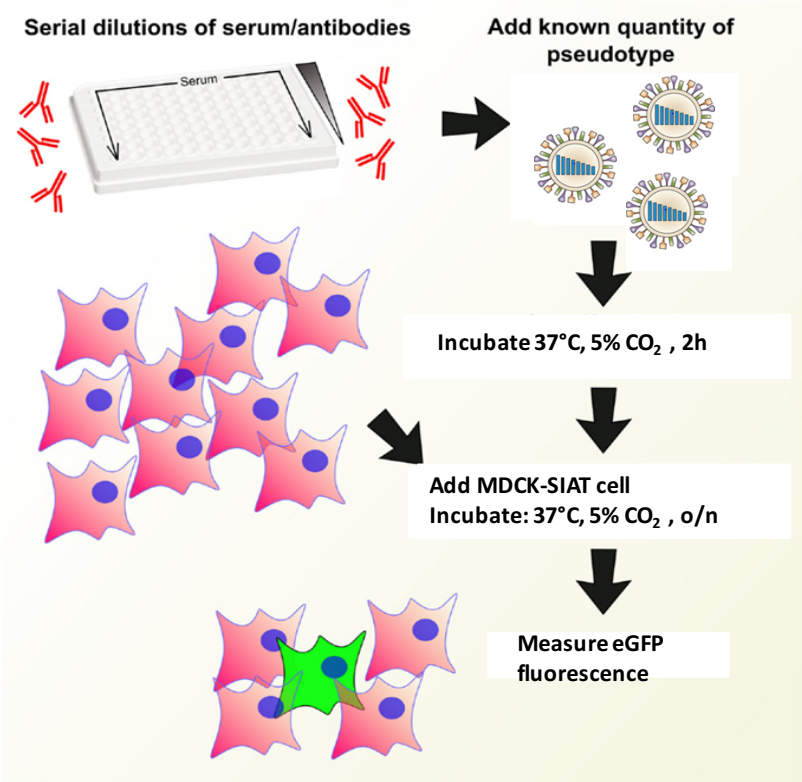

Figure 2. 4 ***Micro neutralisation assay.*** *Figure adapted from (Carnell et al. 2015).*

2.14 Enzyme linked lectin assay (ELLA)

ELLA assay was adapted from the methods described by Schulman et al. (Schulman, Khakpour, and Kilbourne 1968) and Sandbulte et al. (Sandbulte et al. 2009). This assay

detects the inhibition of neuraminidase enzymatic activity on sialic acid by neuraminidase antibodies. The schematic diagram of the assay is shown in figure 2.4. Viruses or recombinant neuraminidase proteins were used as the source of neuraminidase. Virus growth medium was used to dilute antibodies and viruses. A NUNC plate was plated overnight with 25 µg/ml fetuin (Sigma, #F3385). Two-fold serial dilutions of sera or monoclonal antibodies performed in duplicates were incubated together with a fixed amount of titrated neuraminidase source. Column 11 of a plate was used for NA source only control, and column 12 was used for medium only control. After 2 h incubation, antibody/NA mix were transferred to the PBS washed fetuin plate and incubated for 18-20 h at 37 ºC buffered by CO_2 as for tissue culture. Next day, the contents of the plate were discarded and the plate washed with PBS. HRP conjugated peanut agglutinin (PNA-HRP, Sigma, #L7759) at 1 µg/ml was added to the wells. PNA binds to the exposed galactose after cleavage of sialic acid by neuraminidase. After 1 h incubation and PBS wash, signal was developed by adding OPD (o-Phenylenediamine Dichydrochloride) solution (Sigma, #P9187) and the reaction stopped after 5-15 min using 1 M H2SO4. Absorbance was read at 492 nm in a Clariostar platereader (BMG Labtech).

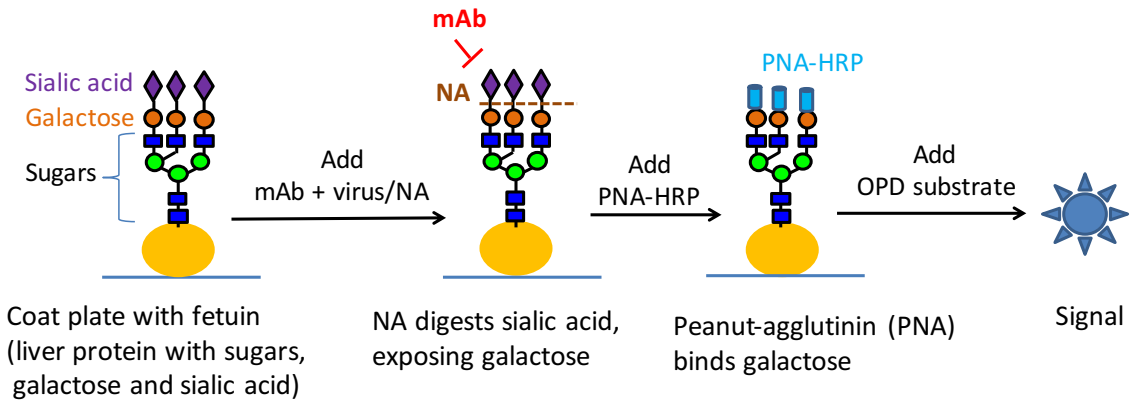

Figure 2. 5 ***Enzyme linked lectin assay (ELLA) for measuring neuraminidase activity and inhibition by antibodies.*** *Antibody and neuraminidase were incubated together*

before adding to the NUNC plate coated with fetuin. Next day, the catalytic activity of NA and inhibition by antibody were read using PNA-HRP which binds to the galactose exposed after removal of sialic acid.

2.15 Antibody cross-inhibition binding of the antigen for epitope mapping

Competition ELISA or IFA was performed to find out if a known/reference antibody with a defined binding site is blocked by the testing antibody and vice versa.

Antibody was biotinylated using EZ-link Sulfo-NHS-LC-biotin (Life Technologies, #21327). Biotinylated reference antibody and competing mAb (in 10-fold excess over biotin-mAb) were mixed, and transferred to an antigen coated plate for competition binding. A monolayer of MDCK-SIAT1 cells expressing antigen or purified antigen bound to plastic were used. As secondary Extravidin-FITC (diluted 1:400) (Sigma, #E2761) or Extravidin-peroxidase (diluted 1:1600) (Sigma, #E2886) were used. When FITC was used, cells were fixed and fluorescence was measured by a Clariostar platereader (BMG Labtech). When Extravidin-peroxidase was used, signal was developed by adding OPD substrate (Sigma, #P9187) and the reaction stopped with 50 µl 1 M H_2SO_4. Mean and 90% confidence interval of eight replicate measurements were calculated. Using peroxidase on cells gave higher background than FITC.

2.16 Escape mutant virus selection by antibodies for epitope mapping

Selecting escape mutants in the presence of saturating levels of neutralising antibody is one accurate method for determining the binding epitope by identifying amino acid substitutions that prevent neutralisation. Mutation frequency in cloned virus is estimated to be approximately 10^{-5} (Yewdell, Webster, and Gerhard 1979). Therefore, we used 10^5 $TCID_{50}$ of virus per well with a concentration of neutralising antibody 5 to 10-fold higher

than the neutralising EC_{50} concentration of the antibody (normally 1 μg/ml for head antibodies and 4 μg/ml for stem antibody). From one 96-well plate we expected to get 10 or more escape clones. However, the amount of escape clones obtained was different for different antibodies. Some antibodies yielded more than expected resistant clones, and some none.

To select escape clones, a MDCK-SIAT1 cell monolayer was prepared the day before. Antibody and virus were incubated together for 1-2 hours, then diluted in VGM and added to the PBS washed cell monolayer (100 μl/well). After 1 hour incubation at 37 °C, 100 μl of VGM/trypsin (2 μg/ml) was added. Plates were incubated for 48 h at 37 °C after which the supernatants were transferred to a U-bottomed 96-well plate and the cell monolayer was fixed and stained for NP expression. Selected escape mutant viruses were recloned by limiting dilution in the presence of antibody. Finally, the virus was expanded to 3 ml – 50 ml batch for future tests and sequencing.

Only 140 μl is required for RNA extraction (Qiagen viral RNA mini kit). The protocols for RNA extraction and RT-PCR were obtained from WHO Influenza CC, the Crick Institute. PCR and sequencing of the genes were performed by Rod Daniels at the Crick Institute. In brief, primers to two halves overlapping fragments of the HA and NA genes were used to perform one step reaction of reverse transcription and DNA amplification using Superscript III one-step RT-PCR with Platinum *taq* polymerase (Invitrogen, #12574018). PCR products were observed on a gel, gel purified and sequenced.

2.17 Thermolysin Digestion of Ebola glycoprotein

Thermolysin digestion of the Ebola glycoprotein expressed on cells was performed to analyse if antibody recognises thermolysin cleaved GP. It is known that GP proteolysis

by cathepsins removes mucin-like domain and glycan cap, and is essential for binding of GP to NPC1 receptor. Thermolysin mimics cathepsins and the proteolytic activity is active at physiological pH whereas cathepsins require strongly acidic pH which is toxic to living cells (Dube et al. 2009; Bale et al. 2011).

Thermolysin (Sigma, #P1512) was dissolved in HM buffer (20 mM HEPES,130 mM NaCl and 20 mM MES and pH adjusted to 7.5). Thermolysin faintly precipitates in HM buffer. EBOV glycoprotein expressing cells were trypsinised from the flask and treated with 0.25 mg/ml thermolysin diluted in HM buffer containing 2 mM $CaCl_2$ for 1 hour at 37 ºC. Then cells were washed with PBS and passed through cell strainer as cells tend to form clumps after thermolysin treatment.

To analyse antibody binding to thermolysin treated GP, 25 μg/ml antibody was incubated with cells for 1 h. FITC conjugated anti-human IgG (Life Technologies. #62-8411) was used for binding detection in FACS. Antibody binding to untreated GP expressing cells was done in parallel for binding comparison.

2.18 Site-directed mutagenesis

Amino acid substitutions associated with virus escape can be confirmed by introducing appropriate mutations in an expressable cDNA encoding HA or GP. Agilent Quick change lightning site directed mutagenesis kit and Quick change primer design in Agilent website were used to mutate one or more nucleotides in the HA or Ebola-GP constructs.

2.19 *In vivo* protection studies

DBA/2OlaHsd mice used for protection against X179A and BALB/cOlaHsd for PR8 and X31 viruses were purchased from Envigo, UK and housed in individually vented cages in

a special unit for infectious diseases. Six mice per group were used as the minimum size group to obtain statistical significance with 5-6 survivors v nil in the control group. The dose of viruses used in prophylaxis experiments are shown in table 4. Mice were anesthetised by isofluorane (Abott) and 50 µl of virus was administrated intranasally 24 hours after the intraperitoneal administration of 10 mg/kg antibody (500 µl). Mice were under regular observation and weighed. Mice with weight loss ≥20 percent or morbid clinical scores were euthanized by rising concentration of CO_2. Antibodies were tested for therapy of influenza by treatment at 24 hrs after infection. For Ebola therapy, antibodies were tested in the Scripps BSL-4 containment facility by the group of Erica Saphire. BALB/c mice were infected with a lethal dose of mouse-adapted Ebola virus and treated with a single dose of 100 µg of antibody (approximately 5mg/kg) i.p. after 48 hrs.

Table 2. 4 List of viruses and their dose used in animal experiments.

Virus	Mice Type	TCID50 per mice	HAU per mice	~ MD50 based on (≥20% weight loss)
X179A (H1N1)	DBA/2	$1.1x\ 10^4$	0.32	150 fold
PR8 (H1N1)	BALB/C	10^4	0.128	~ 1000 fold
X31 (H3N2)	BALB/C		32-64	

2.20 Data and statistical Analysis

Graphs were generated using GraphPad Prism software (version 7) and Microsoft Excel 2010. The ELISA or MN titres were expressed as half maximal effective concentrations (EC50: midpoint between negative and plateau positive controls) derived by linear interpolation from neighbouring points in the titration curve. Statistical analysis was done by using GraphPad Prism and SPSS. *P* values of less than 0.05 were considered significant. Kaplan Maier test was done on survival curves.

2.21 Haemagglutinin sequence numbering

Sequence numbering of the H1 and H3 haemagglutinin in the thesis are based on H1 and H3 numbering system respectively, used in the annual reports by WHO Collaborating Centre for Reference and Research on Influenza, the Crick Influenza Worldwide Centre.

2.22 Study approval

This study was performed in accordance with the Declaration of Helsinki and Good Clinical Practice guidelines. Protocols and informed consent were reviewed and approved by the Oxford Tropical Research Ethics Committee and the Weatherall Institute of Molecular Medicine. Signed informed consent was obtained from each individual donor who supplied a blood sample. All animal procedures were approved by an internal University of Oxford Ethics Committee and the United Kingdom Home Office. Principle of the 3Rs were applied in designing of experiments.

CHAPTER 3 | Monoclonal antibody repertoire to haemagglutinin of H1N1/2009 in a vaccinated individual

CHAPTER 3 INTRODUCTION

Circulating influenza viruses constantly evolve via antigenic drift, which reduces vaccine effectiveness if the vaccine strain is mismatched with the circulating drifted variant. WHO Collaborating Centres located in various parts of the world collect circulating seasonal influenza strains, sequence the HA and NA genes, and analyse the antigenic relatedness of new viruses to previous ones by performing haemagglutinin inhibition (HI) assays with antisera generated in infected ferrets. Update of the vaccine strain in the annual influenza vaccine is based upon the HI data from ferret sera. Little is known about what drives antigenic drift and prediction of future drift variants is difficult.

Five immunodominant antigenic sites are defined for H1 haemagglutinin (Caton et al. 1982; Gerhard et al. 1981), and these are located on the globular head of the molecule. For the complete loss of neutralising activity of a hyper-immune serum, as many as 12 mutations at multiple positions in HA are required (Das et al. 2013), which should be a rare event, as discussed in the Chapter 1. Focusing of the antibody response on a sub-region of the haemagglutinin, favouring the selection of escape viruses with point mutations, is one of the proposed mechanisms that drives antigenic drift. This was suggested earlier by studying escape mutant virus selected by sera (Lambkin et al. 1994) and monoclonal antibodies (Natali, Oxford, and Schild 1981) from mouse, and sera from humans screened for binding to viruses with single point mutations (Haaheim 1980b) and

selective binding inhibition shown by characterized murine monoclonal Fab fragments (Wang, Skehel, and Wiley 1986).

Thomas Francis noted the power of the first exposure to influenza in humans and animals to shape subsequent antibody responses (Francis 1960). The antibody titre to the virus of first exposure remains high throughout life, and is boosted by subsequent exposures. He proposed that the second and subsequent responses are predominantly, but not exclusively, composed of antibodies cross-reactive with the virus of first exposure. He described this as 'original antigenic sin'. Since the 1960's this term has narrowed in meaning to indicate a situation where the cross reactive antibodies dominate the response but fail to neutralise, where the "sin" refers to the lower neutralising titre against the new virus.

The observation that the response to the first exposure dominates subsequent responses has been confirmed repeatedly and further elaborated by recent studies in the form of "antibody landscapes" followed over a period of years in individuals (Fonville et al. 2014), and longitudinal analysis of antibody titres in donors against viruses spanning a 20-year period (Miller et al. 2013). Cumulatively, they reported that the antibody response is increased against previously encountered viruses offering cross-reactivity to more recent viruses and this is termed 'antigenic seniority' by Lessler et al. (Lessler et al. 2012).

H1N1 pandemic virus has been undergoing continuous *genetic drift* since it first appeared in 2009 but this was not detected as *antigenic drift* by ferret sera raised to the 2009 pandemic virus. The 2009 vaccine strain was therefore maintained until now (2016). In the 2013-2014 season the H1N1pdm09 virus was observed to affect the middle-aged population (age group 45-64 years), although the overall vaccine efficacy for the season

was accounted to be 50-75% against A(H1N1)09 virus (Skowronski, Chambers, et al. 2014; European Centre for Disease Prevention and Control 2014). However, despite this rise in cases, ferret sera didn't detect any antigenic change in H1N1pdm09 viruses (The Crick Worldwide Influenza Centre 2015).

The recent clade which severely affected the middle-aged population is designated as clade 6B. In contrast to the findings with ferret antisera, Linderman et al. reported 42% of middle-aged adults (born between 1965-1979) had reduced serologic reactivity with 2013-2014 H1N1pdm09 viruses and also identified a single amino acid substitution (K163Q, H1 Numbering) to be responsible for this loss of reactivity (Linderman et al. 2014). This study was based on serological analysis and neither the clonal analysis of the antibodies from the donors, nor the selection of escape variants by sera were investigated. Other groups have also seen this amino acid substitution (K163E/Q) in escape viruses selected by occasional human monoclonal antibodies *in vitro* (Krause, Tsibane, Tumpey, Huffman, Briney, et al. 2011; Li et al. 2016).

In this chapter, we have studied the antibody repertoire to H1 haemagglutinin following vaccination in a middle-aged human donor who was exposed to the pandemic H1N1/2009 for the first time (Huang et al. 2015). Our aim was to perform a clonal analysis of the monoclonal antibody response, and ask the question whether antibodies of this kind could be responsible for antigenic drift of the pdmH1N1 virus. We isolated 157 monoclonal antibodies, of which 88% were focused on the K163 site in the head region of haemagglutinin. These head antibodies, although they recognised the A/USSR/90/1977 virus to which the donor may have been exposed in his childhood, failed to neutralise the clade 6B viruses with the characteristic K163Q substitution and/or the neighbouring S162N glycosylation. K163 lies within a patch of surface residues conserved between

A/USSR/90/1977 and the 2009 H1N1, and recently mutated in the clade 6B viruses. Resistant variants selected *in vitro* with these monoclonal antibodies introduced substitutions at position 163, exactly recapitulating the antigenic drift that had occurred in nature. Our results showed that antibodies primed in the donor's childhood to a conserved region of the molecular surface were selectively recalled in 2009 and expanded to form a focused response, which favoured the selection of antigenic drift variants with substitution at K163 and S162.

CHAPTER 3 RESULTS

3.1 Response to influenza-virus after vaccination

A healthy donor referred to as 'donor H', aged 42, was selected for isolation of monoclonal antibodies. Donor H had received trivalent vaccine in 2008 and 2009 before receiving the vaccine containing novel haemagglutinin from H1pdm09 in 2011. The vaccine antigens from these years are shown in table 3.1.

Table 3. 1 Influenza vaccination History of donor H.

Date	Vaccine Composition
11 Nov 2008	A/Brisbane/59/2007 H1N1-like virus A/Brisbane/10/2007 H3N2-like virus B/Florida/4/2006
26 Nov 2009	A/Brisbane/59/2007 H1N1-like virus A/Brisbane/10/2007 H3N2-like virus B/Brisbane/60/2008-like virus
10 Nov 2011	A/California/07/2009 H1N1-like virus A/Perth/16/2009 H3N2-like virus B/Brisbane/60/2008-like virus

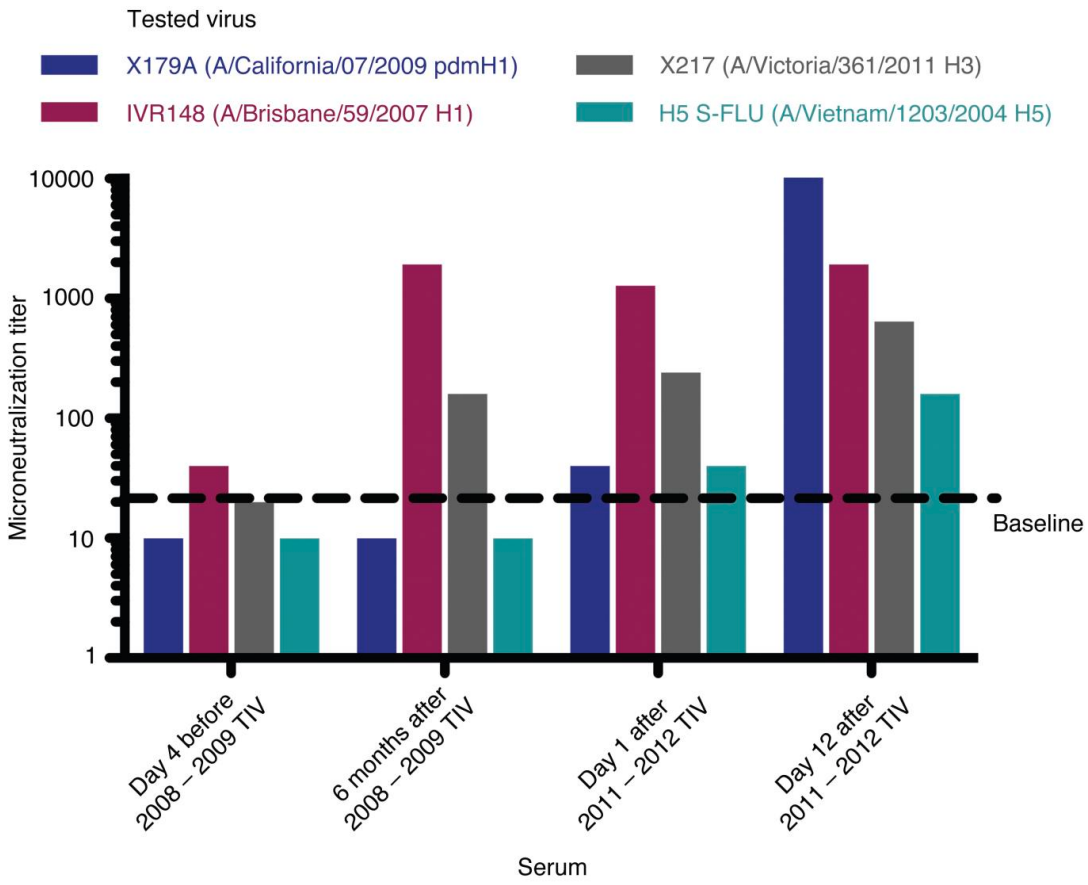

Figure 3. 1 ***The serological neutralisation titres for former seasonal H1, H3, H1pdm09, and H5-pseudotyped influenza viruses in donor H before and after trivalent seasonal influenza vaccination.*** *Donor H received the 2008–2009, 2009–2010, and 2011–2012 influenza vaccines, which contain antigens from the viruses listed in table 1. The assay was performed in duplicate and means are shown. Pseudotyped influenza viruses are more sensitive to stem antibodies than wild-type viruses. TIV: trivalent seasonal influenza.*

Neutralisation of former seasonal H1, H3, H1pdm09 and H5 viruses by serum isolated from donor H at different time points of vaccination are shown in figure 3.1. Before first vaccination in 2008, the titres to all viruses are at baseline. Six months after the first vaccination in 2008, a response is seen to former seasonal H1 (IVR148, A/Brisbane/59/2007) and H3 (A/Victoria/361/2011) which is not cross-reactive to

H1pdm09 and H5. After the third vaccination in 2011, which was the first exposure of donor H to pdmH1, a strong response to H1N1pdm09 was detected. Day 12 serum neutralisation titres revealed a low-level cross-reactivity to pseudotyped H5 virus, owing to the possible emergence of cross-reactive stem antibodies or cross reactivity between similar regions of HA. The response to H3 and seasonalH1 remained unchanged.

Post 2011 vaccination serum from this donor showed 4 to 6-fold reduced neutralisation to recently evolved clade 6B viruses. We isolated and characterised monoclonal antibodies from this donor to analyse the clonal basis for this reduction in serum neutralisation titre (Huang et al. 2015).

3.2 Sorting of HA-specific plasmablasts

PBMC isolated from day 7 after the 2011 vaccination from the donor H were stained and sorted as described in chapter 2. We have shown the proof of principle for use of haemagglutinin protein for antigen specific sorting of plasmablasts in Chapter 2 Figure 2.3. H1 purified haemagglutinin protein with a biotin tag stained approximately 26% of the plasmablasts (identified as $CD3^{neg}/CD20^{neg\&low}/CD19^{pos}/CD38^{high}/CD27^{high}$) (Figure 3.2). A total of 288 HA-specific B cells were sorted singly and 167 cells were positive on PCR for both heavy and light (kappa or lambda) chains, from which 167 monoclonal antibodies were developed. Of the 167 antibodies, 157 bound to HA antigen expressed on the cell surface, which were further tested by ELISA, haemagglutinin inhibition (HI), specific neutralisation and western blot. Sorting and isolation of antibodies were done in collaboration with Arthur Huang, and characterization was aided by Alain Townsend and Lisa Schimanski.

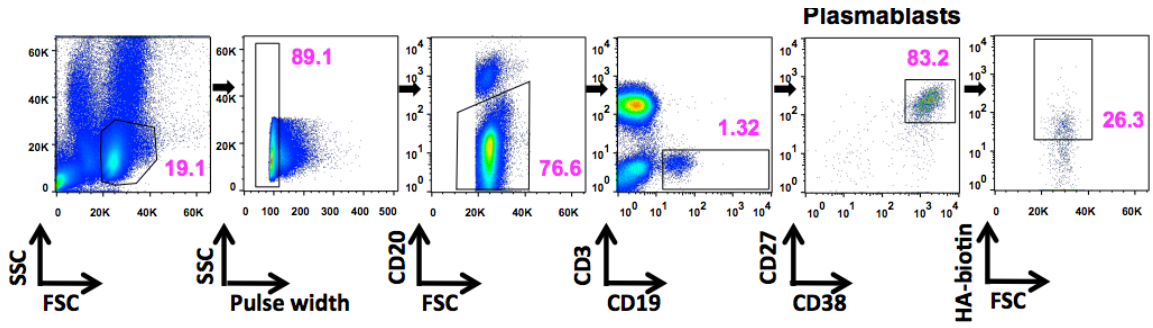

Figure 3. 2 ***Day 7 plasmablasts from donor H following 2011-12 influenza vaccination****, stained with biotinylated H1N1pdm09 (A/England/195/2009) HA protein for antigen specific single plasmablast sorting. The percentage of cells selected in each gate is shown in pink.*

Table 3. 2 Summary of the antibodies and their VH gene analysis.

					Characteristics of the largest clone			
Specificity	V_H gene	No. of antibodies	No of clones	Size of the largest clone	HCDR3 length	V_H	D	J_H
Head S	3-7	88	6	73	18	3-7*01	3-16*01	6*02
	3-33	12	2	10	17	3-33*01or05or06	1-26*01	6*02
	1-18	20	5	15	17	1-18*01	2-21*02	6*02
Head CR	3-15	18	3	16	17	3-15*01or02	3-22*01	4*02
Stem CR	1-69	8	5	5	13	1-69*01or1-69D*01	2-2*02	6*03
	3-23	4	3	2	17	3-23*01or3-23D*01	3-22*01	4*02
	3-30	3	2	2	18	3-30-3*01	3-3*02	6*03
	4-39 (Stem)	1						
	4-59	1						
	3-21	1						
	3-9	1						
First six dominant sets		150						
Total antibodies		157						

S: Specific, CR: Cross-reactive, HCDR: Heavy complementarity determining region

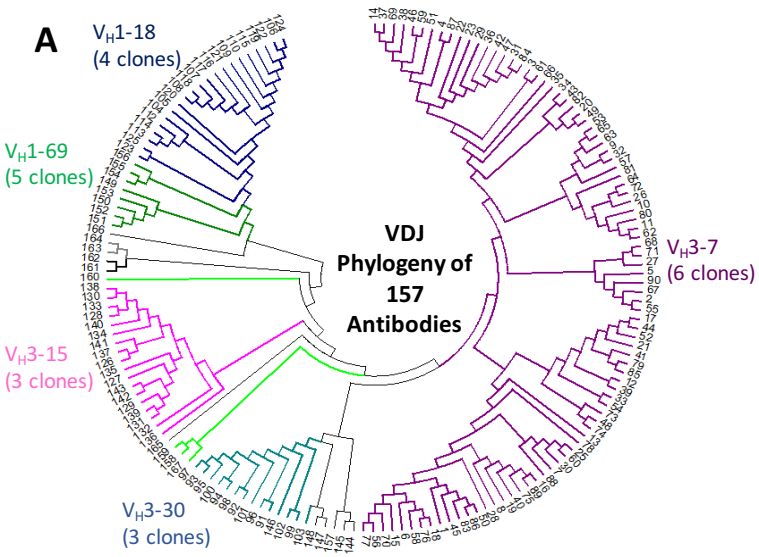

B **Clonality within VH3-7 set of antibodies**

Color code	V_H	D_H	J_H	Reading frame	Size of the clone
	3-7*01	3-16*01	6*02	2	73
	3-7*03	3-16*01	6*02	2	2
	3-7*01	3-3*01	6*02	3	7
	3-7*01	3-3*01	6*02	2	3
	3-7*01	3-3*02	6*02	3	2
	3-7*01	3-16*01	6*01	2	1

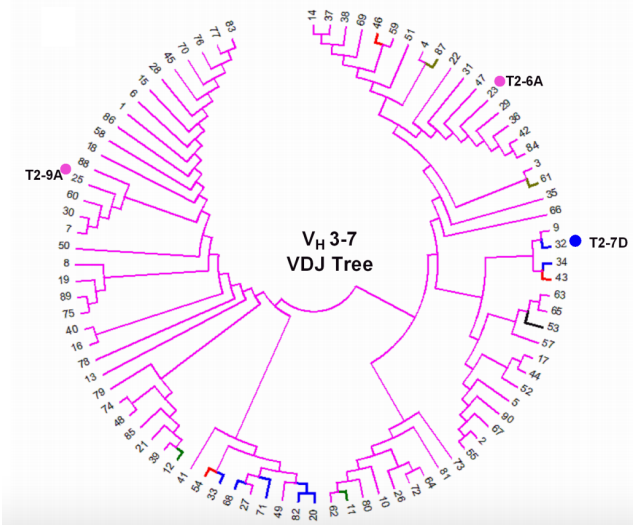

Figure 3. 3 ***Antibody response in donor H is polyclonal as shown by VDJ heavy chain gene rearrangement of 157 antibodies.*** ***A)*** *More than 21 clones are present in 150 antibodies encoded by 6 major VH genes. Clones are here defined by a unique combination of V, D and J segments and the D reading frame in the heavy chain.* ***B)*** *The amino acid sequence dendrogram of the largest set of HA head specific-binding antibodies, encoded by the VH3-7 gene segment. The largest set of VH3-7 antibodies was dominated by a clone (pink) encoded by VDJ: 3-7*01/3- 16*01/6*02 and reading frame*

2. The dendrogram was generated based on the protein sequence with MEGA software version 6.06 using neighbour-joining tree.

3.3 Antibody repertoire following vaccination in donor H

Each of the 157 antibodies had a unique sequence as analysed by the International Immunogenetics Information System (IMGT) (Lefranc et al. 1998). These antibodies can be divided into 11 sets based on their coding VH genes (Table 3.2) and 150 out of 157 (96%) are encoded by the six largest VH sets (Table 3.2 and Figure 3.3A). Within each set, a number of clones were identified based on their specific VDJ rearrangements and D-region reading frame (Table 3.2) in the heavy chain. These clones were further diversified by a unique pattern and frequency of somatic mutations. The largest set containing 88 antibodies, encoded by VH3-7, was derived from 6 clones. A single dominant clone diversified to 73 unique antibodies (Figure 3.3B) with different patterns of somatic mutations. Selected antibodies from the six VH sets were expanded and their antibodies were purified and tested for neutralisation of a variety of viruses.

150 antibodies from six VH sets were divided into three functional groups which are shown in figure 3.4. The first group of 120 antibodies encoded by VH3-7, 3-33 and 1-18, referred as 'Head Specifics' neutralise pdmH1N1 viruses and do not cross-react on recent pre-2009 seasonal H1N1 viruses. The second group called 'Head Cross-reactives' composed of 18 antibodies were encoded by the VH3-15 gene. These antibodies bind to the head region as suggested by haemagglutination inhibition and they are cross-reactive to former seasonal H1N1 strains (1994-2007 so far tested). Twelve antibodies form a third group 'Stem Cross-reactives' and were encoded by two VH genes VH1-69 and VH3-23. They compete for binding by the classic stem antibody C179 (Okuno et al. 1993), do

not inhibit haemagglutination, and are cross-reactive to former seasonal H1N1 strains and H5 subtype viruses. These three functional groups are discussed in detail in later sections.

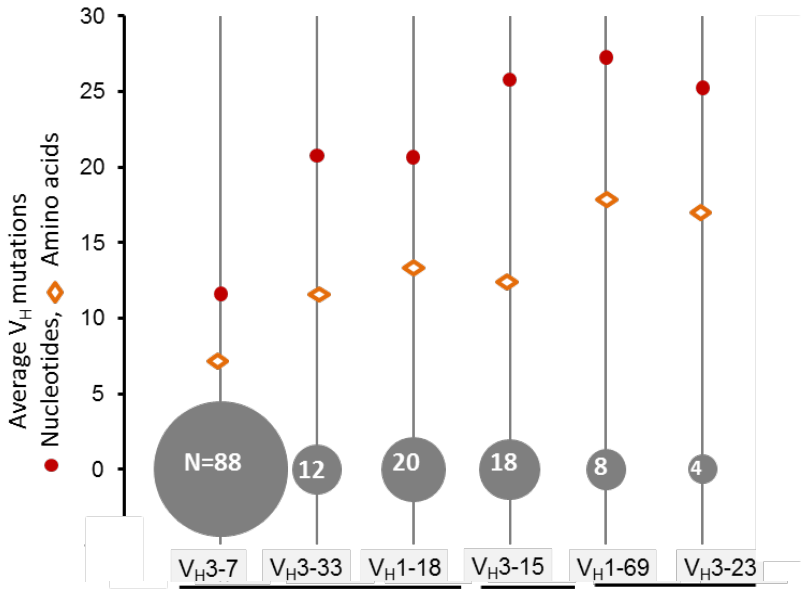

	Head Specifics	Head Cross-Reactives	Stem Cross-Reactives
Inhibit hemagglutination	+++	++	—
Neutralize 2009 H1	+++	++	+
Neutralize seasonal H1 (1994-2007)	—	++	+
Neutralize 1977 H1	+++	++	—
Neutralize H5	—	—	+

Figure 3. 4 ***The 6 largest VH-related sets of HA-binding antibodies derived from day 7 H1 HA-specific B cells.*** *The average number of VH nucleotide and amino acid replacements in the 6 largest sets of HA-binding antibodies are shown. The representative HI and MN results of head-specific (Head S), head cross-reactive (Head CR), and stem cross-reactive (Stem CR) antibodies are summarised in the figure. –, negative; +, EC_{50} ~366 ng/ml; ++, EC_{50} ~70 ng/ml; +++, EC_{50} ~7 ng/ml for neutralisation of X179A virus (A/California/07/2009 H1pdm09).*

3.4 Antibodies to H1N1 globular head

Of the total 157 antibodies, 150 bind to the head region of haemagglutinin, as recognised by inhibition of haemagglutination of human red cells by X179A (A/California/07/2009) virus (Figure 3.4).

3.4.1 Antibodies specific to H1N1pdm09 viruses

The majority of the antibodies (56%, 88 of 157) were derived from a dominant VH3-7 set, most frequently associated with JH6*02/DH3-16*01 and VL1-40*01/JL2*01 (Table 3.2 and Figure 3.3). These antibodies are diversified to at least 6 clones based on their heavy chain VDJ recombination and D-chain reading frame. All antibodies resulted in a CDR3 length of 18 amino acids (Table 3.2). One dominant clone diversified to 73 sequences, generated by introduction of somatic mutations. There are 7 amino acids somatic mutations per sequence in antibodies encoded by VH3-7 (Figure 3.3). Clonal dendrogram of VDJ amino acid sequences of these antibodies (Figure 3.3B) shows the diversity in these sequences generated by somatic mutations and clonal D-J combinations. This result is in accordance to findings by Krause et al. (Krause, Tsibane, Tumpey, Huffman, Briney, et al. 2011) and Jackson et al. (Jackson et al. 2014), who published a similar set of antibodies (VH3-7/JH6) targeting the Sa site of H1N1pdm09 HA.

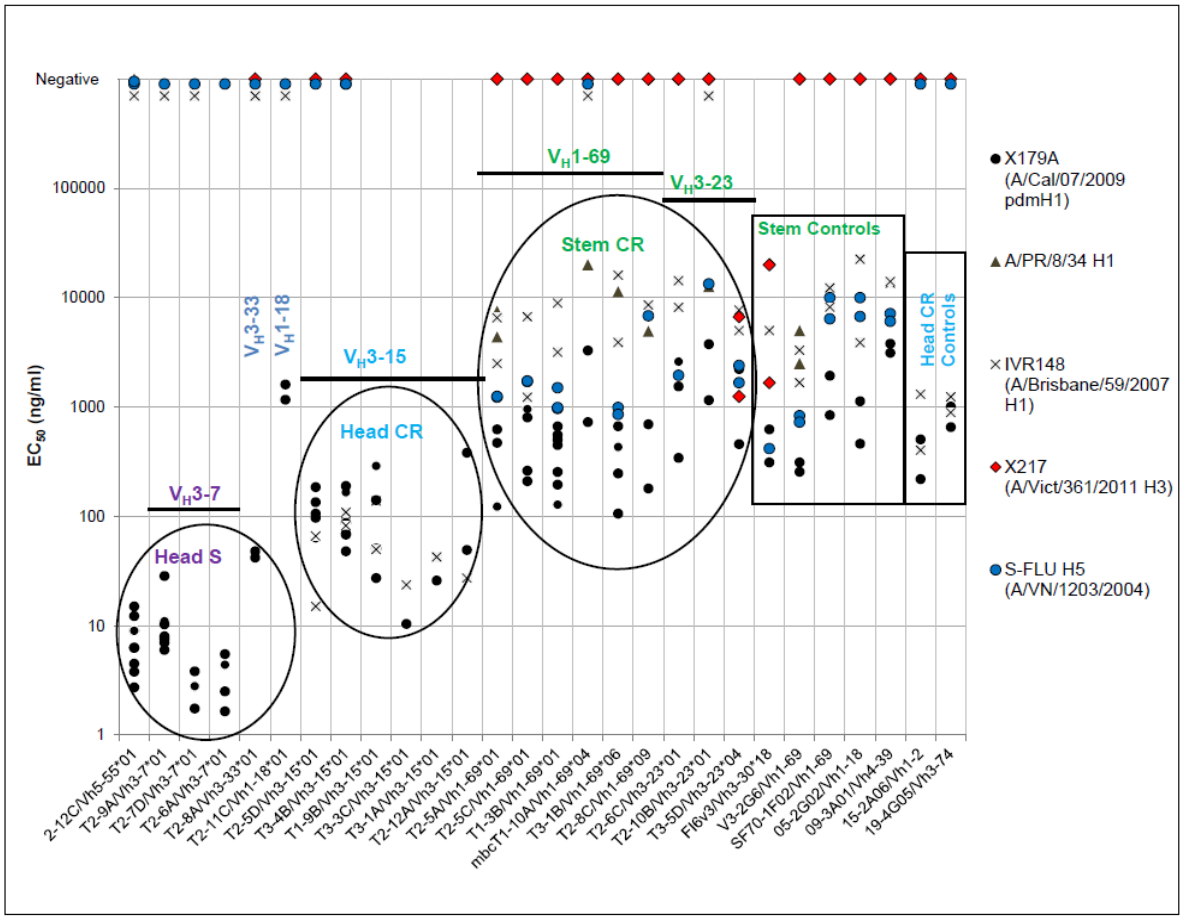

Figure 3. 5. ***Antibodies of 3 specificities with varying in-vitro neutralisation potency****. Neutralisation titres of head-specific (Head S), head cross-reactive (Head CR), and stem cross-reactive (Stem CR) antibodies for former H1, H3, H1pdm09, and H5 viruses. Two H1 head-specific, 15-2A06 and 19-4G05 (Li, Chiu, et al. 2012), and 5 stem-reactive, FI6v3 (Corti et al. 2011), V3-2G6 (Thomson et al. 2012), SF70-1F02 (Wrammert et al. 2011), and 05-2G02 and 09-3A01 (Li, Chiu, et al. 2012), reference antibodies were included as controls, kindly supplied by Rafi Ahmed and Antonio Lanzavecchia. Each symbol represents an independent measurement. Some measurements overlap. MN titres were assayed at least twice for each antibody. The mean EC_{50} for neutralisation for the 6 largest sets of HA-binding antibodies in the MN assay was analysed by 1-way ANOVA, and a P value less than 0.05 was considered significant.*

Initial screening of the antibody supernatants revealed that clones from the VH3-7 set inhibited haemagglutination by H1N1pdm09 (X179A A/California/07/2009) virus. We selected three antibodies from this set, purified and titrated them against various viruses in HI and micro-neutralisation assays. These are the most potent antibodies we have isolated with neutralisation EC50 for H1N1pdm09 virus of approximately 7 ng/ml (~5x 10^{-11} M), but these failed to HI or neutralise past seasonal (pre-2009) H1N1 strains (Figure 3.5 and Table 3.3).

Escape variants of the virus X179A (A/California/07/2009) were selected using the VH3-7 antibody T2-6A, in order to identify the site recognised by the VH3-7 clones. Sequencing of the mutant and wild type viruses were done by Rod Daniels at the WHO Collaborating Centre, The Crick Institute. Antibody T2-6A selected a single mutation K163E in the Sa site of the head of the haemagglutinin (Figure 3.6) and this mutation is associated with loss of binding (Figure 3.7) and neutralisation (Table 3) by other members of VH3-7 set. The K163E substitution corresponds to K166E in escape virus selected by antibody 4K8 (encoded by VH3-7*01) isolated by Krause et al. (Krause, Tsibane, Tumpey, Huffman, Briney, et al. 2011). The numbering system used in our work is based on the WHO annual reports from the Crick Worldwide Influenza Centre.

Additional two VH sets: VH3-33 (12 of 157 mAbs) and VH1-18 (20 of 157 mAbs) showed similar properties to VH3-7 family. They also were polyclonal (Table 3.2) and specific to H1N1pdm09 (Figure 3.5 and Table 3.3), but tended to require higher concentrations of antibody for neutralisation and contained more somatic mutations than the VH3-7 set (Figure 3.4: 21 ± 2 nucleotide changes for VH3-33 and 20 ± 3 for VH1-18). The representative antibodies from these sets also failed to bind (Figure 3.7) and

neutralise the K163E variant virus (Table 3.3) selected by the VH3-7 clone, and thus appeared to bind to an overlapping site.

Table 3. 3 MN of natural variants and in vitro antibody-selected variant viruses

			Past H1N1 viruses								Clade 6B viruses*				Antibody selected mutants		
Antibody	V_H	Specificity	A/USSR/90/1977	A/Bayern/7/1995	A/Beijing/262/1995	A/N.Caledonia/20/1999	A/Brisbane/59/2007	IVR148 (A/Brisbane/59/2007)	A/Bayern/69/2009 (G155E)	X179A (A/California/07/2009)	A/Malta/MV14319/2013 (K163I)	A/Belgium/14G0500/2014 (K163Q)	A/Serbia/NS-601/2014 (SKS 162-164 NQS, +CHO)	A/England/621/2013 (SKS 162-164 NNS, +CHO)	T2-6A ΔX179A (K163E)	T3-4B ΔX179A (K163Q)	2-12C ΔX179A (K130E)
Donor H Serum day 12^										1:10240							
Donor H Serum day 7 ^			1:320							1:2560	1:640	1:640	1:480	1:480	-	-	1:2560
T2-9A	3-7*01	Head S		-	-	-	-	-	++++	++++							
T2-6A	3-7*01	Head S	++++	-	-	-	-	-	++++	++++	-	-	-	-	-	-	++++
T2-7D	3-7*01	Head S	++++				-	-	++++	++++	-	-	-	-	-	-	++++
T2-8A	3-33*01	Head S	+++					-		+++	-	-	-	-	-	-	+++
T2-11C	1-18*01	Head S	+++					-		++	-	-	-	-	-	-	+++
T2-5D	3-15*01	Head CR	+++	+++	+++	+++	+++	+++	++	+++	-	-	-	-	-	-	+++
T3-4B	3-15*01	Head CR	+++	++	++	+++	+++	+++	+++	+++	-	-	-	-	-	-	+++
T1-9B	3-15*01	Head CR	+++	+++	-	+++	+++	+++	++	+++	-	-	-	-	-	-	+++
T2-12A	3-15*01	Head CR		+++	++			+++		++					-	-	++
T3-3C	3-15*01	Head CR	+++	+++	-			+++		+++	-	-	-	-	-	-	+++
T3-1A	3-15*01	Head CR		+++	-			+++		+++					-	-	+++
Controls																	
2-12C	5-55*01	Head S	-	-	-	-	-	-	++	++++	++++	++++	++++	++++	++++	++++	-
Q11A6	3-21*01	Head S	-					-		+++	++	++	+	+	++	++	-
15-2A06	1-2	Head CR	++					++		++	-	-	-	-	-	-	+++
19-4G05	3-74*01	Head CR	+					++		++	-	-	-	-	-	-	++
T1-3B	1-69*01	Stem CR	-	-	-	+	++	+	+	++	++	++	+	+			
FI6v3	3-30*18	Stem CR	-							++	++	++	+	++			

Scale	MN EC_{50}
++++	0 - 20 ng/ml
+++	20 - 200 ng/ml
++	0.2 - 2 µg/ml
+	2 - 20 µg/ml
+/-	20-80 µg/ml
-	Not Detected

* Replication based microneutralization assays

^Donor sera were obtained after vaccination in 2011. S: Specific; CR: Cross Reactive; CHO: Glycosylation

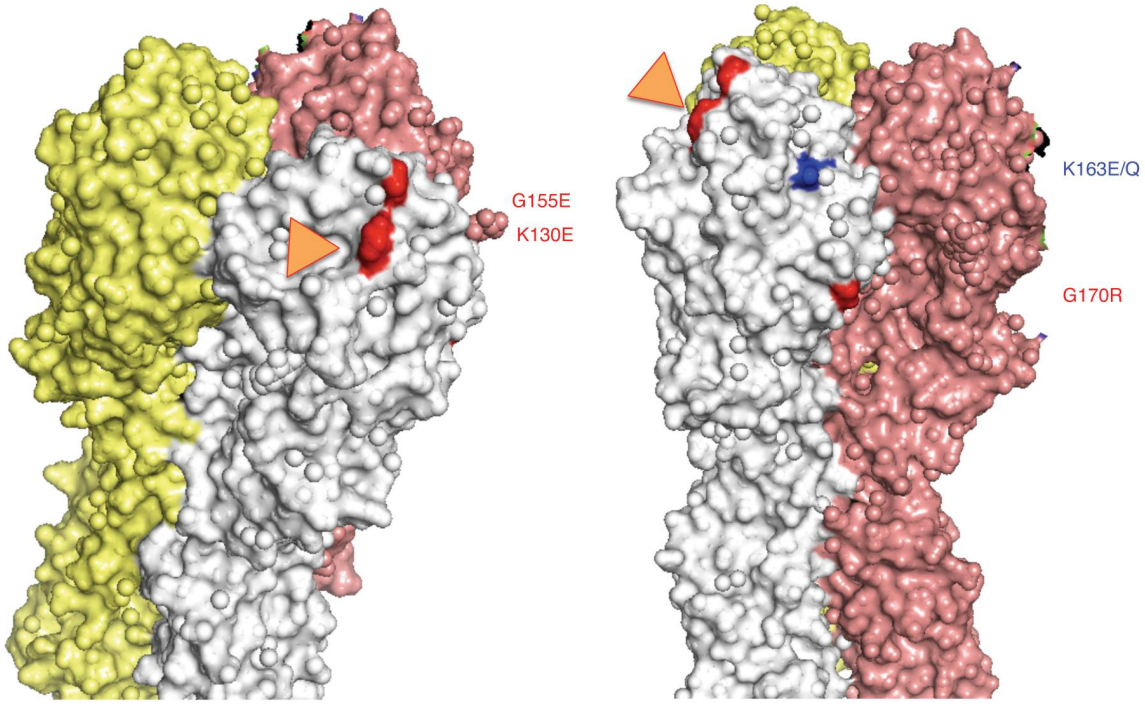

Figure 3. 6 ***Mapping of K163E/Q substitutions selected by head-specific T2-6A (V_H 3-7) and head cross-reactive T3-4B (V_H 3-15) antibodies.*** *K130E, G155E, and G170R (shown in red) resulted in loss of binding by the 2-12C control antibody. The G170R amino acid substitution, co-selected by the control antibody 2-12C, is thought to be coincidentally associated with K130E. The orange triangle indicates the position of the sialic acid–binding site. K163E/Q is shown in blue. Mutations were mapped with PYMOL version 1.7 onto PDB:3LZG (Xu et al. 2010)). These mutant and wild type viruses were sequenced by Rod Daniels, at the WHO Collaborating Centre, The Crick Institute.*

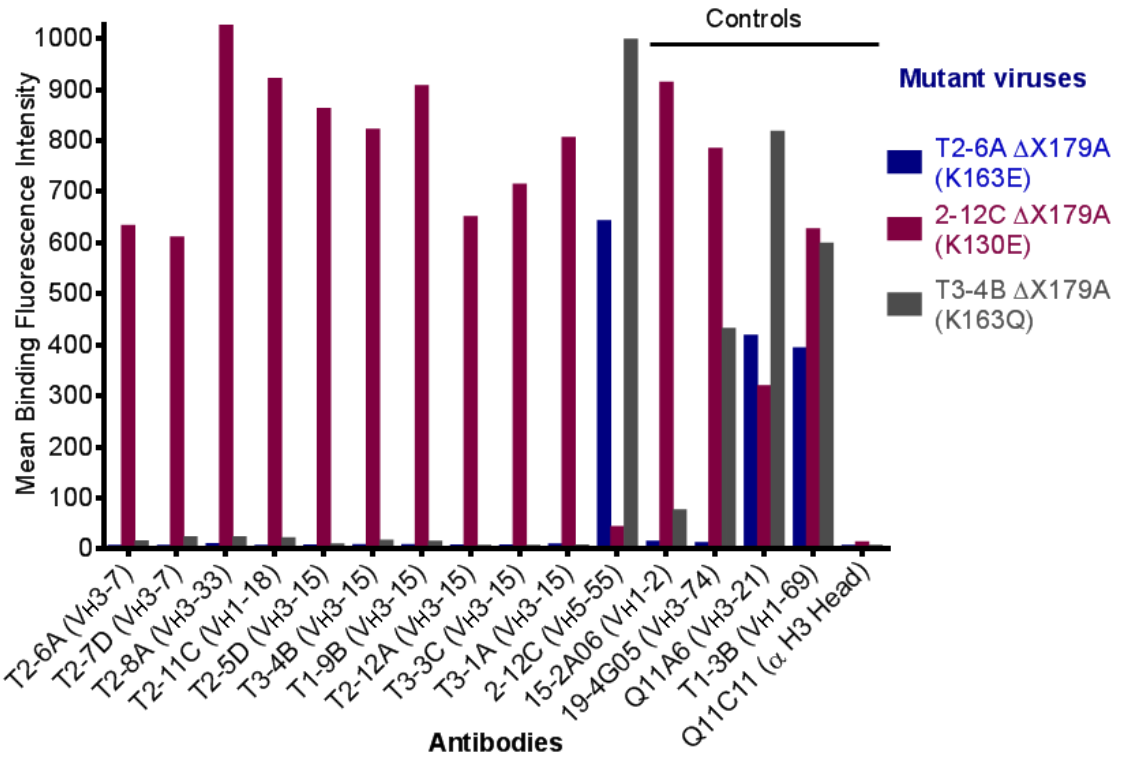

Figure 3. 7 ***Binding activity of HA head-specific and head cross-reactive antibodies on cells infected with the variant viruses.*** *A selection of head-specific (VH 3-7, 3-33, 1-18) and head cross-reactive (VH3-15) antibodies and controls, including the stem cross-reactive antibody T1-3B (VH1-69), were tested for binding to MDCK-SIAT1 cells infected with variant viruses selected with monoclonal antibody T2-6A (VH3-7) that selected the K163E substitution, T3-4B (VH3-15) that selected K163Q, and the control 2-12C (VH5-51) that selected (K130E/G170R). The assay was done twice with equivalent results.*

3.4.2 Head antibodies cross-reactive to seasonal (pre-2009) H1N1 and H1N1pdm09 viruses

A second dominant set was encoded by VH3-15, and was comprised of 18 antibodies (11%) (Table 3.2). These neutralised and inhibited haemagglutination activity of seasonal (A/Brisbane/59/2007) and H1N1pdm09 (A/California/09/2007) viruses almost equally. These antibodies did not cross-compete for binding with stem antibody C179. These

results combined suggest that these antibodies recognise an epitope in the HA head which is conserved between seasonal H1N1 and H1N1pdm09 viruses. This set of antibodies also carry a higher number of somatic mutations (average nucleotide mutations 25 ± 4) which is significantly higher than that for the VH3-7 antibodies (ANOVA $P<0.001$) suggesting these may have been stimulated from memory B cells that had passed repeatedly through the germinal centre. MN neutralisation titre of a selection of VH3-15 antibodies was ~70 ng/ml for X179A (Figure 3. 5), which is about 10-fold higher than that of head VH3-7 antibodies (ANOVA, $P<0.001$). These antibodies also neutralised former seasonal H1N1 strains back to 1994 so far tested. As controls we used 15-2A06 and 19-4G05 antibodies (Li, Chiu, et al. 2012) which also reacted broadly to the H1 head with equivalent neutralisation EC50 to our VH3-15 antibodies (Figure 3. 5 and Table 3.3).

We selected an escape mutant using a representative VH3-15 antibody T3-4B to define the binding epitope. This antibody selected substitution K163Q in Sa site, exactly the same position as selected by VH3-7 antibody T2-6A which selected K163E. K163Q is the substitution which characterises the clade 6B viruses which have evolved recently (The Crick Worldwide Influenza Centre 2015).

3.4.3 Antibodies to the head are focused on K163

After identifying the K163 as an epitope for both VH3-7 and VH3-15 antibodies, we then tested the binding and neutralisation of these K163E/Q variant viruses with head specific antibodies belonging to all 4 VH related sets (which makes up 138 of total 157 antibodies, Figure 3.4). These mutations abolished the binding (Figure 3.7) and neutralisation (Table 3.3) by all 4 antibody sets (VH 3-7, 3-33, 1-18 and 3-15) implying that they are all binding around the same epitope. These mutations at K163 also prevented the neutralisation by two control antibodies from Rafi Ahmed 15-2A06 (VH1-2) and 19-

4G05 (VH3-74) suggesting that these 2 antibodies bind closely related epitopes. It is noteworthy that 19-4G05 although it lost neutralisation, retained some binding to K163Q virus.

An antibody from a different individual, 2-12C (VH5-51) was not affected at all by the K163E/Q mutations in binding or neutralisation. We sequenced the escape mutants generated by the 2-12C antibody and found that it selected separate mutations at K130E near the sialic acid binding site associated with G170R (Figure 3. 6). This variant resulted in loss of neutralisation by its own selecting antibody 2-12C and another antibody Q11A6 (VH3-21) from a third individual, but didn't affect the binding or neutralisation by any of the head antibodies from donor H, which were susceptible to K163E/Q substitutions. Q11A6 is a second example of an antibody that retained some binding to the mutant HA (Figure 3.8), but lost the ability to neutralise the variant virus bearing the mutated HA (Table 3.3). In binding and neutralisation assays to mutant variants, stem antibody T1-3B (VH1-69) was unaffected by both substitutions (K163E/Q or K130E and G170R) in the head. The antibody 2-12C also had significantly reduced neutralisation and HI titres to H1N1pdm09 virus (A/Bayern/69/2009) which carries the G155E substitution compared to the HA of A/California/07/2009 virus (Table 3.3 and Appendix 3.1)

The substitutions selected by the antibodies were mapped on to the 3D structure of H1 HA, which showed that residues 130 and 155, recognised by the clone 2-12C, are in neighbouring sites around the receptor binding site (shown in red in Figure 3.6). On the contrary, residue 163, (shown in blue in Figure 3.6), indispensable to the donor H head antibodies and 2 broadly reactive control antibodies 15-2A06 and 19-4G05, is further away from the 130 site but in closer proximity to the receptor binding site; enough to block haemagglutination. The G170R substitution co-selected by 2-12C may be

coincidental as it is distant from K130 and the receptor binding site. Also, it is not present in A/Bayern/69/2009 (G155E) virus, which also showed reduced neutralisation by 2-12C.

3.4.4 Effect of somatic mutations on the fine specificity of antibodies for drifted viruses

Six VH3-15 antibodies sharing the same VDJ recombination but differing in somatic mutations, were tested for neutralisation of A/Beijing/262/1995 and A/Bayern/7/1995 in table 3. This revealed that antibodies that differ only by somatic mutations can distinguish between these closely related drifted viruses. All six antibodies neutralised A/Bayern/7/1995 but only three antibodies neutralised A/Beijing/262/1995. These two viruses differ at several positions, including K163N.

3.4.5 Cross-inhibition by antibodies to pdm09 HA

Lisa Schimanski in the lab performed cross-inhibition of binding to purified HA by the various sets of head antibodies from donor H (recognising K163) and compared them to antibody 2-12C (recognising K130) and stem antibody T1-3B. We found that 4 representative antibodies from the VH sets 3-7, 3-33, 1-18 and 3-15 blocked each other's binding but were not inhibited by 2-12C or stem antibody T1-3B (Figure 3.8) except for T3-4B (VH3-15) antibody which was partially inhibited by 2-12C. By contrast, none of the selected head antibodies from donor H inhibited the binding of control antibody 2-12C. The unidirectional inhibition of binding of VH3-15 antibody T3-4B by 2-12C may suggest an overlap of the binding footprints or steric hindrance between these two antibodies.

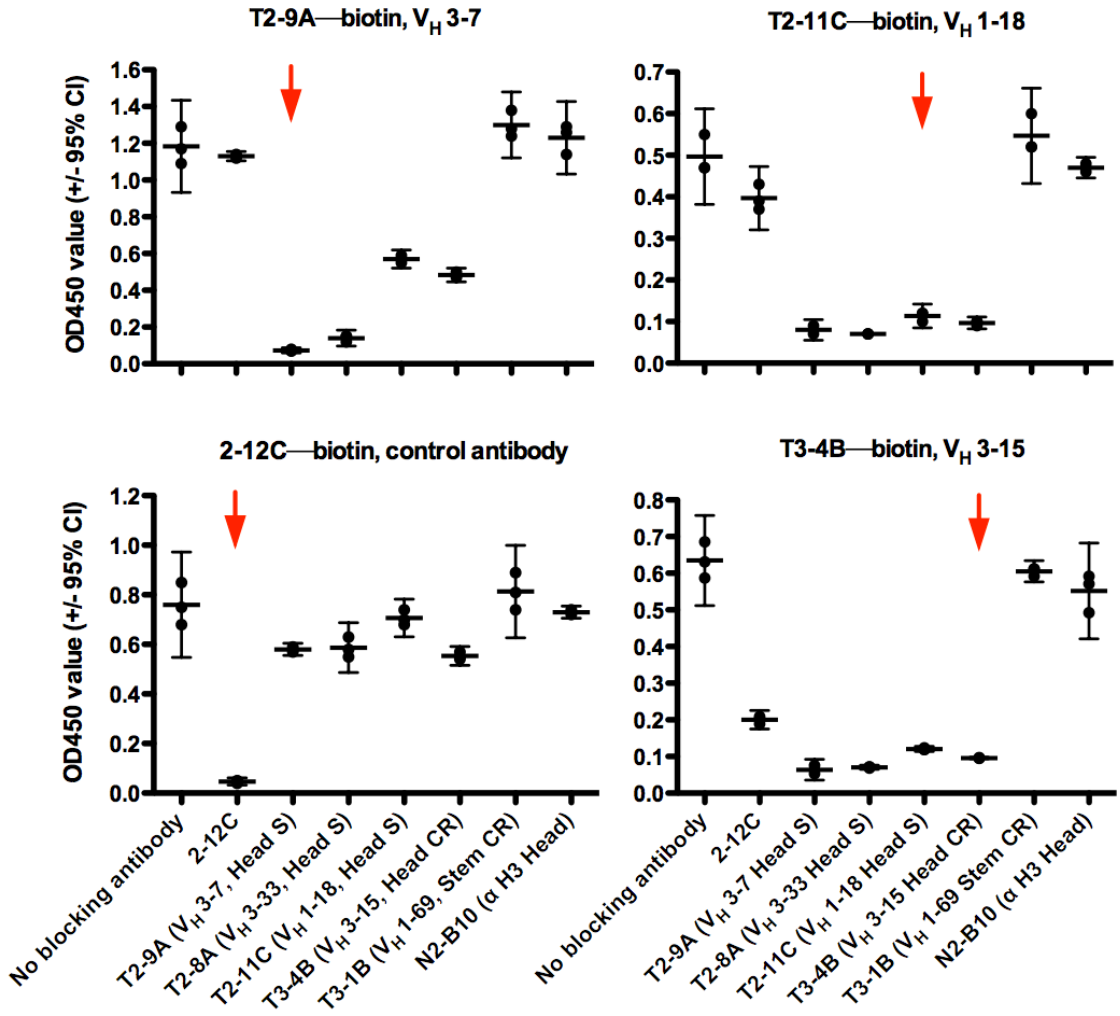

Figure 3. 8 ***Competitive binding to purified A/England/195/2009 HA by the various sets of antibodies that are sensitive to K163E/Q.*** *The head-specific antibody 2-12C recognizing K130, G155, a typical VH1-69 stem reactive antibody and an anti-H3 antibody were included as controls. Arrows indicate self-inhibition by the unlabelled version of each antibody. Measurements were in triplicate. Means and 95% confidence intervals are shown. The assay was done twice with equivalent results.*

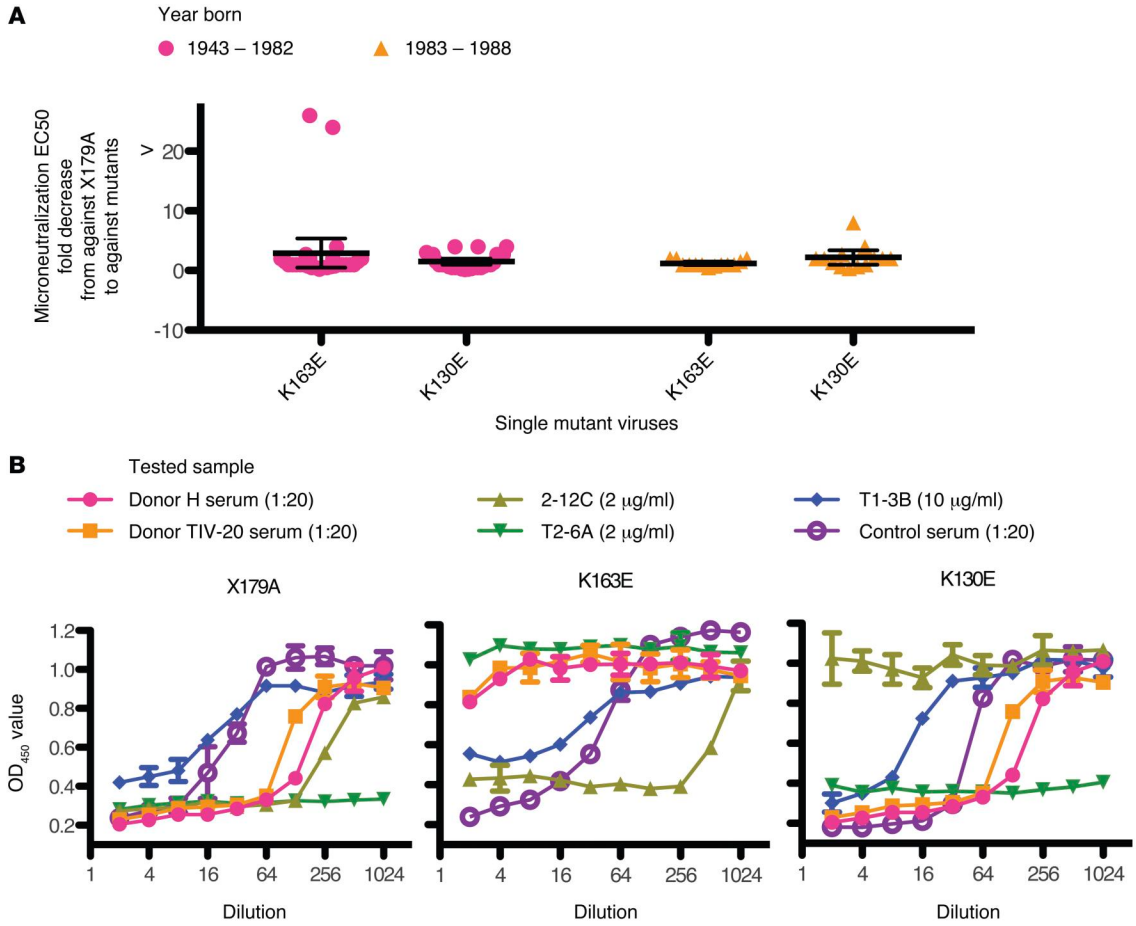

Figure 3. 9 ***Neutralising activities by sera and monoclonal antibodies from vaccinated individuals against the variant viruses.*** *(**A**) Sera from recently vaccinated individuals born between 1943 and 1982 (n = 28) and 1983 and 1988 (n = 13) were tested for neutralisation of X179A and HA variants carrying single amino acid substitutions. Sera from two individuals (donor H and TIV-20) failed to neutralise the K163E variant of X179A, and their response was focused on the Sa site. Sera from two individuals born between 1983 and 1988 were focused on K130 (Ca2 site). Mean and 95% confidence interval are shown. (**B**) Serum after vaccination and the VH 3-7 antibody T2-6A from donor H, together with serum after vaccination from another donor (TIV-20), neutralised X179A strongly but failed to neutralise the K163E virus variant. Their neutralising activity was unaffected by the K130E substitution. T1-3B and control serum had similar neutralisation titres to all the viruses. The MN assays were performed in duplicate.*

3.4.6 Reactivity with natural antigenic drift variants of H1N1pdm09 with K163 change

Ferret sera were unable to detect the antigenic change in 2013/14 clade 6B viruses. We were particularly interested to see if the monoclonal antibodies, and the serum from donor, which should be polyclonal, were affected by the K163 change in natural clade 6B viruses.

Comparison of MN titres of the antibodies and serum are shown in Table 3.3 and the HI titres are shown in Appendices 3.1 and 3.2 (performed by Rod Daniels at the WHO Influenza Centre). The EC50 neutralisation titres of day 7 sera from donor H after vaccination was reduced from 2560 to 480-640 on a selection of clade 6B 2013-2014 viruses, which have either the K163Q substitution or the epitope is masked by glycosylation at N162. In accordance with serum results, selected head antibodies from four VH sets (VH 3-7, 3-33, 1-18 and 3-15) representing 138/157 antibodies (88%) did not neutralise these viruses (Table 3.3).

These head antibodies representing 4 VH sets were also tested for HI of various clades of H1N1pdm09 viruses, where they failed to inhibit haemagglutination by clade 6B viruses, thus matching the neutralisation data (Appendix 3.1). Nine of these tested clade 6B viruses had the characteristic S162N substitution along with K163Q. S162 is contiguous with K163, and forms part of a N-linked glycosylation sequence N-X-S/T. It appeared in 2015 and was positively selected in association with K163Q to become dominant by 2016 (Figure 3. 13).

The control antibody 2-12C which recognised residues 130 and 155, had relatively similar HI titres to all H1N1 viruses tested except viruses A/Bayern/69/2009 and the A/California/07/2009 E4/E2 isolate, which had been passaged in eggs (Appendix 3.1).

Reduced titre to A/Bayern/69/2009 can be explained by G155E substitution. Titres to A/California/07/2009 E4/E2 are lower for all antibodies because of the selection of 223R substitution (known to affect receptor binding) in egg-grown viruses (Wang et al. 2010), which may be an example of an adsorption mutation with global effects on neutralisation by antibodies (discussed in Chapter 1). It is a good example of why egg propagation for human vaccines should be avoided if possible.

Ferret sera against A/California/07/2009 failed to detect the K163 change in clade 6B viruses (Appendices 3.1 and 3.2) because it is known to focus on the Sa site around positions 153-155 (Chen et al. 2010), which is conserved in the clade 6B viruses. The control antibody 2-12C, which is mapped to residues 130 and 155, retained neutralisation with EC50 <10 ng/ml to all clade 6B viruses (Table 3.3). The retention of neutralisation of clade 6B viruses by ferret sera and antibody 2-12C is consistent with the fact that the amino acid sequence between 128 and 159 is identical for A/California/07/2009 and the clade 6B viruses. Another control antibody Q11A6 with similar epitope to 2-12C, also retained neutralisation for clade 6B viruses.

Control antibodies 15-2A06 and 19-4G05, for which the neutralisation was affected by K163E/Q substitution also lost neutralisation to clade 6B viruses (Table 3.3).

3.4.7 Cross-reactivity to A/USSR/90/1977

To test whether the antibodies we had isolated reacted with a virus that would have been circulating during the childhood of donor H, representative head specific (VH3-7, 3-33, 1-18) and head cross-reactive antibodies (VH3-15) were tested for neutralisation of A/USSR/90/1977. All of the antibodies representing these four 4 VH sets, which were mapped to the K163 site, also neutralised A/USSR/90/1977 virus with an equal EC50 concentration to A/California/07/2009 (Table 3.3).

The donor H was a child when the USSR virus appeared in 1977, during which time the donor may have been exposed and generated a primary memory B cell pool. A relatively rare subpopulation of these memory cells may have been stimulated by the cross-reacting epitopes in the 2009 vaccine which were limited to the surface around K163. The residues conserved in A/USSR/90/1977 and A/Brisbane/59/2007 compared to A/California/07/2009 are mapped onto the 3D structure in figure 3.10. It shows that K163 (Sa site) is situated in the centre of a patch of conserved surface in these haemagglutinins. This site is conserved also in 1918 H1 haemagglutinin and the VH3-7 antibodies to this site were found to cross-neutralise this virus also (Krause, Tsibane, Tumpey, Huffman, Basler, et al. 2011).

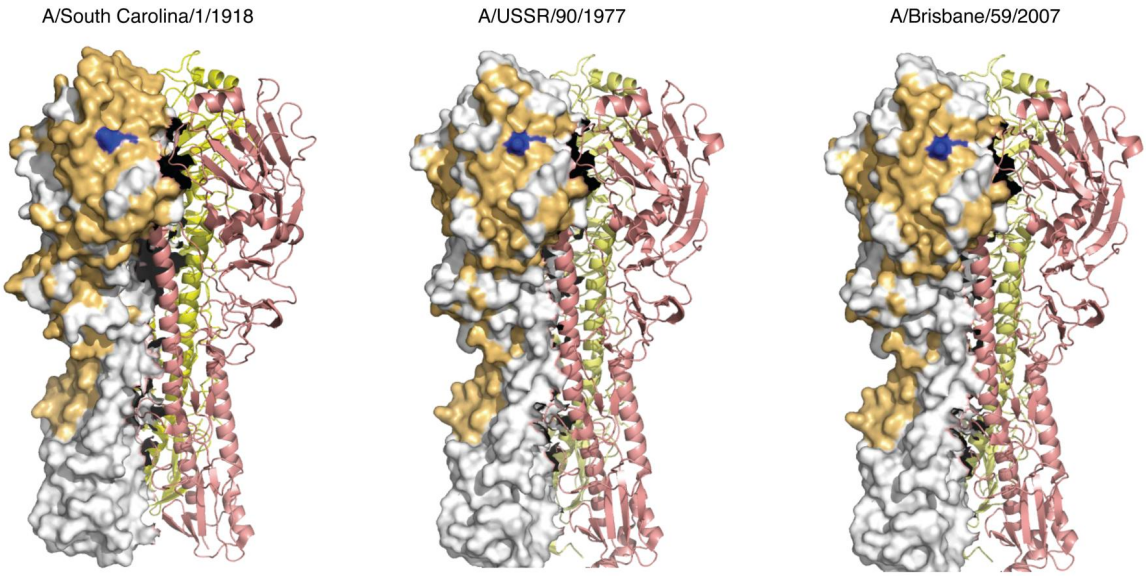

Figure 3. 10 ***Mapping of the HA1 K163 residue in former H1N1 viruses.*** *Conserved HA1 residue K163 (shown in blue), which was selected for substitution by the VH3-7*01 and 3-15*01 antibodies, is situated in a patch (coloured gold) of surface conserved between A/California/07/2009, A/Brisbane/59/2007, A/USSR/90/1977, and A/South Carolina/1/1918 HAs. Conserved residues were mapped with PYMOL version 1.7 onto PDB:3LZG (Xu et al. 2010)*

3.4.8 The antibody response from donor H is focused

Having shown that 88% of the antibodies we isolated were focused around position 163, we tested the donor's serum on the variant viruses we had selected with representative monoclonal antibodies with a single substitution at K163 (Figure 3. 9). We found that the donor H serum also lost almost all its ability to neutralise the K163 variants indicating that the majority of the antibodies in the serum must be focused on this site, as indicated by the collection of monoclonal antibodies we isolated from donor H.

Combining these data which include: i) failure of binding (Figure 3. 7) and neutralisation by head antibodies (88% of the total response) (Table 3.3, Figure 3.9B), ii) loss of neutralisation by donor sera to escape mutant virus (K163E/Q) selected by representative antibodies (Figure 3.9B), iii) cross-inhibition of binding to HA (Figure 3. 8), and iv) reduced neutralisation by mAbs and sera to clade 6B viruses (Table 3.3), it becomes clear that the antibody response generated by vaccination with HA from H1N1pdm09 (A/California/07/2009) was focused on a small patch of the HA head (Sa site) including residue K163, which was substituted in clade 6B viruses which evolved in 2013.

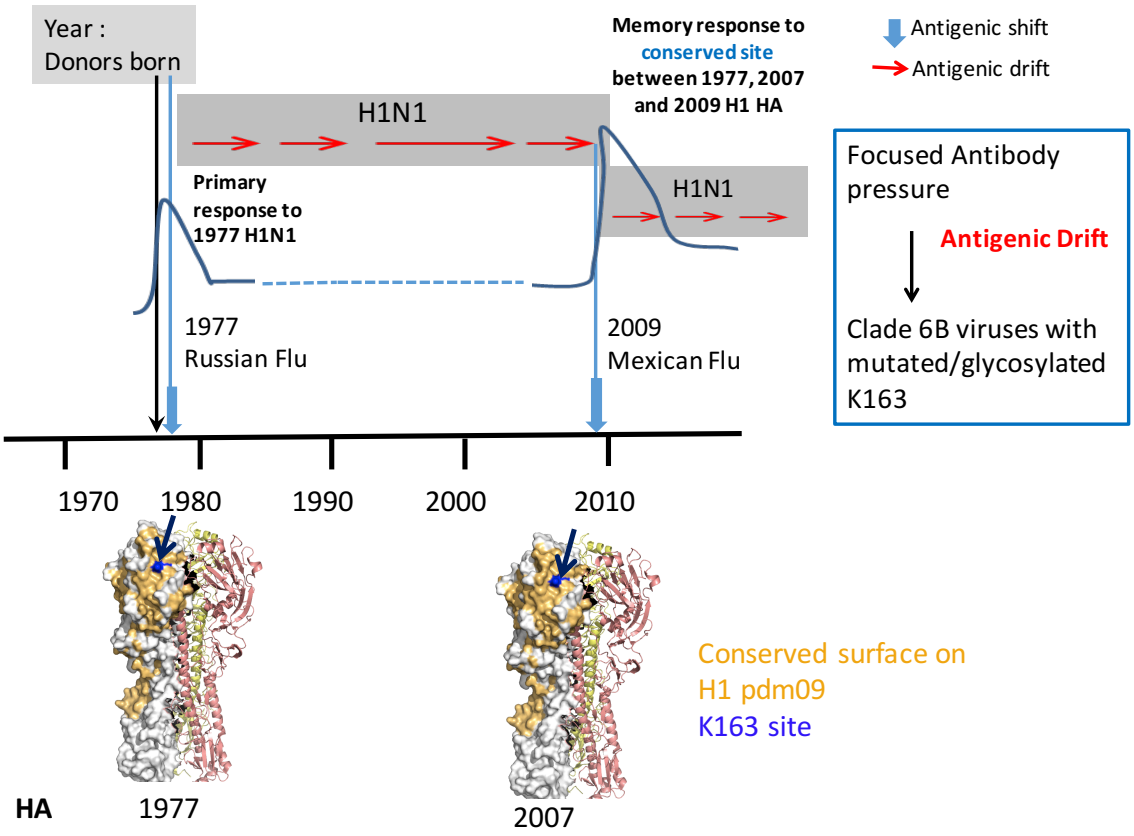

Figure 3. 11 ***Graphical summary of the finding in this chapter****. Monoclonal antibodies isolated post pdmH1N109 vaccination from donor H, born before 1977 H1N1, showed a repertoire of head antibodies with cross reactivity to 1977 and a subset of antibodies also reactive to seasonal H1N1 strains between 1977-2007. This spectrum was possible since the donor was primed during his childhood to 1977 H1N1 haemagglutinin and memory B cells to the conserved surface (golden conserved surface mapped on to 2009 H1 (PDB:3LG)) were selected by exposure to the 2009 H1. The K163 residue lies within the conserved patch to which the secondary response was focused. This focusing of antibodies to one site in a middle-aged donor such as donor H, made the response functionally monoclonal, favouring the selection of escape variants which gave rise to and spread of clade 6B drift viruses.*

3.4.9 Additional donor sera focused to K163 site

We compared the reactivity of sera from 41 donors post vaccination and infection, against A/California/07/2009, K163 variants and the clade 6B viruses. We found a second donor's sera (TIV-20) who also lost neutralisation to H1N1 viruses with K163 substitutions (Table 3.3 and (Figure 3. 9). These findings are in line with the serological survey of Linderman et al. (Linderman et al. 2014), who reported 42% of sera from donors born before 1979 showed reduced reactivity with clade 6B isolates. Both donors focused to K163 site in our study were born before 1982 (2 of 28).

In supplementary figure 3.2, Rod Daniels compared HI titres of serum against various clades of H1N1pdm09 viruses and found that sera from donor H, TIV-20 and another donor TRE (collected by Antonio Lanzavecchia's lab) had reduced HI titres to clade 6B viruses, while the sera from other donors (M, J and N) had HI titres equivalent to A/California/07/2009 and clade 6B viruses (Appendix 3.2).

3.4.10 The rise of clade 6B viruses

Clade 6B viruses emerged in 2013/14 with the characteristic mutation in K163 and other residues (Figure 3. 12). This clade has dominated since then and now has branched out as clade 6B.1 virus (in 2015/16), which has the additional neighbouring S162N substitution resulting in glycosylation of the site (Figure 3. 13). The clade 6B.1 is now predominant in both southern and northern hemispheres. The H1N1 vaccine strain for 2016/17 season in the Southern hemisphere has now been updated to clade 6B.1 virus A/Michigan/45/2015. Ferret sera have still not detected a major antigenic change in these viruses, but on the basis of the evidence that a selection of human sera and antibodies failed to recognise the clade 6B.1 viruses the WHO committee decided to update the vaccine. Our data was presented by our collaborator Rod Daniels at the 2016 Vaccine Selection Meeting and

contributed to the evidence that drove this decision. This is the first time that an influenza A vaccine has been updated in the absence of data derived from ferret antisera.

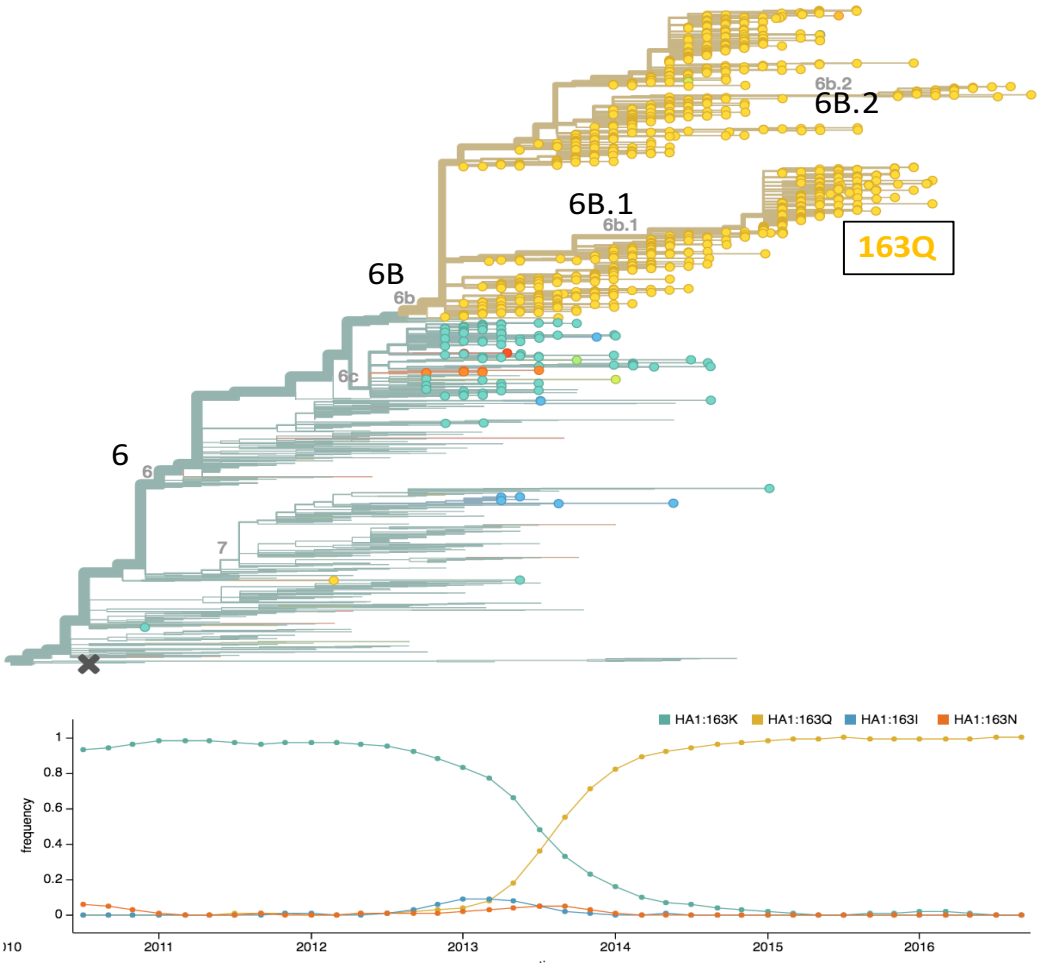

Figure 3. 12 ***Emergence of clade 6B viruses with characteristic substitution in K163Q****. The figure was generated using nextflu.org (Neher and Bedford 2015). Cross denotes the vaccinating strain. Note that on the website the authors use lower case 6b, but the Worldwide Influenza Centre reports and other publications use the convention of upper case 6B.*

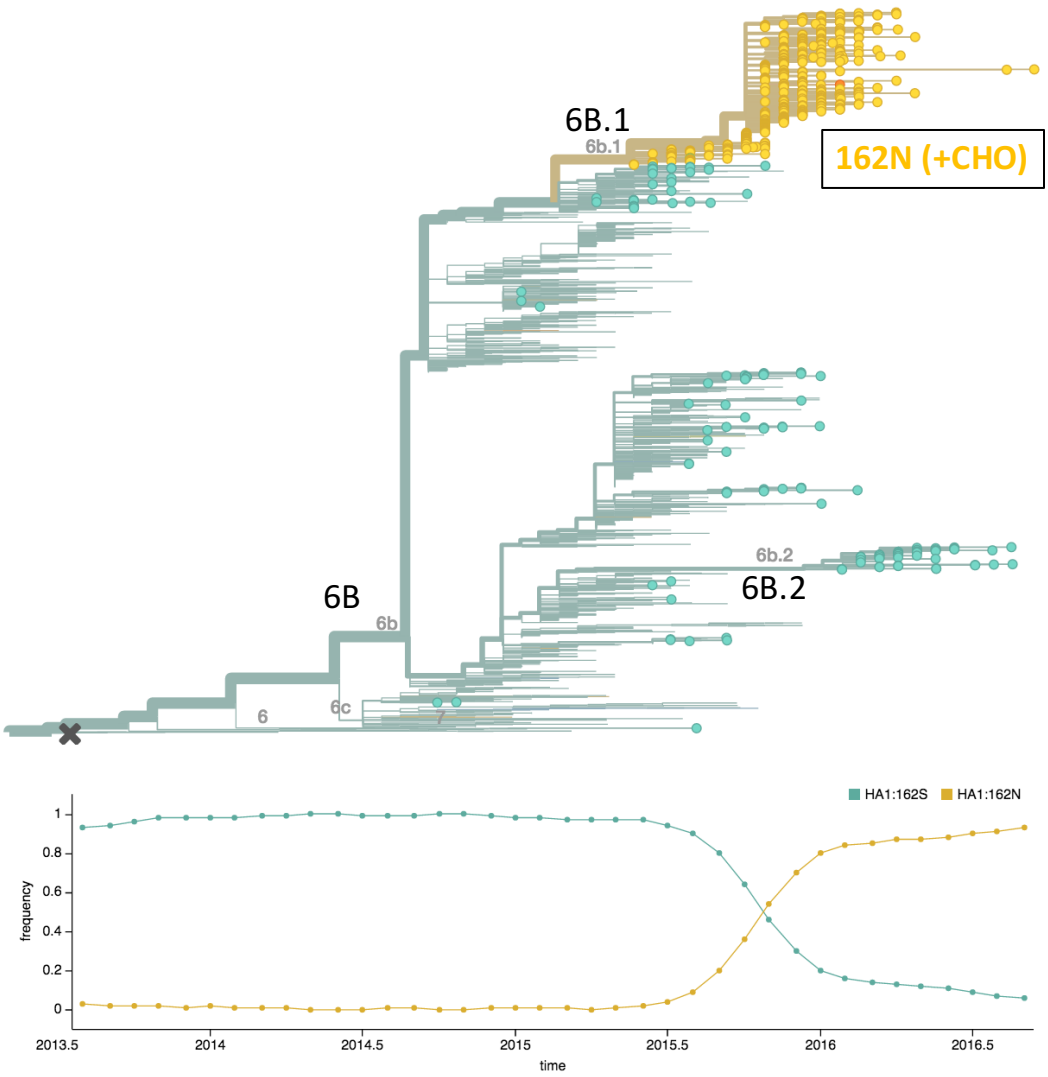

Figure 3. 13 ***Emergence of clade 6B.1 in 2015/16 with S162N substitution resulting in glycosylation and masking of the residue 163 Sa site****. The figure was generated using nextflu.org (Neher and Bedford 2015).*

3.5 Broadly cross-reactive stem antibodies

Besides head antibodies, there were 13 antibodies directed to the stem of haemagglutinin (13 out of 157, 8.2%). Eight antibodies were encoded by VH1-69, four by VH3-23 and one by VH4-39 ((Figure 3. 4) and (Table 3.2)). The stem antibodies were identified by a combination of assays: binding to HA protein, lack of haemagglutination inhibition activity, cross-competition for binding with stem antibody C179 (Okuno et al. 1993), lack

of reactivity in western blots and heterosubtypic neutralisation of H5 influenza pseudotyped virus. The EC50 concentration of the stem antibodies required to neutralise H1N1pdm09 virus (X179A) was significantly higher (average 366 ng/ml for VH1-69 antibodies) than that for head specific antibodies (ANOVA, $P<0.001$) (Figure 3. 5). However, the EC50 for neutralisation by stem antibodies was found to be approximately 40-fold lower when pseudotyped influenza viruses were used. This was also the case with broadly reactive stem antibodies in the literature which neutralised the lenti-pseudotyped viruses at ~1000-fold lower concentration than wild type viruses (Corti et al. 2010). Our stem antibodies also neutralised H5-pseudtoyped influenza virus (coated with H5 HA A/Vietnam/1203/2004) with EC50 ~ 1 µg/ml (Figure 3. 5), which matches the neutralisation of H5-psedutotyped virus by serum post vaccination (Figure 3. 1). As found by others (reviewed in (Corti and Lanzavecchia 2013; Ekiert and Wilson 2012)) we isolated rare stem antibodies (T3-5D in Figure 3.5) that cross-reacted between H1 and H5 (Group 1) and H3 (Group 2) haemagglutinins. We have since isolated a second example, mAb Z3B2 from a Chinese child with an asymptomatic infection with the H7N9 virus (data not shown).

3.6 Therapeutic Potential

Testing of the protective effect of these antibodies was done by Timothy Powell. Representative antibodies from three groups representing different specificities: head specific, head cross-reactive and stem, at a dose of 10 mg/kg, were inoculated by intraperitoneal injection in DBA/2 mice 24 h post challenge with X179A virus (that contained HA from A/California/07/2009 virus). The DBA/2 mice strain is extremely sensitive to influenza infection (Srivastava et al. 2009) and we used approximately 150 LD50 virus (1 LD50 means dose required to cause 20% weight loss in at least 50% of the recipients). All three antibodies as therapy protected mice from more than 20% weight

loss ($P<0.01$) and reversed the weight loss after 3 days (Appendix 3.3). The control head specific antibody from another donor 2-12C (VH5-55) also protected all mice (n=6) from more than 20% weight loss. In contrast, the control H3 head specific antibody Q11C11 and PBS given mice showed no protection from infection by the H1N1 challenge virus.

It is noteworthy that the VH3-15 antibodies, although they lost reactivity to the recent clade 6B viruses, would have been effective therapeutics against H1N1 viruses for at least 19 years (1994-2013).

CHAPTER 3 DISUCSSION

This chapter describes the isolation and characterisation of monoclonal antibodies from an individual whose sera showed reduced neutralisation to drift variants of H1N1pdm09 - clade 6B viruses. Clade 6B appeared in the 2013/14 season, which is known for vaccine mismatch and severe influenza infection in the middle-aged population (European Centre for Disease Prevention and Control 2014). The majority of the response from this donor was towards the head region of haemagglutinin, and focused to the K163 site, which is a defining mutation for the clade 6B viruses.

Possible weaknesses of this study

In our sorting experiments, we enriched for specific B cells by staining with haemagglutinin. The drawback of specific sorting is that plasmablasts that may have lost expression of surface B-cell receptor would be missed. In addition, our PCR technique selects for IgG expressing clones. Thus, we acknowledge that our collection of antibodies may not represent the complete repertoire of B cells specific for HA. However, we can rule out the possibility that use of HA for sorting may have selected antibodies specific to certain epitopes. We have shown that our HA protein preparation bound to

antibodies to different sites, provided by various labs around the world. Moreover, we were able to reproduce the results from monoclonal antibodies with the donor's serum.

VDJ gene use

A relatively limited number of VH and VK/L genes have been used by donor H in response to H1 haemagglutinin. Out of a total of 11 VH sets used for encoding 157 antibodies, six VH-related sets provided 96% of the response. Although the response is markedly polyclonal, a single clone expanded from each VH set is seen to dominate. Here a "clone" is defined by a unique heavy chain VDJ gene rearrangement and the D region reading frame. Clonally expanded antibodies were diversified by extensive somatic mutations to the extent that each of the 157 antibodies had a unique amino acid sequence. The high frequency of somatic mutations ranging from 7 (for head specific antibodies) to 17 (for head cross-reactive and stem cross-reactive antibodies) compared to 2-5 mutations in novel Ebola antibodies discussed in Chapter 6, indicates that these may have been derived from pre-existing memory B cells that had undergone a germinal centre reaction more than once (Victora and Wilson 2015). These antibodies are high affinity and cross-reactive (to seasonal H1N1 and/or A/USSR/70/1977), suggesting they may have been selected based on their affinity and cross-reactivity to the new strain (H1N1pdm09). This finding fits with the theory of 'original antigenic sin' (OAS) envisaged by Thomas Francis (Francis 1960) or 'antigenic seniority' (Lessler et al. 2012).

As the antibodies from the pool of memory B cells gets selected, and undergoe Somatic Hyper-Mutation (SHM) and expansion in germinal centres (Gitlin, Shulman, and Nussenzweig 2014), the response gets narrower leading to immunodominance to one or more epitopes. Immunodominance and focusing of antibody responses to a single antigenic site has also been shown in primary influenza infection in mice (Patera et al.

1995). This contrasts to studies showing that the primary antibody response in mice was very diverse after a single intranasal infection (Staudt and Gerhard 1983). The discrepancy may be due to different vaccination protocols and adjuvants.

The clone VH3-7*01/JH6*02 antibodies are predominant in our set representing 56% of the response. These antibodies rearranged with D gene 3-16*01, 3-3-*01 and 3-3*02. Head antibodies to the same epitope encoded by VH3-7/JH6 have been seen in other individuals as well (Krause, Tsibane, Tumpey, Huffman, Briney, et al. 2011), where they were rearranged with a different group of D gene segments (3-16*02, 3-22*01, 6-13*01 and 4-17*01). However, these D gene segments are closely related and share a 'DTY' motif at the D-J junction. Moreover, the Krause et al. antibody 4K8 (VH3-7*01) (Krause, Tsibane, Tumpey, Huffman, Briney, et al. 2011), selected the identical K163E substitution as our antibody T2-6A (VH3-7). Krause et al. also showed that although their antibodies fail to cross-react with former seasonal H1 strains (including A/Brisbane/59/2007), they neutralised the H1N1 viruses from 1977 and 1918. The region surrounding K163, is conserved in these 2009, 1977 and 1918 viruses.

Additionally, from the deep sequencing of B cells after a week of influenza vaccination, Jackson et al. found that use of clonal lineage VH3-7/JH6 with a HCDR3 of 18 amino acids was the most prominent feature (Jackson et al. 2014), similar to our donor. This is described as the convergent signature antibody response to 2009 H1 haemagglutinin. This finding that the dominant focused clone can be detected by deep sequencing of peripheral blood lymphocytes seven days after vaccination may be a very useful way of quickly identifying clones of antibodies that are likely to be playing a significant role in selecting antigenic drift viruses in the community.

Antibody Footprints

Antibodies from VH3-7 and VH3-15 sets recognise the same site around K163, however their footprints on the haemagglutinin may differ as they show more cross-reactivity with earlier seasonal viruses. This difference is reflected also in H1pdm09 clade 6A viruses. Clade 6A viruses have a glycosylation site at K119N but no K163 change. The VH3-7 antibodies recognise clade 6A viruses in the HI assay (done at the Crick Worldwide Influenza Centre), unlike VH3-15 clones T2-5D and T1-9B that do not (Appendix 3.1). The head specific VH-18 clone is also severely affected. The K119 residue may be within the footprint of VH3-15 and VH1-18 antibodies, but missed by the VH3-7 set (Appendix 3.1).

Subtle differences in footprint are also seen within the clones of the VH3-15 set, which have the same VDJ rearrangement but differ by somatic mutations. For example, clones T2-5D and T1-9B have the same VDJ rearrangements and light chains, but one neutralises A/Beijing/262/1995 (Table 3.3) and the other does not. In this case the somatic mutations must be responsible for this subtle change in specificity. This diverse repertoire of naturally produced human antibodies derived from the same clone but differing by somatic mutations, mirrors the classic studies on clonal antibody diversity in individual BALB/C mice by testing binding to 51 similar or antigenically drifted viruses (Staudt and Gerhard 1983). That study demonstrated a similar VH gene restricted usage with polyclonality and suggested the role of somatic mutations for this fine “paratypic” diversity (Clarke et al. 1985; Radic 2008; Corti and Lanzavecchia 2013).

Antigenic sin in the modern sense

We didn't come across antibodies from donor H that cross react for binding on drifted viruses, but which are now non-neutralising, i.e. “antigenically sinful” in its modern

usage. However, we did find some control antibodies with this property. For example, the antibody Q11A6 from a different individual binds the K130E mutant haemagglutinin (Figure 3. 7), but this affinity was not enough for neutralisation. If these medium affinity non-neutralising antibodies were selected in the germinal centre for expansion, they could become dominant and weaken the overall humoral response. Examples of this happening after exposure to certain combinations of viruses (for instance the H1 viruses A/PR/8/34 and A/FM/1/1947) has been well described in the mice (Kilbourne et al. 2002; Skountzou et al. 2010) and ferret (Huang et al. 2013; Carter et al. 2013), and may account for occasional problems with reduced protection after repeat vaccination in humans (Ohmit et al. 2014). It would be explained by the affinity for antigen required for selection of a B cell in the germinal centre being lower than that required for neutralisation, for which there is now compatible evidence (Kuraoka et al. 2016).

The link between antibody focusing and selection of actual drift variants

Linderman et al. related the appearance of clade 6B viruses in 2013/14 with a high frequency of severe infections in the middle-aged population (Linderman et al. 2014). We have extended these results by showing that multiple monoclonal antibodies from such individuals can focus to a single site to such an extent that they could select and spread antigenic drift viruses that are now circulating in nature. The virus may spread with success when there are enough susceptible individuals in the population, and they could transmit the drift variant to other individuals with different histories of antigen exposure and focusing on different antigenic sites. Ours is the first study to show the link between antibody focusing and selection of actual drift variants in humans. Although this concept has existed for a long time, it was not directly demonstrated (Haaheim 1980a, 1980b;

Patera et al. 1995; Gerber, Loosli, and Hambre 1955; Natali, Oxford, and Schild 1981; Lambkin et al. 1994; Hensley et al. 2009).

Focusing at the site defined by K130 has been found in a different age cohort (born 1983-96) by Li et al. (Li et al. 2013). Our antibodies 2-12C and Q11A6, isolated from different donors, lost neutralisation to K130E virus and may represent this focused response. The K130 site is widely separated from K163 and is a mutually exclusive epitope. In serological analysis, we found two donors (born after 1983) whose neutralisation titre was reduced by the K130 substitution, which corresponds to the serological analysis by Li et al. (Li et al. 2013). Li et al. have shown that individuals who were born between 1983-1996, who were primed by H1 haemagglutinin which retained a Lysine (K) at position 130, narrowly focused their response on this region on exposure to H1N1pdm09. This K130 residue is intact in most recent circulating viruses, which indicates that there is no immune pressure for this site to change at the moment. However, there are rare strains which have acquired changes at this site, for example A/Moldova/15808/2015 which has acquired a K130N mutation. This suggests that mutation at K130 in post 2009 H1 viruses is not completely prohibited by fitness costs. Given that K130 has been involved in major antigenic change in the past, this site needs to be in the watch list for the next season.

We haven't studied the mechanism of focusing but there are three possibilities, i) a limited response in the first exposure resulting in a limited pool of memory B cells (Wang, Skehel, and Wiley 1986; Patera et al. 1995) ii) selection of cross-reacting B cells from the available repertoire induced by primary exposure to a related influenza virus (Francis 1960; Destgroth and Webster 1966; Morens, Burke, and Halstead 2010; Xu et al. 2010; Wrammert et al. 2011; Lessler et al. 2012; Li et al. 2013; Miller et al. 2013; Fonville et al. 2014) and iii) selection of B cells that influence antigen processing and

presentation to T cells in the germinal centre by the antibody altering the degradation of antigen - a process called "T-B reciprocity" (Manca et al. 1985; Gitlin, Shulman, and Nussenzweig 2014; Barnett et al. 1989; Moss, Tree, and Watts 2007; Watts et al. 1998; Shirai et al. 1999). These mechanisms may act together and are not mutually exclusive. The first possibility is not well supported as the primary response to new antigens appears to be very diverse and encoded by many VH families, as discussed for the response to Ebola GP in Chapter 6.

Human Monoclonal Antibodies versus Ferret antisera

Ferret antisera raised to primary infection by human influenza have been used to monitor antigenicity of new viruses since the 1930's. In general, antigenic changes detected by ferret sera have correlated well with antigenic changes linked to epidemics, particularly for the H3N2 viruses (Koel et al. 2013).

However, we have clearly shown by using human monoclonal antibodies and sera from vaccinated individuals that clade 6B pdmH1N1 viruses are antigenically different from A/California/07/2009 virus, whereas the ferret antisera used by the WHO Collaborating Centre failed to distinguish between these two clades of viruses. It is known that the ferret antibody response to A/California/07/2009 is focused on residues 153-155 (Chen et al. 2010). The loss of reactivity to A/Bayern/69/2009 with the G155E substitution by ferret sera to A/California/07/2009 in standard HI assays supports this (Appendix 3.1, 3.2). Therefore, the ferret antisera were unable to distinguish the drifted clade 6B viruses.

These observations are evidence that human individuals can focus their antibodies to an antigenic site, different to that by the ferret. Using ferret antisera to determine the antigenic relatedness between virus isolates may not always predict the specificity of human antibody responses (Li et al. 2013; Linderman et al. 2014; Huang et al. 2015).

We propose that panels of selected human monoclonal antibodies, that have been characterised by their selection of variants matching existing drifted viruses detected in isolates from humans, could be used alongside ferret antisera to improve the prediction of antigenic drift. Moreover, the monoclonal antibodies may prove to have therapeutic value.

FUTURE PLANS

We have shown in this chapter that in principle monoclonal antibodies isolated from appropriate individuals can be used to recapitulate antigenic drift *in vitro,* and thus could be used to predict the direction of evolution that the circulating virus may take. We were lucky in this study to find an individual whose serum showed the characteristic loss of neutralisation of the latest clade 6B viruses described by Linderman et al. (Linderman et al. 2014).

These experiments were retrospective. In future studies, we hope to be able to predict antigenic drift *before it happens.* The question then arises how to identify the individuals who can donate the most informative antibodies for this to work. The recent evidence from the pdmH1N1 viruses clearly shows that certain age cohorts can become susceptible to new variants as they focus their antibody responses on the localised regions of the HA surface that have recently mutated, presumably under selective pressure from the same antibodies in these cohorts. The particular age cohort that focuses sufficiently to select variant viruses most likely depends on their particular exposure history, as revealed in the variety of antibody landscapes in different age cohorts (Fonville et al. 2014). Screening age stratified cohorts by deep sequencing of peripheral blood lymphocytes at day seven post vaccination may identify dominant clones of relevant B cells (Jackson et al. 2014). An alternative approach would be to randomly sample monoclonal antibodies from all

age cohorts, select variant viruses, compare the sequences to the pool of circulating viruses, and select those represented at some frequency for screening against age stratified sera for neutralisation.

We are now developing panels of informative human monoclonal antibodies for distribution to the WHO Collaborating Centres (in collaboration with John McCauley, Rod Daniels and Arthur Huang) to be used to monitor antigenic change in H1N1 and H3N2 circulating influenza viruses. Information obtained from these panels, together with the ferret HI data and virus phylodynamics (nextflu.org), may provide stronger predictions of future antigenic drift. This could improve overall vaccine efficacy with the capacity to reduce mortality from influenza infection.

Appendix 3. 1 Antigenic analysis of influenza A(H1N1)pdm09 viruses: post-infection ferret antisera and human monoclonal antibodies

(Data by Rod Daniels, Worldwide Influenza Centre, The Francis Crick Institute).

				Haemagglutination inhibition titre																		
				Post-infection ferret antisera												Human monoclonal antibodies[*2,3]						
Viruses		Collection date	Passage history	A/Cal 7/09	A/Bayern 69/09	A/Lviv N6/09	A/Chch 16/10	A/Astrak 1/11	A/St. P 27/11	A/St. P 100/11	A/HK 5659/12	A/Sth Afr 3626/13	A/Slov 2903/15	A/Slov 2903/15	A/Scot P2/15	1 T2-6A	2 T2-7D	3 T2-8A	4 T2-11C	5 T2-5D	6 T1-9B	7 2-12C
	Passage history			Egg	MDCK	MDCK	Egg	MDCK	Egg	Egg	MDCK	Egg	MDCK	Egg	Egg	VH3-7	VH3-7	VH3-33	VH1-18	VH3-15	VH3-15	VH5-55
	Ferret number			NIB F05/14[*1]	F09/15[*1]	F14/13[*1]	F15/14[*1]	F22/13[*1]	F26/14[*1]	F24/11[*1]	F30/12[*1]	F3/14[*1]	F01/16[*1]	F02/16[*1]	F03/16[*1]	Head S	Head S	Head S	Head S	Head CR	Head CR	Head S
	Genetic group			1	1	1	4	5	6	7	6A	6B										Control
REFERENCE VIRUSES																						
A/California/7/2009	1	2009-04-09	E3/E2	1280	640	ND	640	640	640	2560	2560	1280	2560	2560	2560	2560	10240	640	640	320	320	2560
A/California/7/2009	1	2009-04-09	E4/E2	640	320	320	320	640	320	1280	1280	640	ND	640	ND	320	1280	320	320	160	160	640
A/Bayern/69/2009	1	2009-07-01	MDCK5/MDCK1	<	320	320	160	80	40	80	80	80	ND	<	ND	640	1280	320	320	160	80	640
A/Lviv/N6/2009	1	2009-10-27	MDCK4/SIAT1/MDCK3	80	1280	640	320	80	80	80	160	80	ND	80	ND	640	2560	320	320	160	160	1280
A/Christchurch/16/2010	4	2010-07-12	E1/E3	1280	1280	1280	5120	1280	640	2560	2560	1280	2560	2560	2560	320	2560	2560	40	80	40	5120
A/Astrakhan/1/2011	5	2011-02-28	MDCK1/MDCK5	1280	640	640	640	1280	640	2560	1280	1280	2560	2560	2560	2560	5120	5120	320	320	160	2560
A/St. Petersburg/27/2011	6	2011-02-14	E1/E4	1280	1280	640	640	1280	640	2560	2560	1280	2560	2560	5120	5120	20480	20480	640	320	320	5120
A/St. Petersburg/100/2011	7	2011-03-14	E1/E3	2560	1280	640	640	1280	1280	2560	2560	1280	2560	2560	5120	5120	20480	20480	640	640	320	5120
A/Hong Kong/5659/2012	6A	2012-05-21	MDCK4/MDCK2	320	160	160	160	320	160	640	640	320	640	640	640	1280	5120	5120	40	<	<	1280
A/South Africa/3626/2013	6B	2013-06-06	E1/E3	1280	640	640	640	1280	640	1280	640	1280	1280	1280	2560	<	<	<	<	<	<	2560
TEST VIRUSES																						
A/Slovenia/2903/2015	6B	2015-10-26	MDCKx/MDCK2	1280	640	ND	1280	1280	640	2560	1280	1280	2560	2560	2560	<	<	<	<	<	<	2560
A/Slovenia/2903/2015	6B	2015-10-26	E4	2560	640	640	1280	1280	1280	5120	2560	1280	5120	2560	2560	<	<	<	<	<	<	2560
A/Scotland/P2/2015	6B	2015-11-19	E4	1280	640	ND	1280	1280	1280	5120	2560	1280	5120	2560	2560	<	<	<	<	<	<	2560
A/Lisboa/30/2015	6B	2015-11-08	MDCK1/MDCK1	640	320	ND	640	640	320	1280	1280	640	2560	2560	1280	<	<	<	<	<	<	2560
A/Iran/116675/2015	6B	2015-11-28	E1/E1	1280	640	ND	1280	1280	640	2560	1280	1280	2560	2560	2560	<	<	<	<	<	<	1280
A/Iran/109635/2015	6B	2015-10-08	SIAT1/MDCK1	1280	640	ND	1280	1280	640	2560	1280	1280	2560	2560	2560	<	<	<	<	<	<	2560
A/St. Petersburg/349/2015	6B	2015-11-25	C1/MDCK1	1280	640	ND	1280	1280	640	2560	1280	1280	2560	2560	2560	<	<	<	<	<	<	2560
A/Finland/546/2015	6B	2015-11-26	MDCK 1/MDCK1	640	320	ND	640	640	640	2560	1280	1280	2560	2560	2560	<	<	<	<	<	<	1280
A/England/357/2015	6B	2015-10-26	SIAT1/MDCK1	1280	640	ND	320	1280	640	2560	1280	640	2560	2560	2560	<	<	<	<	<	<	2560
A/Antsirabe/4186/2015	6B	2015-09-29	MDCK1/MDCK1	1280	640	ND	640	1280	640	2560	1280	1280	2560	2560	2560	<	<	<	40	<	<	2560
A/Maevatanana/4189/2015	6B	2015-09-24	MDCK2/MDCK1	1280	640	ND	640	1280	640	1280	1280	1280	2560	2560	2560	<	<	<	<	<	<	1280
A/Mecklenburg-Vorpommern/19/201!	6B	2015-12-21	C2/MDCK1	640	320	ND	320	640	320	1280	640	640	1280	1280	1280	<	<	<	<	<	<	1280
A/Bayern/148/2015	6B	2015-11-24	C2/MDCK1	640	320	ND	320	640	320	1280	640	640	1280	1280	1280	<	<	<	<	<	<	1280
A/Austria/891161/2015	6B	2015-11-24	SIAT1/MDCK1	640	320	ND	320	640	320	1280	640	640	1280	1280	1280	<	<	<	40	<	<	1280
				Vaccine																		

HI assay conducted with turkey RBCs

* Superscripts refer to antiserum properties (< relates to the lowest dilution of antiserum used)

[1] < = <40; [2] < = <40 where an initial concentration of 10µg/ml mAb (titre of 40 equivalent) was used (so a titre of 20480 = ~20ng/ml); [3] mAbs have been described in Huang et al (2015) *J Clin Invest* 125, 2631-45: the 'T' series of mAbs are sensitive to HA1 K163Q/E substitutions (and addition of cho at position 162) while 2-12C is sensitive to HA1 K130E substitution

Appendix 3. 2 Antigenic analysis of influenza A(H1N1)pdm09 viruses: post-infection ferret antisera and human post-vaccination antisera

(Data by Rod Daniels, Worldwide Influenza Centre, The Francis Crick Institute).

				Haemagglutination inhibition titre														
				Post-infection ferret antisera										Human sera[*1]				
Viruses		Collection date	Passage history	A/Cal 7/09	A/Bayern 69/09	A/Lviv N6/09	A/Chch 16/10	A/Astrak 1/11	A/St. P 27/11	A/St. P 100/11	A/HK 5659/12	A/Sth Afr 3626/13	A/Slov 2903/2015	donor M	donor J	donor N	TIV20	donor H	TRE
	Passage history			Egg	MDCK	MDCK	Egg	MDCK	Egg	Egg	MDCK	Egg	Egg						
	Ferret number			F05/14[*1]	F09/15[*1]	F14/13[*1]	F15/14[*1]	F22/13[*1]	F26/14[*1]	F24/11[*1]	F30/12[*1]	F03/14[*1]	F02/16[*2]						
	Genetic group				1	1	4	5	6	7	6A	6B	6B.1						
REFERENCE VIRUSES																			
A/California/7/2009	1	#########	E4/E3	1280	320	320	320	640	320	1280	1280	640	640	160	320	80	160	320	160
A/Bayern/69/2009	1	2009-07-01	MDCK5/MDCK1	<	320	320	160	80	40	80	80	80	<	160	160	<	80	80	80
A/Lviv/N6/2009	1	2009-10-27	MDCK4/SIAT1/MDCK3	80	1280	1280	320	80	80	80	160	80	80	640	640	80	320	320	320
A/Christchurch/16/2010	4	2010-07-12	E1/E3	1280	1280	1280	2560	2560	640	2560	2560	1280	2560	640	640	160	80	160	160
A/Astrakhan/1/2011	5	2011-02-28	MDCK1/MDCK5	1280	640	640	1280	1280	640	2560	2560	1280	2560	320	640	80	160	320	320
A/St. Petersburg/27/2011	6	2011-02-14	E1/E4	1280	640	640	640	1280	640	2560	1280	1280	1280	320	640	80	160	320	320
A/St. Petersburg/100/2011	7	2011-03-14	E1/E3	1280	1280	640	1280	1280	640	2560	2560	2560	2560	160	320	80	160	160	160
A/Hong Kong/5659/2012	6A	2012-05-21	MDCK4/MDCK2	320	160	160	320	320	320	1280	640	640	640	320	320	80	160	320	320
A/South Africa/3626/2013	6B	2013-06-06	E1/E3	640	640	640	640	640	640	2560	1280	1280	1280	320	320	80	<	40	40
A/Slovenia/2903/2015	6B.1	2015-10-26	E4	1280	640	640	2560	2560	1280	5120	2560	1280	2560	320	320	160	40	40	40
TEST VIRUSES																			
A/Oman/6329/2015		2015-11-17	SIAT2/MDCK1	1280	640	640	1280	1280	640	2560	2560	1280	2560	640	640	80	<	<	40
A/Oman/6337/2015		2015-11-18	SIAT2/MDCK1	1280	640	320	640	1280	640	2560	1280	1280	2560	80	40	80	<	<	80
A/Oman/6268/2015		2015-12-11	SIAT2/MDCK1	1280	640	320	640	1280	640	2560	2560	1280	2560	640	640	80	<	<	40
A/Istanbul/201/2015		2015-12-31	MDCK1/MDCK1	1280	640	320	640	640	320	2560	1280	1280	2560	80	80	<	<	<	<
A/Moldova/45.03/2016		2016-01-20	MDCK1	1280	640	320	640	1280	640	2560	2560	1280	2560	640	320	80	<	<	40
A/Moldova/47.03/2016		2016-01-20	MDCK1	1280	640	640	640	1280	640	2560	2560	1280	2560	640	640	80	<	<	40
A/Moldova/59.03/2016		2016-01-21	MDCK1	1280	640	320	640	1280	640	2560	2560	1280	2560	640	320	80	<	<	40
A/Moldova/62.03/2016		2016-01-22	MDCK1	1280	1280	320	640	1280	640	2560	2560	1280	2560	640	640	80	<	<	40
A/Greece/65/2016		2016-01-22	MDCK1	1280	640	640	640	1280	640	2560	2560	1280	2560	640	640	80	<	<	40

HI (Turkey RBC) — Vaccine

* Superscripts refer to antiserum properties (< relates to the lowest dilution of antiserum used) — Egg-propagated viruses

[1] < = <40; [2] < = <80

Appendix 3. 3 Protection against influenza challenge with the antibodies described in the text. *The in vivo therapeutic effect of antibodies: head specific VH3-7, head cross-reactive VH3-15, stem cross-reactive VH1-69, head specific VH5-51, and H3 head specific Q11C11 in X179A challenged mice (n=6 per group). Twenty-four hours after intranasal infection with 150 LD50 X179A virus, DBA/2 mice were treated with a single dose of 10 mg/kg antibody or PBS administered to the peritoneal space.*

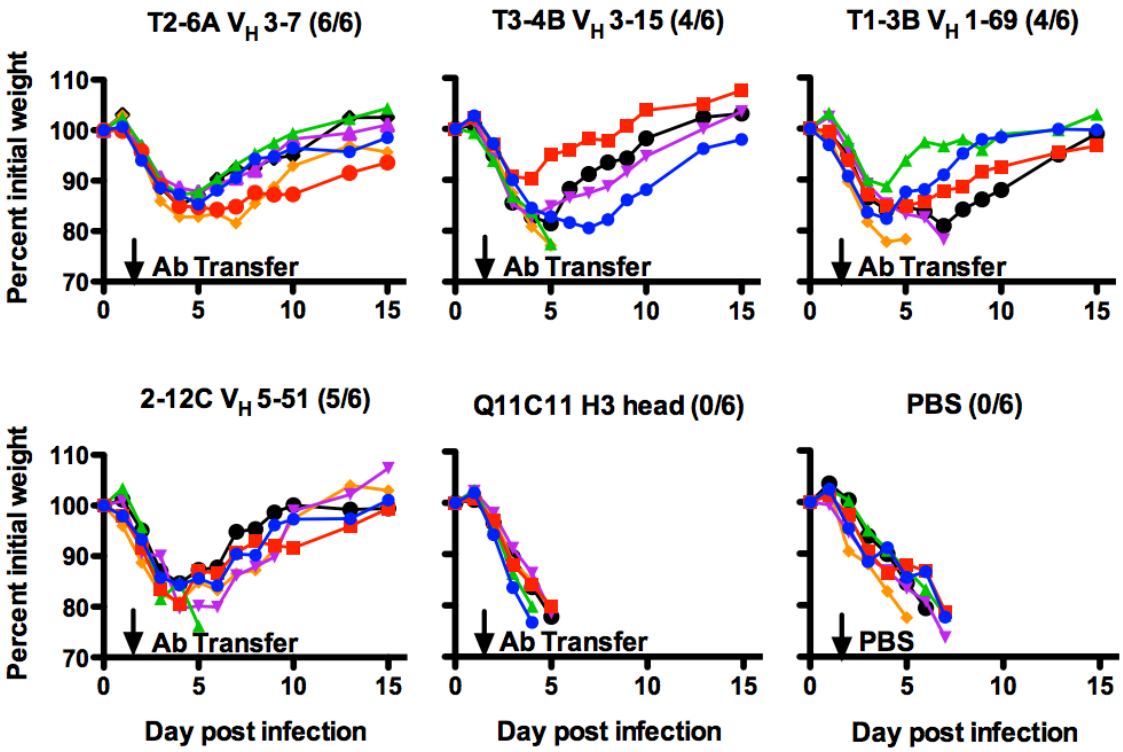

CHAPTER 4 The evolution of H3N2 influenza studied by application of human monoclonal antibodies

CHAPTER 4 INTRODUCTION

H3N2 virus after entering the human population in 1968 established itself until now as a seasonal influenza. Unlike the H1N1 viruses, which disappeared between 1958-1976, and have recently undergone an antigenic shift in 2009, the H3N2 viruses have been undergoing continuous evolution in humans since 1968. More than 30 vaccine updates have been recommended to keep pace with the evolution of this virus. In some years, the number of H3N2 infections were more than expected, often associated with vaccine mismatch. Better vaccine efficacy is possible with more accurate monitoring and prediction of antigenic drift.

For H3N2, the antigenic sites in the globular head domain of haemagglutinin are described as sites A-E based on murine monoclonal antibody variant selection, and sequence changes in natural virus isolates (Webster and Laver 1980; Webster et al. 1980; Wiley, Wilson, and Skehel 1981; Wilson, Skehel, and Wiley 1981; Skehel et al. 1984). Each site has a variety of epitopes definable with murine monoclonal antibodies, and a change in one amino acid may cause the antibody to lose its binding or neutralisation or both. As the virus evolves these sites acquire amino acid substitutions, and a subset of these (N-X-S/T) result in the epitopes becoming masked by N-linked glycosylation. H3 hemagglutinin has continually increased the number of glycosylation sites since 1968. The combination of new glycosylation sites and sequence changes close to the receptor

binding site has been associated with a continuous lowering of affinity for α-2,6 sialic acid, and almost complete loss of binding to α-2,3 (Lin et al. 2012).

This loss of affinity for sialic acid has resulted in the associated loss of the ability to agglutinate red cells in more than half of recent isolates (The Crick Worldwide Influenza Centre 2016), which has led to technical problems in defining antigenicity using the standard haemagglutination inhibition (HI) assay (Gulati et al. 2013). In addition, the neuraminidase can now contribute to sialic acid binding to such a degree that the traditional HI assay must be done in the presence of neuraminidase inhibitors in order to interpret the results (The Crick Worldwide Influenza Centre 2016). Finally, the loss of binding to α-2,3 sialic acid results in frequent adaptive mutations in or near the sialic acid binding site when the viruses are grown in the allantoic cavity of fertilised chicken eggs (where α-2,3 sialic acid predominates), and this in turn can alter the antigenicity of the hemagglutinin to such an extent that it may cause vaccine mismatch and even failure, as occurred in 2011 in Canada (Skowronski, Janjua, et al. 2014).

In order to circumvent these issues in screening for relevant human monoclonal antibodies, we have developed a neutralisation assay with replication deficient S-FLU coated (pseudotyped) in H3 haemagglutinins that are fixed in sequence (Powell et al. 2012). As described in chapter 2, S-FLU is grown in MDCK cells that provide the HA coating the virus from a stable transduced gene encoding H3 HA. These are synthesised as codon optimised cDNA from a sequence defined by PCR amplification of virus isolates after minimal culture *in vitro* in MDCK-SIAT cells that maintain wild-type sequences of the HA (McWhite, Meyer, and Wilke 2016). These H3 sequences were chosen through consultation with our collaborators John McCauley and Rod Daniels at

the Crick Worldwide Influenza Centre. For selection of antibody resistant isolates, we necessarily had to use viruses capable of replication in MDCK cells.

Antigenic sites A and B of H3 hemagglutinin are known to be immunodominant in humans, based on serological evidence (Sato et al. 2004; Popova et al. 2012; Xie et al. 2015; Nobusawa et al. 2012) and phylogenetic analysis (Bush et al. 1999). Also, the major antigenic drifts in the past were predominantly due to substitutions at these sites (Koel et al. 2013; Huang and Yang 2011). By studying the antigenic cartography of past H3N2 strains, Koel et al. identified seven residues around the receptor binding site (Site A: 145, and Site B: 155, 156, 158, 159, 189, and 193) that were associated with the major antigenic changes in the past. Our analysis of antibody escape mutants will frequently refer to this study (Koel et al. 2013). The Koel study with H3N2 viruses was based on the reactivity of primary ferret sera, which reflected human serology accurately in comparison to the recent experience with drifted variants of the pandemic H1N1 virus ((Linderman et al. 2014) and discussed in Chapter 3).

The majority of infections with influenza that resulted in hospital admission in 2012-2013 were due to H3N2 infections (Public Health England 2013). In the current scenario, the low vaccine effectiveness in 2014-2015 in the northern hemisphere was attributed to H3N2 vaccine mismatch. New drifted viruses had acquired changes in antigenic site B in the globular head of the hemagglutinin, namely clade 3C.2a and 3C.3a characterised by the substitutions F159Y and F159S respectively. The vaccine strain chosen for the 2015/16 season was clade 3C.3a (A/Switzerland/9715293/2013), but unfortunately the great majority of infections were with clade 3C.2a for which the chosen vaccine was essentially useless (Public Health England 2016; Li et al. 2015). The recommended vaccine for this season 2016/17 is now clade 3C.2a (A/Hong Kong/4801/2014). The

F159S change as a single mutation in site B was detected by a reduced titre in human sera post 2006, 2008 (Popova et al. 2012) and 2014 (Chambers et al. 2015) seasons, which suggested many humans were focusing their antibodies on this site, which could be driving viral evolution. Popova et al. also used a human monoclonal antibody isolated post 2006 to select mutations in H3 HA, one of which selected for the F159S substitution. The significance of this substitution was also reflected in reduced HI titres of standard ferret anti-sera at the Worldwide Influenza Centre (The Crick Worldwide Influenza Centre 2015).

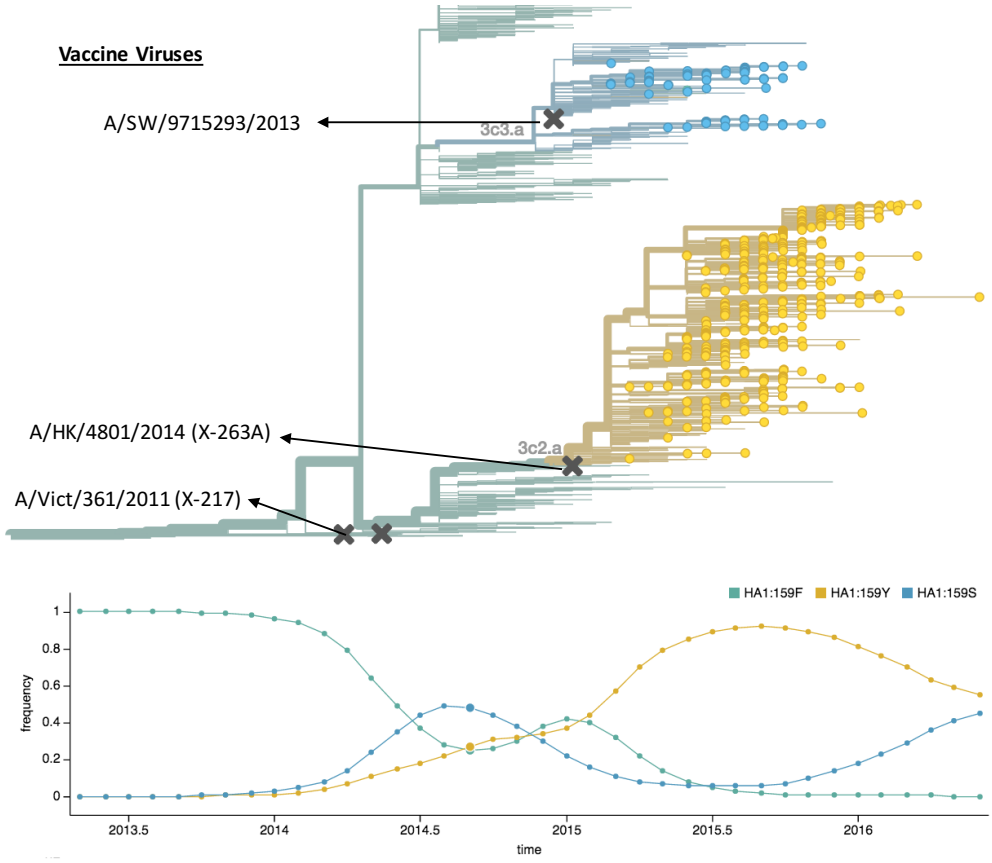

Figure 4. 1 ***The evolution of clade 3C.2a and 3C.3a H3N2 viruses in 2014****. These clades carry characteristic F159Y and F159S substitutions. Crosses denote the vaccine strains. The figure was made using nextflu.org (Neher and Bedford 2015).*

In this project, we have recapitulated antigenic drift *in vitro* by selection of escape viruses with *human* monoclonal antibodies specific for H3N2 viruses. Having shown the proof of principle in chapter 3 with antibodies to H1N1 viruses, we were interested to see if our approach to predicting antigenic drift could be generalised, given the very different evolutionary histories of H1N1 (group 1) and H3N2 (group 2) viruses.

CHAPTER 4 RESULTS

4.1 The majority of isolated antibodies are head specific and potent binders and neutralisers

About 20 monoclonal antibodies to H3 HA were isolated from a young donor (Q) vaccinated in 2012/2013 and one antibody from an elderly donor (N) vaccinated in 2011/2012. Another three antibodies were isolated in 2015/2016 from infected individuals by Arthur Huang in Taiwan.

The H3N2 vaccine strain for years 2011-2013 was A/Victoria/361/2011. Recombinant H3 protein matching this virus was used to specifically sort plasmablasts expressing anti-H3 antibodies from donor Q using the methods outlined in chapter 2. All of the H3 antibodies isolated from these donors were against the globular head region of the HA. They inhibited the haemagglutination of human red blood cells. However, there is a discrepancy in the HI titres when performed with human RBC and turkey RBC. Turkey RBC are used by the WHO collaborating centres to determine the HI titres of ferret sera.

Hemagglutination inhibition (HI): The monoclonal antibodies were either very weak or failed to inhibit the haemagglutinin of the turkey RBC (tRBC) by influenza viruses, whereas they inhibited agglutination of human RBC (hRBC) very well (Table 4.1). In table 4.1, both viruses A/Perth/16/2009 and A/Brisbane/10/2007 are egg-grown and even

though their receptor binding site may have been adapted to α-2,3 sialic acid (SA) they agglutinate hRBC well and our antibodies inhibit the agglutination better than on tRBC. Human RBC contain both 2,3 and 2,6 SA whereas turkey RBC expresses disproportionately more 2,6 SA than 2,3 SA (Ito et al. 1997).

Antibody Q11C11 inhibits hemagglutination of H3N2 viruses from year 1997 to 2012 (Table 4.1). The epitope may have been conserved for this 15-year period. Subtype specific antibodies with reactivity for viruses isolated over long periods are reported in chapter 3 (H1N1) as well.

Table 4. 1 HI titres (in ng/ml) of H3N2 antibodies against various H3N2 viruses using human and turkey RBC

H3N2 Viruses	N2B10		Q11C9		Q11C11		Q11D4
	hRBC	tRBC	hRBC	tRBC	hRBC	tRBC	hRBC
A/Texas/50/2012		>5000		>5000		>5000	
A/PR/16/2009	625	>5000	>5000	—	625	>5000	—
A/Brisbane/10/2007	78	>5000	312	—	78	>5000	156
A/Fuijan/411/2002		—		—		>5000	
A/Sydney/5/1997	—	—	—	—	1666	>5000	—
X31 (1968)	—	—	—	—	—	—	—

Binding and neutralisation: The binding of these antibodies to recombinant H3 HA protein revealed EC50 <20 ng/ml (Figure 4.2A). The antibodies N2B10 and Q11C11, though from two different individuals are encoded by the same VH gene 4-61 and they cross-inhibit each other (data not shown). Figure 4.1 B, C shows the neutralisation of reassortant vaccine viruses X187 (A/Victoria/210/2009) and X217 (A/Victoria/361/2011) viruses respectively. All three antibodies shown are strong neutralisers and require <100 ng/ml for 50% inhibition, except Q11C9 which is weak on X187 (A/Victoria/210/2009).

It is an interesting observation that N2B10 and Q11C11 have a higher number of somatic mutations (VH amino acid changes – 8 and 9 respectively) compared to Q11C9 (4 amino

acids) which has a lower number of somatic mutations and may be a newly formed clone (Appendix 4.1). N2B10 and Q11C11 may have passed through several cycles in the germinal centre and gained better neutralisation via somatic mutations and affinity maturation.

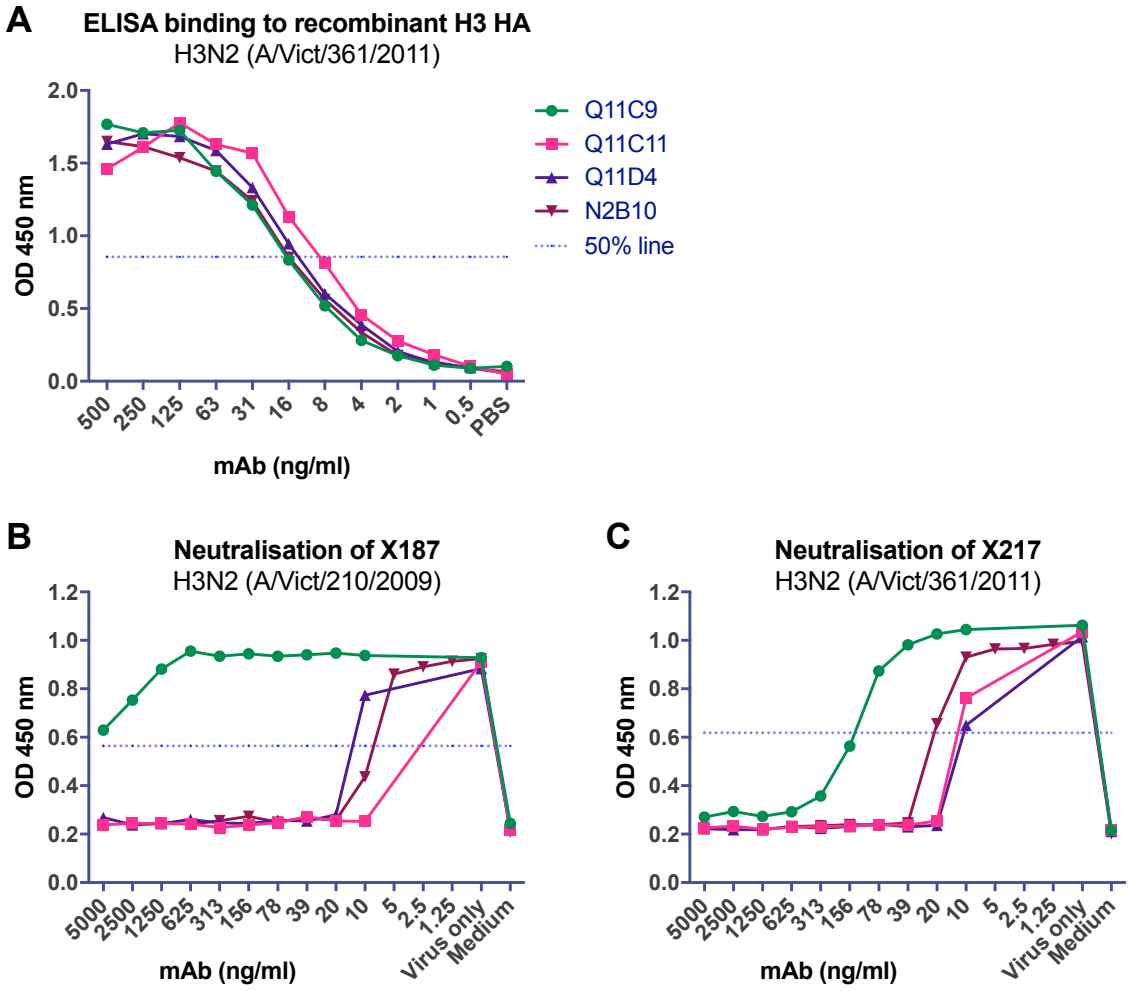

Figure 4. 2 ***Binding and neutralisation by H3 HA antibodies. A)*** *Binding of H3N2 antibodies to recombinant H3 HA protein* ***(B, C)*** *Neutralisation of 2009 and 2011 H3N2 seasonal vaccine viruses by monoclonal antibodies.*

4.2 Cross-reactivity of H3 antibodies to past H3N2 strains

These antibodies are cross-reactive to past H3 strains as well. Their cross-reactivity IC50 titres are shown in table 4.2 along with stem antibodies from donor Z. Donor Z is a Chinese child donor who developed an asymptomatic infection with the H7N9 virus which elicited many H3/H7 cross-reactive antibodies directed at the group 2 stem.

Among the antibodies, head antibody Q11C11 is the most cross-reactive and inhibits past H3 strains from 1994 and 1985 (Table 4.2). These antibodies mirror the head cross-reactive H1 antibodies described in chapter 3 which see H1N1 viruses back to A/USSR/90/1977. Q11C9 is weaker on 2009 virus compared to 2007 or 2011 viruses. Stem antibodies are cross-reactive to viruses from different years, however they require a much higher concentration for neutralisation *in vitro* than head antibodies. It is remarkable that head antibodies can be almost as cross-reactive as stem antibodies.

Table 4. 2 Cross reactivity of H3 head and stem antibodies to antigenically drifted viruses from different years.

Antibody	VH gene	Specificity	A/Texas/50/12	X217 (2011)	X187 (2009)	A/Perth/16/09	A/Brisbane/10/07	A/Sydney/5/97	A/JHB/33/94	A/Missisippi/1/85	X31 (1968)
N2B10	4-61	Head	++++	+++	++++	+++	+++	—	—	—	—
Q11C9	4-59	Head	+++	+++	+/-	+/-	++	—	—	—	—
Q11C11	4-61	Head	+++	++++	++++	+++	+++	++	+++	+/-	—
Q11D4	3-9	Head	+++	+++	+++	++	++	—	+++	—	—
Z3A8	3-23	Stem	++	+	+	+/-	+	—	+	—	+/-
Z3A9	3-30	Head	++	+	+	+/-	+	—	+	—	—
Z3A10	3-23	Stem	+/-	+/-	+/-	+/-	+/-	—	+/-	—	+/-
Z3B2	3-53	Stem	+/-	+/-	+/-	+/-	+/-	—	+/-	—	+/-

	ng/ml
++++	1-10
+++	10-100
++	100-1000
+	1000-5000
+/-	>5000
—	no neutralization

4.3 Reactivity to recent clades 3C.2a and 3C.3a

All of the head antibodies described above either lost or reduced their neutralisation to the recent H3N2 virus clades 3C.2a and 3C.3a (Table 4.3). The neutralisation IC50 ranges in figure 4.2 are derived from the neutralisation of pseudotyped (S-FLU) H3N2 viruses. The stem antibodies neutralised pseudotyped viruses better than wild type viruses (Table 4.3). There is a difference of ~100 fold in IC50. This effect is similar to the one seen in neutralisation of H1 and H5 pseudotyped viruses by stem cross-reactive antibodies in chapter 3.

Those antibodies which lost neutralisation to recent clades were used to select escape mutants of X217/2011 virus to see if they selected substitutions which later occurred in nature. Although we tried to select escape mutants with all the head antibodies in table 4.3, not all antibodies selected mutants. In some cases, the mutant didn't grow which may mean it had a fitness cost and didn't survive in following subsequent passages.

Table 4. 3 Neutralisation reactivity of antibodies to recent clade 3C.2a and 3C.3a viruses.

mAbs	Specificity	A/Vict/210/09 (clade 3)	A/Vict/361/11 (Clade 3)	A/HK/5738/14 (clade 3C2.a)	A/SW/9715293/13 (clade 3C3.a)	Selected escape variant
Q12A3	Head	+++	++	—	—	
Q12A6	Head	++++	++++	+	+	
Q12C5	Head	+	+++	—	—	Yes
Q12C6	Head	++++	++++	—	—	
Q12C9	Head	++++	++++	—	—	Yes
Q12D6	Head	++++	++++	—	—	Yes
Q12D9	Head	++++	+++	—	—	Yes
N2B10	Head	++++	++++	—	—	Yes
Q11C9	Head	+++	+++	++	—	Yes
Q11C11	Head	++++	++++	—	—	
Q11D4	Head	++++	++++	—	+/-	Yes
T35D	Stem	+++	++	—	—	
Z3A8	Stem	+++	++	—	—	
Z3A9		+++	++	—	—	
Z3A10	Stem	++	+	+	+/-	
Z3B2	Stem	+++	++	++	+	Yes

	ng/ml
++++	1-10
+++	10-100
++	100-1000
+	1000-5000
+/-	>5000
—	no neutralization

4.4 Human monoclonal antibodies select escape mutants that recapitulate natural antigenic drift.

Eight antibodies successfully selected escape viruses in cell culture. Escape viruses were re-cloned in the presence of antibody and grown to sequence the HA and NA vRNAs. At least two escape clones for each antibody were sequenced. The RNA isolation and sequencing of the genes was done by Rod Daniels at the Worldwide Influenza Centre, The Crick Institute. Substitutions in escape viruses were compared to the parental viruses and are shown in table 4.4. No accompanying neuraminidase mutations were found in any of these escape mutant clones.

Table 4. 4 Amino acid substitutions in escape mutant viruses selected by the antibodies to X217 (A/Victoria/361/2011) virus.

Antibody	VH gene	Variant	Specificity	Substitution
Q11C9	VH4-59	Clone 1	Site A	R142G
		Clone 2		K82R
		Clone 3		K82E
Q12C5	VH1-3	Clone 1	Site A	R142G
		Clone 2		N144K (-cho)
Q12C9	VH3-48	Clone 1	Site B	K189N
		Clone 3		K189N
Q12D6	VH1-18	Clone 1	Site B	K189R
		Clone 2		K189R, S265R
		Clone 3		K189R
Q12D9	VH3-48	Clone 1	Site B	157-158 del
		Clone 2		K189N
		Clone 3		F159S
N2B10	VH4-61	Clone 1	Site B	F159S
		Clone 2		F159S
		Clone 3		F159S
Q11D4	VH3-9	Clone 1	Site B	157-158 del
		Clone 2		157-158 del
		Clone 3		157-158 del
Z3B2	VH3-53	Clone 1	Stem	HA2: I45N
		Clone 2		HA2: I45F
		Clone 3		HA2: I45F

Table 4. 5 Amino acid substitutions selected by human monoclonal antibodies analysed comparing to the past and circulating H3N2 virus strains.

Amino acids	Specificity	Recent isolate	Positive selection	Koel 7	Alternative AA	Selected by mAbs (n)
R142G	Site A	2013 (WHO)	Yes (nf)	No	G/K/E/S	2
K82R	Site A	2015 (nf)	No	No	R/E/T/N	1
K82E	Site A	2012 (fs)	No	No	R/E/T/N	1
N144K(-cho)	Site A	2015 (nf)	Yes for N144S	No	S/Q/K/R/G/T/I	1
K189N	Site B	2016 (nf)	No	Yes	S/R/N	2
K189R	Site B	2013 (fs)	Yes in past	Yes	S/R/N	1
S265R	Internal	No	No	No	G	1
F159S	Site B	2014 (WHO)	Yes	Yes	Y/S/N	2 (from 2 individuals)
157-158 del	Site B	No	No	Yes		2
HA2: I45N	Stem	H1 2011 (Li 2012)	No	No	H3 V/T, H1 F/V/N	1
HA2: I45F	Stem	H1 2016 (nf)	No	No	H3 V/T, H1 F/V/N	1

WHO = WHO annual reports, fs = fluserver, nf = nextflu.org

Sequences of the genes revealed substitutions in site A and site B of the head of the haemagglutinin. Some antibodies selected more than one substitution but all within the surface of one antigenic site involving neighbouring residues. The antibody Q12D9 selected three substitutions in Site B (residues 189, 157-158del and 159) (Table 4.4 and Figure 4.3), all of which have been reported as sites of major antigenic changes in the past (Koel et al. 2013).

The amino acid substitutions selected by each antibody are shown in table 4.5. Almost all the substitutions selected by head antibodies are surrounding the receptor binding site (Figure 4.3). The substitutions R142G, K82R/E and N144K (-CHO) are in site A and K189R/N, 157-158 del and F159S in site B. Residue 82 is not immediately surrounding the sialic acid binding site. Antibodies to epitopes distant from the receptor binding site do not directly affect receptor binding but act by obstructing the binding site by steric hindrance (Knossow et al. 2002).

Interestingly many of these exact amino acid substitutions selected by these monoclonal antibodies have been detected in past and recent H3N2 seasonal strains. The timing of these changes in circulating viruses 2011-2016 are shown in table 4.5, figure 4.2 and their positions are shown in figure 4.3. Among them, R142G, N144S and F159S were positively selected in nature and were responsible for antigenic drift in the 3C.2a and 3C.3a strains circulating since 2013. N144K (antigenic site A) with loss of a glycosylation site, is gaining momentum in recent 2016 isolates (Figure 4.2).

Substitutions at positions 159 (F159Y) and 189 (K189E) selected by antibodies were also reported by another study (Li et al. 2016). F159Y appeared in clade 3C.2a viruses, but the K189E change has not yet been seen in H3 HAs from 2004 – 2016. However, this position has acquired other substitutions that are circulating at low frequency (Table 4.5).

K189N/R were selected by three of our antibodies. This amino acid replacement at this position was responsible for a cluster transition in 1975, and in combination with positions 155 and 159 caused major antigenic change in 1987 (Koel et al. 2013). It therefore seems possible that substitution at position 189 may be responsible for another major antigenic change in the near future.

The substitution R142G, selected by two independent antibodies from donor Q, first appeared in 2012. Currently almost 60% H3N2 viruses have Arginine and 30% Glycine at 142, indicating recent positive selection at this position (Figure 4.4C). Glycine is dominant at position 142 in 3C.3a viruses and present in low frequency among 3C.2a viruses. The other substitutions at position 142 now circulating at low frequency include K, E, Q and S (Table 4.5).

The change at position 144 (site A) from N to K resulted in removal of an N-linked glycosylation site, which appears to have abrogated neutralisation by antibody Q12C5. The N144S substitution is largely seen in post-2014 H3 viruses whereas N144K is seeming to rise in recent 2016 strains (Figure 4.4D). This residue wasn't involved in past antigenic change but the neighbouring residue 145 played a key role in cluster transition in the past (Koel et al. 2013). It is unusual for the binding of an antibody to be dependent on the *presence* of a glycosylation site, as glycosylation is often associated with loss of antibody binding (as seen for glycosylation at H1 162 for the set of antibodies to H1 hemagglutinin described in chapter 3).

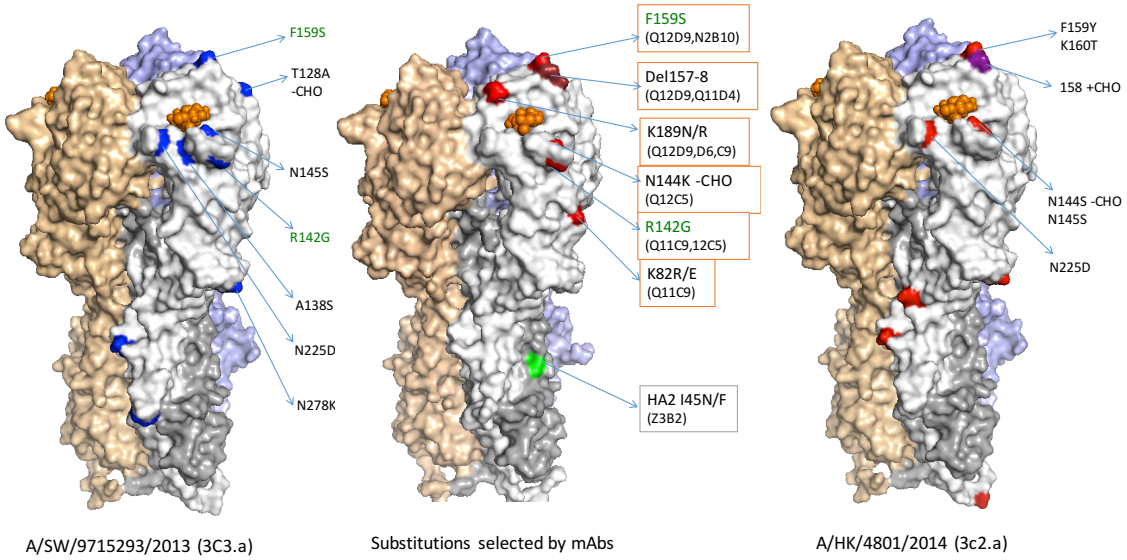

Figure 4. 3 ***The amino acid substitutions selected by antibodies to X217 (A/Victoria/361/2011) virus****; shown on PDB:5HMG as red (head antibodies) and green (stem antibody). On the left and right are shown the natural substitutions that have occurred in recently circulating viruses from clade 3C.3a and clade 3C.2a respectively. The substitutions selected by human antibodies are in site B (F159S, Del157-158, K189N/R) and site A (N144K causing loss of glycosylation, R142G and K82R/E) surrounding the receptor binding site (shown in orange). The substitutions in green font have been reported in recently circulating strains. F159S, which is responsible for a major antigenic change, defines clade 3C.3a viruses. The substitution I45N/F in HA2 (highlighted as green patch) was selected by the broadly cross-reactive stem antibody Z3B2. These Pymol graphs are used with kind permission from Alain Townsend.*

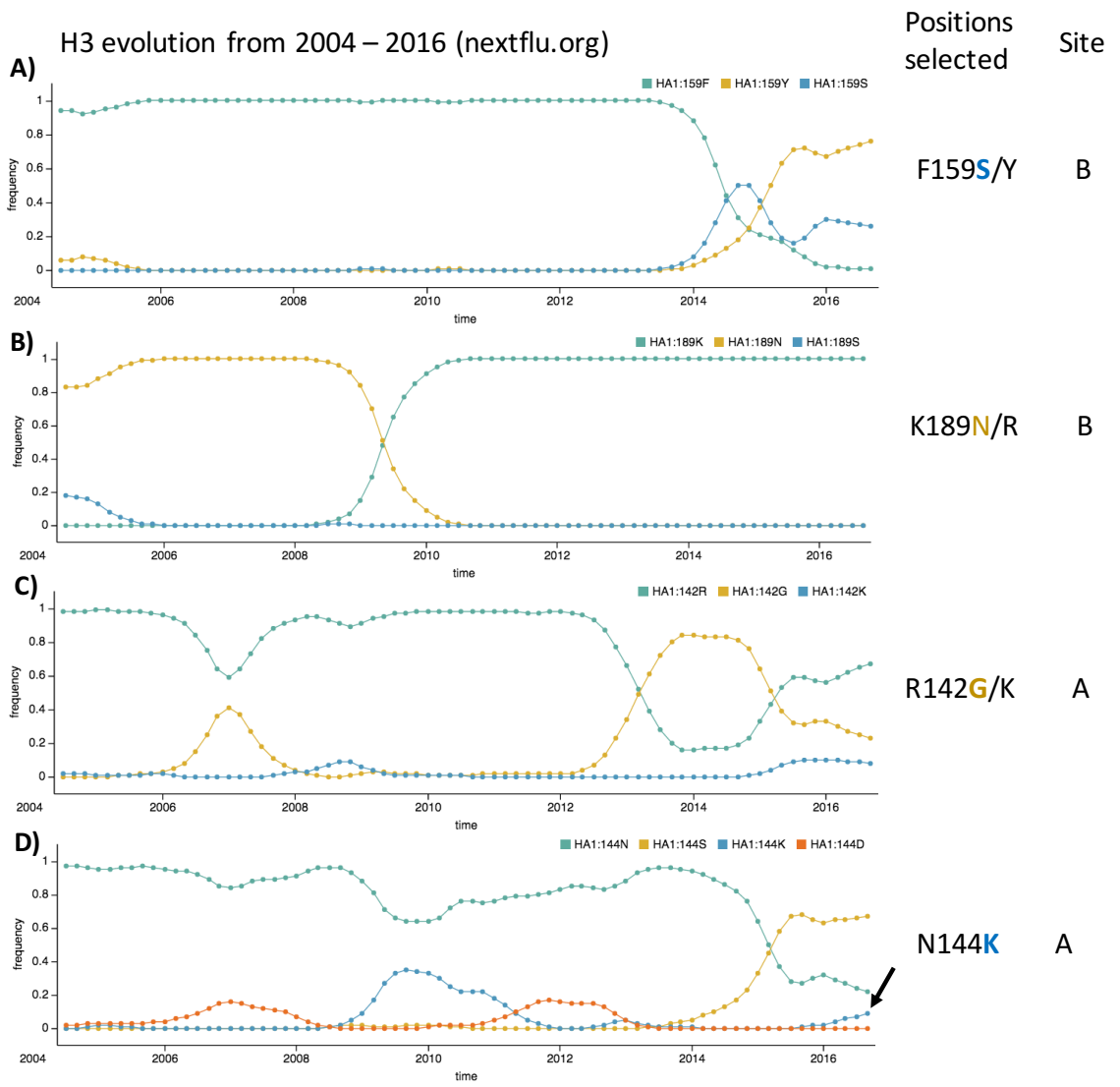

Figure 4. 4 ***Evolution of H3N2 viruses with different amino acid changes in the major antigenic sites of the haemagglutinin head.*** *These residues around the receptor binding site were reported to be associated with antigenic drift in the past (Koel et al. 2013). Substitutions seen in recent strains are in bold and coloured.* ***A)*** *At position 159, phenylalanine was consistent from 2004 to 2014, and then was substituted by serine and tyrosine giving rise to antigenically variant clades 3C.2a and 3C.3a. Serine is predicted in the escape virus selected by the antibody.* ***B)*** *Lysine at position 189 (site B) present in recent viruses was a change from asparagine in 2009. The monoclonal antibody selected the substitution back to N or R.* ***C)*** *Residue 142 at site A had a glycine and arginine*

interchangeably with lower frequency of lysine. Glycine was predominant in 2014. ***D)*** *Position 144 is dominated by residue serine in recent strains with the declining frequency of asparagine which was stable from 2004 until 2014. There is a low frequency of viruses with lysine at this position that are taking a rising toll in 2016 (indicated by an arrow). The figure was made using nextflu.org (Neher and Bedford 2015).*

Besides the head antibodies, the stem antibody Z3B2, which is similar to FI6 (Corti et al. 2011) and MEDI8852 (Kallewaard et al. 2016), selected substitutions in the alpha- helix A of HA2 at I45N/F. HA2 I45F has been seen in recent H1N1 viruses in China (Li, Shao, et al. 2012), and other changes at this site have been recorded sporadically in recent H3N2 viruses (Nextflu.org). Z3B2 required almost 5-fold EC50 concentration for neutralisation of clade 3C.3a virus compared to 2011 virus. Other stem antibodies also require higher concentration to neutralise clade 3C.3a and 3C.2a viruses, suggesting substitutions in the head may have affected the activity of stem antibodies, perhaps by an effect on the fusion pH optimum as described by Daniels et al. (Daniels et al. 1987).

4.5 Antibodies that may predict future antigenic drift.

The work described above tested the principle that human monoclonal antibodies could recapitulate antigenic drift of influenza in vitro, and thus provide predictive information. However, the design of these experiments was deliberately retrospective. The antibodies were selected for their lack of reactivity with clade 3C.2a and 3C.3a viruses to see if the substitutions selected in earlier viruses matched changes that later actually appeared in nature. In the next set of experiments, we set out to find new antibodies that were able neutralise the H3N2 viruses circulating currently, to see if our approach can predict future antigenic drift.

Our collaborator in Taiwan (Arthur Huang's group) recently isolated H3 antibodies from H3N2 infected young donors aged 6 and 16. These antibodies neutralised A/Victoria/361/2011 and A/HK/5738/2014 (clade 3C.2a) virus, however, they did not neutralise A/SW/9715293/2013 (clade 3C.3a) virus. As clade 3C.2a viruses are dominant now, they are likely to be the substrate for further antigenic drift in the future. Human monoclonal antibodies that neutralise these viruses were then used to select resistant variants of the vaccine viruses X217 (A/Victoria/361/2011) and X263A (A/Hong Kong/4801/2014).

We tried to select escape mutants with both viruses. Interestingly, each antibody selected escape mutants with only one virus. It is possible that mutations around the receptor binding site imposed a fitness cost to the drifted variant and could not grow further. Antibody AQ6A selected escape mutants with X217 (A/Victoria/361/2011) and not with X263A (A/Hong Kong/4801/2014) and vice versa for antibodies AM3C and AR1D.

The substitution F159S was selected by the antibody AQ6A with substrate virus X217 (Table 4.6), exactly confirming the earlier results with the antibodies Q12D9 and N2B10 (Table 4.4). It is remarkable that three antibodies (AQ6A, Q12D9 and N2B10), encoded by three different VH genes (1-2, 3-48 and 4-61), from three different donors (aged 6, 23 and >65), selected the same amino acid substitution at the same position. Popova et al. (Popova et al. 2012) also selected an escape mutant carrying substitution F159S by a human monoclonal antibody specific for a 2006 virus. The ferret and human serological study by Chambers et al. associated this substitution with the low vaccine efficacy in the 2013-2014 season (Chambers et al. 2015).

Table 4. 6 Substitutions selected by monoclonal antibodies that neutralise clade 3C.2a virus

Antibody	Donor (age)	VH gene	Escape selection parent virus	Variant	Specificity	Substitution
AQ6A	PNEU-10 (6 y)	1-2*02	X217 (A/Victoria/361/2011)	Clone 1	Site B	F159S
				Clone 2		F159S
				Clone 3		F159S
				Clone 4		F159S
AM3C	PNEU-10 (6 y)	3-49*04	X263A A/Hong Kong/4801/2014)	Clone 1	Site B	F193Y (140I + 225G)
				Clone 2	Site A	R222K (140I + 225G)
				Clone 3		F193Y (140I + 225G)
AR1D	PNEU-15 (16 y)	3-7*03	X263A (A/Hong Kong/4801/2014)	Clone 1	Site B	F193L (140K + 225D)
				Clone 2		F193V (140K + 225D)
				Clone 3		F193L (140K + 225D)

140 (90%K + 10%I) and 225 (80%D + 20%G) are two polymorphisms shown by parent X263A virus
F193S/Y/L (one of Koel 7 site) seen in 2016 clades 3C.3a and 3C.2a viruses (WIC Report 2016 September and Nextflu)
R222K seen in 2016 clade 3C.2a (Nextflu)

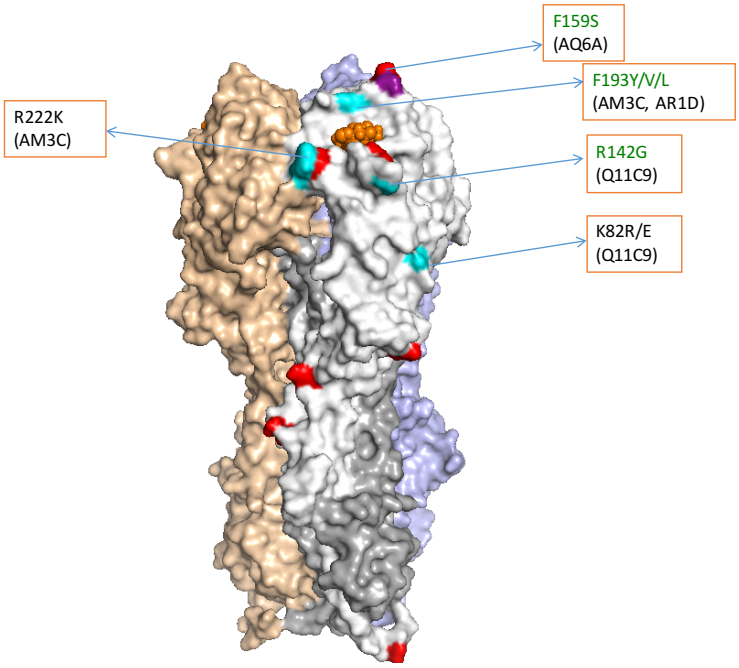

Figure 4. 5 Substitutions selected by antibodies that neutralise clade 3C.2a virus.

Two other antibodies AM3C and AR1D from two donors aged 6 and 16 years, encoded by germline VH genes 3-49 and 3-7 and which neutralise clade 3C.2a viruses, both selected a substitution at position F193 (Table 4.6 and Figure 4.5). AM3C selected F193Y and AR1D F193L/V. It is noteworthy that all these substitutions have emerged in both clades 3C.2a and 3C.3a viruses within the last year (WIC Report September 2016

and nextflu.org) (The Crick Worldwide Influenza Centre 2016). Residue 193 lies within the antigenic site B surrounding the receptor binding site, next to other important residues 159, 156, 157, 158 and 189 (Figure 4.5). This residue is one of the "Koel-7" residues (Koel et al. 2013) and has been associated with major antigenic drift in the past. This is an accessory and cluster-transition mutation site that interchanged between S193D (1968), D193N (1975), N193K (1987), N193S (1989), S193F (2006) and is continuing to evolve. The F193Y/V/L selected by our antibodies may be predictive for future antigenic change. In the past F193 has also been part of a dual change with an additional residue. For example, A/Sydney/1/87 vs. A/Victoria/7/87 with only two amino acid differences S138A (site A) and K193N (site B) were antigenically different as shown by ferret HI titre (Lee and Chen 2004). Similarly, cluster transition from A/Sichuan/2/1987 to A/Beijing/353/89 was accompanied by S193N change that co-occurred with drift mutation N145K ((Koel et al. 2013), Fig S4F).

Besides F193Y, antibody AM3C also selected substitution R222K in site A. This is the first antibody we have encountered that selected mutations in both sites A and B, suggesting the footprint for this antibody may span the sialic acid binding site. The R222K residue change hasn't notably occurred in the past. However, a low frequency of clade 3C.2a viruses recently circulating in late 2016 now carry this mutation (Nextflu.org).

There were polymorphic adaptation mutations at positions 140 (90%K + 10%I) and 225 (80%D + 20%G) shown by parent X263A virus grown in MDCK-SIAT1 cells (Table 4.6). The original X263A virus with majority K140 and D225 agglutinated human red cells very well. However, when we used HI assays to identify escape mutant viruses none of them agglutinated. Escape mutant viruses were later identified by staining for surface

HA or NP expression. We would have missed the escape viruses if we had only relied on HI assays. Many studies have reported the alteration in positions 193 (S193F/R) (Medeiros et al. 2001) and 225 (D225N/G) (Mochalova et al. 2003) as a cause for altering the specificity and/or affinity of H3 HAs (Lin et al. 2010; Daniels et al. 1987) for sialic acid. Thus, the mutation at position 225 may have caused the loss of haemagglutination by our escape viruses.

CHAPTER 4 DISCUSSION

Vaccine mismatch is a big problem in influenza vaccination against H3N2 viruses. Every year there is uncertainty whether the vaccine strain decided on by the WHO based on sequence and antigenic analysis (mainly using ferret anti-sera) of circulating viruses will be protective against the virus predominating in the upcoming season. In addition, the egg grown vaccine strains often acquire egg-adaptive mutations that contribute to vaccine mismatch (Skowronski, Janjua, et al. 2014). Here we have shown, using monoclonal antibodies isolated from vaccinated and infected donors to select escape mutant viruses, that we can extend the work on H1N1 (group 1) to predict antigenic drift in H3N2 (group 2) viruses. We hope that this type of information will contribute to improved vaccine virus selection. Our data will be presented for discussion at all future vaccine selection meetings by our collaborators John McCauley and Rod Daniels.

Efforts to use murine monoclonal antibodies in similar studies with H3 viruses in the years following the development of hybridoma technology in 1975 (Kohler and Milstein 1975) failed to provide very useful information. The murine response was extremely diverse and the majority of antibodies did not select for amino acid substitutions that were deemed epidemiologically significant (Webster et al. 1980). Why then does it appear that human monoclonal antibodies are more predictive? The answer may lie in the fact that

unlike mice, humans are repeatedly exposed to influenza, and as discussed in chapter 3, tend to select B cells from the pool of memory cells laid down by the first exposure to influenza in childhood (Francis 1960; Destgroth and Webster 1966; Li et al. 2013; Linderman et al. 2014; Fonville et al. 2014). This selection process occurs in the germinal centre (Victora and Wilson 2015) and inevitably tends to narrow the repertoire of B cells that are selected during repeated rounds of affinity maturation, by the combination of somatic hyper-mutation and Darwinian selection of the most efficiently stimulated B cells. This results in a tendency in individuals with particular antigenic exposure histories to focus their antibody responses to limited regions of the haemagglutinin surface, and this may drive antigenic drift.

Our efforts to use human monoclonal antibodies to predict antigenic drift in H3N2 viruses is at an early stage, and we have isolated relatively few antibodies. However, we aim to produce a panel of informative antibodies that through our collaboration with the Worldwide Influenza Centre at the Crick institute, can be distributed to the WHO Collaborative Centres around the world for monitoring antigenic change alongside the standard ferret sera. In addition, the analysis could be made more informative by screening human sera from a range of birth cohorts for loss of reactivity to the growing panel of antibody selected virus variants. In this way, the age group most likely to select a given variant, and be at risk of infection if that variant grows out, can be identified. In addition, ferrets can be immunized with our monoclonal antibody selected variants and the range of reactivity generated compared to human sera.

Vaccination strategies to combat antigenic drift and vaccine mismatch

How can vaccines be designed to deal with antigenic drift? In the first place the contribution of egg adaptation mutations can be removed by immunizing with

recombinant proteins of fixed sequence. The recent licensing of FluBlok (Cox et al. 2015), a vaccine prepared in bacculovirus infected cells, should remove this tiresome issue. In addition, improved regulation to ensure an adequate content of neuraminidase would enhance the protective capacity of the vaccine (discussed in chapter 5) and provide a second level of immunity when HA mismatching does occur.

A popular concept in the literature is the development of methods to boost the immune response to the conserved stem region of haemagglutinin, and thus avoid the problem of antigenic drift altogether (Krammer and Palese 2013). There is a notion that stem antibodies hardly select escape mutant viruses, perhaps because there is a fitness cost to these mutations due to structural constraints of stem epitopes (Sui et al. 2009). However, the first described antibody to the H2 stem was able to select several resistant mutations by standard methods (Okuno et al. 1993).

In our experiments, we isolated escape mutants of H3N2 virus with our group 1 and 2 cross-reactive stem antibody Z3B2 in the first attempt. It may be possible that some stem antibodies select escape viruses more easily than others. The stem antibody CR8020 selected two escape mutations after 4 passages (Laursen and Wilson 2013). The escape mutants (at position HA2 I45) selected by the stem antibody Z3B2 are found in circulating natural viruses albeit at low frequency (Li, Shao, et al. 2012), which suggests there is no absolute fitness cost preventing the evolution of these viruses. We still haven't tested the cross-reactivity of other stem antibodies, ours and others, with the escape mutant virus with the HA2 I45N/F substitution. However, it is noteworthy that the amino acid I45 and other residues in helix A of the HA2 domain collectively forms a hydrophobic groove where many stem antibodies insert their HCDR (Dreyfus, Ekiert, and Wilson 2013; Kallewaard et al. 2016; Wu et al. 2015; Friesen et al. 2014) . It is not

unlikely that if the immune response is focused towards the stem region by specific vaccination, as advocated by Krammer et al. (Krammer, Palese, and Steel 2015) escape viruses with mutations in the stem domain may come to dominate.

As prediction of antigenic drift improves, it may be possible to immunise "pre-emptively" with a vaccine preparation containing the most likely drift variants of the immediate future. This concept also introduces the possibility of expanding the B cell repertoire by vaccinating with mixtures of haemagglutinins, so that future exposures have a larger repertoire to choose from. This concept was actually considered and shown to work in a small clinical trial in the 1950s (Davenport and Hennessy 1957), but has since been abandoned. It was based on the observation that while the elderly population was more likely to become ill following influenza infection, they become infected less frequently than younger generations. This relative protection was associated with the accumulation of a broader range of antibodies after multiple exposures. Finally, a complete vaccine should induce a local protective T cell response in addition to neutralising antibody. There are exciting recent developments in methods for attenuating influenza to a single cycle of replication, that should allow local administration by aerosol to the lung that could provide a complete local immune response (Baz et al. 2015; Broadbent et al. 2016; Morgan et al. 2016; Si et al. 2016) .

Appendix 4. 1 Variable Heavy and light genes of the H3N2 antibodies

	Heavy Chain							Light Chain						
Antibody	**V-GENE and allele**	**J-GENE and allele**	**D-GENE and allele**	**V-REGION identity %**	**V-REGION Nb of AA changes**	**CDR-IMGT lengths**	**AA JUNCTION**	**Locus**	**V-GENE and allele**	**J-GENE and allele**	**V-REGION identity %**	**V-REGION Nb of AA changes**	**CDR-IMGT lengths**	**AA JUNCTION**
AQ6A	1-2*02	3*01, or 3*02	6-19*01	91	16	8.8.16	CARPGYSSDWYHGAFYLW	Kappa	2-28*01, or 2D-28*01	1*01	97	6	11.3.9	CMQGLQTPRTF
AM3C	3-49*04	6*02	5-12*01	97	6	8.10.19	CTRGKSGYDWNHYYYYGMDVW	Kappa	1-39*01, or 1D-39*01	4*01	95	10	6.3.9	CQQTYTLPLTF
AR1D	3-7*03	6*02	5-24*01	92	16	8.8.16	CASLYGYKEGYYYGADLW	Kappa	1-33*01, or 1D-33*01	4*01	92	16	6.3.10	CQQYDDVLALSF
Q12C9	3-48*03	3*02	2-21*01	93	11	8.8.14	CARASLELLDHAFDTW	Lambda	3-25*02	1*01	97	4	6.3.10	CQSADSRVPYVF
Q12B11	4-61*02	6*03	2-21*01	92	14	10.7.26	CAKSPCGGNCYIGEGEGWDFYYSYMDIW	Lambda	1-51*01	2*01, or 3*01	93	12	8.3.11	CGTWDSALSAVVF
Q12C5	1-3*01	4*02	3-22*01	94	12	8.8.11	CARYHYDDYFDYW	Lambda	1-44*01	2*01, or 3*01	99	1	8.3.11	CAAWDDSLNGVVF
Q12D9	3-48*02	2*01	4-11*01	97	6	8.8.12	CARASTTFWYFDLW	Lambda	3-25*02	1*01	98	4	6.3.12	CQSADSSNTYPYVF
Q12A6	4-61*02	6*03	2-15*01	93	13	10.7.26	CARSPCGGNCYIGEGEGWDFYYHYMDVW	Lambda	1-51*01	2*01, or 3*01	93	11	8.3.11	CGTWDSSLSALVL
Q12D6	1-18*01	4*02	3-10*01	95	9	8.8.16	CARDLMVEGVISMGFDSW	Lambda	3-25*02	1*01	98	2	6.3.11	CQSADSSNTYRVF
Q12C6	4-61*02	6*03	2-21*01	92	13	10.7.26	CARSPCGGNCYIGEGEGWDFYYYYMDVW	Lambda	1-51*01	2*01, or 3*01	92	15	8.3.11	CGTWDSALAAVVF
Q12A3	1-18*01	6*03	3-10*01	94	15	8.8.22	CSRHMLQGFVITPGNFYYYYMDVW	Kappa	3-11*01	3*01	96	6	6.3.10	CQHRSNWRDSLF
Q11C9	4-59*08	5*02	6-19*01	98	4	8.7.14	CARQDGSGWQNWFDPW	Lambda	3-21*02	2*01, or 3*01	97	6	6.3.11	CQVWDSSSDHAVF
Q11C11	4-61*02	6*03	2-21*01	95	10	10.7.26	CARSPCGGNCYIGEGEGWDFYYSYMDVW	Lambda	1-51*01	2*01, or 3*01	96	8	8.3.11	CGTWDSSLSAVVF
Q11D4	3-9*01	6*03	2-2*01	92	14	8.8.7	CTVPSMDVW	Lambda	1-47*01	3*02	95	7	8.3.12	CAAWDDRLSGPWVF
N2B10	4-61*01	4*02	3-3*02	96	9	10.7.13	CATPHFWSGYQFDYW	Lambda	1-40*01	2*01, or 3*01	97	4	9.3.12	CQSYDSSLSGYVIF
Z3B2	3-53*01	6*02	3-9*01	94	9	8.7.18	CARFLVLRYFDWPNYAMDVW	Lambda	2-8*01	2*01, or 3*01	98	5	9.3.11	CSTHAGSNNLVLF

CHAPTER 5 | Broadly cross-reactive human monoclonal antibodies to neuraminidases

CHAPTER 5 INTRODUCTION

Although the importance of antibodies to neuraminidase for virus inhibition has been highlighted in humans and animal models (reviewed in Chapter 1), studies on NA specific monoclonal antibodies are limited compared to HA antibodies. There exist a few protective NA antibodies isolated from mice (Wan et al. 2013; Shoji et al. 2014; Wan et al. 2015) and rabbit (Doyle, Li, et al. 2013). These antibodies either have restricted specificity to one or more sub-groups of viruses or need enormous doses for protection. The mouse antibody CD6 isolated against pdmH1N109 virus doesn't cross-react with earlier seasonal N1 neuraminidases and has lost reactivity to recent H1N1 (post 2013/14) strains (Wan et al. 2015). There is an unmet need for broadly cross-protective neuraminidase antibodies isolated from humans.

In this chapter, I present a set of human monoclonal antibodies to neuraminidases N1, N2 and N9 and have shown that they inhibit neuraminidase activity in ELLA assays and protect mice from a lethal dose of virus infection. Moreover, some of these are novel broadly cross-reactive antibodies which hold therapeutic potential against seasonal and pandemic influenza viruses.

CHAPTER 5 RESULTS

5.1 Neuraminidase antibody screening

Isolation of human monoclonal antibodies to neuraminidase was done according to the methods described in chapter 2. Two N1 antibodies (AG7C and AF9C) were isolated by Arthur Huang's group in Taiwan from the recipients of seasonal vaccine, and sent to us for characterisation as part of an ongoing collaboration. N9 antibodies were isolated from H7N9 infected donors, in collaboration with Beibei Wang in Beijing, China. Three of the N9 antibodies isolated from a H7N9 infected but asymptomatic child donor were cross-reactive to N1. One of these, antibody Z2B3, is broadly cross-reactive. The N2 antibody (M6B12) was isolated by a visiting Masters student Philipp Janesch in the Townsend laboratory, under my supervision.

Antibodies were screened for binding to MDCK-SIAT1 cells infected with test viruses: H1N1 and H3N2 (Figure 5.1), and for the absence of binding to the HA protein expressed in transduced cells. Specificity for neuraminidase was confirmed by radiolabelled immune-precipitation (data not shown) or detecting binding to 293T cells transfected with an NA gene of interest (Figure 5.1). Neuraminidase binding antibodies were tested for inhibitory function in ELLA assays, as described in chapter 2. In ELLA assays, viruses or recombinant neuraminidase proteins, were used as a source of enzyme. Some of the ELLA assays reported in this chapter were performed by Alain Townsend.

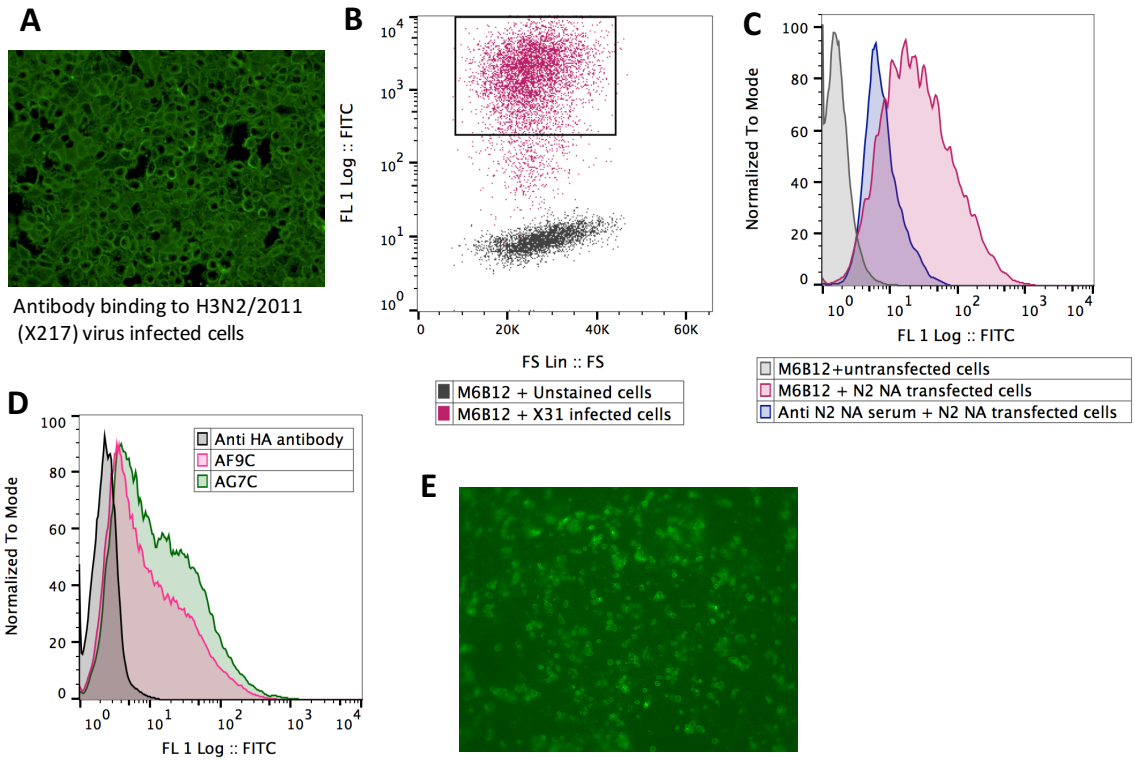

Figure 5. 1 ***Screening for antibody to neuraminidase by different methods. A)*** *Indirect immunofluorescence binding of antibody to virus infected MDCK-SIAT1 cell. Magnification 40x.* ***B)*** *Analysis of antibody binding to virus infected MDCK-SIAT1 cells by FACS.* ***C)*** *Binding of antibody to 293T cells transfected with N2 (X31/1968) neuraminidase gene and analysed by FACS. Sheep anti N2 sera to H3N2 (2011) is control which is poorly cross-reactive to X31 neuraminidase.* ***D)*** *Cross-reactivity of N1 antibodies to H5N1 (A/Egypt/NAMRU-2321/2007 clade 2.2.1) neuraminidase shown by binding to NA expressed on the surface of 293T cells.* ***E)*** *Binding of N9 antibody Z2B3 to N9 (A/Anhui/1/2013) NA transfected 293T cells. Magnification 40x.*

5.2 Broadly-inhibiting N1 mAbs from human individuals

Two antibodies AG7C and AF9C were isolated from two Taiwanese individuals who received seasonal influenza vaccine. These antibodies are able to inhibit the neuraminidase activity of the N1 viruses from 1934 to 2014, so far tested (Figure 5.2).

H1N1 virus after appearing in 1918 continued as a seasonal virus until 1957 when it was replaced by H2N2 and later H3N2. This virus re-appeared in 1977, continuing as a seasonal virus until the 2009 pandemic strain wiped it out. N1 NA in recent circulating H1N1 is of avian-origin transferred via swine (Garten 2009). These NA antibodies inhibit both the human and swine-lineage neuraminidases.

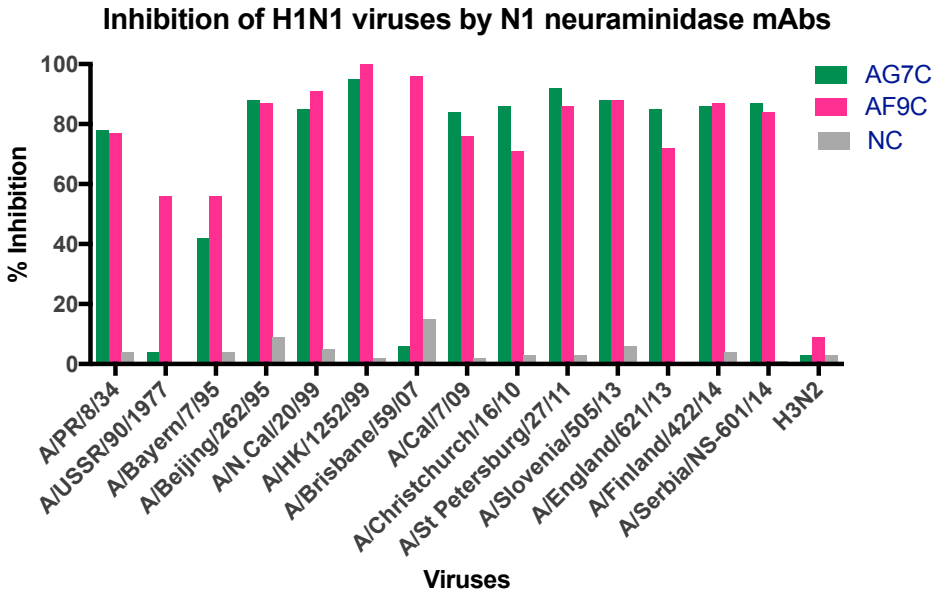

Figure 5. 2 ***ELLA screening of antibodies for inhibition of various H1N1 viruses from year 1934 to recent 2014 strains.*** *Percentage inhibition of NA activity by N1 antibodies AG7C and AF9C at 20 µg/ml are shown. H3N2 (2011) is used as a negative control virus and irrelevant HA antibody is used as a negative control antibody.*

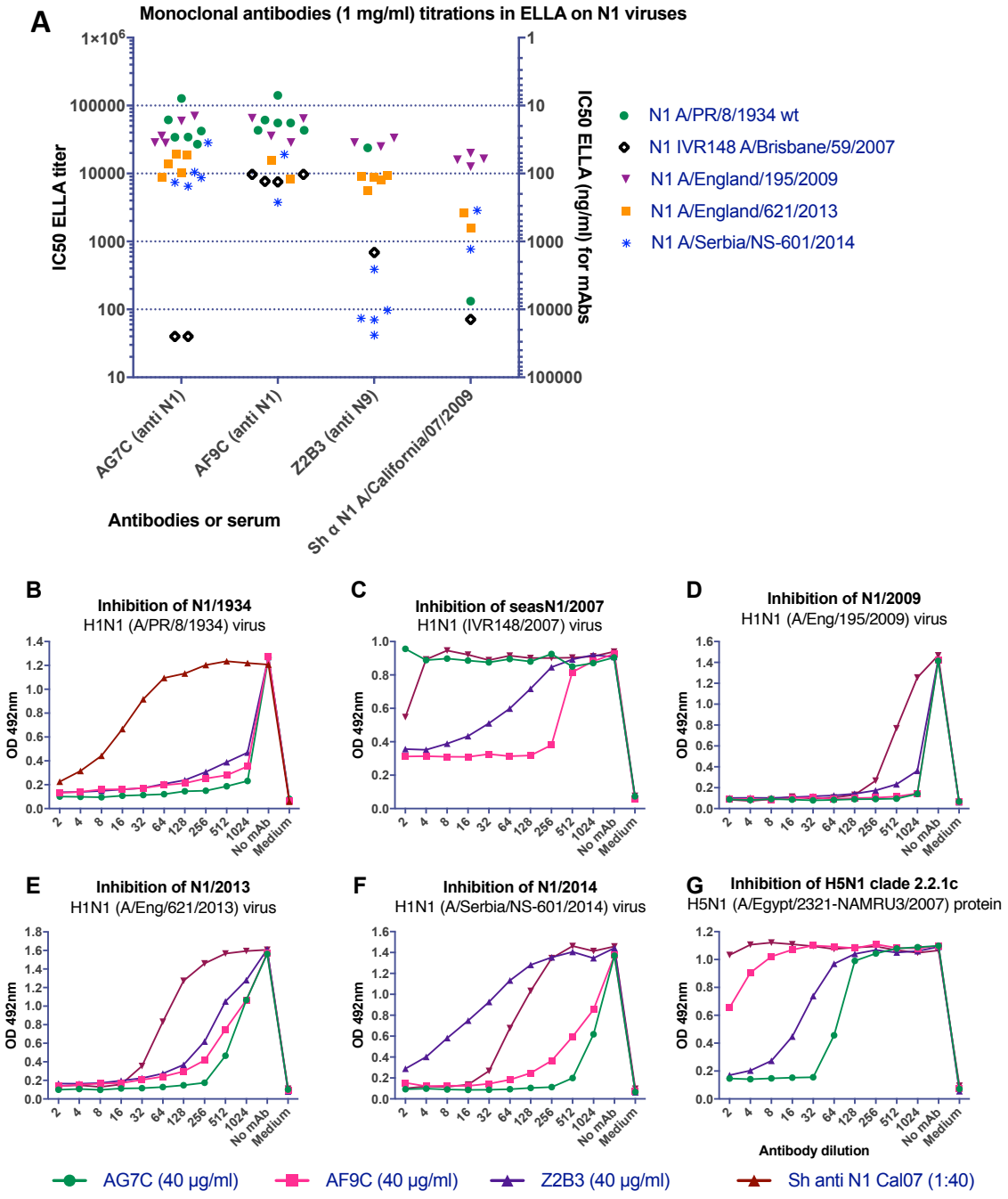

Figure 5. 3 ***ELLA inhibition titres of antibodies to N1 neuraminidases from H1N1 or H5N1 viruses.*** *AG7C and AF9C are N1 specific antibodies. Z2B3 is a cross-reactive N1/N9 antibody. Sheep anti N1 (A/Cal/07/2009) serum is a positive control.* ***A)*** *All three N1 NA mAbs inhibited 1934, 2009 and 2013 N1 neuraminidases. Antibody Z2B3 significantly lost its reactivity to 2014 clade 6B.1 virus. Sheep sera to N1 A/California/07/2009 also has reduced titre to 2013 and 2014 pdmH1N1 viruses by*

almost 10-fold. ELLA titration curve to different neuraminidase are shown in B-G. ***B)*** *A/PR/8/1934 virus* ***C)*** *Pre-2009 seasonal H1N1 virus* ***D)*** *2009 pandemic H1N1 virus* ***E)*** *pdmH1N1 2013 clade 6B virus* ***F)*** *pdmH1N1 2014 clade 6B.1 virus* ***G)*** *N1 protein from H5N1 clade 2.2.1.*

AF9C is reactive to viruses isolated over a period of 80 years. Mab AG7C is different from AF9C because it failed to inhibit A/Brisbane/59/2007 and A/USSR/90/1977 NAs. Both mAbs inhibit NA activity at IC50 concentration of ~ 10-200 ng/ml to most of the N1 NA neuraminidases (Figure 5.3). AF9C has lower IC50 for 1934 and 2009 neuraminidases (<30 ng/ml) compared to the 2007 N1 (158 ng/ml). Sheep sera generated against 2009 N1 neuraminidase has the strongest IC50 titre to the 2009 N1 and has significantly reduced titres to 1934, 2007, 2013 and 2014 neuraminidases, suggesting some low level of cross-reactivity of N1/09 antibodies to pre2009 human N1 and recent avian N1 neuraminidases. Reduction in titres to recent 2013-2014 N1 neuraminidases indicates the antigenic drift of neuraminidase of H1N1 virus. Sheep sera to 2009 N1 also have low level of cross-reactivity to avian origin H5N1 neuraminidase.

Another antibody Z2B3 shown in figures 5.3 and 5.4 is a cross-reactive antibody isolated from a H7N9-infected child donor. This antibody is as strong as AF9C at inhibiting NA activity of 1934, 2007 and 2009 N1 neuraminidases. In a later section, this antibody is shown to inhibit recombinant N9 NA at higher concentration. The cross-reactivity between N1 and N9 is unusual and suggests that this antibody may have been stimulated from a memory B cell to N1 NA upon exposure to N9. This is discussed in detail in later section.

The mAb Z2B3 requires a significantly higher concentration to inhibit the 2014 clade 6B.1 viruses, compared to 2009 or 2013 H1N1 viruses. There are only two substitutions

(K432E and A386K, N1 numbering) in N1 of A/Serbia/NS-601/2014 compared to N1 A/England/621/2013 (Figure 5.12). K432 is a known antigenic site for anti-N9 antibodies NC10 and NC41 (Tulip et al. 1992; Malby et al. 1994). The crystal structure study of Z2B3 in complex with N9 also revealed that K432 is part of the epitope (Figure 5.9).

5.2.1 N1 mAbs cross-react on pandemic H5N1 neuraminidase

Both N1 mAbs bind the H5N1 neuraminidase clade 2.2.1-c (A/Egypt/2321-NAMRU3/2007). Figure 5.1D shows the binding of the antibodies to NA protein stably expressed on the surface of 293T cells. Titration of the antibodies to this neuraminidase is shown in figure 5.3G. AG7C and Z2B3 inhibit NA activity well (average IC50 323 and 1165 ng/ml respectively) but AF9C is a poor inhibitor (IC50 11 μg/ml).

Besides clade 2.2.1 H5N1 (A/Egypt/2321-NAMRU3/2007) NA, these three antibodies cross-inhibit neuraminidases to various degrees from other clades, isolated from different regions around the world including China, Indonesia, Vietnam and Egypt. AG7C is broadly reactive on all the H5N1 NA clades tested, unlike AF9C which was a relatively weak inhibitor of the H5N1 NAs. Z2B3 almost failed to inhibit A/Vietnam/14012902/2014 clade 1.1.2 but inhibited other clades. Sheep sera to N1 A/Cal/07/2009 is almost not cross-reactive to other N1s from H5N1 viruses.

Inhibition of the enzyme activity of recombinant NA proteins required ~ 10-fold higher concentration of antibody than viruses as a source of NA (figures 5.3 and 5.4 respectively). The reason for this is not known, but could be explained if only a small proportion of the recombinant protein was enzymatically active.

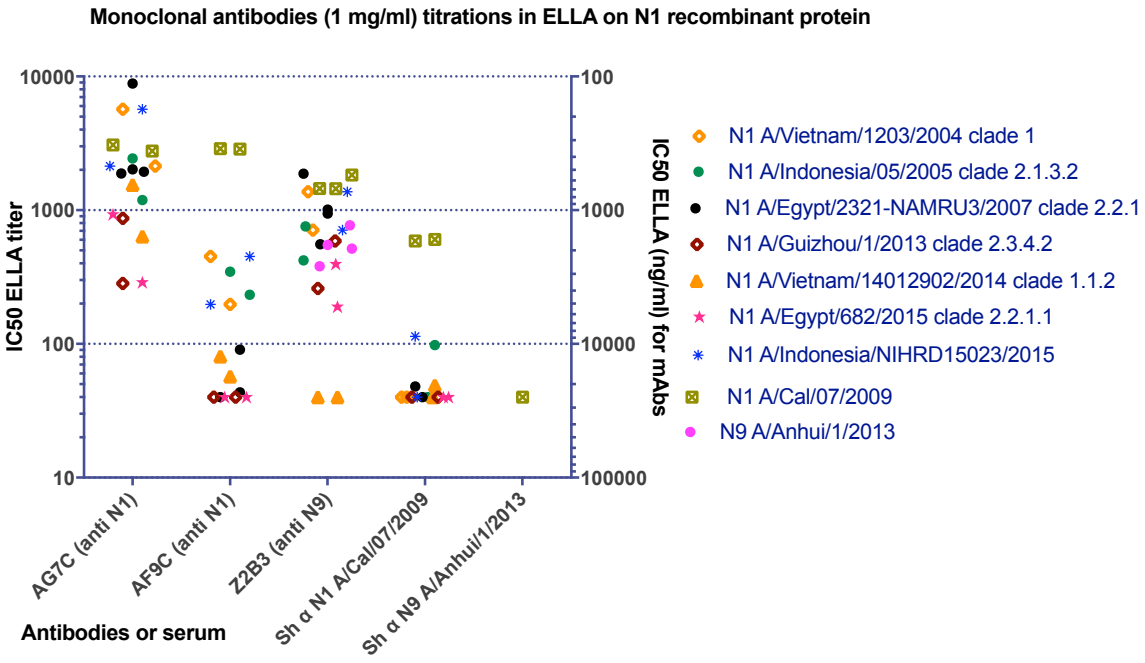

Figure 5. 4 Titration of anti-N1 antibodies on recombinant neuraminidase proteins derived from different H5N1 clades.

5.3 Broadly reactive N2 mAb isolated from a vaccinated individual

Microscope picture (Figure 5.1A) and FACS binding (5.1B) of the antibody to virus infected cells and NA transfected 293T cells (5.1C) presents an example of screening and confirmation of N2 neuraminidase specific antibodies. This N2 mAb, M6B12, was isolated in year 2014 following seasonal vaccination and binds to both X31 (1968) and X217 (2014) infected cells.

In figure 5.5, we have shown that antibody M6B12 inhibits activity of N2 NA from years 1968 (IC50 <70 ng/ml) and 2007-2012 (IC50 100-1000 ng/ml). However, it lost its reactivity from 1975 to 2002. M6B12 was isolated from a donor who was born before 1968 and may have been exposed to H3N2/1968 virus during his childhood.

Heterosubtypic antibody Z2B3 is cross-inhibitory to H3N2 neuraminidase from years 2009 and 2012 (tested so far) but requires very high concentration (figure 5.5 B, D, F).

This antibody requires testing on more N2 neuraminidases to confirm its broad-reactivity to N2 neuraminidases.

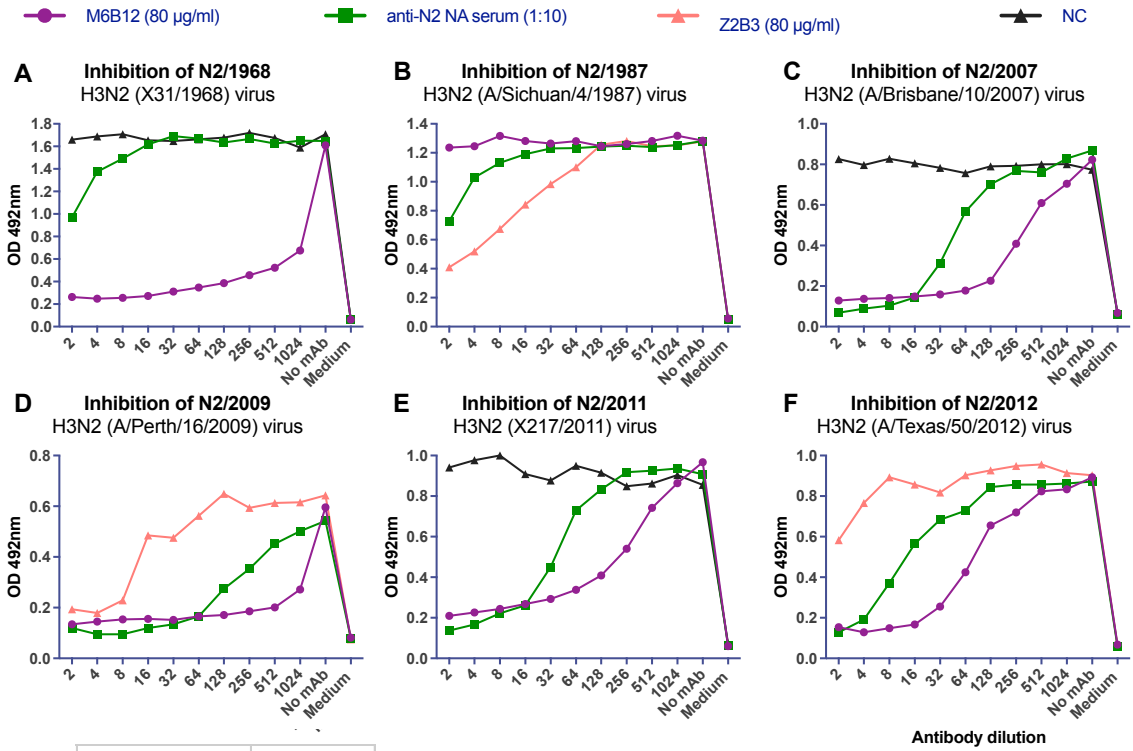

G

H3N2 Viruses	NA inhibition
X31 (1968)	Yes
A/Victoria/3/1975	No
A/Texas/1/1977	No
A/BG/11/1979	No
A/MS/1/1985	No
A/Schiuan/4/1987	No
A/JHB/33/1994	No
A/Fuijian/411/2002	No
A/Brisbane/10/2007	Yes
A/Perth/16/2009	Yes
X217 (2011)	Yes
A/Texas/50/2012	Yes

Figure 5. 5 ***Inhibition titration of N2 antibody M6B12 to H3N2 viruses. A)*** *1968 virus B) 1987 virus C) 2007 virus D) 2009 virus E) 2011 virus F) 2012 virus G) Summary of inhibition The N2 sheep serum was raised to 2003 N2.*

5.4 Antibodies to N9 isolated from H7N9 infected patients

Six antibodies to N9 were isolated from H7N9 infected donors. Figure 5.1E shows the representative screening of antibody for immunofluorescence binding to N9 transfected 293T cells.

Among the six, three antibodies namely, Z2B3, W1C7 and Z2C2, inhibit the neuraminidase activity of N9 recombinant protein (figure 5.6A). Z2B3 inhibits at average IC50 920 ng/ml whereas the other two antibodies require much higher concentration (>8 μg/ml).

5.4.1 N9 antibodies synergistic effect

We performed the binding of biotin-labelled antibodies in the presence of other antibodies to look for synergy. Antibodies did not block each other, but we found some evidence for synergy in binding. The binding of antibodies Z2C2, W1C7 and Z2B3 were increased in the presence of mAb P17C (Figure 5.7B). The binding synergy was more obvious with antibody Z2C2 where the binding was increased by 4.5-fold.

This synergy in binding translated to enhanced inhibition of N9 NA (Figures 5.6 and 5.7A). The non-inhibiting antibody P17C enhanced the inhibition by other inhibiting antibodies. The IC50 for antibody W17C decreased by about 3-fold and Z2C2 by about 5-fold (Figures 5.6 and 5.7B). Slight enhancement was seen with antibody Z2B3 as well.

These findings are preliminary and need more detailed analysis of kinetics and synergy at different concentrations. However, the evidence is suggestive that antibodies in a cocktail or serum may work better together than individual antibodies. In polyclonal sera, even the non-inhibiting antibodies may be helpful by improving the overall inhibition titre.

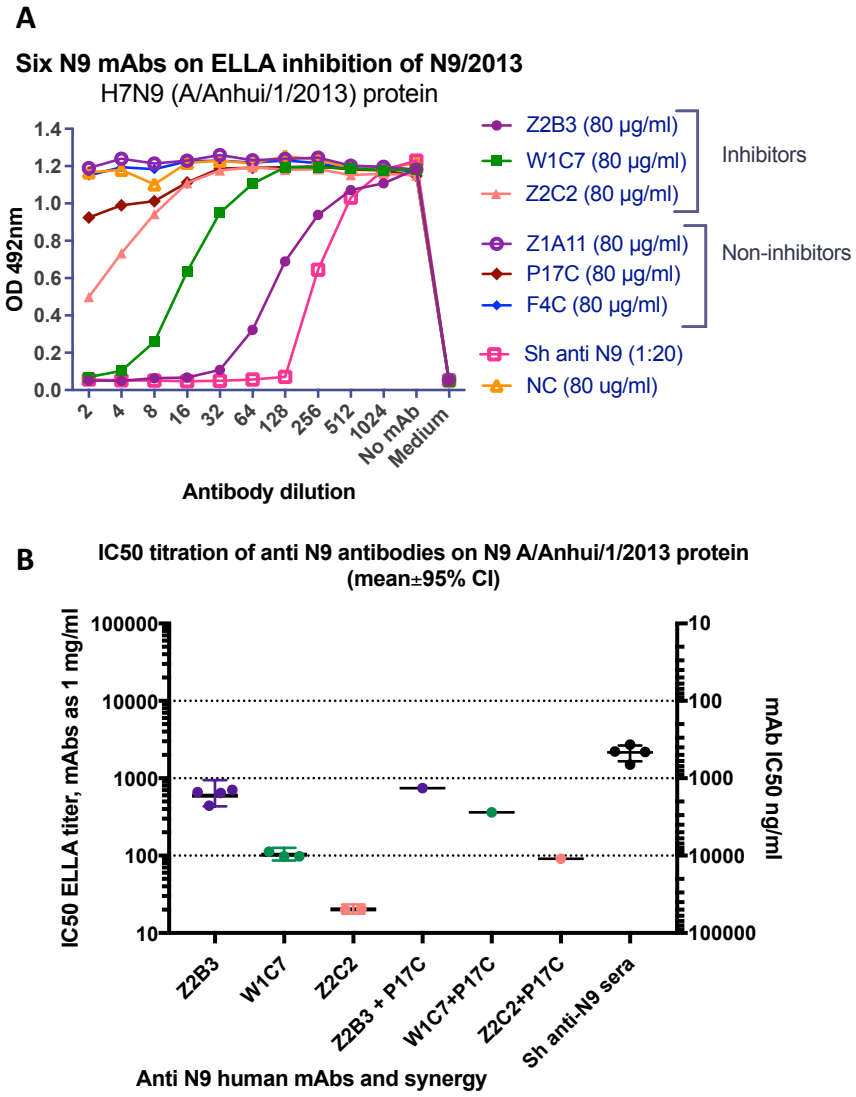

Figure 5. 6 ***Inhibition of N9 neuraminidase enzymatic activity by anti N9 antibodies on enzyme-linked lectin assay.*** *A) Titration of antibodies for inhibition. Sheep anti N9 sera (A/Anhui/1/2013) is a positive control and anti H7 HA antibody is a negative control. B) Inhibition concentration at 50% (IC50) values are shown for three inhibiting antibodies Z2B3, W1C7 and Z2C2. X axis: IC50 titres of antibodies as 1 mg/ml. Y axis: IC50 of mAbs in ng/ml. IC50 of these antibodies in presence of equal amount of non-inhibiting antibody P17C is also shown. IC50 is reduced for antibodies Z2C2 and W1C7 in synergy with mAb P17C.*

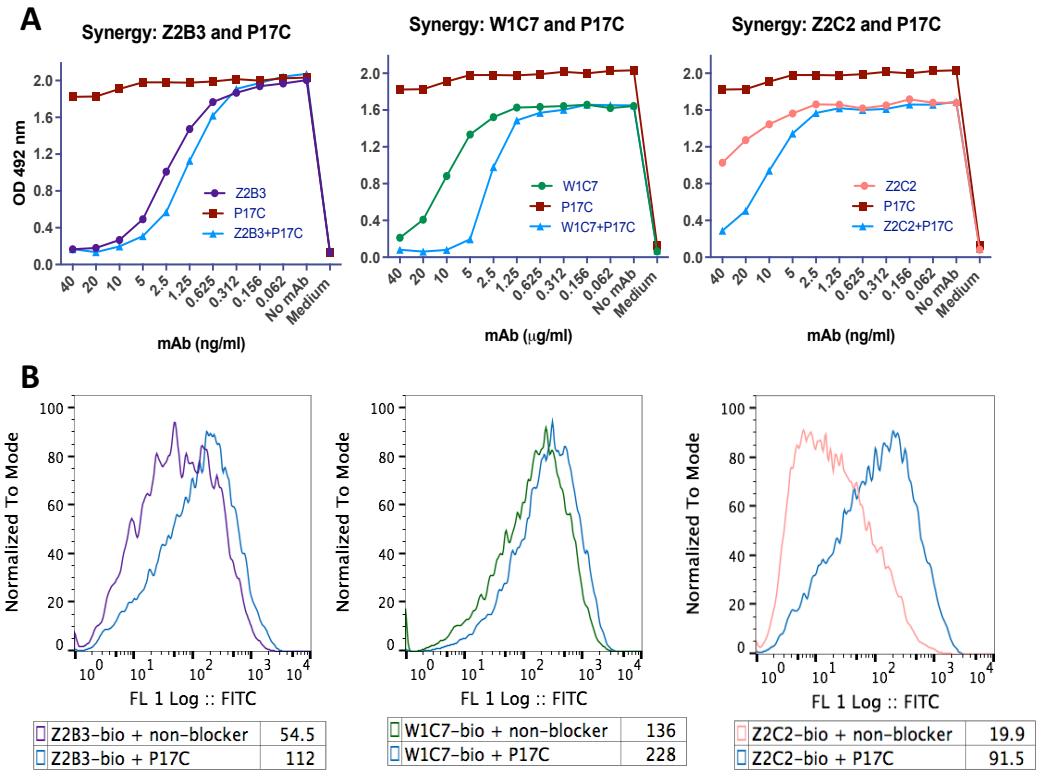

Figure 5. 7 ***Binding synergy of N9 antibodies****. **A)** Synergy of antibodies in N9 neuraminidase inhibition. P17C: a non-inhibiting antibody enhances the function of other antibodies especially Z2C2 and W1C7. **B)** Binding synergy of the antibodies. Binding of antibodies Z2B3 and W1C7 is increased slightly in presence of P17C and that of Z2C2 is greatly improved. Mean fluorescence intensity are shown.*

5.4.2 N9 antibodies may have arisen from memory cells to N1 neuraminidase

N9 and N1 NAs fall into two distantly related groups phylogenetically. We tested the inhibition of N1 by anti-N9 antibodies. Antibodies from donor Z (Z1A11, Z2C2 and Z2B3) inhibited the N1 neuraminidase almost as strongly as N1 antibody AG7C. Another antibody P17C also inhibited N1 but required higher concentration.

These antibodies from donor Z have a higher number of somatic mutations (VDJ, 8-13 amino acids mutations) (Appendix 5.1) suggesting that they pre-existed in the memory B

cell repertoire of the donor Z as a response to seasonal N1 neuraminidase. The epitope seen by these antibodies may be conserved in N1 and N9 neuraminidases. The antibody P17C (VDJ somatic mutation, 1 amino acid) seems to be either a newly formed antibody in response to N9 that gained cross-reactivity to N1 or had been in the memory B cell population without being selected previously in a germinal centre reaction.

Other antibodies W1C7 and F4C seem to be newly originated in response to H7N9 infections based on their number of VDJ somatic mutations. The heavy chain of W1C7 is a germline sequence without somatic change.

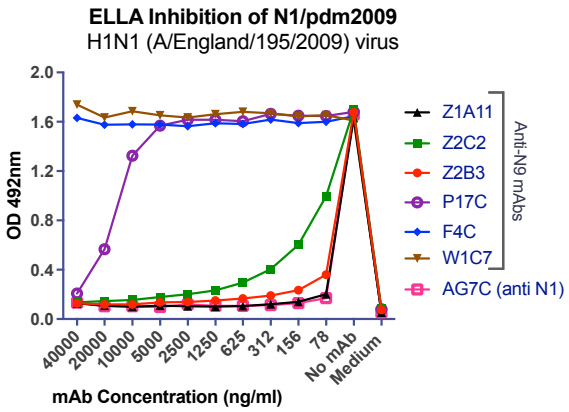

Figure 5. 8 ***Cross-reactivity of N9 antibodies to N1 NA.*** *Some N9 antibodies, including all three antibodies from donor Z (asymptomatic H7N9 child donor), cross-inhibit N1 H1N1pdm09, which indicates a probable origin from memory B cells.*

5.5 Residue K432E is indispensable for antibody Z2B3 inhibition.

Z2B3 showed reduced inhibition of N1 from clade 6B.1 virus (A/Serbia/NS-601/2014). The N1 from this isolate differs from the sensitive N1 from A/England/621/2013 NA at two amino acids K432E and N386K (Figures 5.3 and 5.13D). K432 (sequence **K**ENT, N1 numbering) is most likely to be part of the epitope as it is near the receptor binding

and catalytic site, and in addition this residue is conserved between N1 and N9 neuraminidases (Figure 5.13C), which are both inhibited by antibody Z2B3.

The crystal structure of the antibody Z2B3 bound to recombinant N9 was solved by Haihai Jiang and Yi Shi in George Gao's lab at CAS, China. This revealed a unique structure that shows the CDR3 of Z2B3 diving into the conserved active site of the enzyme and making many amino acid contacts with conserved residues in the site (Figure 5.9). The negatively charged residue D102 in HCDR3 of the antibody formed a salt bridge with positively charged residue K432 of neuraminidase, which may explain the loss of activity of Z2B3 on viruses with an E substitution at this position that would disrupt the salt bridge. Lisa Schimanski has since showed that replacing D102 with the positively charged amino acids K or R restored the antibody inhibition titres to N1 A/Serbia/NS-601/2014 (E432) (data not shown), most probably by reforming the salt bridge in reverse.

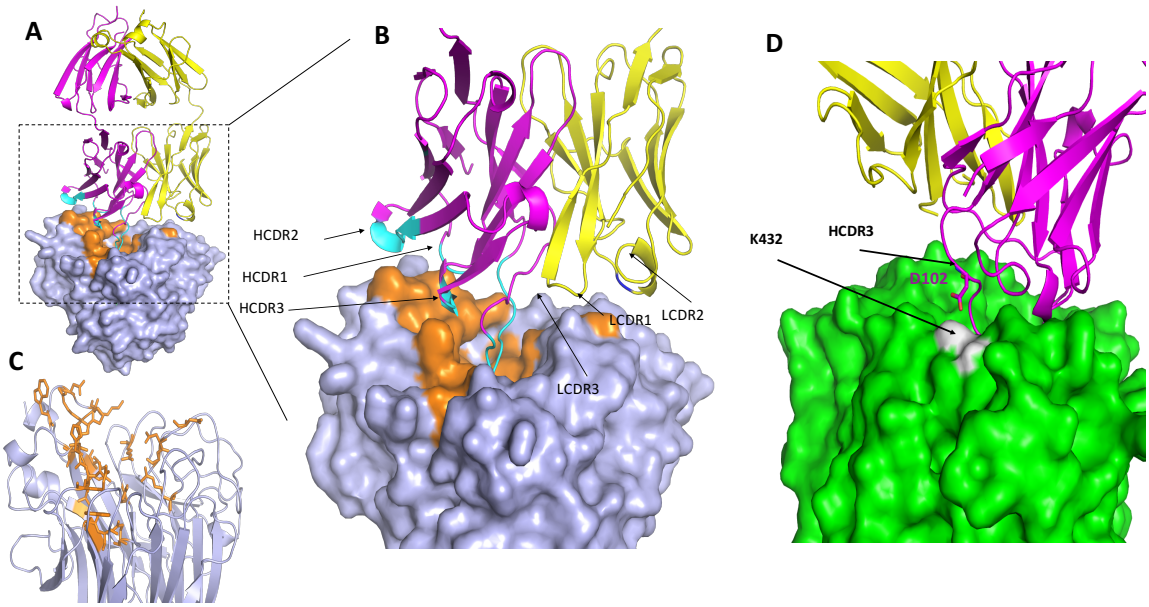

Figure 5. 9 ***Antibody Z2B3 complexed with N9 neuraminidase****. **A)** Neuraminidase is grey coloured; Variable heavy and variable light chains are pink and yellow respectively. Orange coloured regions are the contact residues of antibody Z2B3 on N9 NA. **B)** HCDR1-3 and LCDR1-3 are labelled. HCDR1-3 are labelled in cyan. **C)** Residues in the neuraminidase active site that contact antibody are shown. **D)** A salt bridge interaction is formed between positively charged residue Lys432 of N9 NA and negatively charged residue Asp102 of Z2B3 HCDR3. The antibody-N9 complex was crystalized by Haihai Jiang and analysed by Yi Shi in George Gao's lab, Institute of Microbiology, CAS, China.*

It is of interest that the K432E substitution has become dominant in the clade 6B.1 viruses isolated after 2014 (The Crick Worldwide Influenza Centre 2015). This suggests the possibility that antibodies similar to Z2B3, perhaps through cross-selection by N1s pre- and post-2009, have exerted an evolutionary pressure at this residue.

5.6 Cross-reactive N1 and N2 mAbs protect mice from lethal influenza infection

Both of the N1 NA mAbs, AG7C and AF9C, protected 100% mice from 10^4 TCID50 of H1N1 A/PR/8/1934 virus (equivalent to 150 LD50) when given as a 10 mg/kg dose 24 h before infection (Figure 5.10 A,B; $p<0.001$). They inhibited any weight loss whereas mice that received control anti N2 antibody M6B12 succumbed to 20% or more weight loss by day 5 and were culled. Heterosubtypic NA antibody Z2B3 also protected 100% mice without weight loss (data not shown).

AG7C and AF9C also protected hyper-sensitive DBA/2 mice from 10^4 TCID50 of pdmH1N1/2009 (X179A A/California/7/2009) virus (Figure 5.10 C,D; $p<0.001$). In the case of prophylaxis with antibody AG7C, 1 out of 6 mice was culled on day 11 after

losing >20% weight. T1-3B (Huang et al. 2015) and Z3B2 are stem HA antibodies (positive controls) both protective to PR8 and X179A viruses.

N2 antibody protected Balb/C female mice completely against lethal dose of X31 virus, with some weight loss ($p<0.001$) (Figure 5.11). Combination of HA (Z3B2) and NA (M6B12) each at 10 mg/kg seemed to prevent more weight loss comparatively, but this did not reach statistical significance. Lung virus titres weren't measured to see the differences, but the average weight loss shows that the group given both anti HA and NA antibodies have slightly lower weight loss than the groups that received individual antibodies. For treating human infections, combining HA and NA antibodies is logical, and may be more beneficial. The chances for selection of escape mutants would be minimised when both surface glycoproteins are targeted. Two different mechanisms of action are implemented, where one acts at virus entry and the other at virus exit.

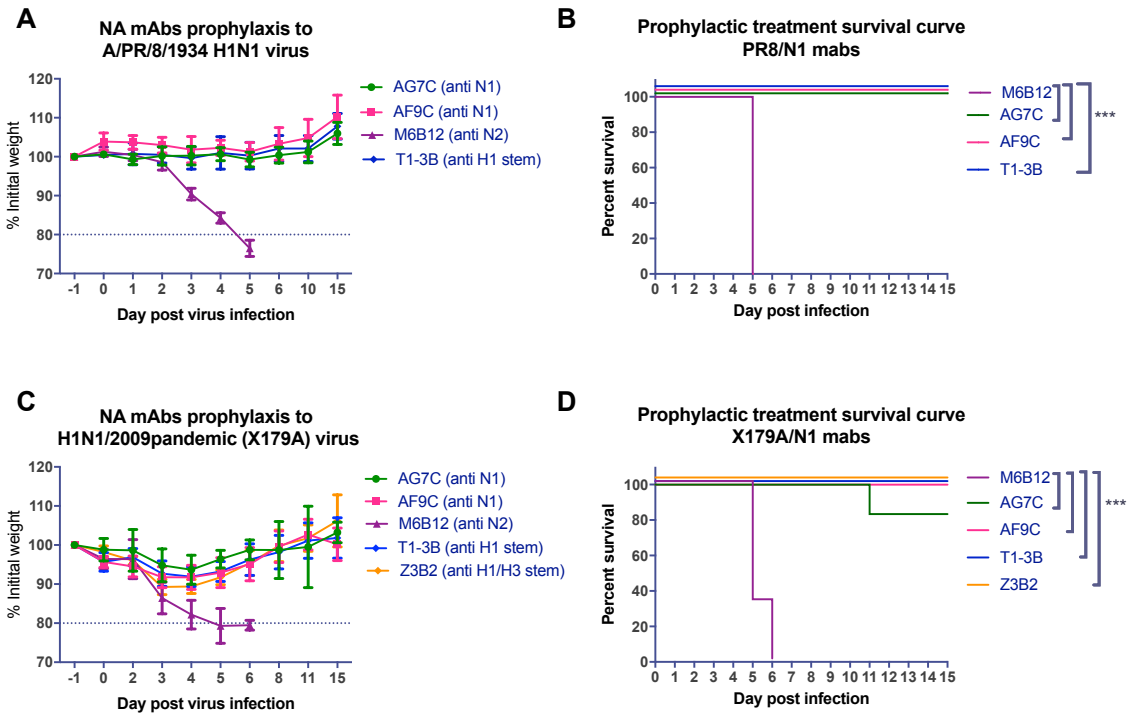

Figure 5. 10 ***In vivo prophylaxis with N1 antibodies*** *AG7C and AF9C, n=6/group and mAb dose is 10 mg/Kg. Loss in weight following infection was measured and >20%*

weight loss was considered as an endpoint. Anti-H1stem antibody (T1-3B) cross-reactive to X179A and PR8 viruses is a positive control and anti-N2 specific antibody M6B12 is a negative control. Experiments were performed at least twice and data from one experiment are shown here. ***(A, B)*** *N1 antibodies protect Balb/C female mice completely against* 10^4 *TCID50 of PR8 virus, without any weight loss (p<0.001).* ***(C,D)*** *N1 antibodies protect DBA/2 female mice completely against lethal dose of ~150 LD50 X179A virus, with about 5-10% weight loss (p<0.001). One mouse treated with AG7C became sick on day 8 and was culled after losing >20% weight on day 11. mAb may have selected an escape mutant in this mouse.*

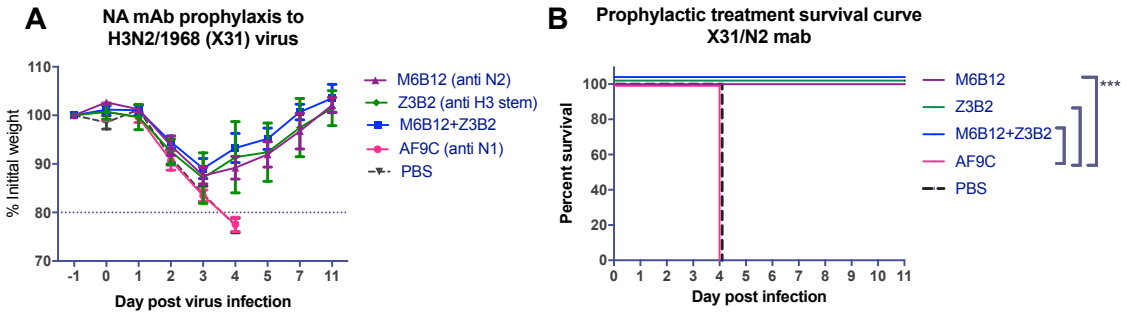

Figure 5. 11 ***In vivo prophylaxis treatment with N2 antibody M6B12****, n=6/group and mAb dose is 10 mg/kg. Loss in weight following infection was measured and >20% weight loss was considered as an endpoint. Anti-H3 cross-reactive stem antibody Z3B2 is a positive control and anti-N1 specific antibody AF9C is a negative control. Experiments were performed at least twice, and data from one experiment are shown.*

CHAPTER 5 DISUCSSION

Aim of the project

We have isolated and characterised human monoclonal antibodies to seasonal and pandemic neuraminidases with the aim of identifying epitopes, analyse cross-reactivity, and explore therapeutic potential.

Cross-reactivity

We have seen that hyperimmune sheep anti Cal7/09 NA sera is poorly cross-reactive to the immediately prior seasonal H1N1 BR59/07 virus, earlier era viruses, and H5N1 viruses (Figures 5.3A and 5.4). Also, mouse polyclonal serum to PR8/34 has no detectable cross-reactivity to Cal7/09 virus (personal communication with Alain Townsend). The residues surrounding the catalytic site of neuraminidase are conserved in N1 NAs from 1934, 2009 and avian N1s (Figure 5.12), and most of the differences are found on surface residues at some distance from the catalytic site (Figure 5. 13). This suggests that most antibodies in a polyclonal serum raised against a single NA are directed at variable surface residues distant from the catalytic site.

By contrast, our N1 mAbs cross-react to N1 neuraminidases over a period of 80 years. These N1 antibodies may have been stimulated from rare memory B cells to the human N1 lineage, which were selected out upon exposure to avian lineage N1, leading to this level of cross-reactivity. This reflects the general tendency for influenza antigens to select B cells from the memory population laid down early in life in preference to the generation of new specificities (Victora and Wilson 2015). The number of somatic mutations in the VH region (15 and 16 for AG7C and AF9C respectively, Appendix 5.1) indicate that they may have undergone several germinal centre reactions, and is suggestive of a memory B

cell origin. This mirrors the cross-reactivity of antibodies to the pdmH1 HA globular head described in chapter 3. Exposure to novel neuraminidases may program the humoral response to select cross-reactive antibodies from the memory pool. These cross-reactive memory cells may be rare but they can dominate in the germinal centre and be selected for expansion.

Sandbulte et al. has also shown that mice sera to humanN1 (NC20/1999) offered some cross-protection against avian virus H5N1 (Sandbulte et al. 2007). Further human sera with good NA titres to human N1 lineage also offered partial protection against avian H5N1 virus (Sandbulte et al. 2007). Isolation of more antibodies from vaccinated individuals may yield more cross-reactive neuraminidase antibodies offering protection against both human and avian N1 lineage viruses.

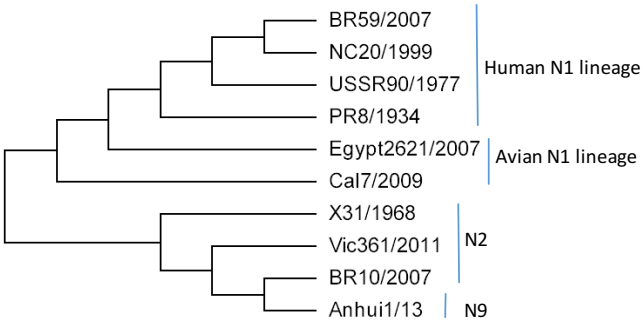

Figure 5. 12 ***Phylogeny of neuraminidases in this chapter****. This shows avian and human N1 lineage from group 1 and, N2 and N9 from group 2 neuraminidases.*

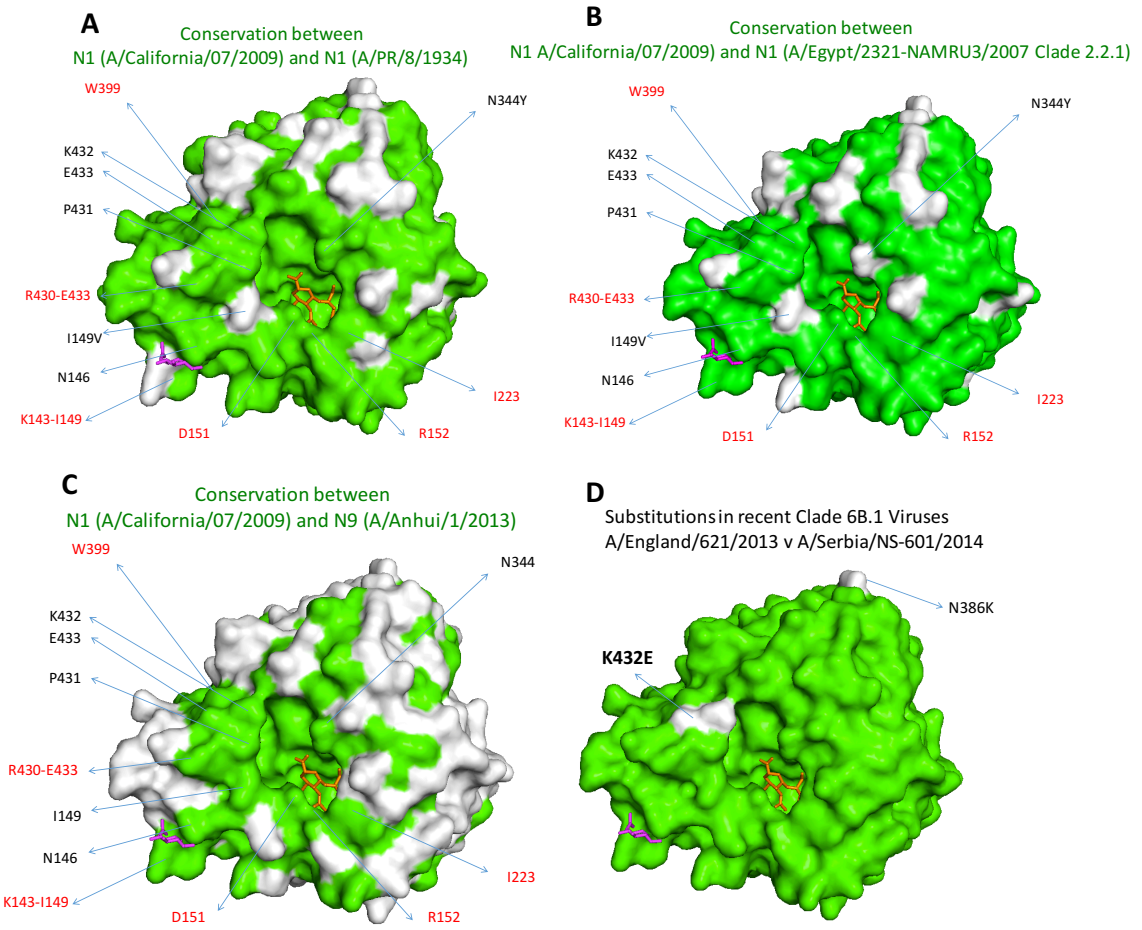

Figure 5. 13 ***Conservation between N1 (A/California/07/2009) and other N1 and N9 neuraminidases shown on PDB 4B7J.*** *Conserved residues are shown in green and substitutions in grey. Residues surrounding the active site and those that are different in neuraminidases are labelled in the picture. Orange coloured sialic acid is sited on the catalytic groove.* ***A)*** *Conservation between N1 (A/California/07/2009) and N1 (A/PR/8/1934)* ***B)*** *Conservation between N1 (A/California/07/2009) and N1 (H5N1 A/Egypt/2321-NAMRU3/2007 clade 2.2.1)* ***C)*** *Conservation between N1 (A/California/07/2009) and N9 (H7N9 A/Anhui/1/2013)* ***D)*** *Two substitutions including K432E in N1 A/Serbia/NS-601/2014 clade 6B.1 virus that resulted in reduction in activity of antibody Z2B3, compared to N1 A/England/621/2013. These Pymol graphs are used with a kind permission from Alain Townsend.*

H7N9 infection may have favoured the selection of Z2B3 and other cross-reactive antibodies from the N1 memory B cell pool, even though these are most distantly related neuraminidases belonging to two separate phylogenetic groups. The low affinity of Z2B3 to N9 (data not shown), suggests that Z2B3 is fundamentally an anti N1 antibody.

Z2B3 has >50 fold higher IC50 to clade 6B.1 virus A/Serbia/NS-601/2014 compared to A/England/621/2013, and the structure of the bound antibody suggests that the K432E substitution is responsible for this loss of activity. The K432E change near the NA active site has become dominant in new clade 6B.1 since 2014. This suggests that antibodies similar to Z2B3 may have played a significant role in the population to select this change. By contrast, N1 antibodies AG7C and AF9C are not affected by the K432E substitution. They cross-react on nearly all seasonal N1 neuraminidases. These two antibodies may see slightly different epitopes because AG7C doesn't react to USSR90/1977 and BR59/2007 but AF9C does. Further, AG7C is stronger on several clades of H5N1 neuraminidases than AF9C.

N2 antibody M6B12 may also have arisen from the memory B cell pool of the donor primed in his childhood against 1968 virus. The epitope changed in the years 1975-2002, but reappeared after this and could select memory cells laid down in 1968.

The structural basis for the cross-reactivity of AG7C, AF9C and M6B12 is under investigation through crystallography studies.

Inhibition of enzymatic activity and *in vivo* protection

The antibodies block neuraminidase activity by binding near to the enzymatic active site. We still have to assess the binding epitopes for these antibodies, however based on their reactivity to different viruses, they may recognise different epitopes, and may work in

synergy. Some level of synergy is seen with N9 antibodies where non-inhibiting antibody enhanced the binding and ELLA activity of an inhibiting antibody.

Inhibition of enzymatic activity *in vitro* may be the first indicator of *in vivo* protection although non-inhibiting antibodies are reported to aid in protection via other mechanisms (Kim et al. 2016). In a recent paper DiLilo et al. have stated that broadly cross-reactive antibodies to HA, even the non-neutralizing or non-inhibiting ones, are protective in mice via Fc-FcYR interaction and a cell cytotoxicity mechanism (DiLillo et al. 2016). This was shown with IgG2a antibodies in mice. In the case of humans, Jegaskanda et al. have shown that humans also elicit ADCC antibodies following seasonal vaccination and they may play role in protection (Jegaskanda et al. 2016). *In vivo* protection was seen with non-inhibiting NA antibodies suggesting that antibody effector functions such as ADCC and complement-dependent cytotoxicity may play a role (Wan et al. 2013). We will look at the ADCC function of these antibodies in protection against virus in the future.

Comparison with other NA antibodies

Mouse antibody CD6 isolated by Eichelberger's group is specific to avian N1 unlike our N1 antibodies (Wan et al. 2013; Wan et al. 2015). It binds residues bridging adjacent monomers in the NA tetramer. This epitope may be different from our N1 antibodies, as CD6 failed to inhibit recent clade 6B.1 virus (K432 and N369 substitutions) whereas AG7C and AF9C are reactive to these NAs.

The murine N9 antibodies NC10 and NC41 isolated by Webster et al in 1987, showed reduced binding to substitution at K432 (**K**EDK) (Webster et al. 1987). Similar to Z2B3, the D56 in HCDR of mAb NC10 formed a long salt bridge link with the K432 of the N9 NA (Malby et al. 1994) (Appendix 5.2). Our N9 antibody Z2B3, which is cross-reactive to N1, is also affected by the K432E substitution. However, NC10 and NC41 are not

cross-reactive to N1 NA. Z2B3 formed multiple amino acid contacts with neuraminidase, in accord with other NA antibodies (15-30 amino acids, reviewed in Chapter 1), but uniquely many of these contacts were in the conserved active site.

An antibody that is cross-reactive to all neuraminidase subtypes has been isolated from hyperimmune rabbits (Doyle, Hashem, et al. 2013). This antibody is directed to a conserved peptide derived from the active site. However, it is a very low affinity antibody and requires three doses of 60 mg/kg for prophylaxis protection in mice, compared to a single dose of 10 mg/kg for our antibodies. This major difference may be because the Doyle antibody was raised to a synthesised linear peptide that is very unlikely to conserve the tertiary structure of the active site from which it was derived (Doyle, Hashem, et al. 2013).

Implications for vaccination and therapy

The protective effect of neuraminidase antibodies in humans is now beyond doubt. It therefore seems reasonable that the regulatory authorities should insist that the standard subunit vaccine should contain a sufficient quantity of immunogenic NA protein to induce a protective antibody response. This would ensure some protective effect of the vaccine even in years where antigenic drift of HA has reduced the efficacy of the vaccine, and help prevent the selection of new escape variants in HA.

The binding affinity of H3 haemagglutinin for sialic acid in recent H3N2 viruses has steadily decreased, and in some cases binding has been subsumed by the neuraminidase (Lin et al. 2010). In addition, it has been possible to produce viable H1N1 viruses *in vitro* where this has occurred (Hooper and Bloom 2013). It may be that the evolution of human seasonal influenza is heading towards a state where NA takes over the sialic binding function from HA, and HA retains only fusion activity. If this happens, antibodies that

block NA may become crucial. It would seem wise to prepare for this situation by ensuring a strong antibody response to NA in modern vaccines.

We have shown that it is possible to find antibodies with very broad reactivity to NA, which can bind to conserved residues within the active site of the enzyme. This is an exciting period for the isolation of broadly cross-reactive antibodies, which arise from exposure of the human population to a new neuraminidase. This raises the question of whether a vaccine could be designed that selected for such antibodies. The difficulty lies with the observation that in general residues at some distance from the active site, that are undergoing genetic drift, tend to be highly immunogenic and attract most of the attention in the immune response. Given the propensity of the conserved parts of the NA active site to select B cells from the memory pool at times when there is a major shift in sequence of the NA, perhaps a simple strategy would be to immunise humans sequentially with recombinant NAs based on the phylogenetically most distant sequences. This is the exact opposite of the present fashion for attempting to match the HA and NA to the most recently drifted variants.

The recent introduction of broadly reactive antibodies to the HA stalk for therapy could be supported by the broadly reactive NA antibodies described here. This would be entirely logical as the two classes of antibody act at different points of the virus life cycle, anti HA at entry and anti NA at release, and should complement each other's activities.

Appendix 5. 1 V(D)J genes of neuraminidase antibodies with number of somatic mutations and CDR lengths

	Heavy Chain								Light Chain						
Antibody	**V-GENE and allele**	**J-GENE and allele**	**D-GENE and allele**	**D-REGION reading frame**	**V-REGION identity %**	**V-REGION Nb of AA changes**	**CDR-IMGT lengths**	**AA JUNCTION**	**Locus**	**V-GENE and allele**	**J-GENE and allele**	**V-REGION identity %**	**V-REGION Nb of AA changes**	**CDR-IMGT lengths**	**AA JUNCTION**
AG7C	4-31*03, or 4-31*06	4*01, or 4*02	5-24*01	3	89.0	15	10.7.11	CARDLEGHTFHDW	Kappa	1-39*01, or 1D-39*01	2*01	88.5	17	6.3.9	CQQSHSAPYTF
AF9C	1-69*01, or 1-69D*01	6*02	4-17*01	2	91.7	16	8.8.19	CARDLAPYGDRFYFHYGMDVW	Kappa	1-9*01	5*01	94.6	9	6.3.9	CQQLNNYPFTF
M6B12	3-48*03	4*02	4-17*01	2	93.8	11	8.8.19	CARDRLPDRDSGDYESRFDFW	Kappa	1-33*01, or 1D-33*01	2*01	93.2	12	6.3.9	CQQYFKIPYTF
Z2B3	1-69*01, or 1-69D*01	6*02	5-18*01	1	96.5	8	8.8.25	CARDLQDTPMVDRIIGSYYYYNG LDVW	Lambda	2-14*01	2*01, or 3*01	96.9	8	9.3.10	CSSYTRSSSVVF
Z2C2	3-66*01, or 3-66*04	6*02	2-21*02	2	93.3	13	8.7.27	CASWSFCGGDCYPDRMQEKFH YSYGMDVW	Kappa	1D-12*01	4*01	95.7	9	6.3.9	CQQAYSFPLTF
Z1A11	1-46*01, or 1-46*02 or 1-46*03	6*02	3-22*01	2	92.7	17	8.8.19	CARNSYYYDTDRPYYNGMDVW	Kappa	2-28*01, or 2D-28*01	5*01	96.9	5	11.3.9	CMQAVQTPRTF
W1C7	3-9*01	3*02	4-17*01	2	99.7	0	8.8.13	CAKDVGGDYHAFDIW	Kappa	3-15*01	4*01	99.6	1	6.3.10	CQQYNNWPPLTF
P17C	3-23*04	5*02	2-15*01	1	99.3	1	8.8.14	CAKDGRWLLGNWFDPW	Lambda	2-14*01	1*01	99.3	2	9.3.10	CSSYTSSSTFVF
F4C	4-59*01	4*02	4-17*01	2	99.7	1	8.7.10	CARGYYGDYDYW	Lambda	1-40*01	2*01, or 3*01	100.0	0	9.3.11	CQSYDSSLSGVVF

Appendix 5. 2 Structure of antibody NC10 Fab complexed with N9 neuraminidase PDB:1NMB *(Malby et al. 1994). N9 is labelled green, Heavy and light chains are labelled orange and pink respectively. D56 of H-chain formed a salt bridge with K432 of NA.*

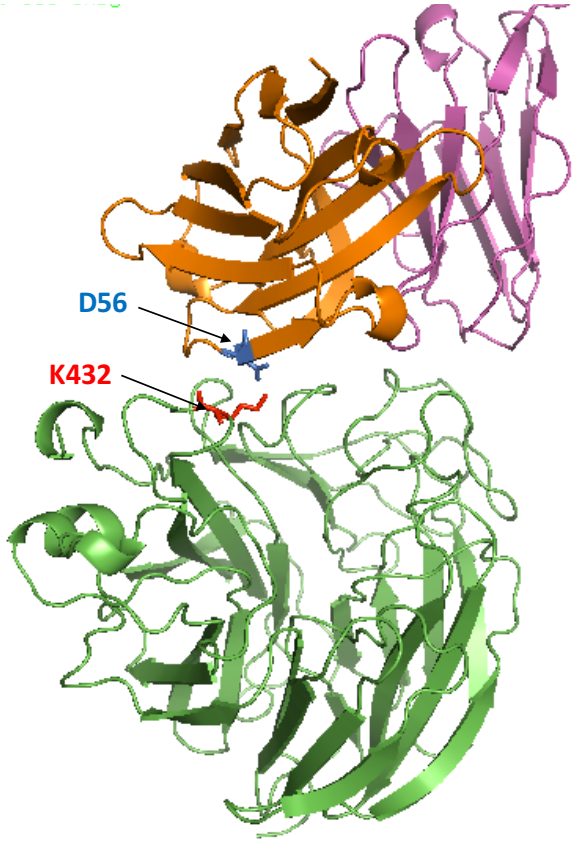

CHAPTER 6 | Human monoclonal antibodies to Ebola glycoprotein

CHAPTER 6 INTRODUCTION

When the Ebola outbreak started in 2014, there was a lot of interest and need for research, because there were no specific therapies available and mortality from the disease was greater than 50% (reviewed in the Chapter 1). We took the opportunity to apply our methods of isolation and characterisation of influenza antibodies to isolate monoclonal antibodies from Ebola vaccinated donors. Our aim was to form a therapeutic cocktail of potent neutralising human antibodies binding to non-overlapping epitopes that would curtail the risk of escape due to the selection of resistant mutant viruses (Kugelman et al. 2015).

The only available promising antibody cocktail against Ebola virus at the time of the epidemic was ZMapp (Qiu et al. 2014). Now it is known from the clinical trial of ZMapp that it appeared to be beneficial but it did not meet the set threshold for efficacy (Prevail Team 2016). There is a need for efficacious antibodies to form a better cocktail. These antibodies isolated from human will also provide valuable information on epitopes and serve as tools to study virus biology.

In the Ebola vaccine trial at the Jenner Institute, 60 volunteers were vaccinated with a priming dose of ChAD3 EBO Z (Chimpanzee Adeno virus expressing Zaire GP) vaccine and 30 of them received a booster with recombinant MVA-BN Filo (Modified Vaccinia expressing Zaire, Sudan and Marburg GPs and NP from the Tai Forest strain) vaccine (Ewer et al. 2016). We were unable to isolate antibodies from primed PBMC at day 10

after the priming dose with recombinant Adeno virus, as the plasmablast frequency was too low and the antibody PCR positivity was also low. Thus, we used day 7 post boost PBMC from 8 donors who received the boosting dose of recombinant MVA, to isolate monoclonal antibodies.

In collaboration with Simon Draper's group at the Jenner Institute and Antibody Discovery Unit at the company UCB (Slough, UK), we have isolated 82 monoclonal antibodies to date. Our antibodies were isolated from FACS sorted plasmablasts (Smith et al. 2009). UCB employed a different method comprised of isolation by micro-manipulation of cultured memory B cells identified by plaque staining of an underlying monolayer of GP transfected MDCK-SIAT1 cells supplied from us. Screening of the antibodies was done using immunofluorescence assays on GP expressing MDCK-SIAT1 cells referred to as E-SIAT cells. We performed binding, neutralisation and epitope mapping for these antibodies. Further characterisation and the potential therapeutic value of these antibodies are being studied.

CHAPTER 6 RESULTS

6.1 Principle of antigen specific cell sorting

Antibody development from a single cell is tedious and time consuming. The success rate depends on many factors including vaccine potency, plasmablast frequency and individual variation in response. In some donors, the antigen specific cells may comprise as few as 10% of the plasmablasts identified by their size and the CD27 and CD38 surface markers. However, for some individuals up to 40% of the isolated antibodies may be antigen specific. Screening serum or plasma before antibody isolation may help in identifying the best donors for antibody isolation. Using antigen for staining specific plasmablasts may help to increase the efficiency of isolation of antigen specific

antibodies, and if successful can save much labour. To test the practicality of this idea, we expressed the transmembrane forms of specific human IgG1 in transfected 293T cells to mimic plasmablasts (as described in Materials and Methods Chapter 2). We used purified soluble glycoprotein (GP) to bind the membrane antibody, and then detected the bound GP with a previously characterised and biotinylated antibody. We chose to develop this sandwich technique rather than direct labelling of the GP protein, as the GP protein was in short supply. In addition, the sandwich technique has the advantage that the antigen preparation used to stain the cells need not be purified to homogeneity, as the third layer antibody ensures specificity, and in addition the antigen is not altered by biotinylation or another coupling. The disadvantage of this approach is that for detection at least one characterised antibody to the antigen is required.

In figure 6.1, 293T cells were transfected with three human IgG1 immunoglobulins converted to the transmembrane form (as described in Materials and Methods Chapter 2). TM-3CSY (transmembrane 3CSY) is a synthesised form of the defined antibody KZ52 (Lee et al. 2008) that binds to the base of GP; TM-P7 is the first antibody I isolated that binds the glycan cap of GP; and TM-Z4B2 is a negative control antibody specific for the stem of H7 influenza haemagglutinin. Transfected cells were exposed to soluble Ebola GP or H7 haemagglutinin (20 μg/ml), washed and then exposed to biotinylated antibodies specific for Ebola GP (3CSY-Bio and P7-Bio) or the globular head of H7 haemagglutinin (4A-14-Bio) or anti IgG1-Bio. Finally, after a further wash the biotinylated antibodies were detected by Streptavidin-PE. In column 1 staining with Ebola GP is detected with 3CSY-Bio on cells expressing TM-P7 as expected, but not on cells expressing the control antibody TM-Z4B2. In the case of GP+3CSY-bio there is self-competition hence the frequency of positive stained cells is less. The same phenomenon is seen in case of P7 expressed as transmembrane IgG in column 2. 3CSY-biotin antibody stained well but P7-

biotin did not. Specificity of the staining is shown in column 4 where cells transfected with TM-Z4-B2 are stained with H7 protein and detected with 4A-14-Bio. Finally, all of the cells transfected to express TM-IgG1 are stained by the anti-Ig-Bio reagent in column 6.

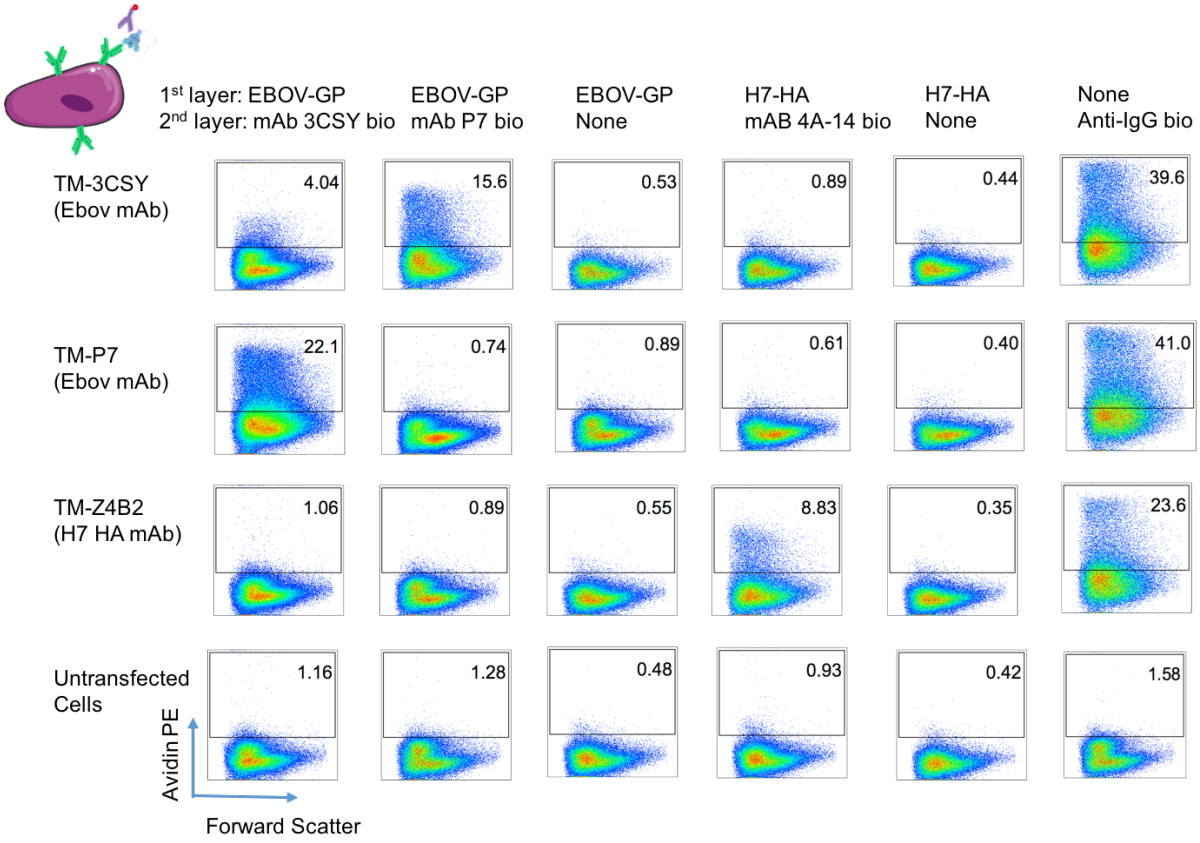

Figure 6. 1 ***Principle for antigen specific cell sorting using antigen + biotinylated-mAb sandwich technique****. 293T cells transfected with transmembrane forms of IgG1 specific for Ebola GP (TM-3CSY and TM-P7) or H7 haemagglutinin (TM-Z4B2), were stained with antigen and secondary biotinylated monoclonal antibody. Stained cells are shown as percentage of total cells. Anti-human IgG antibody binds to TM-IgG transfected cells irrespective of the antibody specificity. 3CSY and P7 are anti-EBOV-GP mAbs, and 4A-14 and Z4B2 are anti-H7 haemagglutinin mAbs isolated from H7N9 infected donors.*

Note that "3CSY" is the lab name given to our synthesised version of KZ52, based on the PDB sequence 3CSY.

Having established the principle of staining antibody-expressing cells with antigen we applied it in some experiments to sort plasmablasts, but with variable success. Staining did not seem to be as efficient as for TM-Ig expressing 293T cells, perhaps because the plasmablasts are beginning to convert their IgGs to the secreted form.

6.2 Plasmablast cell sorting and antibody screening

PBMC from 8 vaccinated donors were sorted in our laboratory. Figure 6.2A shows the GP-ELISA titre of plasma pre-vaccination (red) and post-MVA boost (green) from 8 donors. Pre-immune plasma showed some level of reactivity to Ebola glycoprotein. Since Ebola glycoprotein is a novel antigen and there is very little chance that donors may have been previously exposed, these may be low level cross-reactive antibodies to previously encountered antigens. After vaccination, the antibody level increased 2- to 8-fold in seven donors. Donor 19 was exceptional because the ELISA EC50 titre reached >600. These are only indicative titres. To find out actual titres we need to test post day 14 plasma or sera since the blood antibody level peaks at day 14. Plasma ELISA titre did not match the size of the plasmablast population induced by vaccination. Although donor 19 had the highest ELISA titre, the plasmablast population was only 0.6 % of B cells. The highest plasmablast frequency was 3% for donor 66, and we isolated many antibodies from this donor. By contrast, in the response to influenza the plasmablast frequency normally ranges from 2-30%. The difference may be because our donors were being exposed to Ebola antigens for the first time, whereas most individuals have been exposed to influenza multiple times through infection or vaccination.

A)

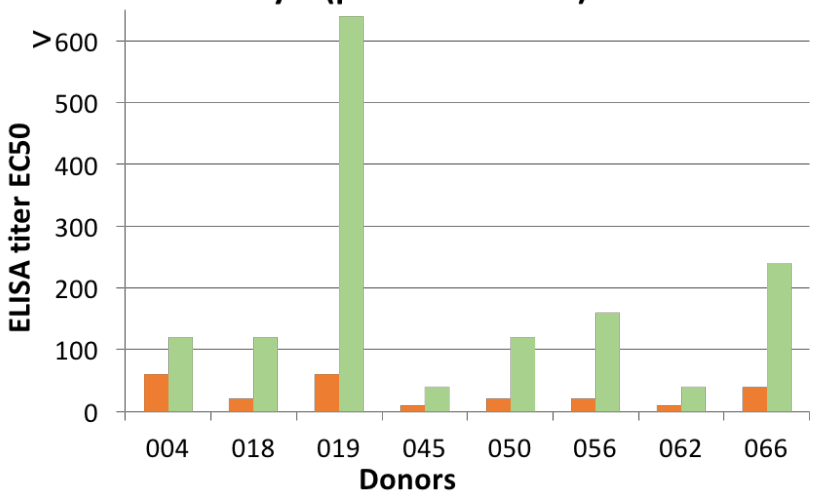

B)

Donor	% Plasmablasts of total B cells
004	0.5
018	1.2
019	0.6
045	1.1
050	1.1
056	0.7
062	2.3
066	3

Figure 6. 2 ***GP-ELISA and plasmablasts measurement from eight donors from the Ebola vaccine trial.*** *A) Orange bar represents plasma titre before the vaccination and green bar represents plasma day 7 post booster vaccination. There is some level of cross-reactivity in pre-immune sera. Donor 19 and donor 66 have the best ELISA EC50 titres. B) In this figure % plasmablasts out of total B cells are shown for 8 donors. Donor 66 has the highest percentage of plasmablasts. Although donor 19 had the highest ELISA titre, the percentage of plasmablasts was low.*

Figure 6.3 shows an example of plasmablast sorting and screening of the monoclonal antibodies obtained after PCR, cloning, and co-transfection of heavy and light chain plasmids in 293T cells (as described in Materials and Methods). In A) PBMC were stained and plasmablasts were gated as Lymphocytes/Single cells/CD3neg/CD19pos/CD38high/CD27high. Class-switched (IgM and IgD negative) plasmablast were sorted as single cells.

After developing monoclonal antibodies from the single cells (as described in materials and methods), antibody supernatants were screened by indirect immunofluorescence

assay for binding to GP transfected MDCK-SIAT1 cells (referred to as E-SIAT cells) in 96-well plates. Mean Fluorescence Intensity was measured in the Clariostar Plate reader in B), and photographs of the stained cells are shown in C) (Figure 6.3). We had found earlier that unlike other cell types (Sullivan et al. 2005; Mohan et al. 2015), MDCK-SIAT1 (Matrosovich et al. 2003) can express high levels of full length GP in the plasma membrane without showing toxicity. In addition, they are highly adherent and can withstand multiple washing steps without detaching from the plastic well, which makes them convenient for screening.

In the example shown in figure 6.3, mAb P7 was found to be positive for binding. Control positive antibody 3CSY was made in-house by synthesis and expression of codon optimised cDNA encoding the amino acid sequence of the characterised antibody KZ52 (Lee et al. 2008) derived from the crystal structure of this antibody in complex with Ebola GP (PDB 3CSY) described by Murin et al. (Murin et al. 2014). 3CSY antibody and E-SIAT cells were made by my supervisor Alain Townsend.

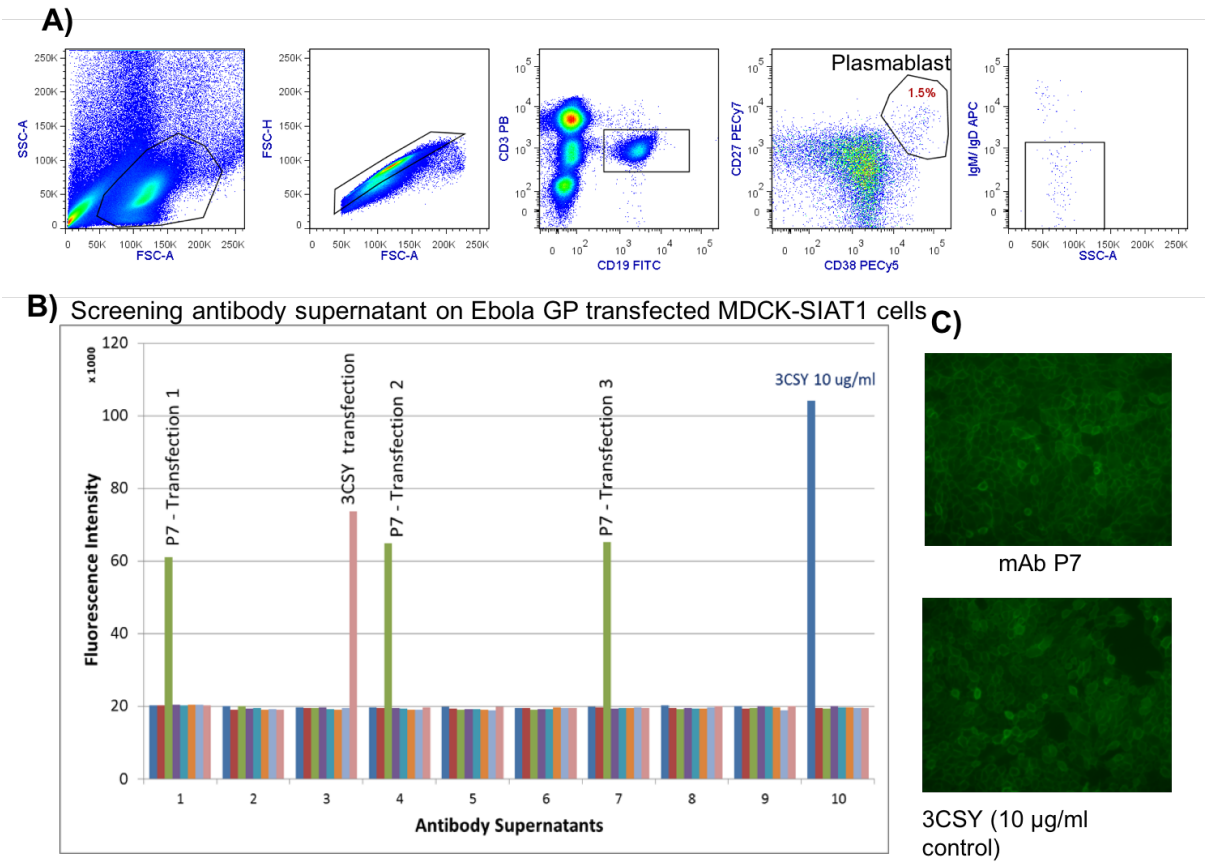

Figure 6. 3 ***Plasmablast sorting and antibody screening A)*** *Sorting of class-switched plasmablasts (Lymphocytes/Singlets/CD19pos/CD3neg/CD38high/CD27high/IgM IgDneg) from donor 018. Out of total CD19^{+} B cells, 1.5% are plasmablasts.* ***B)*** *Antibody supernatants obtained after developing antibody from sorting, cloning and 293T cell transfection were screened for binding to Ebola glycoprotein expressed on MDCK-SIAT1 cell surface. Transfections and screening were done on a 96-well plate system. Binding fluorescence was read by the Clariostar plate reader. In this plate, there are three transfections of mAb P7, which are specific to Ebola glycoprotein. 3CSY is a positive control. C) mAb P7 and control 3CSY staining under the microscope (40x magnification).*

We also tried using purified glycoprotein and known biotinylated GP specific antibody to sort the specific plasmablasts from donor 66 using the sandwich technique. Figure 6.4A shows the gated plasmablast population and GP-specific staining. Out of 38 cells sorted

after GP staining, 22 antibodies were obtained and 9 of them were GP specific, whereas from the unstained plasmablasts 44 antibodies were obtained of which 11 were GP specific (Figure 6.4B). This may represent a true enrichment but did not reach statistical significance (P = 0.256 by Fisher's exact test). We have not done enough comparisons to make a firm statement about this due to lack of sorting time. However, we have got the impression that the use of GP protein to sort improves the yield of specific plasmablasts. This is useful since antibody isolation is a laborious, expensive and time-consuming task.

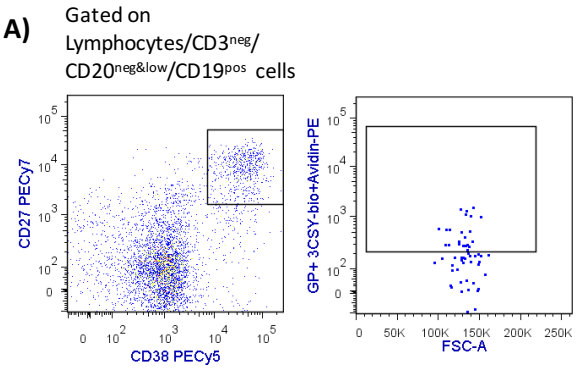

B)

Plate No.	No. of Cell sorted	mAbs made	GP specific mAbs	% of total mAbs
4	48	16	2	13
3	48	28	9	32
6 (GP sort)	38	22	9	41

Figure 6. 4 ***Sorting of plasmablasts and GP-specific plasmablasts from donor 66****. **A)** GP specific plasmablasts were isolated using GP protein + biotinylated antibody, detected by Avidin-PE fluorochrome. **B)** Antibodies derived from plates 3 and 4 are from general pool of plasmablast and from plate 6 from GP-specific plasmablasts. A higher proportion of antibodies were GP-specific when GP protein was used during plasmablast sorting but did not reach statistical significance.*

6.3 Influenza pseudotyped virus to test antibody neutralisation

If possible it would be optimal to test antibodies for neutralisation of wild type Ebola virus. However, Ebola is a highly dangerous pathogen that requires BSL-4 containment. Several surrogates for Ebola have been developed by pseudotyping (coating) various viruses with Ebola Glycoprotein (Wool-Lewis and Bates 1998; Watanabe et al. 2004;

Yonezawa, Cavrois, and Greene 2005; Chandran et al. 2005; Ye et al. 2006). These can be used in neutralisation assays *in vitro* in more convenient containment conditions. The most commonly used are disabled forms of VSV or lentiviruses coated in Ebola GP expressed from a separate codon optimised plasmid (Watanabe et al. 2004; Cronin, Zhang, and Reiser 2005). As our laboratory has developed a pseudotyped influenza particle (Powell et al. 2012) for use as a vaccine for the induction of T cell immunity to influenza, we decided to try pseudotyping S-FLU with Ebola glycoprotein as we have the expertise locally.

S-FLU was designed by Alain Townsend and is based on a recombinant influenza A/PR/8/34 that has been prevented from replication by inactivation of the haemagglutinin signal sequence, and replacement of the coding sequence with eGFP, which makes infected cells fluoresce brightly for detection (Powell et al. 2012). S-FLU is normally grown in MDCK-SIAT1 cells that have been transduced to express a stable high level of an influenza haemagglutinin of choice. In such cells the genetic defect in S-FLU is complemented and the virus replicates and buds out of the cell coated in the haemagglutinin expressed in the MDCK cell plasma membrane. The resulting particles are now coated in haemagglutinin, but do not contain a gene encoding haemagglutinin. They can infect normal cells once only (and are thus single cycle viruses), and infected cells express eGFP instead of haemagglutinin and all the other viral proteins are expressed in the cytosol. For this reason, they are very effective at inducing cell mediated immunity to influenza (Baz et al. 2015). They can also be used in neutralisation assays in vitro, where the prevention of expression of eGFP is a convenient measure of neutralisation, and can be read from 96-well plates in the Clariostar plate reader (BMG Labtech) in a few minutes (as described in Materials and Methods).

MDCK cells expressing full length Ebola GP were tested for their ability to produce pseudotyped S-FLU, after agreement that the replication incompetent A/PR/8/34 progeny coated in Ebola GP, which do not contain any genetic information from Ebola could be handled at BSL-1. Townsend found that S-FLU could be pseudotyped successfully with Ebola GP by these methods, and Julie Xiao (DPhil student) showed that infection of Hela cells was absolutely dependent on the known receptor for Ebola NPC1 (Xiao et al. manuscript in preparation).

The pseudotyped S-FLU virus coated in the Ebola Zaire GP (GenBank KJ660346.2) from the recent outbreak (Table 6.5) is referred to as E-S-FLU. We validated it for neutralisation by control Ebola specific antibodies published in the literature: KZ52 (3CSY described above) (Lee et al. 2008), 100 and 114 ((Corti et al. 2016), kindly provided by Davide Corti and Antonio Lanzavecchia), 6D6 ((Furuyama et al. 2016), kindly provided by Ayoto Takada), and ZMapp components (Qiu et al. 2014), synthesised at the Jenner Institute in the form of chimeric human IgG1 antibodies).

6.4 Neutralising antibodies

A total of 82 antibodies were isolated from 11 vaccinated volunteers (14 mAbs at Jenner, 36 at WIMM and 32 at UCB) from plasmablasts and memory B cells (Table 6.1 and figure 6.5). The greatest number of antibodies (n=29) were isolated from the donor 66.

Table 6. 1 Number of antibodies isolated from vaccinated individuals

Donor	No. of mabs	Neutralizing
66	29	11
4	13	8
49	9	5
56	8	3
3	6	4
12	5	4
18	5	1
14	2	1
45	2	0
68	2	1
19	1	0
Total	**82**	**38**

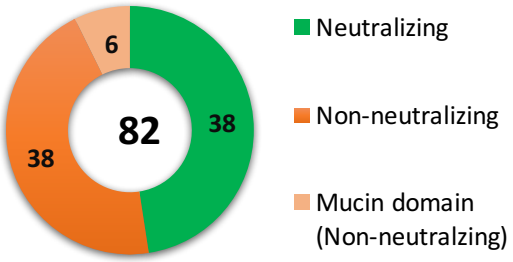

Figure 6. 5 ***Total of 82 antibodies were isolated from 11 vaccinated volunteers****. (14 mAbs at Jenner, 36 at WIMM and 32 at UCB from plasmablasts and memory B cells). Six mucin-like domain dependent and another 38 antibodies are non-neutralising. Almost half of the isolated antibodies are neutralising in in-vitro assays.*

Out of 82 antibodies, 38 inhibited infection by the pseudotyped E-S-FLU virus by at least 50%. We use the 50% inhibition cut off as the definition of "neutralisation". Antibodies that neutralise by this definition can be divided into a subset of 17 "strong neutralisers" that reproducibly reduce infection by >90%, and 21 "partial neutralisers" for which

inhibition of infection plateaus between 50% and 90%, irrespective of the starting concentration of the inhibiting antibody.

Figure 6.6 shows an example of the neutralisation assay, where all Ebola mAbs are neutralising except the influenza mAb (negative control). Microscope pictures show the MDCK-SIAT1 cell monolayer, cell infection by the virus, and virus inhibition by different antibodies at 5 μg/ml concentration. The antibody 66-6-3 neutralised E-S-FLU virus to baseline, whereas 66-4-C12 neutralised only to 60%. IC50 (Inhibitory concentration 50%) and IC90 (inhibitory concentration 90%) of the antibodies are shown in figure 6.7. IC50 ranged from 100 ng/ml to 10,000 ng/ml. This is about 10-fold higher than the neutralisation titres for influenza viruses (see chapter 3). IC90 of the antibodies ranged from 1000 – 10,000 ng/ml. Antibodies 125 and 66-6-3 are the most potent with the lowest IC50 and IC90 respectively.

Among 17 strong neutralisers the IC50 and IC90 values are comparable to the control antibodies 3CSY (equivalent to KZ52) (Lee et al. 2008), 114, 100 (Corti et al. 2016) and ZMapp component 4G7 (Qiu et al. 2014), which gave similar values in our MN assays.

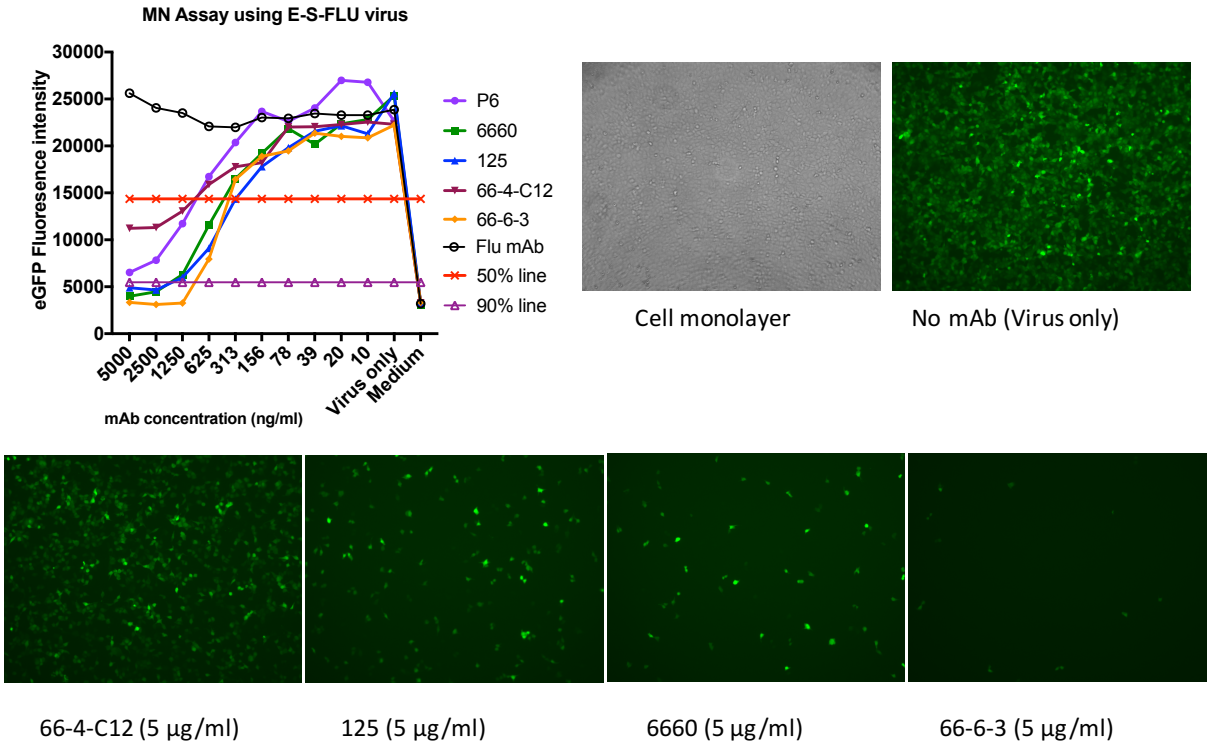

Figure 6. 6 ***Neutralisation of pseudotyped virus E-S-FLU with monoclonal antibodies****. In this non-replicating influenza virus with surface coated with EBOV GP, HA gene is replaced by eGFP which acts as an assay reporter. Antibody 66-4-C12 is a partial neutraliser and other antibodies are strong neutralisers; they suppress cell infection by the virus by at least 90% in the majority of assays. Influenza antibody is a negative control. Microscope pictures are shown for an MDCK-SIAT1 cell monolayer, infection in absence of antibody, and suppression by antibodies. (Magnification 40x)*

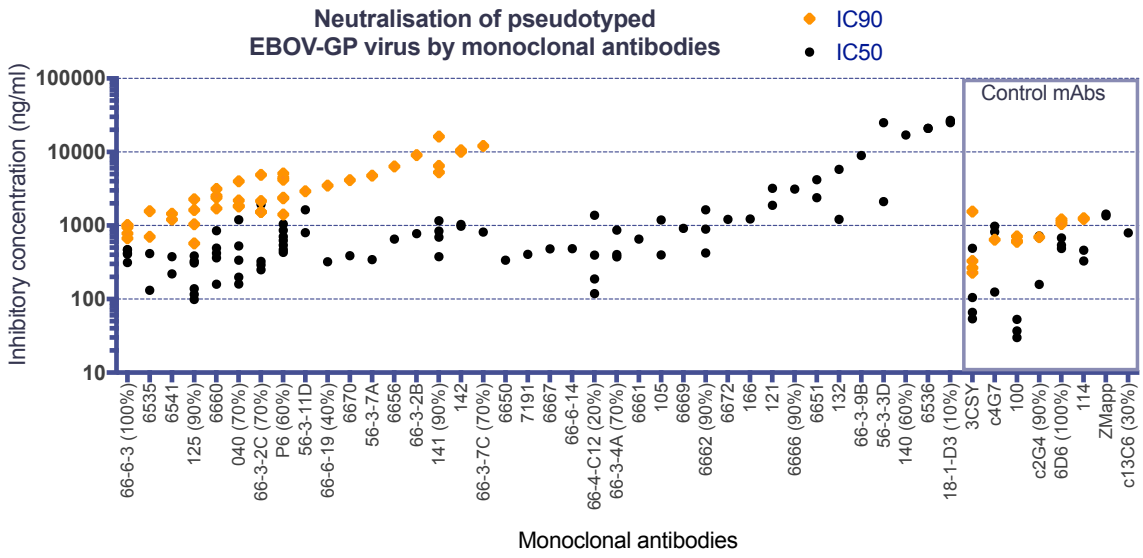

Figure 6. 7 ***In vitro neutralising concentration of monoclonal antibodies shown as IC50 and IC90****. Out of 82 antibodies, 38 are neutralising defined as reaching 50% inhibition of infection. Neutralisation IC50 ranges from 100 ng/ml to 10 µg/ml. Some partially neutralising antibodies have no IC90 values. Almost half of the antibodies have titres comparable to that of the antibodies published in the literature. Percentage of protection of mice from death by Ebola virus infection, are shown for some antibodies in the bracket. Control antibodies were kindly provided by various labs. 100 and 114 (Corti et al. 2016; Misasi et al. 2016): Antonio Lanzavecchia and Davide Corti; Zmapp mAbs c4G7, c2G4, c13C6 (Qiu et al. 2014): Simon Draper's lab and ZGP226 (Marzi et al. 2012): Ayoto Takada's lab. Note that "3CSY" is the lab name given to our synthesised version of KZ52, based on the PDB sequence 3CSY.*

6.5 Partially neutralising antibodies

There are 21 partially neutralising antibodies (defined as reaching 50% but not 90% inhibition of infection) (16 are shown in Table 6.2). These antibodies are mostly encoded by the VH3-15 gene (n=7) and the rest by 7 other VH genes. These antibodies used lambda (n=9) or kappa (n=7) light chains in almost equal numbers. Not all the antibodies

have been assigned epitopes but for the 7 antibodies which have been determined, 4 belong to receptor binding region (RBR) and 3 to the base of GP. Other antibodies to these regions can be strong neutralisers (see below).

Table 6. 2 Partial neutralising antibodies and their properties

mAb	Donor	Epitope	VH	L/K
140	3		1-18*01	λ
6659	4		3-15*01	λ
6655	4		3-21*01	κ
6650	4		3-30*03, or 3-30*18 or 3-30-5*01	κ
6651	4	Base	4-39*07	κ
6665	12		3-15*07	λ
6667	12	RBR	3-15*07	λ
6666	12	RBR	3-15*01	λ
105	49	RBR	3-15*07	λ
132	49		3-15*07	λ
121	49		3-33*01 , or 3-33*06	λ
56-3-3D	56		1-18*01	κ
66-6-10	66	Base	1-2*02	κ
66-3-9B	66		3-23*04 , or 3-23D*02	κ
66-4-C12	66	Base	3-23*04 , or 3-23D*02	κ
6662	68	RBR	3-15*07	λ

We have not found any common denominator for these partially neutralising antibodies that distinguishes them from strong neutralisers. We need to look at antibody affinity and kinetics values to find out if this may be determining the partial neutralising nature of the antibody, alternatively the exact specificity of the antibody might be the factor determining the efficiency of neutralisation.

6.6 The relationship between neutralisation *in vitro* and protection *in vivo*

Our view has been that the demonstration that an antibody can block NPC1 dependent infection of cells *in vitro* should be a good starting point for selecting antibodies that will be protective *in vivo*. Clearly it would not be practical to screen all Ebola specific antibodies for protection of NHPs from wildtype Ebola infection. In our collaboration with Erica Ollmann Saphire, as part of the Viral Haemorrhagic Fever Immunotherapeutic

Consortium (VIC), we have submitted a total of 24 of our antibodies for screening in a battery of tests aimed at selecting the best candidates for a therapeutic cocktail.

The initial *in vivo* screen was by therapy of groups of 10 Balb/c mice infected with mouse adapted Ebola virus for 48 hrs, followed by a single i.p. dose of 100 µg of the test antibody (approximately 5 mg/kg). This was designed as a stringent test for therapy of a developed infection from which to select antibodies for assessment in other models. As controls the 6D6 antibody and the ZMapp components 13C6 and 2G4 were included. 6D6 and 2G4 are strongly neutralising in our assay and provided 100% and 90% protection of mice respectively, 13C6 is partially neutralising and provided 30% protection.

Tables Appendix 6.2 and 6.3 show the results for the 24 antibodies and 3 controls. The 10 non-neutralising antibodies provided varying levels of protection from 10% to 50%. 12 of the 14 neutralising antibodies provided protection between 60% to 100%. A 2x2 contingency table of survivors v non-survivors for animals treated with the 14 neutralising v 10 non-neutralising antibodies (excluding the 6D6, 13C6 and 2G4 controls) is shown below:

	Survived	RIP	Total
Neutralisers	92	48	**140**
Non-Neutralisers	31	69	**100**
Total	**123**	**117**	**240**

Fisher's exact test

The two-tailed P value is less than 0.0001
The association between rows (groups) and columns (outcomes) is considered to be extremely statistically significant.

This indicates that there is a strong association between treatment with an antibody that blocks infection of cells *in vitro* by our E-S-FLU surrogate for Ebola, and survival in this mouse-protection test. However, it is also clear from Tables Appendix 6.2 and 6.3 that

non-neutralising antibodies can provide protection up to 50% (mAbs 66-3-7B and P7), and partially neutralising antibodies that do not reach 90% inhibition of infection *in vitro* can protect 90% of animals from death (mAbs 6662 and 6666), and occasional strong neutralisers are weak in the protection assay (mAb 66-6-19).

6.7 Defining antibody epitopes

The binding sites of the antibodies were analysed using three methods: cross-inhibition for GP binding, screening a yeast display library expressing fragments of GP (in collaboration with Xiao-Ning's lab, Imperial College) and sequencing escape mutants generated *in-vitro* (in collaboration with Kawaoka lab, Wisconsin University). With these assays, we have defined three definitely non-overlapping regions on GP bound by neutralising antibodies, two in the head region (glycan cap and receptor binding region (RBR)) and one at the base.

6.7.1 Yeast display library screening

Libraries of small and large GP segments were expressed on the surface of yeast. Antibodies were allowed to bind to the GP segment expressed on the yeast surface, which were then stained by indirect immunofluorescence and sorted using FACS. The inserts of approximately 20 sorted yeast clones were then grown and sequenced (this was done by Xiao-Ning Xu's lab, Imperial College). For an antibody epitope to be definable in this system the antibody must be able to bind a fragment of protein containing the epitope. Fully conformation dependant antibodies will fail to detect any fragments.

The list of antibodies tested to date and their bound epitopes are shown in table 6.3 and three examples are shown in figures 6.8, 6.9 and 6.10. Among the control antibodies, C6d8 recognises an epitope in GP1 segment amino acids 393-401. However, the

antibodies 4F3 and KZ52 do not bind to small or large peptides, suggesting that these antibodies may recognise more conformational epitopes (Table 6.3). The overlapping region from different clones determines the binding region of the antibody. So far, 14 antibodies have been tested and only six antibodies bind the yeast-displayed segments. Antibody 114 recognised the epitope aa 102-230 (Figure 6.8). This fits with the crystal structure of this antibody bound to the GP trimer (Misasi et al. 2016) where the antibody binds the receptor binding region of GP. Other antibodies P6 and 040 recognise the overlapping GP1 epitopes 220-275 and 228-281 respectively (Figure 6.9 and 6.11). Another antibody 66-3-9C binds the small eight amino acid sequence 286-293 GEWAFWET (Figure 6.10), which has also been detected in the antibody response in non-human primates, and which is highly conserved in Ebola strains (Keck et al. 2016).

Table 6. 3 Antibodies tested on yeast display screening assay

No.	mAb	Origin	Known epitope	FACS sorting	Epitope identified
1	C6d8 (MB-003)	Murine/human chimeric	GP1 (393-401)	+	GP1 (393-402)
2	4F3	Mouse	-	+	GP1 (389-398)
3	KZ52	Human	GP1-GP2 (discontinues)	-	-
4	66-3-9C	Human	-	+	GP1 (286-293)
5	66-3-9A	Human	-	+	GP1 (477-489)
6	40	Human	-	+	GP1 (228-281)
7	114	Human	-	+ (only by large lib.)	GP1 (102-230) Conformational?
8	P6	Human	-	+ (only by large lib.)	GP1 (192-300) Conformational?
9	P7	Human	-	+ (only by large lib.)	GP1 (212-286) Conformational?
10	3CSY	Human	-	-	-
11	19-2-12C	Human	-	-	-
12	100.73	Human	-	-	-
13	133	Human	-	-	-
14	66-3-2C	Human	-	-	-
15	66-3-4A	Human	-	-	-
16	66-3-7C	Human	-	-	-
17	66-4-C12	Human	-	-	-

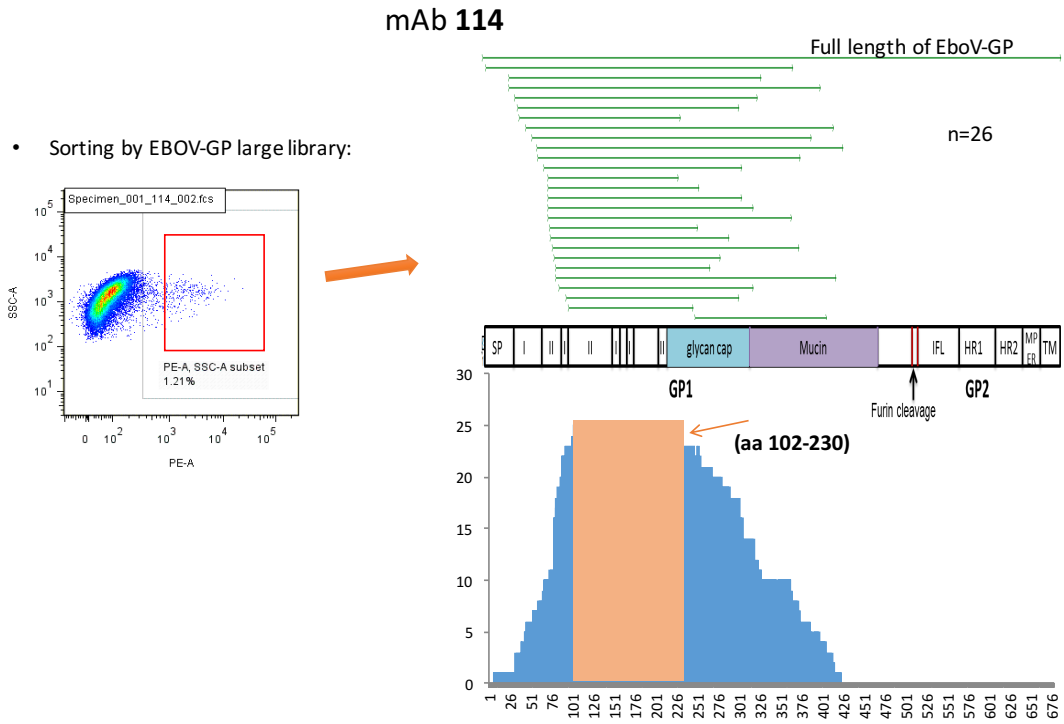

Figure 6. 8 ***Yeast Screen Display of mAb 114****. From the large library screening, aa 102-230 in the GP1 receptor binding region (RBR) was found to be an epitope for antibody 114 which fits with the epitope defined for this antibody in its crystal structure bound to glycoprotein (Misasi et al. 2016). This experiment was performed by Xiao-Ning's lab at Imperial College, London.*

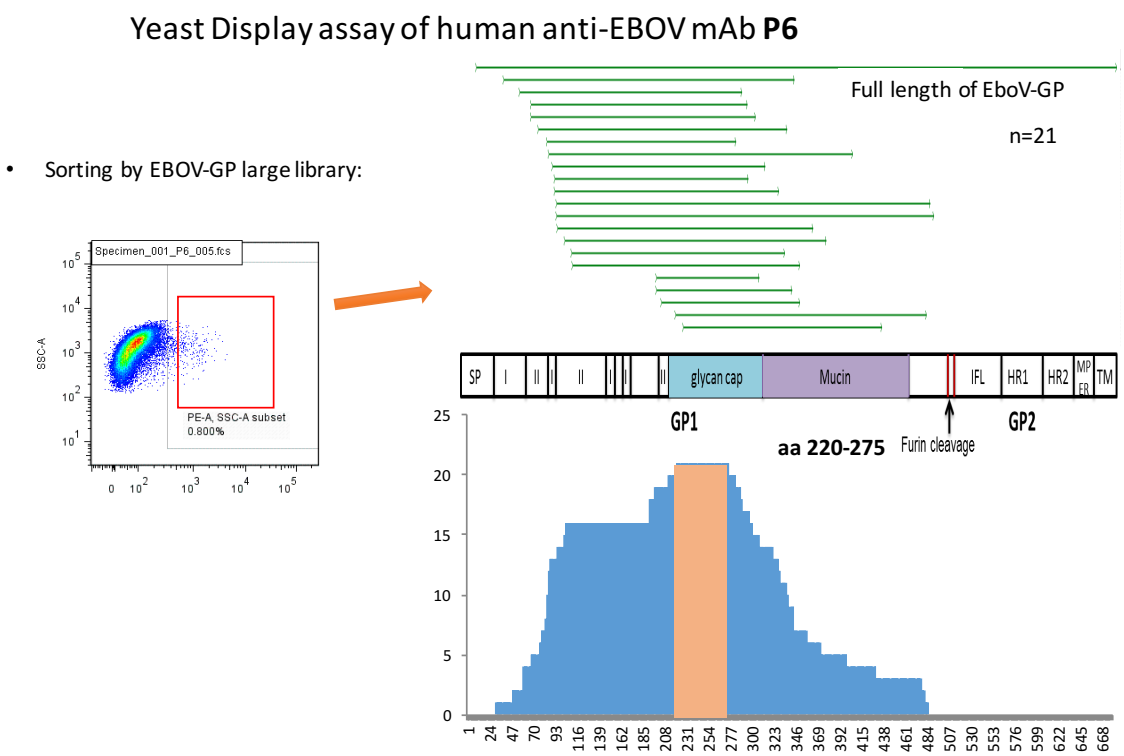

Figure 6. 9 ***Yeast Screen Display of mAb P6****. From the large library screening, aa 220-275 in the GP1 glycan cap was found to contain the epitope for antibody P6. This experiment was performed by Xiao-Ning's lab at Imperial College, London.*

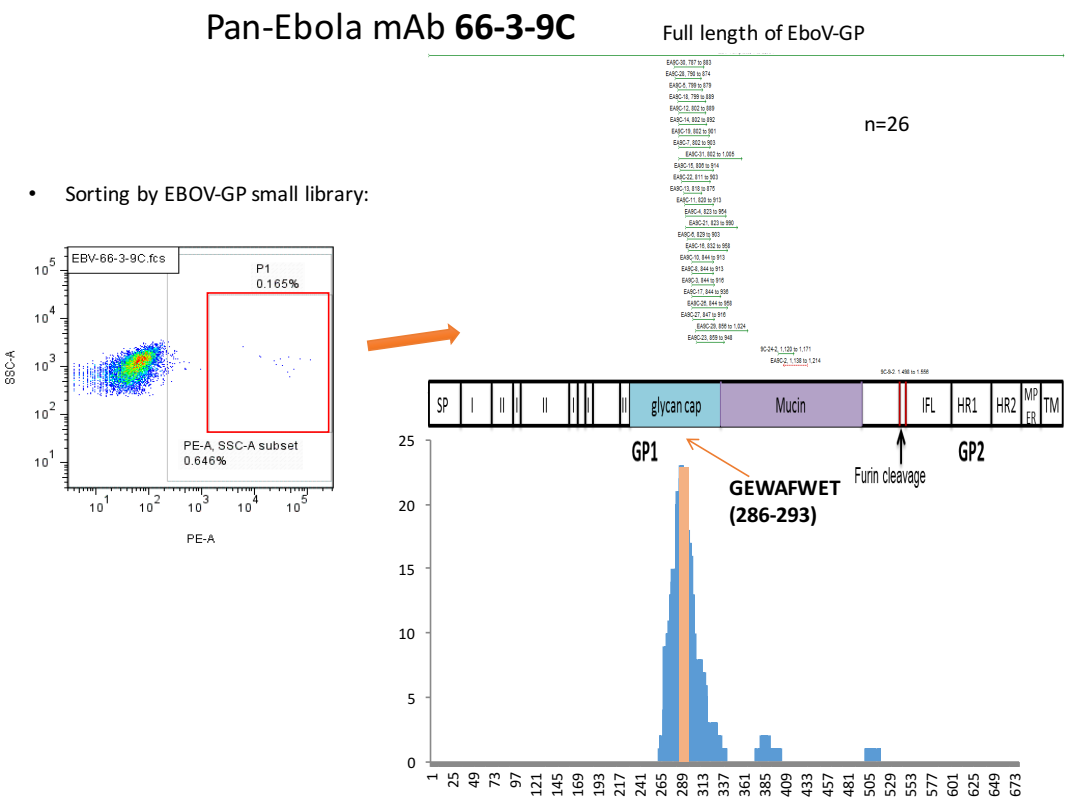

Figure 6. 10 ***Yeast Screen Display of mAb 66-3-9C****. From the small fragment library screening, aa 286-293 (GEWAFWET) in the GP1 glycan cap was found to be the epitope for antibody 66-3-9C. This epitope is conserved in all EBOV subtypes. This antibody is similar to the macaque antibody FVM09 (Keck et al. 2016). This experiment was performed by Xiao-Ning's lab at Imperial College, London.*

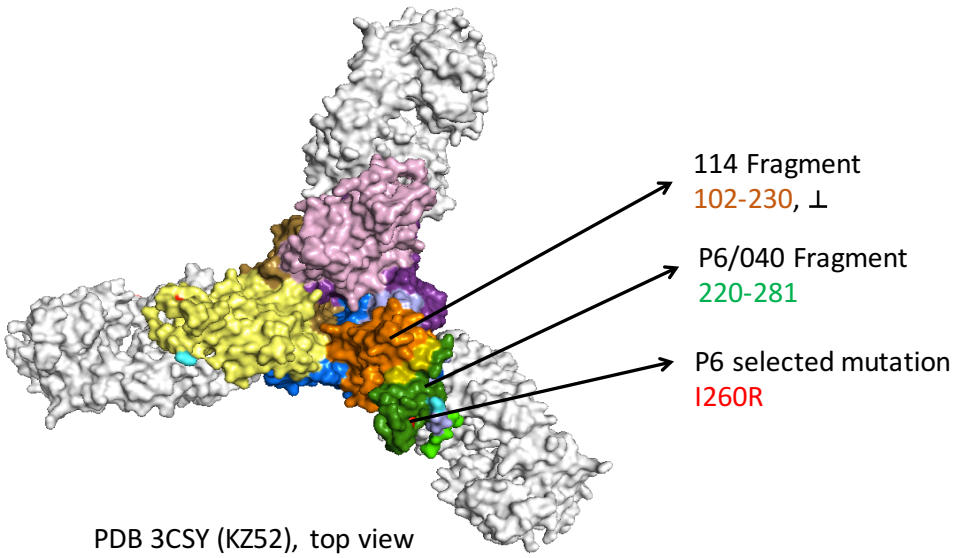

Figure 6. 11 ***Antibody Binding Sites Identified by Yeast Peptide Display.*** *Orange patch (aa 102-230) designates the binding site for mAb 114. This antibody binds perpendicular to the glycoprotein trimer (Misasi et al. 2016). Green patch (aa 220-281) designates the binding site for P6. Within the green patch is a red dot which designates residue I260. I260R substitution was selected as an escape mutation by mAb P6 in another experiment. Grey structures are Fab regions of 3CSY binding the trimeric GP structure at the base (Lee et al. 2008). The mucin like domain (amino acids 314-463) is not shown in the structure as it was removed prior to crystallisation. It would lie contiguous to the green P6 fragment. These sites are shown on the PDB 3CSY crystal structure.*

6.7.2 Escape mutants generated *in vitro*

Escape mutant generation was performed by Peter Halfmann in Kawaoka's lab at Wisconsin University. EBOVΔVP30 virus (Halfmann et al. 2008), handled in BSL3 containment, and Vero cells for infection were used to select escape mutants in the presence of saturating amounts of antibody. The VP30 gene is deleted and replaced with eGFP or the luciferase gene which is used as an assay reporter.

Antibody P6 was first tested to neutralise this near-to-wild type virus *in vitro* in the plaque reduction neutralisation (PRNT) assay. It reduced plaque formation completely at higher dose (1 μg/ml) and it titrated with reducing concentration (Figure 6.12A). Ten-fold of the saturating antibody dose was used to select virus escape mutants. Substitutions S322G and S347P were found respectively in 20/20 and 17/20 escaped clones. These amino acids are in the mucin like domain of the glycoprotein (aa 314-463), which was a surprise given the results with the yeast display library, which localised binding to the fragment 220-281 in GP1. We introduced these two mutations in the Zaire-GP and found no detectable difference in binding compared to wild type GP in indirect immunofluorescence assay by FACS at saturating concentration of antibody (data not shown). Also, we found that the antibody P6 binds strongly to GP from which the mucin-like domain had been deleted (data not shown). Although these mutations do not appear to affect the binding by the antibody, they abolished virus neutralisation of Ebola virus by P6 in the Kawaoka lab (Figure 6.12B). This paradox may be resolved by careful analysis of binding kinetics of the antibody. It is possible that the two mutations in the MLD reduced the affinity of binding sufficiently to prevent neutralisation, but not to be apparent in the indirect immunofluorescence assay at saturating concentration.

Further mutants were selected with P6 in which the I260R mutation was found in escape viruses. I260 is within the GP1 glycan cap (Figures 6.11 and 6.13) and is within the epitope determined by yeast display assay. After introduction of I260R along with S322G+S347P substitutions in Zaire-GP by site directed mutagenesis, screening for binding was done on transiently transfected 293T cells. P6 binding was reduced by 10-fold by FACS (data not shown). MDCK SIAT-1 cells were then established that expressed the mutant GP protein at a stable high level, which also showed the reduced binding by P6 (data not shown). S-FLU pseudotyped with the mutant protein was then

produced, and neutralisation of virus pseudotyped with the mutant GP was found to be selectively abolished for P6 and several other antibodies. This suggests that I260R is the primary mutation that affects P6 binding and neutralisation.

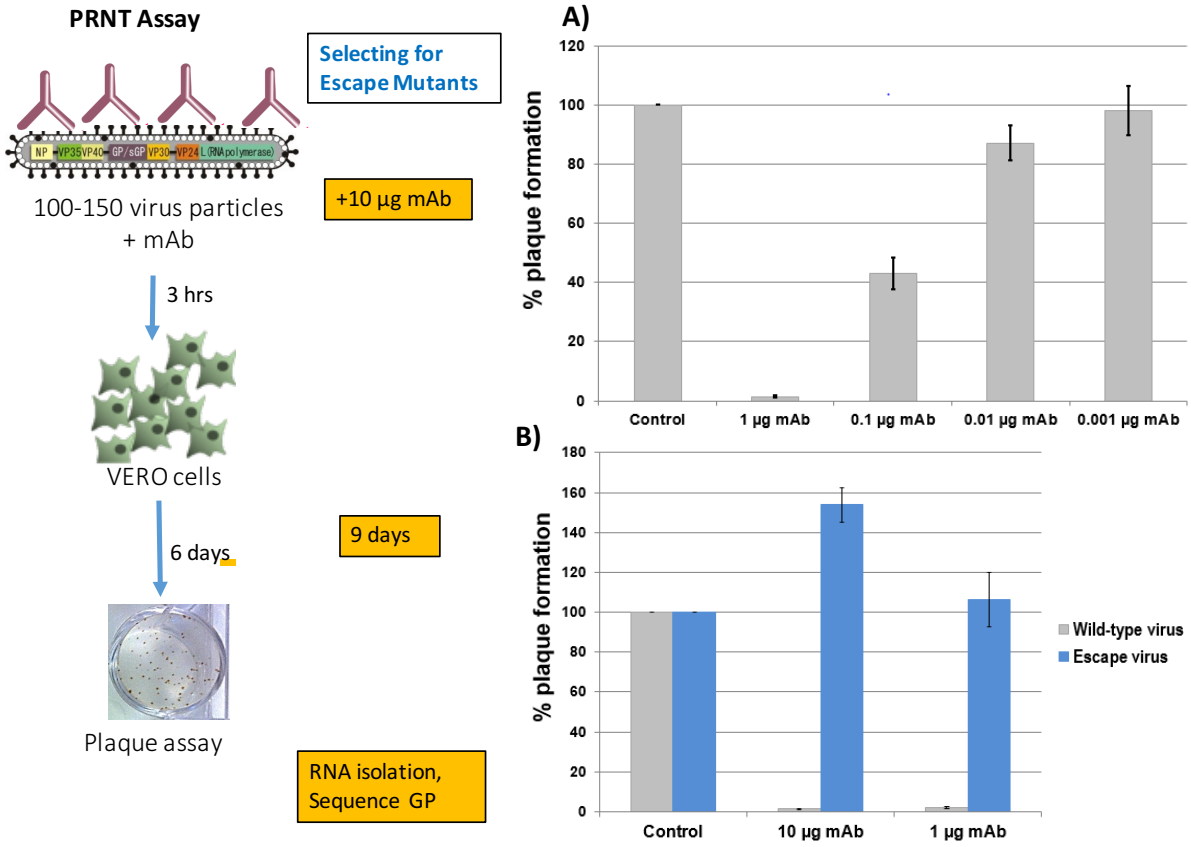

Figure 6. 12 ***Plaque reduction neutralisation (PRNT) assay and selection of escape viruses by mAb P6. (A)*** *The antibody P6 inhibited the Ebola virus plaque formation completely at 1 µg/ml and partially at 0.1 µg/ml.* ***(B)*** *Escape mutant was selected with 10 µg/ml antibody and the mutant virus GP was sequenced. P6 neutralises wild type virus completely but failed to neutralise the escape virus. This experiment was performed by Dr Peter Halfmann in Yoshihiro Kawaoka's lab at Wisconsin University (Halfmann et al. 2008).*

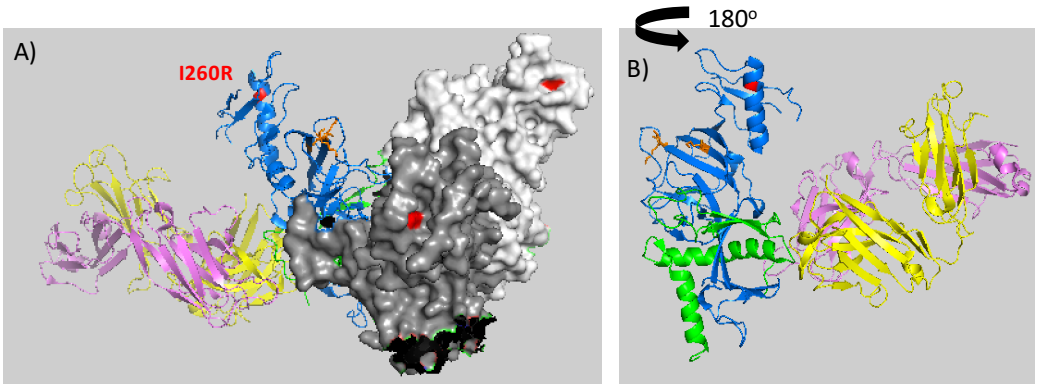

Figure 6. 13 ***MAb P6 recognises a novel site on glycoprotein****. Among three amino acid changes in the glycoprotein of the escape virus selected by mAb P6, I260R is shown as a red patch on the PDB 3CSY. The MLD mutations cannot be shown as this domain was removed before crystallisation.* ***A)*** *Shown on a trimer* ***B)*** *On a monomer, rotated 180° from figure A.*

Once the loss of P6 neutralisation on E-S-FLU I260R/S322G/S347P was established, a range of other antibodies specific for known regions of GP were tested for neutralisation. Antibodies that overlapped the P6 binding site as defined by the cross-inhibition and thermolysin treatment assays (described below) failed to neutralise the mutant pseudotyped virus, but antibodies to the base and receptor binding region (RBR) neutralised both viruses equally (Figure 6.14C). It is noteworthy that this single mutation abolished neutralisation by 10/11 of the glycan cap antibodies isolated from several individuals, and underlines the importance of combining antibodies to several sites to limit the selection of resistant mutants. This site is on the "watch list" developed by Miller et al. based on mathematical modelling of neutralisation sites in GP (Miller et al. 2016).

A)

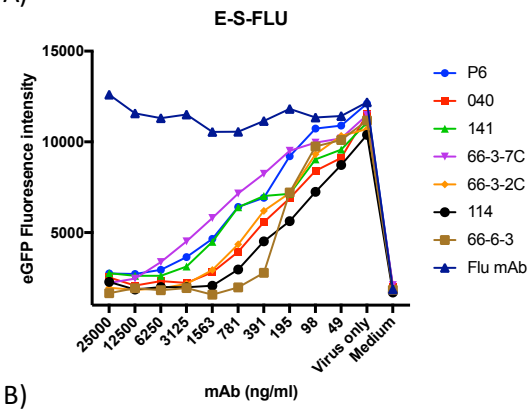

B)

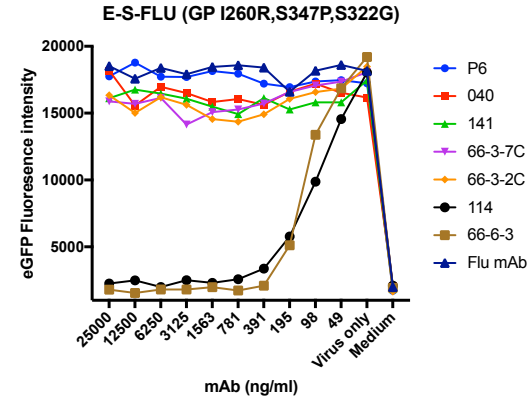

C)

mAbs	Epitope	E-S-FLU	E-S-FLU (GP I260R, S347P, S322G)
P6	Glycan cap	+	-
40	Glycan cap	+	-
141	Glycan cap	+	-
66-3-7C	Glycan cap	+	-
66-3-2C	Glycan cap	+	-
125	Glycan cap	+	-
56-3-7A	Glycan cap	+	-
66-3-7C	Glycan cap	+	-
66-6-19	Glycan cap	+	-
141	Glycan cap	+	-
6535	Glycan cap	+	+/-
114	RBR	+	+
6660	RBR	+	+
c13C6	RBR	+	+
105	RBR	+/-	+/-
6662	RBR	+/-	+/-
6666	RBR	+/-	+/-
6667	RBR	+/-	+/-
66-6-3	Base	+	+
3CSY	Base	+	+
66-6-3	Base	+	+
Flu mAb		-	-

Figure 6. 14 ***Neutralisation profile of the antibodies to wild-type E-S-FLU and E-S-FLU (GP I260R, S322G, S347P) pseudotyped viruses****. **A,C)** All Ebola antibodies neutralise the pseudotyped virus well. **B,C)** P6 and P6-like mAbs fail to neutralise mutant E-S-FLU. Antibodies recognising different sites 114 (RBR) and 66-6-3 (base) are not affected by these substitutions."+" represents neutralisation," +/-" represents partial neutralisation and "–" represents no neutralisation.*

6.7.3 Identification of binding sites by Cross-Inhibition

Biotinylated antibody was cross-competed for binding to glycoprotein with 10-fold higher amount of non-biotinylated counterpart. If the antibodies recognise similar epitopes, they compete and the binding of the biotinylated antibody diminishes. An example of one assay is shown in figure 6.15 where the binding of the biotinylated antibody c2G4 (a component of ZMapp that is known to bind to the base of GP (Murin et

al. 2014)) is inhibited by other base antibodies 3CSY, 100 and c4G7, whereas the other antibodies like P6, 114, 66-3-2C recognise different sites from c2G4 and do not compete with it. Antibodies 125 and c13C6 bind to different sites but may affect the binding of c2G4 slightly by steric hindrance. This is not unusual considering the size of the glycoprotein and antibody is almost same.

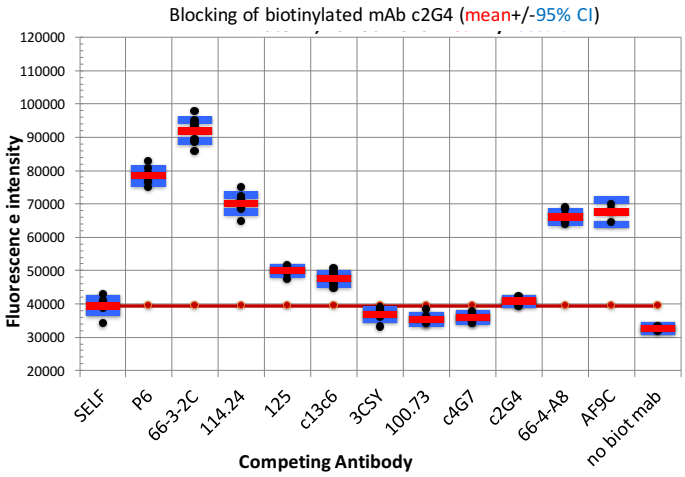

Figure 6. 15 ***An example of competition for binding to ebola glycoprotein****. The biotinylated antibody c2G4 is blocked by unbiotinylated self mAb. Other competing mAbs, 3CSY, 100.73 and c4G7 in this figure, indicate that they recognise a similar epitope. Mucin-like domain (MLD) binding mAb 66-4-A8 and Influenza neuraminidase mAb AF9C are controls which do not block the binding of the biotinylated mAb. Mean (red line) and 95% confidence interval (blue lines) of eight measurements were taken for each antibody. Fluorescence intensity was measured on a Clariostar platereader (BMG Labtech).*

Antibody epitopes were defined for almost all neutralising and some non-neutralising antibodies based on this assay. Collective data are shown in table 6.4. Lower numbers in red means the biotinylated antibody was blocked, and the higher number in green means the binding of the biotinylated antibody is retained in the presence of the competing

antibody. There are three distinct groups in the table. The assignment of the groups to defined regions is by competition with antibodies with known binding sites either from crystallography (3CSY, ZMapp antibodies, 114 and 100) (Lee et al. 2008; Murin et al. 2014; Misasi et al. 2016) or from the yeast expression experiment which define antibodies binding to glycan cap, RBR and GP1-GP2 base.

Table 6. 4 Cross-inhibition of antibodies for mapping epitopes

mAbs	P6	040	66-3-7C	141	66-3-2C	114.24	P7	125	c13C6	66-3-2B	100.73	3CSY	c2G4	c4G7	66-6-3	66-4-C12	142	66-4-A8	Flu mAb
P6 bio	0.1	0.1	0.2	0.1	0.1	1.1	1.0	0.9		1.0	1.0	0.9					0.8	1.0	1.0
66-3-7C bio	0.1	0.1	0.2		0.1	1.8	0.8	1.0			1.0	0.8					0.8	1.0	
040 bio	0.3	0.3	0.6	0.7	0.3	2.0	1.2	0.6			1.0	0.9					1.4	1.0	1.0
66-3-2C bio	0.2	0.2	0.4	0.2	0.2	0.3	0.8	0.9			1.1	1.0					1.2	1.0	1.0
6535 bio	0.4		0.6		0.2	0.1		0.4		1.2	1.1	1.0						1.1	1.0
6656 bio	0.0		0.0		0.0	1.3		0.5		0.7	0.8	0.6					0.7	0.8	1.0
P7 bio	1.1	1.2	1.5	0.5	0.3	0.0	0.1	0.9			1.0	1.0					1.4	1.0	0.9
114.24 bio	0.9	0.9	1.2	1.1	0.8	0.3	0.5	0.8		1.0	1.1	0.8					1.2	1.0	1.0
6660 bio	1.2		1.3		0.7	-0.1		0.8		0.9	0.9	1.0					1.2	0.9	1.0
6670 bio	1.4		1.1		0.6	-0.1		0.8		0.8	0.8	0.7					1.2	0.9	1.0
66-6-14 bio	3.2				0.7	-0.6		0.5	-0.1		1.0	0.9	1.3	1.4				0.9	1.0
66-6-19 bio	-0.4				-0.6	2.0		0.6	0.0		0.8	0.6	1.4	1.5				1.0	1.0
141 bio	-0.2				-0.3	-0.2		0.2	0.0		0.8	0.6	1.1	1.5				0.6	1.0
105 bio	1.5				0.3	-0.2		0.7	0.1		0.5	0.6	0.9	0.8				0.6	1.0
66-3-4A bio	-0.1				-0.1	-0.2		0.4	0.0		0.5	0.6	1.0	1.1				0.8	1.0
c13c6 bio	0.7				0.7	0.1		0.5	0.0		0.5	0.4	0.5	0.8				0.8	1.0
125 bio	0.6	0.6	0.9		0.5	0.6	0.9	0.2	0.0		0.9	0.8					0.8	1.0	
66-3-9C bio	1.0				0.8	0.8		-0.2	1.8		1.1	0.1	4.7	5.6				0.7	1.0
100.73 bio	0.9	1.0	1.0	1.1	0.9	0.9	1.0	1.1		0.8	0.2	0.4					1.1	1.0	1.0
3CSY bio	0.7	1.0	1.0	1.4	0.9	0.9	1.0	1.2			0.2	0.2					0.7	1.0	1.0
142 bio	0.7	1.1	0.7		1.0	0.9	0.8	1.0			0.5	0.1					0.2	1.0	
6541 bio	1.9		1.1		2.1	1.5		0.7		0.9	0.3	0.1						1.3	1.0
66-6-10 bio	1.3				1.8	1.1		0.7	0.3		0.1	0.0	0.2	0.0				0.8	1.0
19-2-12C bio	0.6				0.7	0.6		0.6	0.4		0.4	0.5	0.5	0.5				0.6	1.0
c4G7 bio	1.3				1.5	0.9		0.4	0.3		0.2	0.0	0.0	0.2				0.9	1.0
c2G4 bio	1.4				1.9	1.1		0.4	0.3		-0.1	-0.1	-0.1	0.0				0.9	1.0
66-6-3 bio	0.9		0.9		0.7	1.0		1.0		0.7	0.0	0.2	0.5	0.2	-0.1	0.4	0.8	0.9	1.0
66-4-C12 bio	1.1		0.8		0.6	0.9		1.1		0.6	-0.3	0.0	0.7	0.8	-0.1	0.0	1.0	1.0	1.0
66-3-2B bio	0.8					0.9		1.0		0.6	0.1	0.1	0.4	0.1	0.2	0.3	0.4	1.0	1.0

Antibodies 66-4-A8 (MLD-dependent EBOV antibody) and Influenza antibodies are used as controls for non-inhibiting antibodies. Red designates inhibtion of the biotinylated antibody by the competing antibody. Green designates absence of inhibtion or binding in presence of competing antibody.
Inhibition values are calculated as (X– Min binding)/(Maximum binding – Minimum binding), where X= Binding of the biotinylated mAb in presence of competing mAb, Minimum binding = Blocking of the biotinylated mAb by self or background binding, Maximum binding = Binding of biotinylated mAb in presence of Flu or MLD mAb. Results are average of different experiments and eight replicates were measured in each experiment.

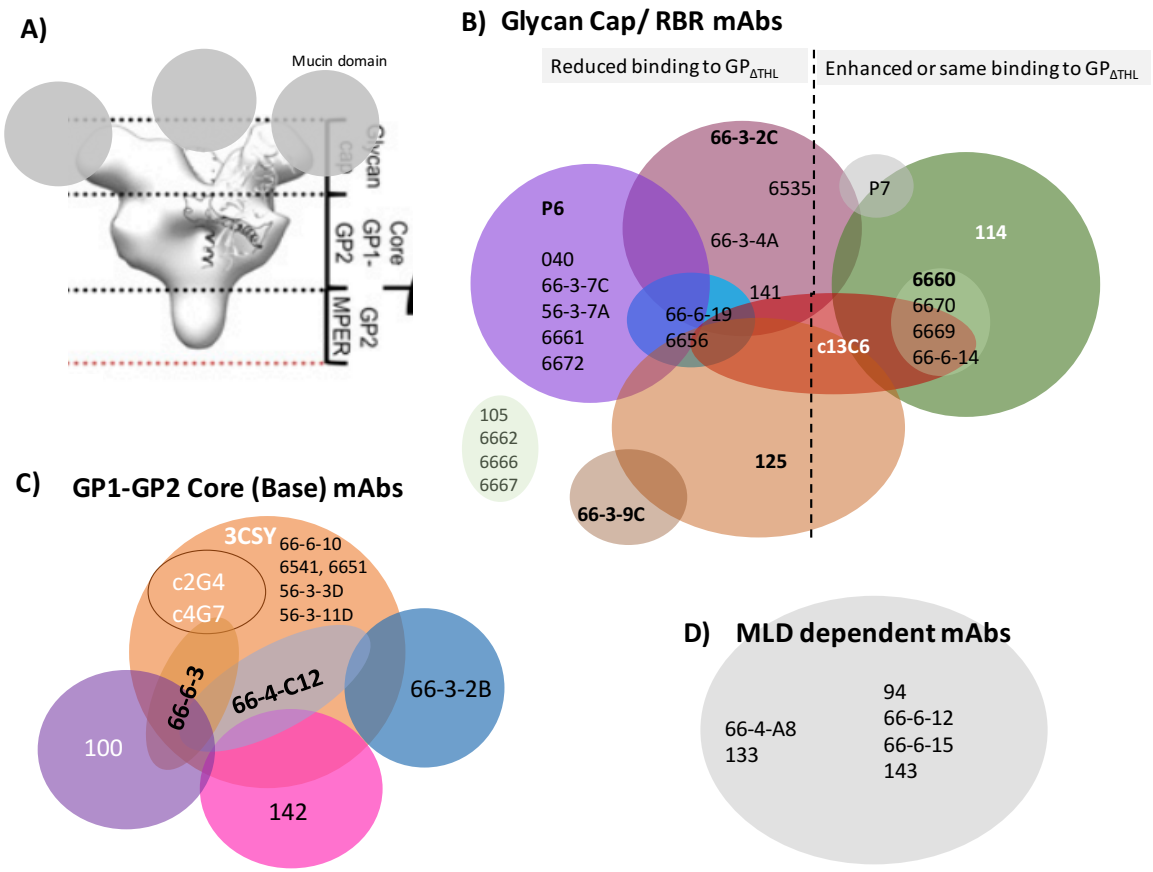

Figure 6. 16 ***Assignment of antibodies to their defined regions based on cross-inhibition assays****. Known antibodies 114, ZMapp (c13C6, c2G4, c4G7), 100 and 3CSY were used as controls to determine the binding regions.* ***A) Structure of glycoprotein****. Picture adapted from Murin et al. (Murin et al. 2014).* ***B) Head antibodies:*** *Within the head region there are about 23 antibodies which can be divided into three groups: P6-like, 114-like and others in-between these epitopes that are blocked by both. P6-like and 114-like are independent epitopes and do not block each other.* ***Thermolysin sensitivity of the head antibodies.*** *Thermolysin mimics cathepsin, which cleaves off the glycan cap and mucin domain from GP during the virus infection inside the cell. Antibodies on the left (P6-like and neighbours) are sensitive to thermolysin cleavage. These are the real glycan cap mAbs. Whereas antibodies on the right (114-like) are resistant to thermolysin cleavage or have enhanced binding after cleavage. These antibodies may recognise the*

receptor binding region defined by antibody 114 (Corti et al. 2016). There are 4 antibodies on a green island, which are thermolysin sensitive but are competed by 114. These are blocked by 114 and c13C6 antibodies and not blocked by P6, 125 or 66-3-2C antibodies. Antibody 66-3-9C (pan-ebola mAb recognising the conserved GP1 loop) binds to a unique site and is blocked by 125 and slightly by 3CSY mAbs. All the antibodies in this figure are neutralising except P7 and 66-3-9C, and the 4 antibodies on the small green island are partially neutralising. ***C) Antibodies to GP1-GP2 core or base****. Nine antibodies are assigned to this site. These antibodies are resistant to thermolysin digestion and may have enhanced binding post-digestion. Antibodies 66-6-3 and 66-4-C12 were studied in detail and they are strong and partially neutralising respectively.* ***D) Mucin-like domain dependent antibodies****. Two antibodies 66-4-A8 and 133 do not bind to GP with the Mucin Like Domain deleted and the other 4 mAbs placed in this group have significantly reduced binding (shown in figure 6.18). Note that "3CSY" is the lab name given to our synthesised version of KZ52, based on the PDB sequence 3CSY.*

There are mainly three groups of antibodies: Head, Base and Mucin-like domain antibodies (Figure 6.16). Within the GP head, there are at least two independent neutralising sites that can be differentiated by sensitivity to thermolysin digestion. Thermolysin mimics cathepsin (Bale et al. 2011), which cleaves off the glycan cap from GP, required before binding to the NPC1 receptor and subsequent fusion events (Cote et al. 2011). One site referred to as the Receptor Binding Region (RBR) is resistant to thermolysin cleavage, and neutralising antibodies binding this site compete with control antibody 114 (Misasi et al. 2016). The group of 114-like antibodies are namely, 6660, 6670, 6669 and 66-6-14. These antibodies also cross-block ZMapp antibody c13C6, which is known to bind to the RBR (Murin et al. 2014). Other antibodies 105, 6662, 6666

and 6667 also recognise mAb 114-epitope, however these are different in that they are partially neutralising and are sensitive to thermolysin digestion.

A second, non-overlapping neutralising epitope in the head of GP is sensitive to thermolysin digestion, and is referred to as the glycan cap. MAbs P6 and 040 represent this region (Figure 6. 9). All P6-like glycan cap mAbs including some of the neighbouring region mAbs 66-3-2C, 125, 141 and 66-6-19 do not neutralise the escape mutant virus E-S-FLU (GP I260R, S347P, S322G) selected by P6 (Figure 6.14).

Besides these two mutually exclusive epitopes on the GP head, there is an epitope overlapping the P6 and 114 epitopes. Antibodies in this group compete to some level for binding with antibodies in both the P6 and 114 like groups. One of the mAbs named 125 is one of the most potent antibodies in our collection (Figure 6. 6).

Another antibody 66-3-9C binds an independent epitope from mAbs P6 and 114. This non-neutralising antibody recognises the thermolysin sensitive epitope GEWAFWET/N conserved in all Ebola subtypes (Figure 6.10). This mAb is like the macaque mAb FVM09 which recognised the GEWAF peptide (Figure 6.17) (Keck et al. 2016). Although FVM09 is non-neutralising *in vitro*, it contributed to partial protection of mice against EBOV infection at day 0 and 3 post infection at a dose of 25 mg/kg. However, this antibody was fully protective when given in a cocktail with another fusion-loop antibody in the NHP model (Keck et al. 2016; Howell et al. 2016).

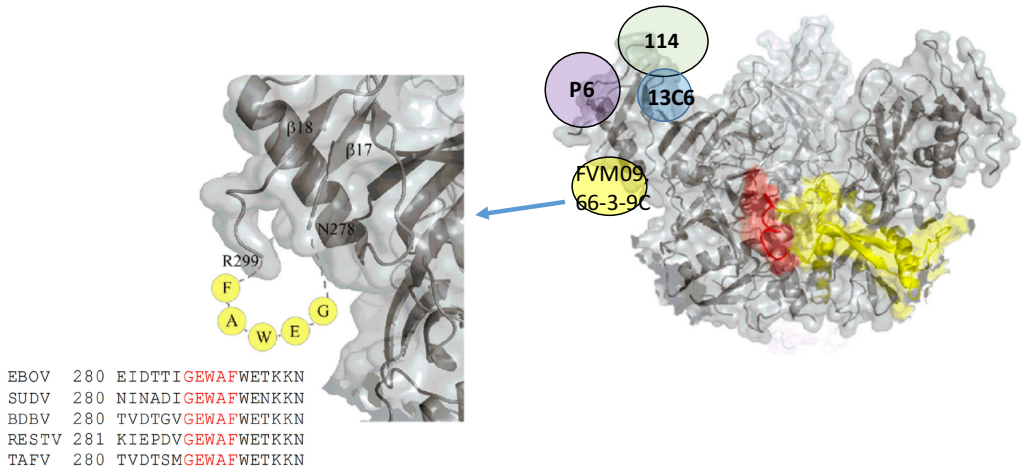

Figure 6. 17 A Pan-Ebola antibody 66-3-9C recognises the small segment GEWAFWET/N. This mAb is homologous to the macaque mAb FVM09 which recognised GEWAF sequence. This sequence is conserved in all Ebola subtypes. Antibodies P6, 114 and 13C6 are shown for reference. Figure adapted from Keck et al. 2016 JVI (Keck et al. 2016).

A group of neutralising antibodies to the base are defined by competition with the control antibodies KZ52 (Lee et al. 2008), 100 (Misasi et al. 2016) and the ZMapp components c2G4 and c4G7 (Murin et al. 2014). There are 9 antibodies to the base. Among them, antibody 66-6-3 is a complete strong neutraliser and 66-4-C12 is a partial cross-reactive neutraliser. Though these antibodies cross-inhibit each other, they may have a slightly different footprint.

6.8 Identification of MLD dependent antibodies

Antibodies specific for the Mucin-like domain (MLD) were identified by screening for binding to a MLD-deleted (aa 314-463) GP expressed in MDCK-SIAT cells, referred to as Emuc-del SIAT. 6/82 antibodies were found to have no binding or highly reduced binding to GPΔmuc compared to GP (Figure 6.16 and 6.18). Other MLD-dependent antibodies B80C18 and G10OC18 shown in figure 6.18 are human monoclonal antibodies

isolated by UCB from a phage expression library derived from RNA isolated from the B cells from an Ebola convalescent donor. Antibodies to the GP head (c13C6) or base (3CSY) bind with similar affinity to GP and GPΔmuc. Among all the antibodies tested, 66-4-C12 (base antibody) and 66-3-9C (GEWAFWET binding antibody) have somewhat reduced binding to the GPΔmuc. In these two cases, it is difficult to distinguish between the MLD contributing to the epitopes recognised by these two antibodies, or some level of distortion of the GP occurring after deletion of aa 314-463.

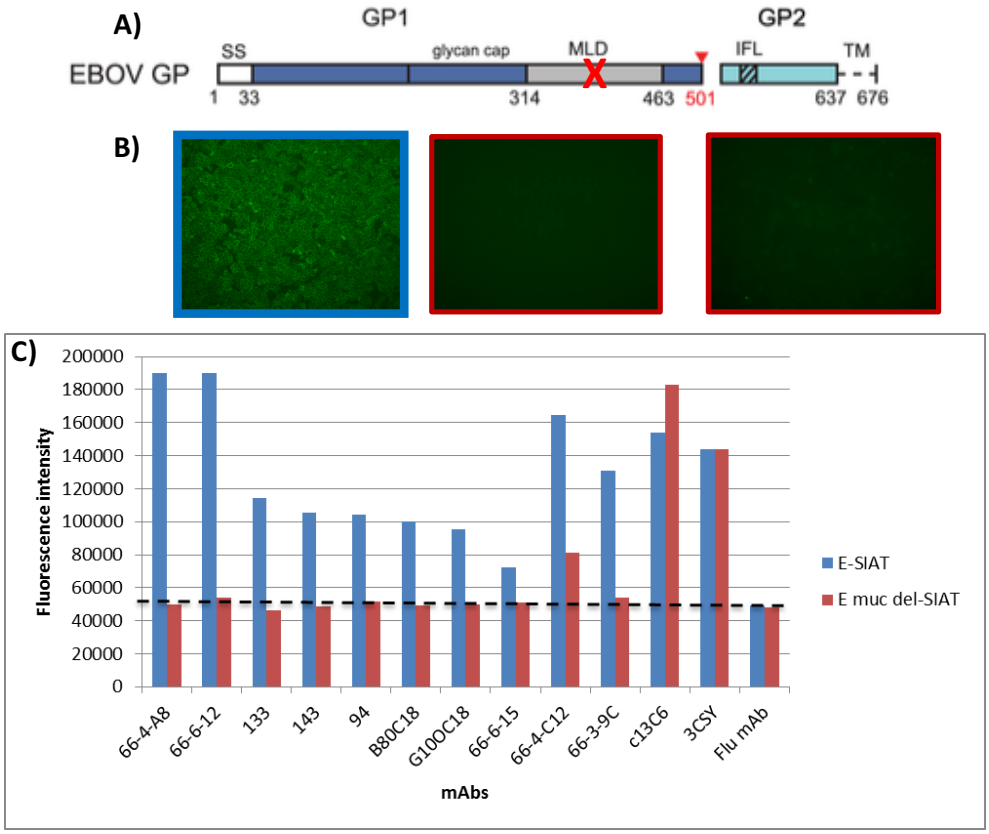

Figure 6. 18 ***Identifying antibodies recognising mucin-like domain of the glycoprotein.*** ***A)*** *MLD domain (amino acids 314-463) was removed from the EBOV GP gene and expressed on the surface of MDCK-SIAT1 cells.* ***B)*** *Picture on left shows the representative binding of the mAbs on E-SIAT cells (cells expressing Ebola full-length glycoprotein). On the middle and right are the antibodies that fail to bind or have*

significantly reduced binding to Emuc del-SIAT cells (expressing MLD-deleted GP). ***C)*** *mAbs c13C6 and 3CSY are controls whose binding is unaffected by MLD deletion. Flu mAb is a negative control, and the rest are MLD dependent mAbs except 66-4-C12 (base mAb). mAbs B80C18 and G10OC18 are mAbs isolated by UCB from a convalescent donor. Fluorescence intensity of the binding was measured using Clariostar platereader (BMG Labtech).*

6.9 Some antibodies may neutralise by blocking cathepsin digestion

It is known that the GP is cleaved by cathepsins in the lysosome to expose the Receptor Binding Region (RBR) that can bind the NPC1 receptor, and then initiate fusion of the viral and lysosomal membranes (Carette et al. 2011; Cote et al. 2011; Bornholdt et al. 2016; Brecher et al. 2012). The enzyme thermolysin has been shown to mimic cathepsin cleavage (Dube et al. 2009) *in vitro*, and is easier to handle in vitro at physiological pH. Most of the antibodies that bind the glycan cap are sensitive to thermolysin digestion but are still neutralising *in vitro*. This seems paradoxical as the glycan cap is removed by cathepsins before binding of GP to its receptor NPC1 and therefore it is hard to see how these antibodies could block virus entry. One possibility is that they bind close enough to the cathepsin cleavage site to block cleavage, and thereby prevent access of the Receptor Binding Region of GP to NPC1. To test this concept, we let GP pre-bind with antibody and then performed thermolysin digestion (as a surrogate for cathepsin) of GP. Binding of antibody to GP was retained when pre-incubated with antibody, which suggests that the antibody blocks the thermolysin dependant removal of the MLD and glycan cap from the glycoprotein. In figure 6.19A, geometric mean intensity (GMI) of P6 binding to GP is 163, while that to GP post thermolysin treatment is 12. When antibody was incubated with GP for one hour prior to digestion, GMI was 384 and when the incubation and digestion were performed simultaneously, the GMI was 142. The difference in intensity

between green and blue histogram is likely due to different times of antibody incubation 60 min versus 20 min. The control base antibody 66-6-3 binding is unchanged to GP and GP post thermolysin (GPΔTHL) (Figure 6.19B). In fact, base antibodies have slightly enhanced binding to GPΔTHL.

We tried to determine if antibodies to the base also block thermolysin digestion. Shedlock et al. have shown that the base antibody KZ52 blocks Cathepsin L (CatL) proteolysis of GP (Shedlock et al. 2010). CatL proteolysis may be slightly different from proteolysis by thermolysin because CatL cleaves off the glycan cap and mucin domain from its original ~130 kDa to an initial 50 KDa GP1 to form a 20 KDa intermediate product which is later further cleaved by CatL/B to the pre-fusion form of 19 kDa. Thermolysin is suggested to cleave GP1 to 19 kDa structure directly ((Dube et al. 2009). We incubated GP with base antibody 66-6-3 prior to thermolysin digestion and let P6-biotinylated antibody bind as an indicator of cleavage. In figure 6.19C, P6 is shown to have some level of binding to GP exposed to thermolysin in the presence of the 66-6-3 antibody (GMI 60), which suggests it may have inhibited the cleavage.

In another experiment performed by Julie Xiao, E-S-FLU virus was digested with thermolysin, and digested virus (after buffer exchange) was used for neutralisation. While the base, 114 and 114-like antibodies neutralised virus equally, P6 and P6-like antibodies no longer neutralise the thermolysin digested E-S-FLU virus (data not shown). These results suggest that some glycan cap antibodies may function by blocking cathepsin digestion, which is essential for virus binding to the NPC1 receptor and subsequent fusion events.

We regard these results as preliminary, and will aim to repeat the assay with more controls, and extend the experiments to direct visualisation of the cleaved products by metabolic or other labelling methods combined with immunoprecipitation.

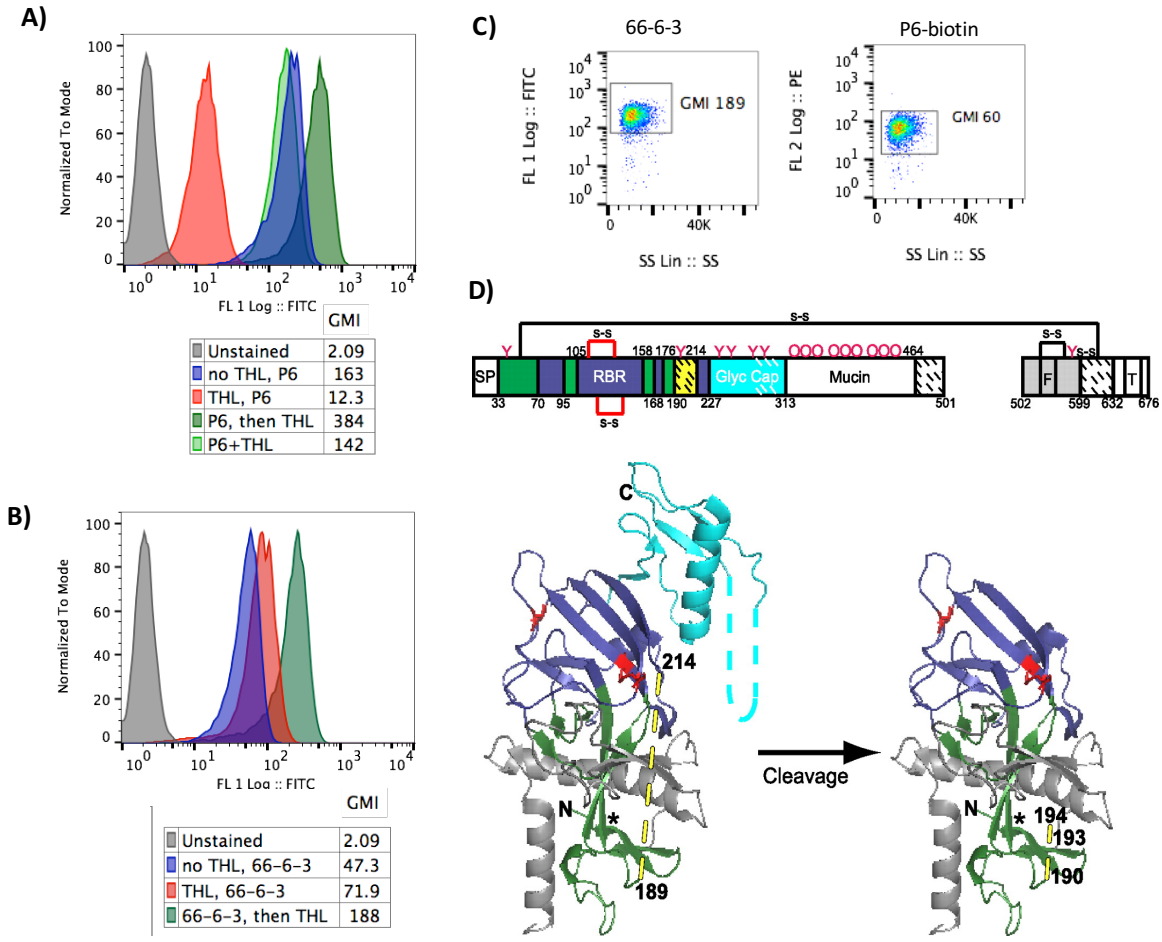

Figure 6. 19 ***MAb P6 blocks the thermolysin cleavage****. **A)** P6 mAb binding to untreated E-SIAT cells (blue) and loss of binding after thermolysin cleavage (red). MAb pre-incubated with E-SIAT cells before thermolysin treatment prevents the cleavage (dark green). Light green shows the binding of mAb during thermolysin treatment. Difference in dark green and blue binding may be due to difference in binding time (60 min vs 20 min). GMI: Geometric mean intensity of the fluorescence.* ***B)*** *66-6-3 is a base mAb which binds to thermolysin cleaved GP. Blue histogram shows binding to untreated E-SIAT cells, red – binding to thermolysin treated E-SIAT cells and green – binding before thermolysin*

treatment. ***C)*** *mAb 66-6-3 was let bind to GP before thermolysin digestion and binding of P6-biotin was detected. 66-6-3 mAb may block thermolysin cleavage to some extent. D) GP construct and model of thermolysin digestion. Figure taken from Dube et al. (Dube et al. 2009).*

6.10 Effect of Combinations of antibodies on virus neutralisation

We performed neutralisation with combinations of antibodies and compared them with the ZMapp cocktail and individual antibodies. The ZMapp antibodies were synthesised from codon optimised cDNA based on the published sequences, and mounted in a human IgG1 scaffold by Simon Draper's group. Antibody selection was mainly based on targeting separate non-overlapping epitopes and antibodies with good IC50 and IC90 values. We selected six mAbs – 4 to the head (including glycan cap and RBR) and 2 to the base to test the combinations in the neutralisation assay (Figure 6.20A). The antibodies were titrated in two-fold dilutions at 10 µg/ml individually and 10 µg/ml of each antibody in combination. IC50 and IC90 values are calculated based on the total concentration of antibody in the reaction. No drastic synergistic effect of one antibody on another was found. For example, antibody 125 is powerful as a single antibody and its IC50 was not improved with addition of another antibody. It can be said that combined antibodies have an additive effect.

Similarly, the combination of three antibodies has an additive effect rather than synergistic effect. Three antibodies to the head: P6, 6660 and 125 tended to give the best IC50 and IC90 values. Also the combinations, 1) 6660, 125 and 66-6-3, 2) 66-3-2C, 6660 and 125, 3) 6660, 125 and 66-4-C12 and 4) P6, 125 and 66-6-3 were among the best. In the case of ZMapp (antibodies 4G7 and 2G4 to overlapping base epitopes and 13C6 to the glycan cap), the individual antibodies have weaker IC50 and they didn't reach 90%

neutralisation at a starting concentration of 5 µg/ml (Figure 6.20C). Antibody c13C6 didn't reach 50% neutralisation. Some of the best three combinations have ~3-fold lower IC50 (~500 ng/ml) compared to the ZMapp combination (1355 ng/ml). These combinations have IC90 <600 ng/ml.

To conclude, we found that combinations of any three of P6-like (glycan cap), 125, 114-like (RBR), and 66-6-3 (base) mAbs may form a good cocktail, based on targeting different epitopes and different mechanisms of action. We also tested these four antibodies together in another experiment. IC50 and IC90 values were similar to that of the combinations of three antibodies.

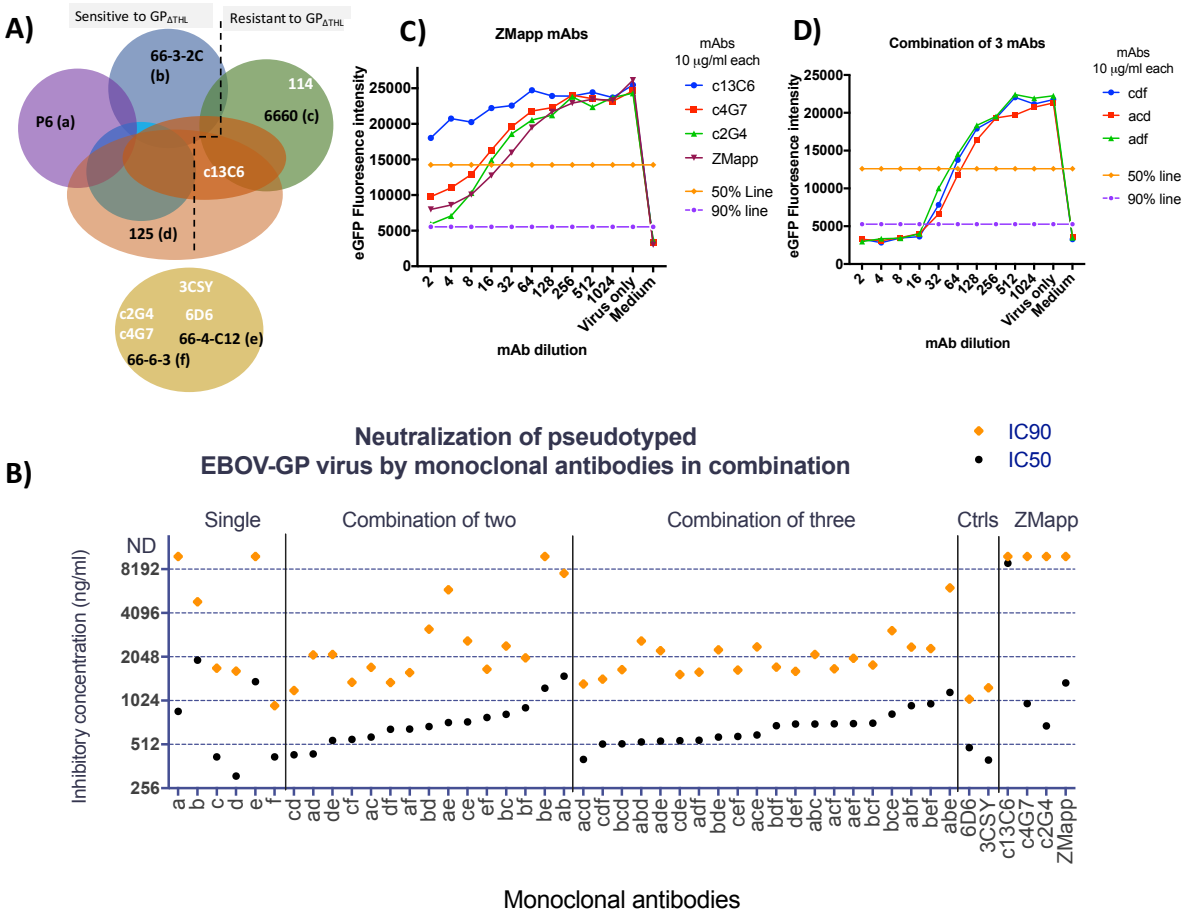

Figure 6. 20 ***Neutralisation of E-S-FLU pseudotyped virus by antibodies in combination****. **A)** Six antibodies (black font) from different sites: 4 from head and 2 from*

base, were selected for a combination neutralisation experiment. mAbs in white are controls belonging to different sites. c13C6, c2G4 and c4G7 are the components of ZMapp cocktail (Qiu et al. 2014). ***B)*** *Inhibitory concentrations at 50% and 90% are shown for individual and combination of mAbs. Good combinations have IC50 <600 ng/ml and IC90 <2000 ng/ml. 6D6 specific for the fusion domain (Furuyama et al. 2016) and 3CSY (KZ52) to base (Lee et al. 2008) are control mAbs. mAb c13C6 didn't have detectable IC50 and IC90 on this experiment. IC90 was not detected also for other two base mAbs c2G4 and c4G7. Combined IC50 for ZMapp in this assay was 1355 ng/ml. ND: Not detected.* ***C)*** *Antibody titration curve of ZMapp cocktail and individual antibodies. Each antibody is tested at 10 µg/ml and ZMapp at 30 µg/ml total.* ***D)*** *Antibody titration curve of selected cocktail of three mAbs which gave better neutralisation. Measurements were done in duplicates in each experiment and the data has been replicated at least twice. Note that "3CSY" is the lab name given to our synthesised version of KZ52, based on the PDB sequence 3CSY.*

Further testing of combinations is warranted, but to date the best is 6660, 125 and 66-6-3 for the most powerful combination of three antibodies to the RBR, glycan cap and base, that do not overlap as assessed by cross-inhibition or loss of neutralisation through the I260R mutation.

6.11 Effect of trypsin on antibody binding

Trypsin sensitive antibodies: We found occasional antibodies that were sensitive to the effect of trypsin digestion for binding to GP expressed on MDCK-SIAT1 cells. These antibodies bind native GP protein (Figure 6.21B), however when E-SIAT cells were trypsin treated binding was lost (Figure 7.21A). We have not identified the trypsin sensitive sites on GP but two antibodies give some information. 66-3-9C, which binds

the conserved short peptide loop 286-293 GEWAFWET (Figure 6. 17), was strongly inhibited by trypsin treatment (not shown), and would have been missed if screening had been done on trypsinised cells in suspension. The bound region GEWAFWET is followed by the sequence KKN, which could be a site for trypsin cleavage. Further the antibody 66-4-A8, which is specific for the mucin-like domain, binds weakly to trypsin treated E-SIAT cells in FACS (not shown here). It is likely therefore that trypsin also cleaves within the MLD.

Trypsin requiring antibodies: We also encountered another set of antibodies which bind to trypsin treated GP only. They didn't bind E-SIAT or Emuc-del SIAT cell monolayer (Figure 7.22A) that had been allowed to recover from trypsinisation overnight. These nine antibodies bind the cells only after they were trypsin treated to form a cell suspension and analysed by FACS. An example of the binding is shown in figure 7.22B. These antibodies are resistant to thermolysin digestion (Figure 7.22B). They were isolated accidentally by UCB when for convenience the cultured B cells were screened for binding to formalin fixed E-SIAT cells in suspension after trypsin treatment.

These results show the need for great care in the design of the screening assay for human monoclonal antibodies, and reveal the extreme diversity of the human antibody response. Considering these observations, follow up studies to dissect the effect of trypsin on glycoprotein processing may be done.

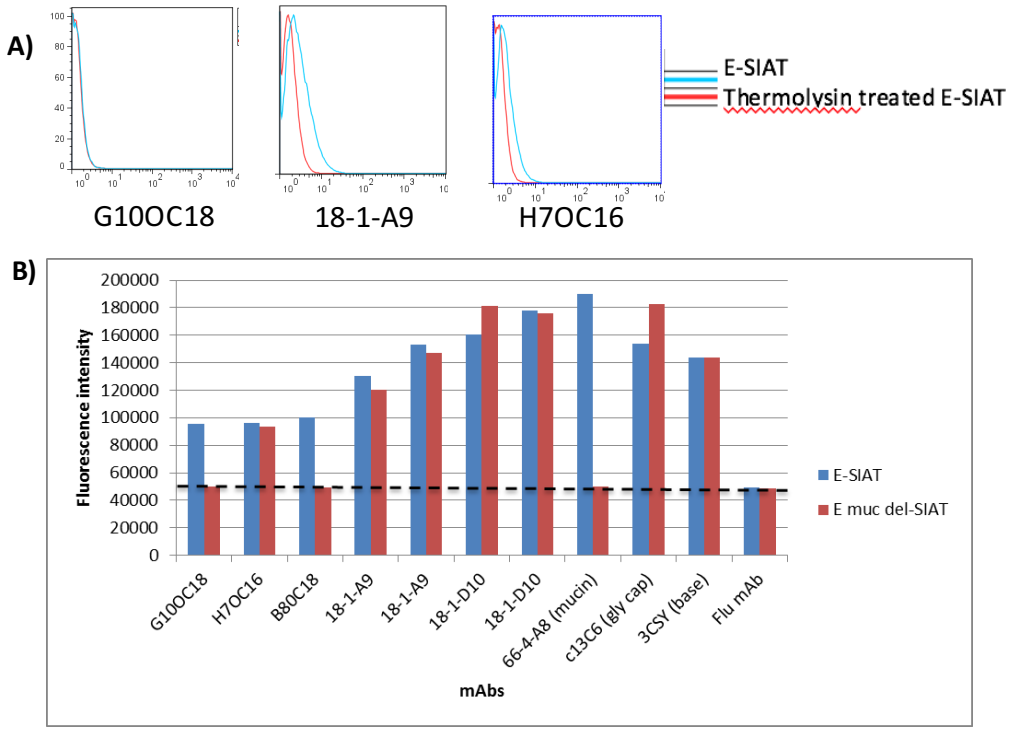

Figure 6. 21 ***Antibodies sensitive to trypsin.*** *Graph shows 3 antibodies (1 MLD dependent and 2 unknown) whose binding epitopes are trypsin sensitive. A) These antibodies do not bind to E-SIAT or thermolysin treated E-SIAT made into cell suspension after trypsin treatment. B) However, these antibodies bind well to E-SIAT cell monolayer.*

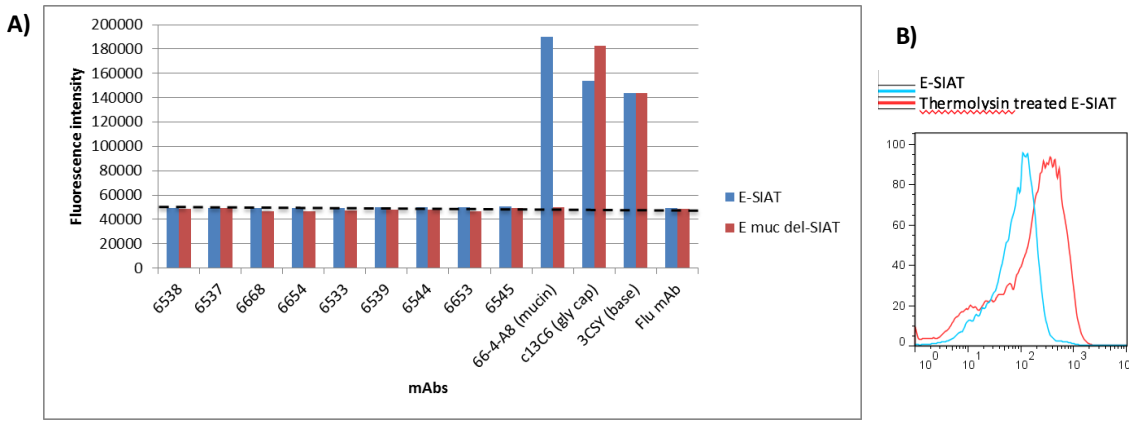

Figure 6. 22 ***Antibodies requiring trypsin cleavage of glycoprotein for binding A)*** *Graph shows 9 antibodies isolated from screening with trypsin-treated and fixed E-SIAT cells, whose binding to E-SIAT cell monolayer is almost undetectable. 66-4-A8 (mucin), c13C6 (glycan cap) and 3CSY (base) mAbs are controls.* ***B)*** *When the cells are in suspension after trypsin treatment, they bind well. These mAbs also bind to E-SIAT cells post thermolysin digestion. This graph is shown as a representative for 9 mAbs.*

6.12 Cross-reactive antibodies to other Ebola species

There is about 50-70% sequence homology of ZEBOV GP to glycoproteins of other Ebola species (Table 6.5 and Figure 6.23) and only ~30% homology to Marburg virus GP (not shown). Most of the amino acid sequence variation is seen in the mucin like domain. We looked for cross-reactivity of our collection of antibodies to other Ebola subtypes Zaire Mayinga 1976 (AF086833), Bundibugyo (NC_014373.1) and Sudan Gulu (NC_006432.1) mentioned in table 6.5. Sudan Gulu and Marburg GP proteins were expressed by the booster MVA vaccine which may have increased the likelihood of stimulating cross-reactive clones. Cross-reactive antibodies definitely exist as shown by 6D6 isolated by the group of Takada (Furuyama et al. 2016). 6D6 is a strongly neutralising antibody specific for the conserved fusion peptide. An ideal cocktail of

antibodies should cross-neutralise at least the Zaire, Bundibugyo and Sudan strains that cause the most severe Ebola disease.

Table 6. 5 Glycoproteins from different Ebola subtypes with % amino acid identity

EBOV Virus	Isolated year	Accession No.	AA identitity to Zaire Makona (%)
ZEBOV Makona	2014	KJ660346.2	100
ZEBOV Mayinga	1976	AF086833	97
BDBV	2007	NC_014373.1	65
SUDV Gulu	2000	NC_006432.1	55

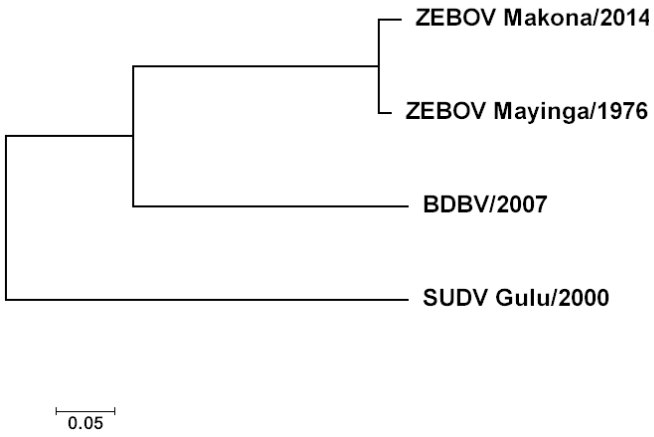

Figure 6. 23 ***Amino acid sequence phylogeny of different Ebola species.***

Figure 6.24 shows the binding of an initial selection of the antibodies to GP-expressing cells in FACS. The assay was done soon after transduction of the MDCK-SIAT1 cells and still contained a proportion of negative cells. The antibody 66-4-C12 is cross-reactive to Sudan and Bundibugyo GP. Mouse mAb 6D6 is a positive control antibody which is reported to bind to all GP of all Ebola subtypes but not Marburg virus (Furuyama et al. 2016).

Another antibody 66-3-9C, specific for the peptide GEWAFWET (Figure 6. 10), is also cross-reactive to these tested GPs (Table 6.6). Although the antibody 66-3-9C binds weakly to these cells which are in suspension after trypsin treatment (see section 6.10), it

binds strongly to soluble GP on ELISA and on trypsin untreated GP-transfected cells bound to plastic (Figure 6.25).

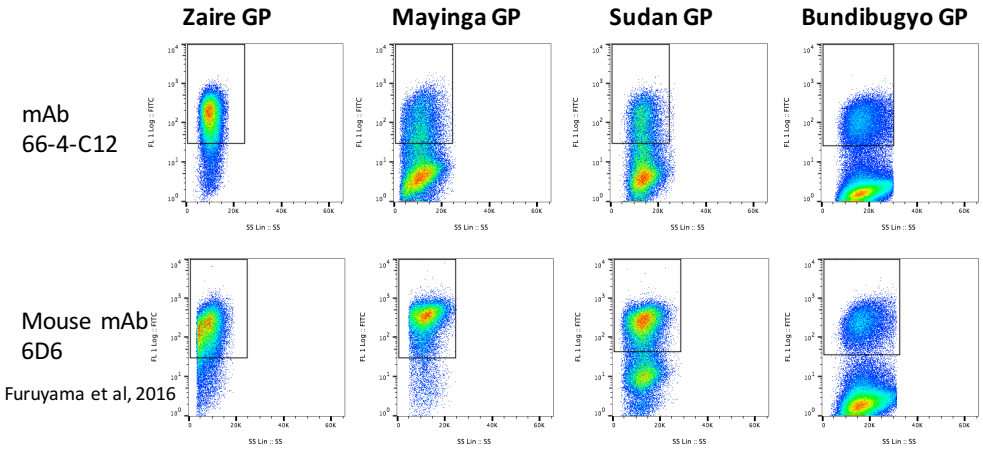

Figure 6. 24 ***FACS plots shows the binding of mAbs to MDCK-SIAT1 cells transfected with glycoproteins of Makona, Mayinga, Sudan and Bundibugyo Ebola viruses.*** *Antibody 66-4-C12 binds strongly to other Ebola GP subtypes as well besides Zaire GP (C15/2014). Mouse antibody 6D6 is positive control pan-Ebola mAb (Furuyama et al. 2016). These cells are mixed populations of transfected and untransfected cells, hence there are two populations.*

Table 6. 6 Cross-reactivity of some of the antibodies tested by FACS

mAb	Zaire GP	Mayinga GP	Sudan GP	Bundibugyo GP
66-6-3	+++	+++	-	-
P6	+++	+++	-	+++
66-4-C12	+++	+++	+++	+++
66-3-9C	++	+	+	+
3CSY	+++	+++	-	-
6D6	+++	+++	+++	+++
Flu mAb	-	-	-	-

We then tested all of the antibodies in our collection at 50 µg/ml concentration on a cell monolayer expressing the Zaire Makona 2014, Zaire Mayinga 1976, Bundibugyo and

Sudan Gulu GPs after the cells had been sorted for expression, and measured binding by indirect immunofluorescence in the Clariostar plate reader. Readings for each antibody were compared (Figure 6.25). Individual comparisons revealed groups of cross-reacting antibodies.

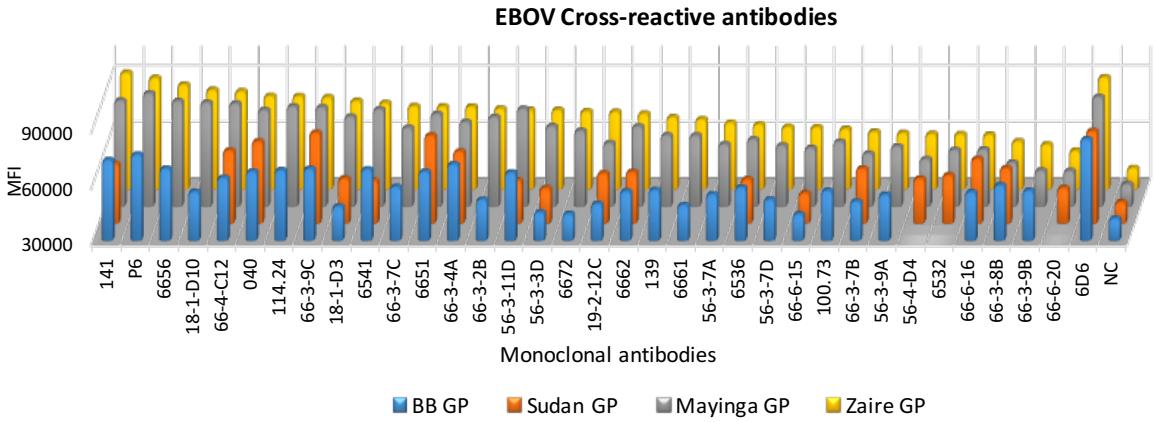

Figure 6. 25 ***Cross-reactive antibodies****. Of total 82 antibodies, there are a set of antibodies which are cross-reactive either to Sudan GP, Bundibugyo GP or both (n=17). All antibodies that bind Zaire Makona GP (2014) also bind to Mayinga Zaire GP (1976) to a similar degree. 6D6 is a pan-Ebola control antibody (Furuyama et al. 2016). Influenza antibody is used as a negative control. Antibodies 114.24 and 100.73 are Zaire GP control antibodies cross-reactive to Bundibugyo but not Sudan GP (Corti et al. 2016). Mean fluorescence intensity (MFI) of antibody binding to GP expressed on cell surface was read by Clariostar plate reader (BMG Labtech).*

A comparison of binding to Zaire Makona 2014 and Zaire Mayinga 1976 revealed a strong correlation in binding, as expected for two proteins that share 97% identity, giving a correlation coefficient of 0.96 (Figure 6.26). By contrast a comparison between Zaire and Bundibugyo revealed some 32 antibodies cross-reactive to Bundibugyo GP (Figure 6.25 and 6.27A).

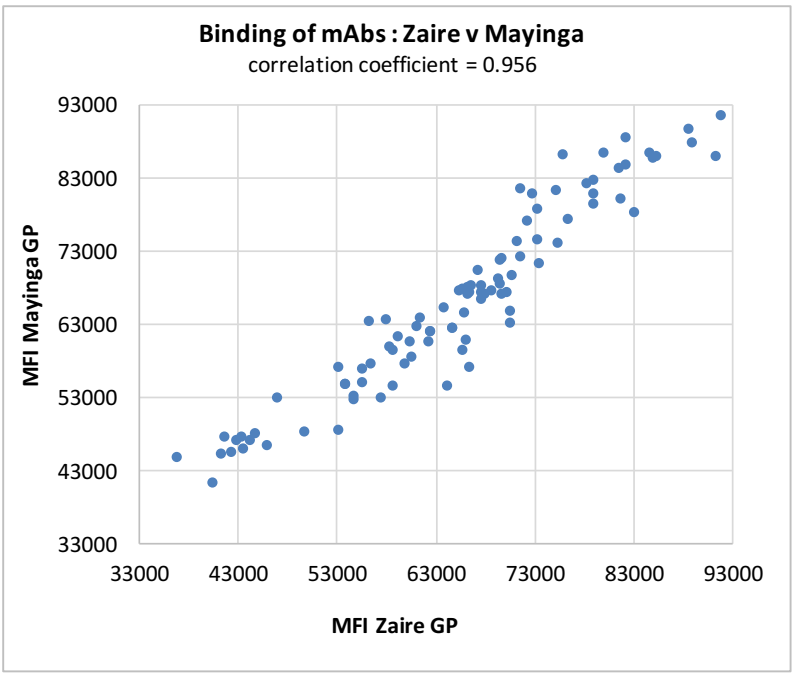

Figure 6. 26 ***Binding of antibodies to glycoprotein of Zaire (C15/2014) and Mayinga (1976) strains****. The correlation coefficient is 0.96.*

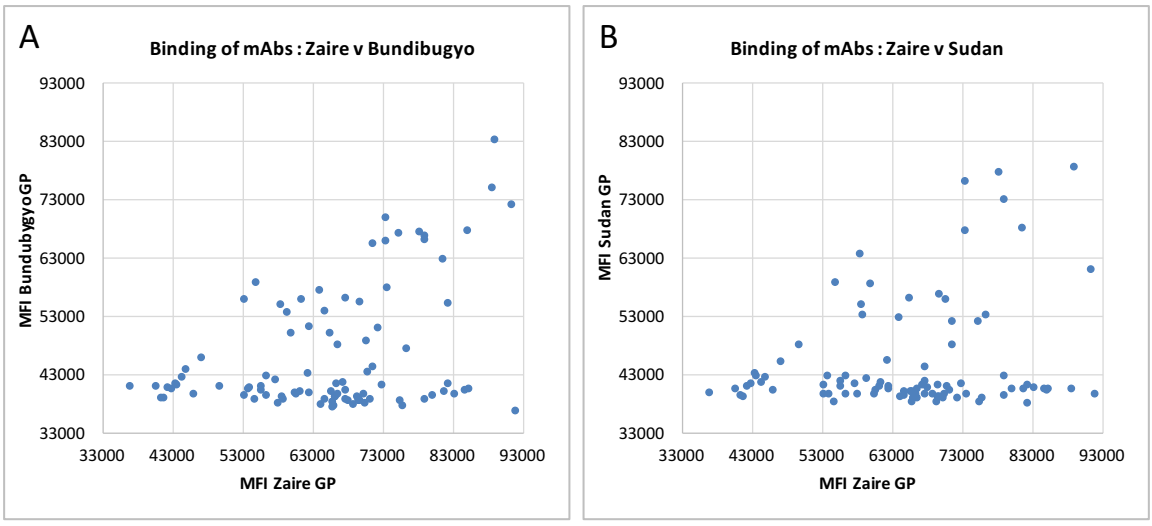

Figure 6. 27 ***Overall cross-reactivity of Zaire antibodies to Sudan and Bundibugyo GPs.*** ***A)*** *Binding of antibodies to glycoprotein of Zaire (C15/2014) and Bundibugyo subtypes.* ***B)*** *Binding of antibodies to glycoprotein of Zaire (C15/2014) and Sudan Gulu.*

The comparison with Sudan GP revealed some 20 cross-reacting antibodies (Figure 6.25 and 6.27B). Finally, a comparison between Bundibugyo and Sudan GPs revealed a subset of 17 antibodies that were cross reactive to both (Figure 6.28).

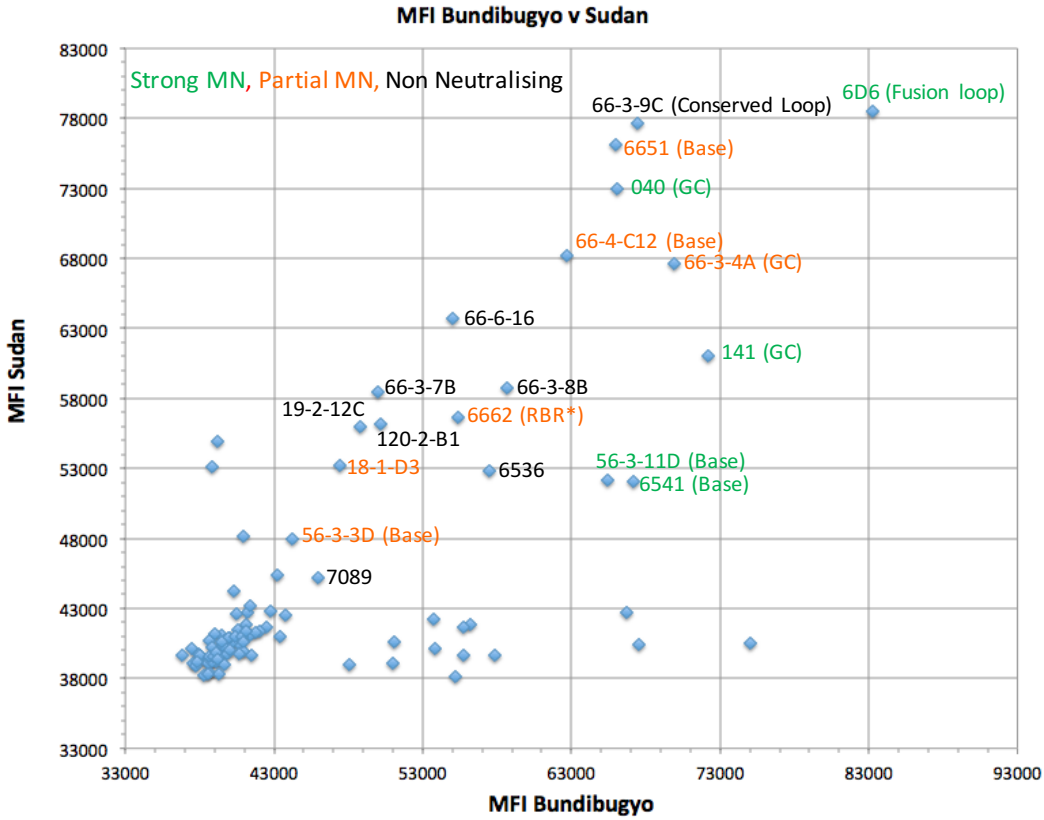

Figure 6. 28 ***Antibodies cross-reactive to Sudan and Bundibugyo GP****. Cross-reactive antibodies that were strongly neutralising are shown in green and partial neutralising antibodies in orange, along with their binding regions. GC: Glycan cap, RBR: receptor binding region. 6D6 is a control antibody binding to the internal fusion loop (Furuyama et al. 2016). 6662 is a cross-reactive RBR antibody but is sensitive to thermolysin digestion.*

The figure shows that several of the cross-reacting antibodies are partial or strong neutralisers of the Zaire E-S-FLU (Figure 6.28). It is encouraging that there is an appreciable frequency of cross-reacting antibodies to the Glycan cap and Base. Only one

cross-reactive antibody binds the RBR (6662) and that is unusual in being sensitive to thermolysin treatment. We have completed preparation of the S-FLU pseudotypes coated in the Mayinga, Bundibugyo and Sudan GPs and will be testing cross-neutralisation of the broadly reacting antibodies.

These data suggest that a cocktail of neutralising antibodies to different sites on GP that cross-react with Zaire, Bundibugyo and Sudan strains of Ebola is a real possibility. Further efforts to search for such antibodies is a definite goal for the future. We have set up a collaboration with the organisers of the EBOVAC-2 vaccine trial (which is very similar in design to the Jenner trial but larger) to continue the search. In addition, an effort will be placed on finding human antibodies similar to the murine 6D6 that binds the fusion loop and cross-neutralises these three strains of Ebola.

6.13 Antibody sequence analysis

More than 23 VH genes have been used to encode the 82 antibodies we isolated, making the VH gene use very diverse within the collection of individuals and within the individuals (Figure 6.29). The most used VH gene was VH3-15 (n=20) as shown in table 6.7. Almost equal numbers of antibodies have used the Kappa (n=39) or Lambda (n=43) light chain locus.

There is no particular VH identified among neutralising antibodies, unlike some viruses like influenza (Jackson et al. 2014) and dengue (Parameswaran et al. 2013) for which signature VH genes were identified (Galson et al. 2014). Interestingly however, all nine 114-like mAbs (antibodies that cross-compete with 114) were encoded by VH3-15 and Vλ1-40 genes (Figure 6.29). Four out of nine of these antibodies were partially neutralising and affected by thermolysin digestion (Figure 6. 16). Antibody 114 is encoded by VH3-13 and VK1-27 (Corti et al. 2016). This restricted usage and varying

neutralising capacity could be the starting point for a detailed analysis of affinity and neutralisation.

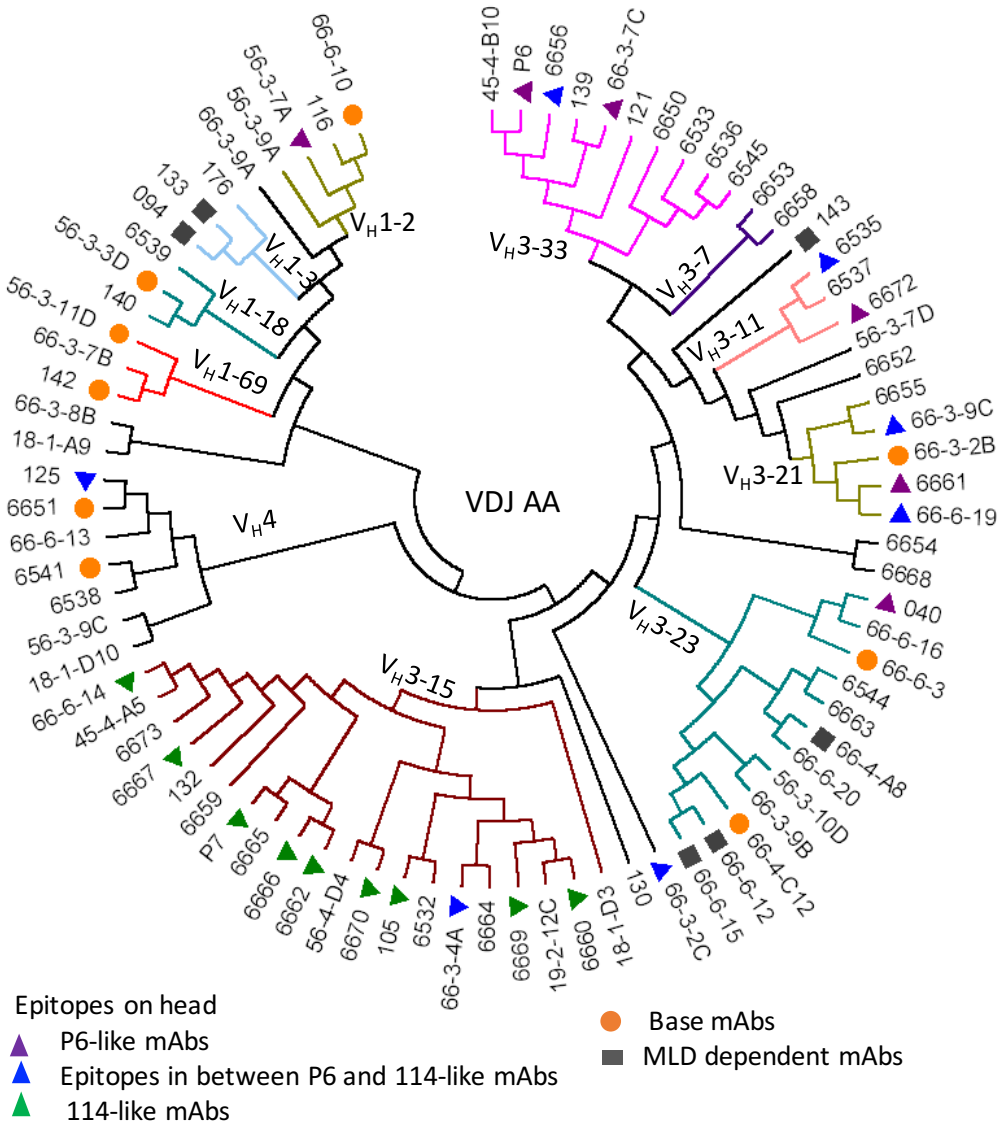

Figure 6. 29 ***Phylogeny of the antibodies based on VDJ amino acid sequences.*** *More than 23 VH genes have been used altogether. VH3-15 was the most commonly used gene and all nine antibodies that recognised the 114-like epitope were encoded by this gene. There was diversity in terms of VH gene use within individuals and within the antibodies to epitopes in the glycan cap and base. The Tree was drawn using MEGA v7 software using Muscle alignment and Neighbour-joining tree settings*

Table 6. 7 Use of VH gene by different donors

Donor	No. mAbs	3-15	3-23	3-21	3-33	3-30	1-2	1-3	1-18	1-69	3-11
66	29	3	9	3	1	3	1		1	1	1
4	13	4	1	2	1	1					
49	9	3			1		1	2			1
56	8	1					2		1	1	
3	6			1	1				1	1	1
12	5	4									
18	5	2			1						
14	2		1					1			
45	2	1			1						
68	2	1									
19	1	1									
	Total	20	11	6	6	4	4	3	3	3	3

6.13.1 HCDR3 length and somatic mutations

Rare broadly neutralising antibodies against HIV that target conserved epitopes, and may have undergone multiple rounds of selection in the germinal centre, tend to be encoded by longer HCDR3 sequences (Corti and Lanzavecchia 2013; Sok, Moldt, and Burton 2013). The HCDR3 lengths of our antibodies to Ebola ranged from 7 to 28 amino acids and LCDR3 from 8 to 13 amino acids (Table 6.8). We could not detect any clear association between the length of the CDR3 and neutralising activity or cross-reactivity, although there is a non-significant trend for partially neutralising antibodies to have shorter HCDR3 length (range 9-18 and average 13) compared to strong neutralising (range 7-28 and average 18) or non-neutralising antibodies (range 8-26 and average 17).

Table 6. 8 HCDR3 length of antibodies

	No. of mAbs	CDR3 length range	Average length
Partial neutralizers	16	9-18	13
Good neutralizers	23	7-28	18
Non-neutralizers	43	8-26	17

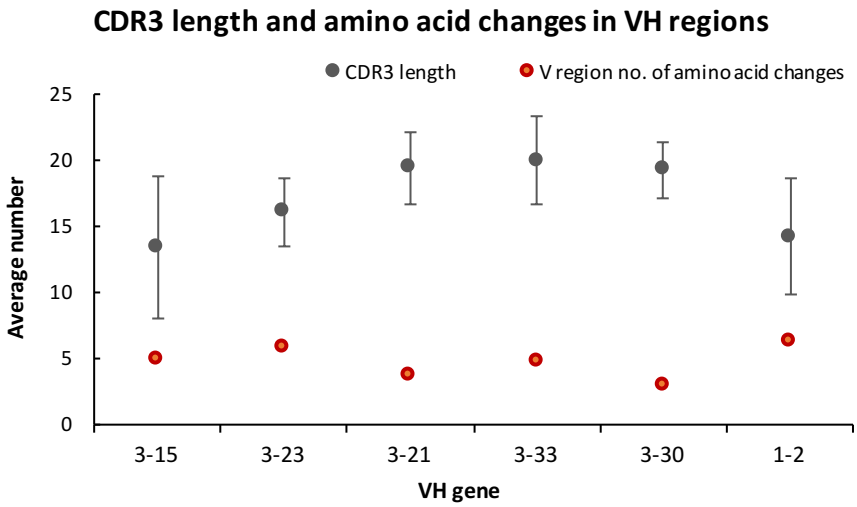

Figure 6. 30 Average HCDR3 length (with standard deviation) and average somatic mutations in the antibodies encoded by different VH genes.

Most of the Ebola specific antibody sequences have high identity to their germline genes with an average of five (range of zero to eight) somatic mutations (Figure 6.30), which is expected for antibodies that have been recently stimulated and that have not gone through several rounds of selection in the germinal centres (Thornburg et al. 2016). We found one example of a non-neutralising antibody, 56-3-9C, that has the identical amino acid sequence to the germline (with 1 silent nucleotide mutation). Such unmutated antibodies were also found occasionally in the response to influenza, particularly in situations of new antigen exposure. For instance, our collaborator Arthur Huang isolated a specific neutralising antibody to H7 haemagglutinin with no somatic mutations at all from an elderly H7N9 infected patient, and I isolated an unmutated antibody to N9 neuraminidase (described in chapter 5).

Overall, the number of somatic mutations in Ebola antibodies is lower than that of influenza antibodies, which gain more access to the germinal centre via frequent antigen

exposure, as discussed in chapter 3 (Huang et al. 2015; Pappas et al. 2014; Wrammert et al. 2011).

CHAPTER 6 DISCUSSION

Aim of the project

We have shown that an experimental Ebola vaccination trial offers a valuable opportunity for the isolation of potentially therapeutic *human* monoclonal antibodies. The main aim of this project was to form a therapeutic cocktail of human antibodies from the vaccinated volunteers to contrast with the murine antibodies in ZMapp (Qiu et al. 2014). In this collaborative project with UCB and Simon Draper's lab, Jenner Institute we isolated more than 82 antibodies. We have characterised these for binding and neutralisation of pseudotyped viruses. Twenty four antibodies were also sent to the International Viral Haemorrhagic Fever Immunotherapeutic Consortium (VIC) initiated by Erica Ollmann Sapphire, Scripps Institute, to help find an optimal therapeutic combination. Our antibodies are being compared to many others for neutralisation of wild type Ebola virus and various in vivo protection tests, but only some results are as yet available. Our own studies are on-going in parallel.

In view of the mutation frequency of Ebola virus (Carroll et al. 2015; Alfson et al. 2015) and the capacity for monoclonal antibodies, even when given in combination, to select resistant mutants during treatment of non-human primates (Kugelman et al. 2015), we aimed to find sets of neutralising antibodies that bound to non-overlapping sites on GP to limit the selection of resistant mutants. We are well ahead with this and have formed a collaboration with PHE Porton Down to test the best three cocktails in the Guinea Pig model of infection (Dowall, Bosworth, et al. 2016), with a comparison to control antibody

114 (Corti et al. 2016) or EBOTAb (ovine polyclonal antibody based product) (Dowall, Bosworth, et al. 2016; Dowall, Callan, et al. 2016), starting therapy at day 3 after infection as described. This experiment is planned to take place early in 2017.

Improving the yield of specific plasmablasts from vaccinated individuals

We see a trend that the use of antigen and a specific monoclonal antibody to stain plasmablasts for isolation may improve the yield of Ebola specific antibodies. Measuring the plasma antibody titres in ELISA may also be helpful in prioritizing the samples, however we haven't found a clear positive correlation between plasma antibody titres and plasmablast frequency in donor's PBMC. It could be because we tested plasma from day 7 and titres are optimal around day 14. The plasmablast frequency post-boost in eight donors ranged from 0.6 to 3% of B cells (Figure 6.2). This is a low frequency compared to influenza vaccination which ranges from 2 to 30% in our studies, and the frequency seen in Ebola virus disease (EVD) patients (McElroy et al. 2015) where the response was between 6 to 49%. This difference may be because of the high viral replication and persistence or longer exposure in EVD patients. The low frequency of antigen specific plasmablasts in the vaccinated volunteers makes the isolation of antibodies laborious, and further efforts to find ways of efficiently staining the antigen specific cells will be made.

Affinity and virus neutralisation

We characterised the binding and neutralisation properties of 82 monoclonal antibodies isolated from 11 vaccinated donors. A systematic comparison of affinity measurements of our antibodies has not been possible yet, but on the average the IC50 concentrations for neutralisation for Ebola virus are higher than for influenza virus (compare Figure 6. 6 with Figure 3.4 in Chapter 3), but as good as and comparable to the ZMapp components

(Davidson et al. 2015), KZ52 (Maruyama et al. 1999) and the therapeutic antibody 114 (Corti et al. 2016).

The binding affinities for a handful of Ebola antibodies to GP measured by Terry Baker at UCB (Appendix 6.1) show that some of them have values comparable to measurements in the literature for mature HA specific antibodies (Schmidt et al. 2015), or antibodies to Ebola isolated from recovered patients (Maruyama et al. 1999) and isolated from hyperimmunised animals (Howell et al. 2016; Furuyama et al. 2016; Keck et al. 2016). It is encouraging that a single dose of the recombinant VSV Ebola vaccine induced a highly protective response in humans even after post exposure to Ebola (Henao-Restrepo et al. 2015), which suggests that a primary response is protective. It is perhaps noteworthy that the two highest affinity antibodies 6661 and 6670 were partially neutralising, but the next highest pair 125 and 66-6-3 were the strongest neutralisers in our collection and protected mice to 90% and 100% respectively.

Mechanism of neutralisation

Preliminary experiments showed that blocking of proteolysis by cathepsins may be one of the mechanisms of virus neutralisation (Figure 6. 19). Blockade of binding to the NPC1 receptor (Howell et al. 2016) and fusion inhibition by binding to the internal fusion loop (Furuyama et al. 2016) may be among other mechanisms of virus neutralisation, which are still left to be studied.

Neutralisation *in vitro* versus protection *in vivo*

There has been much discussion in the literature on this topic (Saphire and Aman 2016; Oswald et al. 2007). Neutralisation assays *in vitro* which are mostly based on blocking of viral entry into cell lines, may miss important protective effects that are operative *in vivo*

such as antibody dependent cellular cytotoxicity, and complement dependent effects. It has been difficult to correlate neutralisation with *in vivo* protection for Ebola antibodies (Schmaljohn and Lewis 2016).

Our results from 24 antibodies tested for protection *in vivo* by Erica Saphire's group show a strong association between neutralisation of our E-S-FLU surrogate for Ebola, and therapeutic action in an established murine infection. A similar correlation between neutralisation of other Ebola pseudotyped viruses and protection has been found at the Scripps (personal communication with Saphire). However, as pointed out above, the correlation is not absolute and non-neutralising antibodies can protect *in vivo*. The neutralisation assay is failing to detect an antibody dependent function that can be protective *in vivo*.

The mechanisms of protection by antibodies against Ebola are not clear, and strong *in vitro* correlations with protection *in vivo* need to be further developed. KZ52 is the classic example of an antibody that showed strong neutralisation *in vitro* (Maruyama et al. 1999) and a good protection profile in mice and guinea pigs (Qiu, Fernando, et al. 2012), but failed to protect NHPs (Oswald et al. 2007). In the context of treatment with a single antibody, and given the high mutation rate of Ebola (Carroll et al. 2015; Alfson et al. 2015), failure could possibly have been due to early selection of resistant mutants. However, this was unlikely since virus isolated from the infected NHPs on sequential days remained sensitive to neutralization by KZ52 *in vitro* (Oswald et al. 2007).

KZ52 is directed to the base of the GP in a very similar configuration to two of the ZMapp components 2G4 and 4G7, and they neutralised our pseudotyped viruses with similar IC50 and IC90 values (Figure 6.7). The third component of ZMapp is 13C6, which performed poorly on *in vitro* neutralisation but made a significant contribution to

protection in the ZMapp cocktail (Qiu et al. 2014). Another example of non-neutralising antibody with *in vivo* activity is FVM09 which was partially protective in mice administrated alone, but completely protective when given together with another fusion loop antibody (Keck et al. 2016).

ZMapp component antibodies are known to also act via Fc engagement and complement fixation (Davidson et al. 2015; Pettitt et al. 2013), and ADCC may be another mechanism which is yet to be studied. It would be useful to test our antibodies further in ADCC and neutralisation in the presence of complement. *In vitro* assays for these functions are being developed (Ana-Sosa-Batiz et al. 2016; Jegaskanda et al. 2016), but standardisation is at an early stage and there are many versions of the assays, so comparison of results between laboratories is difficult. We are planning with Erica Saphire to select a set of assays to compare against the group of antibodies tested in vivo, and extend the *in vivo* testing to enlarge the test-bed to obtain good statistical evaluations.

Synergistic antibodies

In Ebola where therapeutic intervention is better as a cocktail of antibodies, looking at synergy and enhancement is of the utmost interest. There are few examples of antibodies that work synergistically *in vivo*. Combinations of antibodies in ZMapp works together to protect from infection (Davidson et al. 2015; Qiu et al. 2014). In another example, macaques' antibodies FVM02 (non-neutralising fusion loop antibody) and FVM09 (non-neutralising glycan cap conserved loop antibody) both partially protective in mice, when given together were fully protective (Keck et al. 2016). Our antibody 66-3-9C (FVM09-like) uniquely enhanced the binding of base ZMapp antibodies 2G4 and 4G7 by almost 4-fold (Table 6.3) and vice-versa (data not included). Having such cross-reactive synergistic antibodies in a cocktail may be beneficial. We are aiming to offer the 66-3-9C antibody to

the developers of ZMapp for them to explore the possible benefits of adding it to their combination.

Diversity of the antibody response to Ebola GP

The antibody response to Ebola GP in donors was very diverse both in terms of the range of V genes used and the diversity of epitopes detected. Three main groups of cross-inhibiting antibodies (Figure 6.16), were defined to the glycan cap, receptor binding region (RBR), and base or GP1-GP2 core independent of the mucin-like domain. The glycan cap was found to be the major antigenic site based on the numbers of antibodies that were targeted against this site. This is similar to the finding by Flyak et al. from the isolation of antibodies from human survivors of Bundibugyo Ebola virus (Flyak et al. 2016).

These epitopes are similar to the epitopes recognised by antibodies isolated from human, mice or macaque reviewed by Saphire et al. (Saphire and Aman 2016). The epitopes we have defined also match with published antibodies in terms of cross-reactivity to the glycoprotein of Bundibugyo or Sudan Ebola species (Keck et al. 2016; Furuyama et al. 2016; Corti et al. 2016). For example, the antibody 66-3-9C was found to be similar to the pan-ebola antibody FVM09 (Keck et al. 2016) recognising the conserved loop in the glycan cap.

There was further diversity within these groups. For instance, the glycan cap antibodies P6 and 040 looked very similar, but 040 was found to cross-react with Sudan and BB GP, whereas P6 binds BB but not Sudan GP. These two antibodies represent slightly different bindng footprints, analogous to the antibodies from donor H against the HA head in chapter 3. Different epitopes are also identified within the glycan cap, for example the non-cross-inhibiting conserved loop recognised by antibody 66-3-9C and the epitope of

antibody 125 which is cross-inhibited by both GC and RBR antibodies. Even in RBR antibodies, there is a group of antibodies which are 114-like but they are partially neutralising and are affected by thermolysin proteolysis. In addition, the observation that several antibodies could detect the effect of trypsin on the GP suggests that the human Ig repertoire is picking up subtle alterations in the structure of GP.

This profound diversity in the epitopes recognised in the response of vaccinated donors to Ebola GP contrasts with the response to Influenza HA, where in some individuals we have shown that the response is focused onto a localised patch of the HA molecular surface (Chapter 3) (Huang et al. 2015). While the diversity of epitopes in this situation has been narrowed after repeated exposures over the years, the antibodies that make up the response to HA are still polyclonal and encoded by several VH genes (Chapter 3). We see a hint of immunodominance of one or more residues within the glycan cap epitope, where the I260R substitution, along with the other two accessory substitutions in the mucin-like domain, was enough to cause the loss of neutralisation by almost all glycan cap antibodies.

This discrepancy of antibody diversity in monoclonal antibodies to Ebola and influenza could be explained by the evolutionary nature of the antibody response. Humans are exposed to influenza early in life (Francis 1960), and this is followed by repeated exposures by infection or vaccination throughout life to HA molecules that are continuously evolving, and share less common surface as time passes (Jensen et al. 1956). Exposure to the primary antigen shapes the immune response to future exposures by similar antigens (Miller et al. 2013; Lessler et al. 2012; Fonville et al. 2014) . It is known that a second exposure to an antigen preferentially selects antibodies from the memory B cells expanded by the first exposure, and subsequent rounds of hyper-mutation and

competition in germinal centres further refines and narrows the surviving repertoire of antibodies (Victora and Wilson 2015). The result in the end is a relatively focused high affinity response.

The response to Ebola GP is therefore comparable conceptually to the first response by humans to influenza. This is also reflected in the difference in the frequency of productive mutations in the VH genes in the Ebola antibodies (average 5 per VH, Figure 6. 30) as opposed to influenza in our recent study (average 10 per VH, Chapter 3). The Ebola GP specific antibodies have had less opportunity than those to HA to undergo affinity maturation in germinal centres and this may be reflected in a lower average affinity. Whether the relative immaturity of the Ebola antibodies isolated from vaccines will jeopardise their usefulness as therapeutics in humans remains to be seen.

Other groups have successfully isolated antibodies from memory B cells from patients several years after recovery from Ebola infection (Maruyama et al. 1999; Corti et al. 2016; Flyak et al. 2016). These often have a high frequency of mutations suggesting that they may have passed through several rounds of mutation and selection in the germinal centres. This is consistent with a degree of persistence of the virus after infection (Corti and Lanzavecchia 2013).

While the isolation of antibodies from recovered patients may improve the frequency of high affinity antibodies, this is offset by the safety issues provoked by possible exposure to persisting virus (Sow et al. 2016; Diallo et al. 2016).

Broadly reactive antibodies

A secondary aim of the project was to find a more broadly reactive cocktail. The most recent literature describes several neutralising antibodies that cross neutralise GPs of

Zaire, Bundibugyo and Sudan viruses (Howell et al. 2016; Furuyama et al. 2016; Flyak et al. 2016), and we obtained the 6D6 antibody (kindly provided by Ayoto Takada) as a comparator. This antibody is fascinating in terms that it is pan-Ebola and a potent neutraliser that targets the conserved internal fusion loop of GP (Furuyama et al. 2016). We have very recently found two base antibodies (66-4-C12 and 66-6-3) that cross compete with 6D6 for binding, one of which, 66-4-C12 is cross-reactive but poorly protective, and the other 66-6-3 is highly specific but strongly protective. Our efforts in this direction are continuing, and so far, we have been able to find 17 antibodies that cross react in binding to Bundibugyo and Sudan GPs (Figure 6. 25). The influenza pseudotyped viruses to test for neutralisation are in preparation.

We will continue these efforts by screening samples from the EBOVACII trial by Andrew Pollard. We will look specifically for human 6D6 equivalents by screening for antibodies that compete for binding by 6D6, and which fail to bind GP with mutations in the fusion peptide (G528R) in escape virus selected by 6D6.

Antibody cocktail formation for testing in the guinea pig model

The guinea pig infection model is thought to be a better predictor of protection in NHPs than infection of mice (Cross et al. 2015). While the development of assays for Fc dependent functions are in progress, we have taken the view that the selection of antibody cocktails for tests in guinea pigs can proceed based on our neutralisation assay combined with the data from Erica Saphire in the mouse protection assay. We are selecting cocktails of three antibodies directed at spatially separate sites that function well in these two assays (Figure 6. 7). The combinations will be put through a rigorous test for protection of guinea pigs at day 3 of infection (Dowall, Bosworth, et al. 2016; Dowall, Callan, et al. 2016), in collaboration with Miles Carroll at Porton Down in early 2017.

FUTURE PLANS

We will strive to search for pan-Ebola antibodies that neutralise, by isolating more antibodies from EBOVAC II trial (Andrew Pollard, Oxford). Given the diversity of the human antibody response to the Ebola GP that we have demonstrated, we feel it is likely that we can isolate such antibodies from vaccinated volunteers. We will test the 17 broadly reactive antibodies we have already identified in neutralisation assays as soon as the relevant pseudotyped viruses are made. Amongst these we know now that one antibody (66-4-C12) cross-competes with 6D6, and binds the Zaire, Bundibugyo and Sudan species GP equally well (Figure 6.24). However, this antibody is a weak neutraliser (Figure 6.7) and is poorly protective in the mouse protection assay (Appendix 6.3). A careful analysis of the binding kinetics of 66-4-C12 by Terry Baker at UCB, reveals that 66-4-C12 has ~20-fold lower binding affinity than 6D6 for the GP trimer, mainly due to a much faster off-rate: 66-4-C12 Kd 1.7E-4 v 6D6 Kd 4.1E-6 (Appendix 6.1, 6.3). A crystal structure of the bound 66-4-C12 Fab may help in the design of mutations to slow down the off-rate and improve the neutralisation titre. We will collaborate with George Gao, CAS China for the crystallography and Terry Baker at UCB Celltech, Slough for the binding kinetics on this project.

Appendix 6. 1 Affinity of the selected antibodies to Ebola glycoprotein monomer and trimer. *Antibody 125 has the highest binding affinity to trimer. Most of the antibodies have affinity in 1 to 10 nanomolar scale.* Data obtained from Terry Baker at UCB Celltech, Slough.

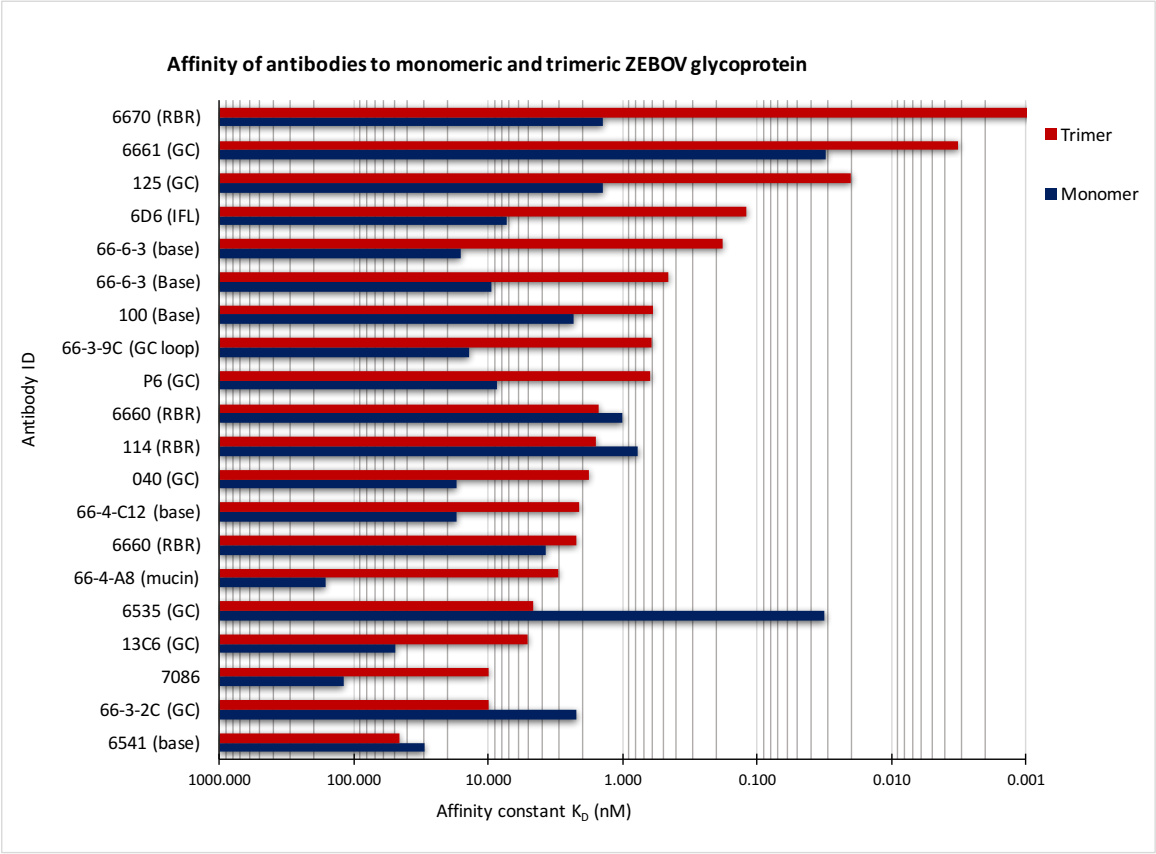

Appendix 6. 2* In vivo *protection of mice against Ebola virus by human monoclonal antibodies given at 100 µg dose 2-day post infection. *Control murine antibodies 2G4 and 13C6 (components of ZMapp) protected 90% and 30% mice from infection. Antibodies 040 and P6 protected 60% and 70% of mice respectively. These antibodies also neutralised 99% of wild type virus in* in vitro *assay. sGP: secreted GP; RBR: Receptor binding region; GPcl: GP cleaved by cathepsins.* Data obtained from Erica Ollmann Saphire lab, Scripps Institute.

mAb	Epitope	Class	in vivo (%)	isotype	Crossreact ELISA	microneut BSL4
P6	glycan cap	sGP, weak GPcl	60	h IgG1	B	99.3
P7	RBR	sGP, weak GPcl	50	h IgG1		97
19-2-12C		sGP, weak GPcl	20	h IgG1	B, S, R	41
56-4-D4		sGP, weak GPcl	30	h IgG1	S	28.3
18-1-A9		unknown	40	h IgG1		0
18-1-D3		unknown	10	h IgG1		0
45-4-B10		sGP	10	h IgG1	B weak	57.2
NC		unknown (no ELISA)	0	h IgG1		5.3
45-4-A5		sGP	30	h IgG1		22.4
40	glycan cap	sGP	70	h IgG1	B, S	99
66-4-C12	base	unknown	20	h IgG1		79.4
Controls						
2G4	base	GPcl: base	90	m IgG2b		99.8
13 C 6	RBR	sGP	30	m IgG2a		61.8
			mice		B = Bundibugyo	
			2 days p.i.		S = Sudan Gulu	
			100 µg dose		R = Reston	
					(x-react with purified ectodomain GP)	

Appendix 6. 3 Combination data including: cross-reactivity, neutralisation, in vivo protection and kinetic analysis for the selected antibodies. *GC: Glycan cap; RBR: Receptor binding region; RBR*: RBR antibodies sensitive to thermolysin proteolysis; S: Sudan; R:Reston; B or BB: Bundibugyo.* Protection data were obtained from Saphire's group at Scripps Institute and Kinetics data from Terry Baker, UCB

Zaire, Sudan and BB Cross-reactive antibodies										
			Neutralization				TRIMER			
	Antibody	Epitope	Zaire	Sudan	BB	Mouse protection	Ka (1/Ms)	Kd (1/s)	KD (M)	
	mouse 6D6	Fusion loop	Strong	Strong	Strong	100%	3.40E+04	4.10E-06	1.20E-10	
	141	GC	Strong	-	Partial Lenti	90%				
	6662	RBR*	Partial	-	-	90%				
	040	GC	Strong	-	-	70%	3.40E+04	6.00E-05	1.80E-09	
	66-3-4A	GC	Strong	-	Partial	70%				
	66-3-9C	GC cons. loop	-	-	-	40%	1.30E+05	7.90E-05	6.10E-10	
	66-4-C12	Base	Partial	Partial	Partial	20%	8.00E+04	1.70E-04	2.10E-09	
	6651	Base	Partial	-	Partial Lenti					
	6541	Base	Strong	-	Strong		8.80E+02	4.00E-05	4.60E-08	
	56-3-11D	Base	Partial	Partial	-					
	120-2-B1		Partial	-	Partial					
Other Antibodies										
			Neutralization					TRIMER		
	Antibody	Epitope	Zaire	Sudan	BB	Mouse protection	Cross-reactivity	Ka (1/Ms)	Kd (1/s)	KD (M)
	66-6-3	Base	Strong			100%	None	3.40E+05	1.60E-04	4.60E-10
	125	GC	Strong			90%	None	4.10E+04	8.10E-07	2.00E-11
	6666	RBR*	Partial			90%	None			
	2G4	Base	Strong			90%				
	66-3-2C	GC	Strong			70%	None			
	140	GC	Partial			60%	None			
	66-3-7C	GC	Strong			60%	BB			
	P6	GC	Strong			60%	BB			
	66-3-7B	?	-			50%	S, BB			
	P7	RBR	Lenti only			50%	None			
	66-6-19	GC	Strong			40%	None			
	18-1-A9	?	-			40%	None			
	56-3-9A	?	-			30%	BB			
	56-4-D4	?	-			30%	S			
	45-4-A5	?	-			30%	None			
	13C6	GC	Weak			30%		7.30E+04	3.70E-04	5.10E-09
	19-2-12C	?	-			20%	BB, S, R			
	66-3-8B	?	-			10%	S, BB			
	18-1-D3	?	Partial weak			10%	B, S(weak)			
	45-4-B10	?	-			10%	None			
	6660	RBR	Strong				None	5.10E+04	7.30E-05	1.50E-09
	6535	GC	Strong				None	1.40E+03	6.30E-06	4.60E-09
	114	RBR	Strong				None	4.60E+04	7.10E-05	1.60E-09
	100	Base	Strong				None	1.70E+05	1.00E-04	6.00E-10
	6670	RBR	Strong				None	7.40E+04	3.90E-08	5.30E-13

BIBLIOGRAPHY

Adalja, A. A., and D. A. Henderson. 2010. 'Original antigenic sin and pandemic (H1N1) 2009', *Emerg Infect Dis*, 16: 1028-9.

Air, G. M. 2012. 'Influenza neuraminidase', *Influenza Other Respir Viruses*, 6: 245-56.

Air, G. M. 2015. 'Influenza virus antigenicity and broadly neutralizing epitopes', *Curr Opin Virol*, 11: 113-21.

Air, G. M. 1981. 'Sequence relationships among the hemagglutinin genes of 12 subtypes of influenza A virus', *Proc Natl Acad Sci U S A*, 78: 7639-43.

Air, G. M., W. G. Laver, and R. G. Webster. 1990. 'Mechanism of antigenic variation in an individual epitope on influenza virus N9 neuraminidase', *J Virol*, 64: 5797-803.

Aleksandrowicz, P., A. Marzi, N. Biedenkopf, N. Beimforde, S. Becker, T. Hoenen, H. Feldmann, and H. J. Schnittler. 2011. 'Ebola virus enters host cells by macropinocytosis and clathrin-mediated endocytosis', *J Infect Dis*, 204 Suppl 3: S957-67.

Alfson, K. J., G. Worwa, R. Carrion, Jr., and A. Griffiths. 2015. 'Determination and Therapeutic Exploitation of Ebola Virus Spontaneous Mutation Frequency', *J Virol*, 90: 2345-55.

Ana-Sosa-Batiz, F., H. Vanderven, S. Jegaskanda, A. Johnston, S. Rockman, K. Laurie, I. Barr, P. Reading, M. Lichtfuss, and S. J. Kent. 2016. 'Influenza-Specific Antibody-Dependent Phagocytosis', *PLoS One*, 11: e0154461.

Andrews, S. F., Y. Huang, K. Kaur, L. I. Popova, I. Y. Ho, N. T. Pauli, C. J. Henry Dunand, W. M. Taylor, S. Lim, M. Huang, X. Qu, J. H. Lee, M. Salgado-Ferrer, F. Krammer, P. Palese, J. Wrammert, R. Ahmed, and P. C. Wilson. 2015. 'Immune history profoundly affects broadly protective B cell responses to influenza', *Sci Transl Med*, 7: 316ra192.

Bale, S., T. Liu, S. Li, Y. Wang, D. Abelson, M. Fusco, V. L. Woods, Jr., and E. O. Saphire. 2011. 'Ebola virus glycoprotein needs an additional trigger, beyond proteolytic priming for membrane fusion', *PLoS Negl Trop Dis*, 5: e1395.

Barnett, B. C., C. M. Graham, D. S. Burt, J. J. Skehel, and D. B. Thomas. 1989. 'The immune response of BALB/c mice to influenza hemagglutinin: commonality of the B cell and T cell repertoires and their relevance to antigenic drift', *Eur J Immunol*, 19: 515-21.

Baz, M., K. Boonnak, M. Paskel, C. Santos, T. Powell, A. Townsend, and K. Subbarao. 2015. 'Nonreplicating influenza A virus vaccines confer broad protection against lethal challenge', *MBio*, 6: e01487-15.

Bedford, Richard Neher; Trevor. 2016. "Nextstrain Ebola: Real-time tracking of Ebola virus evolution." In.

Bianconi, E., A. Piovesan, F. Facchin, A. Beraudi, R. Casadei, F. Frabetti, L. Vitale, M. C. Pelleri, S. Tassani, F. Piva, S. Perez-Amodio, P. Strippoli, and S. Canaider. 2013. 'An estimation of the number of cells in the human body', *Ann Hum Biol*, 40: 463-71.

Bornholdt, Z. A., E. Ndungo, M. L. Fusco, S. Bale, A. I. Flyak, J. E. Crowe, Jr., K. Chandran, and E. O. Saphire. 2016. 'Host-Primed Ebola Virus GP Exposes a Hydrophobic NPC1 Receptor-Binding Pocket, Revealing a Target for Broadly Neutralizing Antibodies', *MBio*, 7: e02154-15.

Brecher, M., K. L. Schornberg, S. E. Delos, M. L. Fusco, E. O. Saphire, and J. M. White. 2012. 'Cathepsin cleavage potentiates the Ebola virus glycoprotein to undergo a subsequent fusion-relevant conformational change', *J Virol*, 86: 364-72.

Broadbent, A. J., C. P. Santos, A. Anafu, E. Wimmer, S. Mueller, and K. Subbarao. 2016. 'Evaluation of the attenuation, immunogenicity, and efficacy of a live virus vaccine generated by codon-pair bias de-optimization of the 2009 pandemic H1N1 influenza virus, in ferrets', *Vaccine*, 34: 563-70.

Bucher, D. J., and E. D. Kilbourne. 1972. 'A 2 (N2) neuraminidase of the X-7 influenza virus recombinant: determination of molecular size and subunit composition of the active unit', *J Virol*, 10: 60-6.

Burnet, FM. 1937. 'Influenza virus on the developing egg. IV. The pathogenicity and immunizing power of egg virus for ferrets and mice. ', *J. Exp. Pathol.*, 18: 37-43.

Bush, R. M., C. A. Bender, K. Subbarao, N. J. Cox, and W. M. Fitch. 1999. 'Predicting the evolution of human influenza A', *Science*, 286: 1921-5.

Carette, J. E., M. Raaben, A. C. Wong, A. S. Herbert, G. Obernosterer, N. Mulherkar, A. I. Kuehne, P. J. Kranzusch, A. M. Griffin, G. Ruthel, P. Dal Cin, J. M. Dye, S. P. Whelan, K. Chandran, and T. R. Brummelkamp. 2011. 'Ebola virus entry requires the cholesterol transporter Niemann-Pick C1', *Nature*, 477: 340-3.

Carnell, G. W., F. Ferrara, K. Grehan, C. P. Thompson, and N. J. Temperton. 2015. 'Pseudotype-based neutralization assays for influenza: a systematic analysis', *Front Immunol*, 6: 161.

Carroll, M. W., D. A. Matthews, J. A. Hiscox, M. J. Elmore, G. Pollakis, A. Rambaut, R. Hewson, I. Garcia-Dorival, J. A. Bore, R. Koundouno, S. Abdellati, B. Afrough, J. Aiyepada, P. Akhilomen, D. Asogun, B. Atkinson, M. Badusche, A. Bah, S. Bate, J. Baumann, D. Becker, B. Becker-Ziaja, A. Bocquin, B. Borremans, A. Bosworth, J. P. Boettcher, A. Cannas, F. Carletti, C. Castilletti, S. Clark, F. Colavita, S. Diederich, A. Donatus, S. Duraffour, D. Ehichioya, H. Ellerbrok, M. D. Fernandez-Garcia, A. Fizet, E. Fleischmann, S. Gryseels, A. Hermelink, J. Hinzmann, U. Hopf-Guevara, Y. Ighodalo, L. Jameson, A. Kelterbaum, Z. Kis, S. Kloth, C. Kohl, M. Korva, A. Kraus, E. Kuisma, A. Kurth, B. Liedigk, C. H. Logue, A. Ludtke, P. Maes, J. McCowen, S. Mely, M. Mertens, S. Meschi, B. Meyer, J. Michel, P. Molkenthin, C. Munoz-Fontela, D. Muth, E. N. Newman, D. Ngabo, L. Oestereich, J. Okosun, T. Olokor, R. Omiunu, E. Omomoh, E. Pallasch, B. Palyi, J. Portmann, T. Pottage, C. Pratt, S. Priesnitz, S. Quartu, J. Rappe, J. Repits, M. Richter, M. Rudolf, A. Sachse, K. M. Schmidt, G. Schudt, T. Strecker, R. Thom, S. Thomas, E. Tobin, H. Tolley, J. Trautner, T. Vermoesen, I. Vitoriano, M. Wagner, S. Wolff, C. Yue, M. R. Capobianchi, B. Kretschmer, Y. Hall, J. G. Kenny, N. Y. Rickett, G. Dudas, C. E. Coltart, R. Kerber, D. Steer, C. Wright, F. Senyah, S. Keita, P. Drury, B. Diallo, H. de Clerck, M. Van Herp, A. Sprecher, A. Traore, M. Diakite, M. K. Konde, L. Koivogui, N. Magassouba, T. Avsic-Zupanc, A. Nitsche, M. Strasser, G. Ippolito, S. Becker, K. Stoecker, M. Gabriel, H. Raoul, A. Di Caro, R. Wolfel, P. Formenty, and S. Gunther. 2015. 'Temporal and spatial analysis of the 2014-2015 Ebola virus outbreak in West Africa', *Nature*, 524: 97-101.

Carter, D. M., C. E. Bloom, E. J. Nascimento, E. T. Marques, J. K. Craigo, J. L. Cherry, D. J. Lipman, and T. M. Ross. 2013. 'Sequential seasonal H1N1 influenza virus infections protect ferrets against novel 2009 H1N1 influenza virus', *J Virol*, 87: 1400-10.

Caton, A. J., G. G. Brownlee, J. W. Yewdell, and W. Gerhard. 1982. 'The antigenic structure of the influenza virus A/PR/8/34 hemagglutinin (H1 subtype)', *Cell*, 31: 417-27.

Centers for Disease Control and Prevention. 2016a. 'Ebola (Ebola Virus Disease)', Accessed 24 November 2016. http://www.cdc.gov/vhf/ebola/about.html.

Centers for Disease Control and Prevention. 2016b. 'Influenza Type A Viruses', Accessed 20 November 2016. http://www.cdc.gov/flu/avianflu/influenza-a-virus-subtypes.htm.

Chambers, B. S., K. Parkhouse, T. M. Ross, K. Alby, and S. E. Hensley. 2015. 'Identification of Hemagglutinin Residues Responsible for H3N2 Antigenic Drift during the 2014-2015 Influenza Season', *Cell Rep*, 12: 1-6.

Chandran, K., N. J. Sullivan, U. Felbor, S. P. Whelan, and J. M. Cunningham. 2005. 'Endosomal proteolysis of the Ebola virus glycoprotein is necessary for infection', *Science*, 308: 1643-5.

Chen, Z., W. Wang, H. Zhou, A. L. Suguitan, Jr., C. Shambaugh, L. Kim, J. Zhao, G. Kemble, and H. Jin. 2010. 'Generation of live attenuated novel influenza virus A/California/7/09 (H1N1) vaccines with high yield in embryonated chicken eggs', *J Virol*, 84: 44-51.

Chertow, D. S., C. Kleine, J. K. Edwards, R. Scaini, R. Giuliani, and A. Sprecher. 2014. 'Ebola virus disease in West Africa--clinical manifestations and management', *N Engl J Med*, 371: 2054-7.

Chu, C. M., C. H. Andrewes, and A. W. Gledhill. 1950. 'Influenza in 1948-1949', *Bull World Health Organ*, 3: 187-214.

Clarke, S. H., K. Huppi, D. Ruezinsky, L. Staudt, W. Gerhard, and M. Weigert. 1985. 'Inter- and intraclonal diversity in the antibody response to influenza hemagglutinin', *J Exp Med*, 161: 687-704.

Colman, P. M. 1994. 'Influenza virus neuraminidase: structure, antibodies, and inhibitors', *Protein Sci*, 3: 1687-96.

Cook, J. D., and J. E. Lee. 2013. 'The secret life of viral entry glycoproteins: moonlighting in immune evasion', *PLoS Pathog*, 9: e1003258.

Cooper-lab. 2013. 'Gibson Cloning'. http://www.cooperlab.wustl.edu/LabMethodsReagentsOperations/GibsonCloning.pdf.

Corti, D., and A. Lanzavecchia. 2013. 'Broadly neutralizing antiviral antibodies', *Annu Rev Immunol*, 31: 705-42.

Corti, D., J. Misasi, S. Mulangu, D. A. Stanley, M. Kanekiyo, S. Wollen, A. Ploquin, N. A. Doria-Rose, R. P. Staupe, M. Bailey, W. Shi, M. Choe, H. Marcus, E. A. Thompson, A. Cagigi, C. Silacci, B. Fernandez-Rodriguez, L. Perez, F. Sallusto, F. Vanzetta, G. Agatic, E. Cameroni, N. Kisalu, I. Gordon, J. E. Ledgerwood, J. R. Mascola, B. S. Graham, J. J. Muyembe-Tamfun, J. C. Trefry, A. Lanzavecchia, and N. J. Sullivan. 2016. 'Protective monotherapy against lethal Ebola virus infection by a potently neutralizing antibody', *Science*, 351: 1339-42.

Corti, D., A. L. Suguitan, Jr., D. Pinna, C. Silacci, B. M. Fernandez-Rodriguez, F. Vanzetta, C. Santos, C. J. Luke, F. J. Torres-Velez, N. J. Temperton, R. A. Weiss, F. Sallusto, K. Subbarao, and A. Lanzavecchia. 2010. 'Heterosubtypic neutralizing antibodies are produced by individuals immunized with a seasonal influenza vaccine', *J Clin Invest*, 120: 1663-73.

Corti, D., J. Voss, S. J. Gamblin, G. Codoni, A. Macagno, D. Jarrossay, S. G. Vachieri, D. Pinna, A. Minola, F. Vanzetta, C. Silacci, B. M. Fernandez-Rodriguez, G. Agatic, S. Bianchi, I. Giacchetto-Sasselli, L. Calder, F. Sallusto, P. Collins, L. F.

Haire, N. Temperton, J. P. Langedijk, J. J. Skehel, and A. Lanzavecchia. 2011. 'A neutralizing antibody selected from plasma cells that binds to group 1 and group 2 influenza A hemagglutinins', *Science*, 333: 850-6.

Cote, M., J. Misasi, T. Ren, A. Bruchez, K. Lee, C. M. Filone, L. Hensley, Q. Li, D. Ory, K. Chandran, and J. Cunningham. 2011. 'Small molecule inhibitors reveal Niemann-Pick C1 is essential for Ebola virus infection', *Nature*, 477: 344-8.

Couch, R. B., J. A. Kasel, J. L. Gerin, J. L. Schulman, and E. D. Kilbourne. 1974. 'Induction of partial immunity to influenza by a neuraminidase-specific vaccine', *J Infect Dis*, 129: 411-20.

Cox, M. M., R. Izikson, P. Post, and L. Dunkle. 2015. 'Safety, efficacy, and immunogenicity of Flublok in the prevention of seasonal influenza in adults', *Ther Adv Vaccines*, 3: 97-108.

Cronin, J., X. Y. Zhang, and J. Reiser. 2005. 'Altering the tropism of lentiviral vectors through pseudotyping', *Curr Gene Ther*, 5: 387-98.

Cross, R. W., K. A. Fenton, J. B. Geisbert, C. E. Mire, and T. W. Geisbert. 2015. 'Modeling the Disease Course of Zaire ebolavirus Infection in the Outbred Guinea Pig', *J Infect Dis*, 212 Suppl 2: S305-15.

Crotty, S. 2015. 'A brief history of T cell help to B cells', *Nat Rev Immunol*, 15: 185-9.

Daniels, R. S., S. Jeffries, P. Yates, G. C. Schild, G. N. Rogers, J. C. Paulson, S. A. Wharton, A. R. Douglas, J. J. Skehel, and D. C. Wiley. 1987. 'The receptor-binding and membrane-fusion properties of influenza virus variants selected using anti-haemagglutinin monoclonal antibodies', *EMBO J*, 6: 1459-65.

Das, K., J. M. Aramini, L. C. Ma, R. M. Krug, and E. Arnold. 2010. 'Structures of influenza A proteins and insights into antiviral drug targets', *Nat Struct Mol Biol*, 17: 530-8.

Das, S. R., S. E. Hensley, W. L. Ince, C. B. Brooke, A. Subba, M. G. Delboy, G. Russ, J. S. Gibbs, J. R. Bennink, and J. W. Yewdell. 2013. 'Defining influenza A virus hemagglutinin antigenic drift by sequential monoclonal antibody selection', *Cell Host Microbe*, 13: 314-23.

Davenport, F. M., and A. V. Hennessy. 1957. 'Predetermination by infection and by vaccination of antibody response to influenza virus vaccines', *J Exp Med*, 106: 835-50.

Davenport, F. M., A. V. Hennessy, and T. Francis, Jr. 1953. 'Epidemiologic and immunologic significance of age distribution of antibody to antigenic variants of influenza virus', *J Exp Med*, 98: 641-56.

Davidson, E., C. Bryan, R. H. Fong, T. Barnes, J. M. Pfaff, M. Mabila, J. B. Rucker, and B. J. Doranz. 2015. 'Mechanism of Binding to Ebola Virus Glycoprotein by the ZMapp, ZMAb, and MB-003 Cocktail Antibodies', *J Virol*, 89: 10982-92.

de Graaf, M., and R. A. Fouchier. 2014. 'Role of receptor binding specificity in influenza A virus transmission and pathogenesis', *EMBO J*, 33: 823-41.

Demaison, C., K. Parsley, G. Brouns, M. Scherr, K. Battmer, C. Kinnon, M. Grez, and A. J. Thrasher. 2002. 'High-level transduction and gene expression in hematopoietic repopulating cells using a human immunodeficiency [correction of imunodeficiency] virus type 1-based lentiviral vector containing an internal spleen focus forming virus promoter', *Hum Gene Ther*, 13: 803-13.

Demicheli, V., T. Jefferson, L. A. Al-Ansary, E. Ferroni, A. Rivetti, and C. Di Pietrantonj. 2014. 'Vaccines for preventing influenza in healthy adults', *Cochrane Database Syst Rev*: CD001269.

Destgroth, S. F., and R. G. Webster. 1966. 'Disquisitions on Original Antigenic Sin .I. Evidence in Man', *Journal of Experimental Medicine*, 124: 331-+.

Deutsch, S., and A. E. Bussard. 1972. 'Original antigenic sin at the cellular level. I. Antibodies produced by individual cells against cross-reacting haptens', *Eur J Immunol*, 2: 374-8.

Diallo, B., D. Sissoko, N. J. Loman, H. A. Bah, H. Bah, M. C. Worrell, L. S. Conde, R. Sacko, S. Mesfin, A. Loua, J. K. Kalonda, N. A. Erondu, B. A. Dahl, S. Handrick, I. Goodfellow, L. W. Meredith, M. Cotten, U. Jah, R. E. Guetiya Wadoum, P. Rollin, N. Magassouba, D. Malvy, X. Anglaret, M. W. Carroll, R. B. Aylward, M. H. Djingarey, A. Diarra, P. Formenty, S. Keita, S. Gunther, A. Rambaut, and S. Duraffour. 2016. 'Resurgence of Ebola Virus Disease in Guinea Linked to a Survivor With Virus Persistence in Seminal Fluid for More Than 500 Days', *Clin Infect Dis*.

Diehl, W. E., A. E. Lin, N. D. Grubaugh, L. M. Carvalho, K. Kim, P. P. Kyawe, S. M. McCauley, E. Donnard, A. Kucukural, P. McDonel, S. F. Schaffner, M. Garber, A. Rambaut, K. G. Andersen, P. C. Sabeti, and J. Luban. 2016. 'Ebola Virus Glycoprotein with Increased Infectivity Dominated the 2013-2016 Epidemic', *Cell*, 167: 1088-98 e6.

DiLillo, D. J., P. Palese, P. C. Wilson, and J. V. Ravetch. 2016. 'Broadly neutralizing anti-influenza antibodies require Fc receptor engagement for in vivo protection', *J Clin Invest*, 126: 605-10.

DiLillo, D. J., G. S. Tan, P. Palese, and J. V. Ravetch. 2014. 'Broadly neutralizing hemagglutinin stalk-specific antibodies require FcgammaR interactions for protection against influenza virus in vivo', *Nat Med*, 20: 143-51.

Dowall, S. D., A. Bosworth, E. Rayner, I. Taylor, J. Landon, I. Cameron, R. Coxon, I. Al Abdulla, V. A. Graham, G. Hall, G. Kobinger, R. Hewson, and M. W. Carroll. 2016. 'Post-exposure treatment of Ebola virus disease in guinea pigs using EBOTAb, an ovine antibody-based therapeutic', *Sci Rep*, 6: 30497.

Dowall, S. D., J. Callan, A. Zeltina, I. Al-Abdulla, T. Strecker, S. K. Fehling, V. Krahling, A. Bosworth, E. Rayner, I. Taylor, S. Charlton, J. Landon, I. Cameron, R. Hewson, A. Nasidi, T. A. Bowden, and M. W. Carroll. 2016. 'Development of a Cost-effective Ovine Polyclonal Antibody-Based Product, EBOTAb, to Treat Ebola Virus Infection', *J Infect Dis*, 213: 1124-33.

Doyle, T. M., A. M. Hashem, C. Li, G. Van Domselaar, L. Larocque, J. Wang, D. Smith, T. Cyr, A. Farnsworth, R. He, A. C. Hurt, E. G. Brown, and X. Li. 2013. 'Universal anti-neuraminidase antibody inhibiting all influenza A subtypes', *Antiviral Res*, 100: 567-74.

Doyle, T. M., B. Jaentschke, G. Van Domselaar, A. M. Hashem, A. Farnsworth, N. E. Forbes, C. Li, J. Wang, R. He, E. G. Brown, and X. Li. 2013. 'The universal epitope of influenza A viral neuraminidase fundamentally contributes to enzyme activity and viral replication', *J Biol Chem*, 288: 18283-9.

Doyle, T. M., C. Li, D. J. Bucher, A. M. Hashem, G. Van Domselaar, J. Wang, A. Farnsworth, Y. M. She, T. Cyr, R. He, E. G. Brown, A. C. Hurt, and X. Li. 2013. 'A monoclonal antibody targeting a highly conserved epitope in influenza B neuraminidase provides protection against drug resistant strains', *Biochem Biophys Res Commun*, 441: 226-9.

Dreyfus, C., D. C. Ekiert, and I. A. Wilson. 2013. 'Structure of a classical broadly neutralizing stem antibody in complex with a pandemic H2 influenza virus hemagglutinin', *J Virol*, 87: 7149-54.

Dube, D., M. B. Brecher, S. E. Delos, S. C. Rose, E. W. Park, K. L. Schornberg, J. H. Kuhn, and J. M. White. 2009. 'The primed ebolavirus glycoprotein (19-kilodalton GP1,2): sequence and residues critical for host cell binding', *J Virol*, 83: 2883-91.

Easterday, B., W. G. Laver, H. G. Pereira, and G. C. Schild. 1969. 'Antigenic composition of recombinant virus strains produced from human and avian influenza A viruses', *J Gen Virol*, 5: 83-91.

Ekiert, D. C., G. Bhabha, M. A. Elsliger, R. H. Friesen, M. Jongeneelen, M. Throsby, J. Goudsmit, and I. A. Wilson. 2009. 'Antibody recognition of a highly conserved influenza virus epitope', *Science*, 324: 246-51.

Ekiert, D. C., and I. A. Wilson. 2012. 'Broadly neutralizing antibodies against influenza virus and prospects for universal therapies', *Curr Opin Virol*, 2: 134-41.

Enserink, Martin. 2011. "Scientists Brace for Media Storm Around Controversial Flu Studies." In *Science*.

European Centre for Disease Prevention and Control. 2014. "Seasonal influenza 2013–14 in the EU/EEA countries." In. Stockholm: ECDC.

Ewer, K., T. Rampling, N. Venkatraman, G. Bowyer, D. Wright, T. Lambe, E. B. Imoukhuede, R. Payne, S. K. Fehling, T. Strecker, N. Biedenkopf, V. Krahling, C. M. Tully, N. J. Edwards, E. M. Bentley, D. Samuel, G. Labbe, J. Jin, M. Gibani, A. Minhinnick, M. Wilkie, I. Poulton, N. Lella, R. Roberts, F. Hartnell, C. Bliss, K. Sierra-Davidson, J. Powlson, E. Berrie, R. Tedder, F. Roman, I. De Ryck, A. Nicosia, N. J. Sullivan, D. A. Stanley, O. T. Mbaya, J. E. Ledgerwood, R. M. Schwartz, L. Siani, S. Colloca, A. Folgori, S. Di Marco, R. Cortese, E. Wright, S. Becker, B. S. Graham, R. A. Koup, M. M. Levine, A. Volkmann, P. Chaplin, A. J. Pollard, S. J. Draper, W. R. Ballou, A. Lawrie, S. C. Gilbert, and A. V. Hill. 2016. 'A Monovalent Chimpanzee Adenovirus Ebola Vaccine Boosted with MVA', *N Engl J Med*, 374: 1635-46.

Falagas, M. E., P. K. Koletsi, E. Baskouta, P. I. Rafailidis, G. Dimopoulos, and D. E. Karageorgopoulos. 2011. 'Pandemic A(H1N1) 2009 influenza: review of the Southern Hemisphere experience', *Epidemiol Infect*, 139: 27-40.

Fazekas de St, Groth, and R. G. Webster. 1966. 'Disquisitions of Original Antigenic Sin. I. Evidence in man', *J Exp Med*, 124: 331-45.

Flyak, A. I., X. Shen, C. D. Murin, H. L. Turner, J. A. David, M. L. Fusco, R. Lampley, N. Kose, P. A. Ilinykh, N. Kuzmina, A. Branchizio, H. King, L. Brown, C. Bryan, E. Davidson, B. J. Doranz, J. C. Slaughter, G. Sapparapu, C. Klages, T. G. Ksiazek, E. O. Saphire, A. B. Ward, A. Bukreyev, and J. E. Crowe, Jr. 2016. 'Cross-Reactive and Potent Neutralizing Antibody Responses in Human Survivors of Natural Ebolavirus Infection', *Cell*, 164: 392-405.

Fonville, J. M., S. H. Wilks, S. L. James, A. Fox, M. Ventresca, M. Aban, L. Xue, T. C. Jones, N. M. Le, Q. T. Pham, N. D. Tran, Y. Wong, A. Mosterin, L. C. Katzelnick, D. Labonte, T. T. Le, G. van der Net, E. Skepner, C. A. Russell, T. D. Kaplan, G. F. Rimmelzwaan, N. Masurel, J. C. de Jong, A. Palache, W. E. Beyer, Q. M. Le, T. H. Nguyen, H. F. Wertheim, A. C. Hurt, A. D. Osterhaus, I. G. Barr, R. A. Fouchier, P. W. Horby, and D. J. Smith. 2014. 'Antibody landscapes after influenza virus infection or vaccination', *Science*, 346: 996-1000.

Francis, T., Jr. 1960. 'On the Doctrine of Original Antigenic Sin', *American Philosophical Society*, 104.

Francis, T., Jr., F. M. Davenport, and A. V. Hennessy. 1953. 'A serological recapitulation of human infection with different strains of influenza virus', *Trans Assoc Am Physicians*, 66: 231-9.

Francis, T., J. E. Salk, H. E. Pearson, and P. N. Brown. 1945. 'Protective Effect of Vaccination against Induced Influenza A', *J Clin Invest*, 24: 536-46.

Francis, T., J. E. Salk, and J. J. Quilligan. 1947. 'Experience with Vaccination Against Influenza in the Spring of 1947: A Preliminary Report', *Am J Public Health Nations Health*, 37: 1013-6.

Friesen, R. H., P. S. Lee, E. J. Stoop, R. M. Hoffman, D. C. Ekiert, G. Bhabha, W. Yu, J. Juraszek, W. Koudstaal, M. Jongeneelen, H. J. Korse, C. Ophorst, E. C. Brinkman-van der Linden, M. Throsby, M. J. Kwakkenbos, A. Q. Bakker, T. Beaumont, H. Spits, T. Kwaks, R. Vogels, A. B. Ward, J. Goudsmit, and I. A. Wilson. 2014. 'A common solution to group 2 influenza virus neutralization', *Proc Natl Acad Sci U S A*, 111: 445-50.

Furuyama, W., A. Marzi, A. Nanbo, E. Haddock, J. Maruyama, H. Miyamoto, M. Igarashi, R. Yoshida, O. Noyori, H. Feldmann, and A. Takada. 2016. 'Discovery of an antibody for pan-ebolavirus therapy', *Sci Rep*, 6: 20514.

Galson, J. D., A. J. Pollard, J. Truck, and D. F. Kelly. 2014. 'Studying the antibody repertoire after vaccination: practical applications', *Trends Immunol*, 35: 319-31.

Geisbert, T. W., and H. Feldmann. 2011. 'Recombinant vesicular stomatitis virus-based vaccines against Ebola and Marburg virus infections', *J Infect Dis*, 204 Suppl 3: S1075-81.

Gerber, P., C. G. Loosli, and D. Hambre. 1955. 'Antigenic variants of influenza A virus, PR8 strain. I. Their development during serial passage in the lungs of partially immune mice', *J Exp Med*, 101: 627-38.

Gerhard, W., J. Yewdell, M. E. Frankel, and R. Webster. 1981. 'Antigenic structure of influenza virus haemagglutinin defined by hybridoma antibodies', *Nature*, 290: 713-7.

Gibson, D. G., L. Young, R. Y. Chuang, J. C. Venter, C. A. Hutchison, 3rd, and H. O. Smith. 2009. 'Enzymatic assembly of DNA molecules up to several hundred kilobases', *Nat Methods*, 6: 343-5.

Gillim-Ross, L., and K. Subbarao. 2007. 'Can immunity induced by the human influenza virus N1 neuraminidase provide some protection from avian influenza H5N1 viruses?', *PLoS Med*, 4: e91.

Gire, S. K., A. Goba, K. G. Andersen, R. S. Sealfon, D. J. Park, L. Kanneh, S. Jalloh, M. Momoh, M. Fullah, G. Dudas, S. Wohl, L. M. Moses, N. L. Yozwiak, S. Winnicki, C. B. Matranga, C. M. Malboeuf, J. Qu, A. D. Gladden, S. F. Schaffner, X. Yang, P. P. Jiang, M. Nekoui, A. Colubri, M. R. Coomber, M. Fonnie, A. Moigboi, M. Gbakie, F. K. Kamara, V. Tucker, E. Konuwa, S. Saffa, J. Sellu, A. A. Jalloh, A. Kovoma, J. Koninga, I. Mustapha, K. Kargbo, M. Foday, M. Yillah, F. Kanneh, W. Robert, J. L. Massally, S. B. Chapman, J. Bochicchio, C. Murphy, C. Nusbaum, S. Young, B. W. Birren, D. S. Grant, J. S. Scheiffelin, E. S. Lander, C. Happi, S. M. Gevao, A. Gnirke, A. Rambaut, R. F. Garry, S. H. Khan, and P. C. Sabeti. 2014. 'Genomic surveillance elucidates Ebola virus origin and transmission during the 2014 outbreak', *Science*, 345: 1369-72.

Gitlin, A. D., Z. Shulman, and M. C. Nussenzweig. 2014. 'Clonal selection in the germinal centre by regulated proliferation and hypermutation', *Nature*, 509: 637-40.

Gong, X., H. Qian, X. Zhou, J. Wu, T. Wan, P. Cao, W. Huang, X. Zhao, X. Wang, P. Wang, Y. Shi, G. F. Gao, Q. Zhou, and N. Yan. 2016. 'Structural Insights into the Niemann-Pick C1 (NPC1)-Mediated Cholesterol Transfer and Ebola Infection', *Cell*, 165: 1467-78.

Gulati, S., D. F. Smith, R. D. Cummings, R. B. Couch, S. B. Griesemer, K. St George, R. G. Webster, and G. M. Air. 2013. 'Human H3N2 Influenza Viruses Isolated from

1968 To 2012 Show Varying Preference for Receptor Substructures with No Apparent Consequences for Disease or Spread', *PLoS One*, 8: e66325.

Haaheim, L. R. 1980a. 'Antibodies to the strain-specific and cross-reactive determinants of the haemagglutinin of influenza H3N2 virus. 3. Selection of antigenic variations in vitro and in vivo', *Acta Pathol Microbiol Scand B*, 88: 341-5.

Haaheim, L. R. 1980b. 'Haemagglutination-inhibition antibodies in human sera to an antigenic mutant of influenza A/Texas/1/77 (H3N2) virus obtained in vitro', *Acta Pathol Microbiol Scand B*, 88: 351-3.

Halfmann, P., J. H. Kim, H. Ebihara, T. Noda, G. Neumann, H. Feldmann, and Y. Kawaoka. 2008. 'Generation of biologically contained Ebola viruses', *Proc Natl Acad Sci U S A*, 105: 1129-33.

Harvey, W. T., D. J. Benton, V. Gregory, J. P. Hall, R. S. Daniels, T. Bedford, D. T. Haydon, A. J. Hay, J. W. McCauley, and R. Reeve. 2016. 'Identification of Low- and High-Impact Hemagglutinin Amino Acid Substitutions That Drive Antigenic Drift of Influenza A(H1N1) Viruses', *PLoS Pathog*, 12: e1005526.

Henao-Restrepo, A. M., A. Camacho, I. M. Longini, C. H. Watson, W. J. Edmunds, M. Egger, M. W. Carroll, N. E. Dean, I. Diatta, M. Doumbia, B. Draguez, S. Duraffour, G. Enwere, R. Grais, S. Gunther, P. S. Gsell, S. Hossmann, S. V. Watle, M. K. Konde, S. Keita, S. Kone, E. Kuisma, M. M. Levine, S. Mandal, T. Mauget, G. Norheim, X. Riveros, A. Soumah, S. Trelle, A. S. Vicari, J. A. Rottingen, and M. P. Kieny. 2017. 'Efficacy and effectiveness of an rVSV-vectored vaccine in preventing Ebola virus disease: final results from the Guinea ring vaccination, open-label, cluster-randomised trial (Ebola Ca Suffit!)', *Lancet*, 389: 505-18.

Henao-Restrepo, A. M., I. M. Longini, M. Egger, N. E. Dean, W. J. Edmunds, A. Camacho, M. W. Carroll, M. Doumbia, B. Draguez, S. Duraffour, G. Enwere, R. Grais, S. Gunther, S. Hossmann, M. K. Konde, S. Kone, E. Kuisma, M. M. Levine, S. Mandal, G. Norheim, X. Riveros, A. Soumah, S. Trelle, A. S. Vicari, C. H. Watson, S. Keita, M. P. Kieny, and J. A. Rottingen. 2015. 'Efficacy and effectiveness of an rVSV-vectored vaccine expressing Ebola surface glycoprotein: interim results from the Guinea ring vaccination cluster-randomised trial', *Lancet*, 386: 857-66.

Heneghan, C. J., I. Onakpoya, M. A. Jones, P. Doshi, C. B. Del Mar, R. Hama, M. J. Thompson, E. A. Spencer, K. R. Mahtani, D. Nunan, J. Howick, and T. Jefferson. 2016. 'Neuraminidase inhibitors for influenza: a systematic review and meta-analysis of regulatory and mortality data', *Health Technol Assess*, 20: 1-242.

Hensley, S. E., S. R. Das, A. L. Bailey, L. M. Schmidt, H. D. Hickman, A. Jayaraman, K. Viswanathan, R. Raman, R. Sasisekharan, J. R. Bennink, and J. W. Yewdell. 2009. 'Hemagglutinin receptor binding avidity drives influenza A virus antigenic drift', *Science*, 326: 734-6.

Herfst, S., E. J. Schrauwen, M. Linster, S. Chutinimitkul, E. de Wit, V. J. Munster, E. M. Sorrell, T. M. Bestebroer, D. F. Burke, D. J. Smith, G. F. Rimmelzwaan, A. D. Osterhaus, and R. A. Fouchier. 2012. 'Airborne transmission of influenza A/H5N1 virus between ferrets', *Science*, 336: 1534-41.

Hoenen, T., D. Safronetz, A. Groseth, K. R. Wollenberg, O. A. Koita, B. Diarra, I. S. Fall, F. C. Haidara, F. Diallo, M. Sanogo, Y. S. Sarro, A. Kone, A. C. Togo, A. Traore, M. Kodio, A. Dosseh, K. Rosenke, E. de Wit, F. Feldmann, H. Ebihara, V. J. Munster, K. C. Zoon, H. Feldmann, and S. Sow. 2015. 'Virology. Mutation rate and genotype variation of Ebola virus from Mali case sequences', *Science*, 348: 117-9.

Holmes, E. C., G. Dudas, A. Rambaut, and K. G. Andersen. 2016. 'The evolution of Ebola virus: Insights from the 2013-2016 epidemic', *Nature*, 538: 193-200.

Hooper, K. A., and J. D. Bloom. 2013. 'A mutant influenza virus that uses an N1 neuraminidase as the receptor-binding protein', *J Virol*, 87: 12531-40.

Howell, K. A., X. Qiu, J. M. Brannan, C. Bryan, E. Davidson, F. W. Holtsberg, A. Z. Wec, S. Shulenin, J. E. Biggins, R. Douglas, S. G. Enterlein, H. L. Turner, J. Pallesen, C. D. Murin, S. He, A. Kroeker, H. Vu, A. S. Herbert, M. L. Fusco, E. K. Nyakatura, J. R. Lai, Z. Y. Keck, S. K. Foung, E. O. Saphire, L. Zeitlin, A. B. Ward, K. Chandran, B. J. Doranz, G. P. Kobinger, J. M. Dye, and M. J. Aman. 2016. 'Antibody Treatment of Ebola and Sudan Virus Infection via a Uniquely Exposed Epitope within the Glycoprotein Receptor-Binding Site', *Cell Rep*, 15: 1514-26.

Huang, J. W., and J. M. Yang. 2011. 'Changed epitopes drive the antigenic drift for influenza A (H3N2) viruses', *BMC Bioinformatics*, 12 Suppl 1: S31.

Huang, K. Y., P. Rijal, L. Schimanski, T. J. Powell, T. Y. Lin, J. W. McCauley, R. S. Daniels, and A. R. Townsend. 2015. 'Focused antibody response to influenza linked to antigenic drift', *J Clin Invest*, 125: 2631-45.

Huang, S. S., Z. Lin, D. Banner, A. J. Leon, S. G. Paquette, B. Rubin, S. Rubino, Y. Guan, D. J. Kelvin, and A. A. Kelvin. 2013. 'Immunity toward H1N1 influenza hemagglutinin of historical and contemporary strains suggests protection and vaccine failure', *Sci Rep*, 3: 1698.

Hunt, C. L., N. J. Lennemann, and W. Maury. 2012. 'Filovirus entry: a novelty in the viral fusion world', *Viruses*, 4: 258-75.

Ito, T., Y. Suzuki, L. Mitnaul, A. Vines, H. Kida, and Y. Kawaoka. 1997. 'Receptor specificity of influenza A viruses correlates with the agglutination of erythrocytes from different animal species', *Virology*, 227: 493-9.

Jackson, K. J., Y. Liu, K. M. Roskin, J. Glanville, R. A. Hoh, K. Seo, E. L. Marshall, T. C. Gurley, M. A. Moody, B. F. Haynes, E. B. Walter, H. X. Liao, R. A. Albrecht, A. Garcia-Sastre, J. Chaparro-Riggers, A. Rajpal, J. Pons, B. B. Simen, B. Hanczaruk, C. L. Dekker, J. Laserson, D. Koller, M. M. Davis, A. Z. Fire, and S. D. Boyd. 2014. 'Human responses to influenza vaccination show seroconversion signatures and convergent antibody rearrangements', *Cell Host Microbe*, 16: 105-14.

Jefferson, T., M. A. Jones, P. Doshi, C. B. Del Mar, R. Hama, M. J. Thompson, E. A. Spencer, I. Onakpoya, K. R. Mahtani, D. Nunan, J. Howick, and C. J. Heneghan. 2014. 'Neuraminidase inhibitors for preventing and treating influenza in healthy adults and children', *Cochrane Database Syst Rev*: CD008965.

Jegaskanda, S., C. Luke, H. D. Hickman, M. Y. Sangster, W. F. Wieland-Alter, J. M. McBride, J. W. Yewdell, P. F. Wright, J. Treanor, C. M. Rosenberger, and K. Subbarao. 2016. 'Generation and Protective Ability of Influenza Virus-Specific Antibody-Dependent Cellular Cytotoxicity in Humans Elicited by Vaccination, Natural Infection, and Experimental Challenge', *J Infect Dis*, 214: 945-52.

Jegaskanda, S., J. T. Weinfurter, T. C. Friedrich, and S. J. Kent. 2013. 'Antibody-dependent cellular cytotoxicity is associated with control of pandemic H1N1 influenza virus infection of macaques', *J Virol*, 87: 5512-22.

Jensen, K. E., F. M. Davenport, A. V. Hennessy, and T. Francis, Jr. 1956. 'Characterization of influenza antibodies by serum absorption', *J Exp Med*, 104: 199-209.

Johansson, B. E., and M. M. Cox. 2011. 'Influenza viral neuraminidase: the forgotten antigen', *Expert Rev Vaccines*, 10: 1683-95.

Kallewaard, N. L., D. Corti, P. J. Collins, U. Neu, J. M. McAuliffe, E. Benjamin, L. Wachter-Rosati, F. J. Palmer-Hill, A. Q. Yuan, P. A. Walker, M. K. Vorlaender, S. Bianchi, B. Guarino, A. De Marco, F. Vanzetta, G. Agatic, M. Foglierini, D. Pinna, B. Fernandez-Rodriguez, A. Fruehwirth, C. Silacci, R. W. Ogrodowicz, S. R. Martin, F. Sallusto, J. A. Suzich, A. Lanzavecchia, Q. Zhu, S. J. Gamblin, and J. J. Skehel. 2016. 'Structure and Function Analysis of an Antibody Recognizing All Influenza A Subtypes', *Cell*, 166: 596-608.

Karlsson Hedestam, G. B., R. A. Fouchier, S. Phogat, D. R. Burton, J. Sodroski, and R. T. Wyatt. 2008. 'The challenges of eliciting neutralizing antibodies to HIV-1 and to influenza virus', *Nat Rev Microbiol*, 6: 143-55.

Keck, Z. Y., S. G. Enterlein, K. A. Howell, H. Vu, S. Shulenin, K. L. Warfield, J. W. Froude, N. Araghi, R. Douglas, J. Biggins, C. M. Lear-Rooney, A. S. Wirchnianski, P. Lau, Y. Wang, A. S. Herbert, J. M. Dye, P. J. Glass, F. W. Holtsberg, S. K. Foung, and M. J. Aman. 2016. 'Macaque Monoclonal Antibodies Targeting Novel Conserved Epitopes within Filovirus Glycoprotein', *J Virol*, 90: 279-91.

Kilbourne, E. D., W. N. Christenson, and M. Sande. 1968. 'Antibody response in man to influenza virus neuraminidase following influenza', *J Virol*, 2: 761-2.

Kilbourne, E. D., W. G. Laver, J. L. Schulman, and R. G. Webster. 1968. 'Antiviral activity of antiserum specific for an influenza virus neuraminidase', *J Virol*, 2: 281-8.

Kilbourne, E. D., B. A. Pokorny, B. Johansson, I. Brett, Y. Milev, and J. T. Matthews. 2004. 'Protection of mice with recombinant influenza virus neuraminidase', *J Infect Dis*, 189: 459-61.

Kilbourne, E. D., C. Smith, I. Brett, B. A. Pokorny, B. Johansson, and N. Cox. 2002. 'The total influenza vaccine failure of 1947 revisited: major intrasubtypic antigenic change can explain failure of vaccine in a post-World War II epidemic', *Proc Natl Acad Sci U S A*, 99: 10748-52.

Kim, J. H., W. G. Davis, S. Sambhara, and J. Jacob. 2012. 'Strategies to alleviate original antigenic sin responses to influenza viruses', *Proc Natl Acad Sci U S A*, 109: 13751-6.

Kim, J. H., A. J. Reber, A. Kumar, P. Ramos, G. Sica, N. Music, Z. Guo, M. Mishina, J. Stevens, I. A. York, J. Jacob, and S. Sambhara. 2016. 'Non-neutralizing antibodies induced by seasonal influenza vaccine prevent, not exacerbate A(H1N1)pdm09 disease', *Sci Rep*, 6: 37341.

Kinoshita, K., A. Shimizu, and T. Honjo. 1991. 'The membrane exons of the pseudo-gamma-chain gene of the human immunoglobulin are apparently functional and highly homologous to those of the gamma 1 gene', *Immunol Lett*, 27: 151-5.

Klein, U., and R. Dalla-Favera. 2008. 'Germinal centres: role in B-cell physiology and malignancy', *Nat Rev Immunol*, 8: 22-33.

Knossow, M., M. Gaudier, A. Douglas, B. Barrere, T. Bizebard, C. Barbey, B. Gigant, and J. J. Skehel. 2002. 'Mechanism of neutralization of influenza virus infectivity by antibodies', *Virology*, 302: 294-8.

Koel, B. F., D. F. Burke, T. M. Bestebroer, S. van der Vliet, G. C. Zondag, G. Vervaet, E. Skepner, N. S. Lewis, M. I. Spronken, C. A. Russell, M. Y. Eropkin, A. C. Hurt, I. G. Barr, J. C. de Jong, G. F. Rimmelzwaan, A. D. Osterhaus, R. A. Fouchier, and D. J. Smith. 2013. 'Substitutions near the receptor binding site determine major antigenic change during influenza virus evolution', *Science*, 342: 976-9.

Kohler, G., and C. Milstein. 1975. 'Continuous cultures of fused cells secreting antibody of predefined specificity', *Nature*, 256: 495-7.

Kondratowicz, A. S., N. J. Lennemann, P. L. Sinn, R. A. Davey, C. L. Hunt, S. Moller-Tank, D. K. Meyerholz, P. Rennert, R. F. Mullins, M. Brindley, L. M. Sandersfeld, K. Quinn, M. Weller, P. B. McCray, Jr., J. Chiorini, and W. Maury. 2011. 'T-cell immunoglobulin and mucin domain 1 (TIM-1) is a receptor for Zaire Ebolavirus and Lake Victoria Marburgvirus', *Proc Natl Acad Sci U S A*, 108: 8426-31.

Krammer, F., and P. Palese. 2013. 'Influenza virus hemagglutinin stalk-based antibodies and vaccines', *Curr Opin Virol*, 3: 521-30.

Krammer, F., P. Palese, and J. Steel. 2015. 'Advances in universal influenza virus vaccine design and antibody mediated therapies based on conserved regions of the hemagglutinin', *Curr Top Microbiol Immunol*, 386: 301-21.

Krammer, F.; Palese, P. 2015. 'Advances in the development of influenza virus vaccines', *Nat Rev Drug Discov*, 14: 167-82.

Krause, J. C., T. Tsibane, T. M. Tumpey, C. J. Huffman, C. F. Basler, and J. E. Crowe, Jr. 2011. 'A broadly neutralizing human monoclonal antibody that recognizes a conserved, novel epitope on the globular head of the influenza H1N1 virus hemagglutinin', *J Virol*, 85: 10905-8.

Krause, J. C., T. Tsibane, T. M. Tumpey, C. J. Huffman, B. S. Briney, S. A. Smith, C. F. Basler, and J. E. Crowe, Jr. 2011. 'Epitope-specific human influenza antibody repertoires diversify by B cell intraclonal sequence divergence and interclonal convergence', *J Immunol*, 187: 3704-11.

Kugelman, J. R., J. Kugelman-Tonos, J. T. Ladner, J. Pettit, C. M. Keeton, E. R. Nagle, K. Y. Garcia, J. W. Froude, A. I. Kuehne, J. H. Kuhn, S. Bavari, L. Zeitlin, J. M. Dye, G. G. Olinger, M. Sanchez-Lockhart, and G. F. Palacios. 2015. 'Emergence of Ebola Virus Escape Variants in Infected Nonhuman Primates Treated with the MB-003 Antibody Cocktail', *Cell Rep*, 12: 2111-20.

Kuhn, J. H., S. Becker, H. Ebihara, T. W. Geisbert, K. M. Johnson, Y. Kawaoka, W. I. Lipkin, A. I. Negredo, S. V. Netesov, S. T. Nichol, G. Palacios, C. J. Peters, A. Tenorio, V. E. Volchkov, and P. B. Jahrling. 2010. 'Proposal for a revised taxonomy of the family Filoviridae: classification, names of taxa and viruses, and virus abbreviations', *Arch Virol*, 155: 2083-103.

Kuraoka, M., A. G. Schmidt, T. Nojima, F. Feng, A. Watanabe, D. Kitamura, S. C. Harrison, T. B. Kepler, and G. Kelsoe. 2016. 'Complex Antigens Drive Permissive Clonal Selection in Germinal Centers', *Immunity*, 44: 542-52.

Lai, K. Y., W. Y. Ng, and F. F. Cheng. 2014. 'Human Ebola virus infection in West Africa: a review of available therapeutic agents that target different steps of the life cycle of Ebola virus', *Infect Dis Poverty*, 3: 43.

Lamb, R. A., and P. W. Choppin. 1983. 'The gene structure and replication of influenza virus', *Annu Rev Biochem*, 52: 467-506.

Lambkin, R., L. McLain, S. E. Jones, S. L. Aldridge, and N. J. Dimmock. 1994. 'Neutralization escape mutants of type A influenza virus are readily selected by antisera from mice immunized with whole virus: a possible mechanism for antigenic drift', *J Gen Virol*, 75 (Pt 12): 3493-502.

Laursen, N. S., and I. A. Wilson. 2013. 'Broadly neutralizing antibodies against influenza viruses', *Antiviral Res*, 98: 476-83.

Laver, W. G. 1978. 'Crystallization and peptide maps of neuraminidase "heads" from H2N2 and H3N2 influenza virus strains', *Virology*, 86: 78-87.

Laver, W. G., P. M. Colman, R. G. Webster, V. S. Hinshaw, and G. M. Air. 1984. 'Influenza virus neuraminidase with hemagglutinin activity', *Virology*, 137: 314-23.

Lee, J. E., M. L. Fusco, A. J. Hessell, W. B. Oswald, D. R. Burton, and E. O. Saphire. 2008. 'Structure of the Ebola virus glycoprotein bound to an antibody from a human survivor', *Nature*, 454: 177-82.

Lee, J. E., and E. O. Saphire. 2009. 'Ebolavirus glycoprotein structure and mechanism of entry', *Future Virol*, 4: 621-35.

Lee, Janis T., and Gillian M. Air. 2002. 'Contacts between Influenza Virus N9 Neuraminidase and Monoclonal Antibody NC10', *Virology*, 300: 255-68.

Lee, M. S., and J. S. Chen. 2004. 'Predicting antigenic variants of influenza A/H3N2 viruses', *Emerg Infect Dis*, 10: 1385-90.

Lee, P. S., and I. A. Wilson. 2015. 'Structural characterization of viral epitopes recognized by broadly cross-reactive antibodies', *Curr Top Microbiol Immunol*, 386: 323-41.

Lefranc, M. P., V. Giudicelli, C. Busin, J. Bodmer, W. Muller, R. Bontrop, M. Lemaitre, A. Malik, and D. Chaume. 1998. 'IMGT, the International ImMunoGeneTics database', *Nucleic Acids Res*, 26: 297-303.

Leroy, E. M., B. Kumulungui, X. Pourrut, P. Rouquet, A. Hassanin, P. Yaba, A. Delicat, J. T. Paweska, J. P. Gonzalez, and R. Swanepoel. 2005. 'Fruit bats as reservoirs of Ebola virus', *Nature*, 438: 575-6.

Lessler, J., S. Riley, J. M. Read, S. Wang, H. Zhu, G. J. Smith, Y. Guan, C. Q. Jiang, and D. A. Cummings. 2012. 'Evidence for antigenic seniority in influenza A (H3N2) antibody responses in southern China', *PLoS Pathog*, 8: e1002802.

Li, C., M. Hatta, D. F. Burke, J. Ping, Y. Zhang, M. Ozawa, A. S. Taft, S. C. Das, A. P. Hanson, J. Song, M. Imai, P. R. Wilker, T. Watanabe, S. Watanabe, M. Ito, K. Iwatsuki-Horimoto, C. A. Russell, S. L. James, E. Skepner, E. A. Maher, G. Neumann, A. I. Klimov, A. Kelso, J. McCauley, D. Wang, Y. Shu, T. Odagiri, M. Tashiro, X. Xu, D. E. Wentworth, J. M. Katz, N. J. Cox, D. J. Smith, and Y. Kawaoka. 2016. 'Selection of antigenically advanced variants of seasonal influenza viruses', *Nat Microbiol*, 1: 16058.

Li, G. M., C. Chiu, J. Wrammert, M. McCausland, S. F. Andrews, N. Y. Zheng, J. H. Lee, M. Huang, X. Qu, S. Edupuganti, M. Mulligan, S. R. Das, J. W. Yewdell, A. K. Mehta, P. C. Wilson, and R. Ahmed. 2012. 'Pandemic H1N1 influenza vaccine induces a recall response in humans that favors broadly cross-reactive memory B cells', *Proc Natl Acad Sci U S A*, 109: 9047-52.

Li, J., T. J. Shao, X. F. Yu, J. C. Pan, X. Y. Pu, H. Q. Wang, and Y. Kou. 2012. 'Molecular evolution of HA gene of the influenza A H1N1 pdm09 strain during the consecutive seasons 2009-2011 in Hangzhou, China: several immune-escape variants without positively selected sites', *Journal of Clinical Virology*, 55: 363-6.

Li, J., Y. Y. Zhou, Y. Kou, X. F. Yu, Z. B. Zheng, X. H. Yang, and H. Q. Wang. 2015. 'Interim estimates of divergence date and vaccine strain match of human influenza A(H3N2) virus from systematic influenza surveillance (2010-2015) in Hangzhou, southeast of China', *Int J Infect Dis*, 40: 17-24.

Li, Q., J. Qi, W. Zhang, C. J. Vavricka, Y. Shi, J. Wei, E. Feng, J. Shen, J. Chen, D. Liu, J. He, J. Yan, H. Liu, H. Jiang, M. Teng, X. Li, and G. F. Gao. 2010. 'The 2009 pandemic H1N1 neuraminidase N1 lacks the 150-cavity in its active site', *Nat Struct Mol Biol*, 17: 1266-8.

Li, Q., X. Sun, Z. Li, Y. Liu, C. J. Vavricka, J. Qi, and G. F. Gao. 2012. 'Structural and functional characterization of neuraminidase-like molecule N10 derived from bat influenza A virus', *Proc Natl Acad Sci U S A*, 109: 18897-902.

Li, Y., J. L. Myers, D. L. Bostick, C. B. Sullivan, J. Madara, S. L. Linderman, Q. Liu, D. M. Carter, J. Wrammert, S. Esposito, N. Principi, J. B. Plotkin, T. M. Ross, R.

Ahmed, P. C. Wilson, and S. E. Hensley. 2013. 'Immune history shapes specificity of pandemic H1N1 influenza antibody responses', *J Exp Med*, 210: 1493-500.

Lieff, Jon. 2014. "The Very Intelligent Ebola Virus Takes Front and Center." In.

Lin, Y. P., V. Gregory, P. Collins, J. Kloess, S. Wharton, N. Cattle, A. Lackenby, R. Daniels, and A. Hay. 2010. 'Neuraminidase receptor binding variants of human influenza A(H3N2) viruses resulting from substitution of aspartic acid 151 in the catalytic site: a role in virus attachment?', *J Virol*, 84: 6769-81.

Lin, Y. P., X. Xiong, S. A. Wharton, S. R. Martin, P. J. Coombs, S. G. Vachieri, E. Christodoulou, P. A. Walker, J. Liu, J. J. Skehel, S. J. Gamblin, A. J. Hay, R. S. Daniels, and J. W. McCauley. 2012. 'Evolution of the receptor binding properties of the influenza A(H3N2) hemagglutinin', *Proc Natl Acad Sci U S A*, 109: 21474-9.

Linderman, S. L., B. S. Chambers, S. J. Zost, K. Parkhouse, Y. Li, C. Herrmann, A. H. Ellebedy, D. M. Carter, S. F. Andrews, N. Y. Zheng, M. Huang, Y. Huang, D. Strauss, B. H. Shaz, R. L. Hodinka, G. Reyes-Teran, T. M. Ross, P. C. Wilson, R. Ahmed, J. D. Bloom, and S. E. Hensley. 2014. 'Potential antigenic explanation for atypical H1N1 infections among middle-aged adults during the 2013-2014 influenza season', *Proc Natl Acad Sci U S A*, 111: 15798-803.

Lingwood, D., P. M. McTamney, H. M. Yassine, J. R. Whittle, X. Guo, J. C. Boyington, C. J. Wei, and G. J. Nabel. 2012. 'Structural and genetic basis for development of broadly neutralizing influenza antibodies', *Nature*, 489: 566-70.

Loeb, M., M. L. Russell, V. Manning, K. Fonseca, D. J. Earn, G. Horsman, K. Chokani, M. Vooght, L. Babiuk, L. Schwartz, B. Neupane, P. Singh, S. D. Walter, and E. Pullenayegum. 2016. 'Live Attenuated Versus Inactivated Influenza Vaccine in Hutterite Children: A Cluster Randomized Blinded Trial', *Ann Intern Med*, 165: 617-24.

Luksza, M., and M. Lassig. 2014. 'A predictive fitness model for influenza', *Nature*, 507: 57-61.

Malby, R. L., W. R. Tulip, V. R. Harley, J. L. McKimm-Breschkin, W. G. Laver, R. G. Webster, and P. M. Colman. 1994. 'The structure of a complex between the NC10 antibody and influenza virus neuraminidase and comparison with the overlapping binding site of the NC41 antibody', *Structure*, 2: 733-46.

Manca, F., A. Kunkl, D. Fenoglio, A. Fowler, E. Sercarz, and F. Celada. 1985. 'Constraints in T-B cooperation related to epitope topology on E. coli beta-galactosidase. I. The fine specificity of T cells dictates the fine specificity of antibodies directed to conformation-dependent determinants', *Eur J Immunol*, 15: 345-50.

Martins, K. A., P. B. Jahrling, S. Bavari, and J. H. Kuhn. 2016. 'Ebola virus disease candidate vaccines under evaluation in clinical trials', *Expert Rev Vaccines*, 15: 1101-12.

Maruyama, T., L. L. Rodriguez, P. B. Jahrling, A. Sanchez, A. S. Khan, S. T. Nichol, C. J. Peters, P. W. Parren, and D. R. Burton. 1999. 'Ebola virus can be effectively neutralized by antibody produced in natural human infection', *J Virol*, 73: 6024-30.

Marzi, A., T. Reinheckel, and H. Feldmann. 2012. 'Cathepsin B & L are not required for ebola virus replication', *PLoS Negl Trop Dis*, 6: e1923.

Marzi, A., R. Yoshida, H. Miyamoto, M. Ishijima, Y. Suzuki, M. Higuchi, Y. Matsuyama, M. Igarashi, E. Nakayama, M. Kuroda, M. Saijo, F. Feldmann, D. Brining, H. Feldmann, and A. Takada. 2012. 'Protective efficacy of neutralizing

monoclonal antibodies in a nonhuman primate model of Ebola hemorrhagic fever', *PLoS One*, 7: e36192.

Matrosovich, M., T. Matrosovich, J. Carr, N. A. Roberts, and H. D. Klenk. 2003. 'Overexpression of the alpha-2,6-sialyltransferase in MDCK cells increases influenza virus sensitivity to neuraminidase inhibitors', *J Virol*, 77: 8418-25.

Matrosovich, M., T. Matrosovich, W. Garten, and H. D. Klenk. 2006. 'New low-viscosity overlay medium for viral plaque assays', *Virol J*, 3: 63.

McCullers, J. A., L. A. Van De Velde, K. J. Allison, K. C. Branum, R. J. Webby, and P. M. Flynn. 2010. 'Recipients of vaccine against the 1976 "swine flu" have enhanced neutralization responses to the 2009 novel H1N1 influenza virus', *Clin Infect Dis*, 50: 1487-92.

McElroy, A. K., R. S. Akondy, C. W. Davis, A. H. Ellebedy, A. K. Mehta, C. S. Kraft, G. M. Lyon, B. S. Ribner, J. Varkey, J. Sidney, A. Sette, S. Campbell, U. Stroher, I. Damon, S. T. Nichol, C. F. Spiropoulou, and R. Ahmed. 2015. 'Human Ebola virus infection results in substantial immune activation', *Proc Natl Acad Sci U S A*, 112: 4719-24.

McWhite, C. D., A. G. Meyer, and C. O. Wilke. 2016. 'Sequence amplification via cell passaging creates spurious signals of positive adaptation in influenza virus H3N2 hemagglutinin', *Virus Evol*, 2.

Medeiros, R., N. Escriou, N. Naffakh, J. C. Manuguerra, and S. van der Werf. 2001. 'Hemagglutinin residues of recent human A(H3N2) influenza viruses that contribute to the inability to agglutinate chicken erythrocytes', *Virology*, 289: 74-85.

MedImmune. 2015. 'A Phase 2a to Evaluate the Safety of MEDI8852 in Adults With Uncomplicated Influenza (MEDI8852)', Accessed 2 January 2017. https://clinicaltrials.gov/ct2/show/NCT02603952.

Medina, R. A., and A. Garcia-Sastre. 2011. 'Influenza A viruses: new research developments', *Nat Rev Microbiol*, 9: 590-603.

Mehedi, M., D. Falzarano, J. Seebach, X. Hu, M. S. Carpenter, H. J. Schnittler, and H. Feldmann. 2011. 'A new Ebola virus nonstructural glycoprotein expressed through RNA editing', *J Virol*, 85: 5406-14.

Mehedi, M., T. Hoenen, S. Robertson, S. Ricklefs, M. A. Dolan, T. Taylor, D. Falzarano, H. Ebihara, S. F. Porcella, and H. Feldmann. 2013. 'Ebola virus RNA editing depends on the primary editing site sequence and an upstream secondary structure', *PLoS Pathog*, 9: e1003677.

Meisner, J., K. J. Szretter, K. C. Bradley, W. A. Langley, Z. N. Li, B. J. Lee, S. Thoennes, J. Martin, J. J. Skehel, R. J. Russell, J. M. Katz, and D. A. Steinhauer. 2008. 'Infectivity studies of influenza virus hemagglutinin receptor binding site mutants in mice', *J Virol*, 82: 5079-83.

Memoli, M. J., P. A. Shaw, A. Han, L. Czajkowski, S. Reed, R. Athota, T. Bristol, S. Fargis, K. Risos, J. H. Powers, R. T. Davey, Jr., and J. K. Taubenberger. 2016. 'Evaluation of Antihemagglutinin and Antineuraminidase Antibodies as Correlates of Protection in an Influenza A/H1N1 Virus Healthy Human Challenge Model', *MBio*, 7: e00417-16.

Miller, C. R., E. L. Johnson, A. Z. Burke, K. P. Martin, T. A. Miura, H. A. Wichman, C. J. Brown, and F. M. Ytreberg. 2016. 'Initiating a watch list for Ebola virus antibody escape mutations', *PeerJ*, 4: e1674.

Miller, M. S., T. J. Gardner, F. Krammer, L. C. Aguado, D. Tortorella, C. F. Basler, and P. Palese. 2013. 'Neutralizing antibodies against previously encountered influenza

virus strains increase over time: a longitudinal analysis', *Sci Transl Med*, 5: 198ra07.

Misasi, J., M. S. Gilman, M. Kanekiyo, M. Gui, A. Cagigi, S. Mulangu, D. Corti, J. E. Ledgerwood, A. Lanzavecchia, J. Cunningham, J. J. Muyembe-Tamfun, U. Baxa, B. S. Graham, Y. Xiang, N. J. Sullivan, and J. S. McLellan. 2016. 'Structural and molecular basis for Ebola virus neutralization by protective human antibodies', *Science*, 351: 1343-6.

Mochalova, L., A. Gambaryan, J. Romanova, A. Tuzikov, A. Chinarev, D. Katinger, H. Katinger, A. Egorov, and N. Bovin. 2003. 'Receptor-binding properties of modern human influenza viruses primarily isolated in Vero and MDCK cells and chicken embryonated eggs', *Virology*, 313: 473-80.

Mohan, G. S., L. Ye, W. Li, A. Monteiro, X. Lin, B. Sapkota, B. P. Pollack, R. W. Compans, and C. Yang. 2015. 'Less is more: Ebola virus surface glycoprotein expression levels regulate virus production and infectivity', *J Virol*, 89: 1205-17.

Moller-Tank, S., A. S. Kondratowicz, R. A. Davey, P. D. Rennert, and W. Maury. 2013. 'Role of the phosphatidylserine receptor TIM-1 in enveloped-virus entry', *J Virol*, 87: 8327-41.

Moller-Tank, S., and W. Maury. 2014. 'Phosphatidylserine receptors: enhancers of enveloped virus entry and infection', *Virology*, 468-470: 565-80.

Moller-Tank, S.; Maury, W. 2015. 'Ebola virus entry: a curious and complex series of events', *PLoS Pathog*, 11: e1004731.

Monto, A. S., J. G. Petrie, R. T. Cross, E. Johnson, M. Liu, W. Zhong, M. Levine, J. M. Katz, and S. E. Ohmit. 2015. 'Antibody to Influenza Virus Neuraminidase: An Independent Correlate of Protection', *J Infect Dis*, 212: 1191-9.

Morens, D. M., D. S. Burke, and S. B. Halstead. 2010. 'The wages of original antigenic sin', *Emerg Infect Dis*, 16: 1023-4.

Morgan, S. B., J. D. Hemmink, E. Porter, R. Harley, H. Shelton, M. Aramouni, H. E. Everett, S. M. Brookes, M. Bailey, A. M. Townsend, B. Charleston, and E. Tchilian. 2016. 'Aerosol Delivery of a Candidate Universal Influenza Vaccine Reduces Viral Load in Pigs Challenged with Pandemic H1N1 Virus', *J Immunol*, 196: 5014-23.

Morita, M., T. Suto, and N. Ishida. 1972. 'Antigenic memory in man in response to sequential infections with influenza A viruses', *J Infect Dis*, 126: 61-8.

Moscona, A. 2005. 'Neuraminidase inhibitors for influenza', *N Engl J Med*, 353: 1363-73.

Moss, C. X., T. I. Tree, and C. Watts. 2007. 'Reconstruction of a pathway of antigen processing and class II MHC peptide capture', *EMBO J*, 26: 2137-47.

Mullarkey, C. E., M. J. Bailey, D. A. Golubeva, G. S. Tan, R. Nachbagauer, W. He, K. E. Novakowski, D. M. Bowdish, M. S. Miller, and P. Palese. 2016. 'Broadly Neutralizing Hemagglutinin Stalk-Specific Antibodies Induce Potent Phagocytosis of Immune Complexes by Neutrophils in an Fc-Dependent Manner', *MBio*, 7.

Murin, C. D., M. L. Fusco, Z. A. Bornholdt, X. Qiu, G. G. Olinger, L. Zeitlin, G. P. Kobinger, A. B. Ward, and E. O. Saphire. 2014. 'Structures of protective antibodies reveal sites of vulnerability on Ebola virus', *Proc Natl Acad Sci U S A*, 111: 17182-7.

Murphy, B. R., J. A. Kasel, and R. M. Chanock. 1972. 'Association of serum anti-neuraminidase antibody with resistance to influenza in man', *N Engl J Med*, 286: 1329-32.

Murphy, Frederick A. 1976. "Electron micrograph of Ebola virus Zaire." In.: CDC.

Murphy, Kenneth. 2011. *Janeway's Immunobiology*.

Natali, A., J. S. Oxford, and G. C. Schild. 1981. 'Frequency of naturally occurring antibody to influenza virus antigenic variants selected in vitro with monoclonal antibody', *J Hyg (Lond)*, 87: 185-90.

Ndifon, W. 2015. 'A simple mechanistic explanation for original antigenic sin and its alleviation by adjuvants', *Journal of the Royal Society Interface*, 12.

Neher, R. A., and T. Bedford. 2015. 'nextflu: real-time tracking of seasonal influenza virus evolution in humans', *Bioinformatics*, 31: 3546-8.

Neher, R. A., T. Bedford, R. S. Daniels, C. A. Russell, and B. I. Shraiman. 2016. 'Prediction, dynamics, and visualization of antigenic phenotypes of seasonal influenza viruses', *Proc Natl Acad Sci U S A*, 113: E1701-9.

Neumann, G., and Y. Kawaoka. 2015. 'Transmission of influenza A viruses', *Virology*, 479-480: 234-46.

NIMR. 2014. 'Chapter 15 Virology', Accessed 29 December 2016. http://www.historyofnimr.org.uk/files/2014/07/chapter15.pdf.

Nobusawa, E., K. Omagari, S. Nakajima, and K. Nakajima. 2012. 'Reactivity of human convalescent sera with influenza virus hemagglutinin protein mutants at antigenic site A', *Microbiology and Immunology*, 56: 99-106.

Nogales, A., and L. Martinez-Sobrido. 2016. 'Reverse Genetics Approaches for the Development of Influenza Vaccines', *Int J Mol Sci*, 18.

Oh, D. Y., I. G. Barr, J. A. Mosse, and K. L. Laurie. 2008. 'MDCK-SIAT1 cells show improved isolation rates for recent human influenza viruses compared to conventional MDCK cells', *J Clin Microbiol*, 46: 2189-94.

Ohmit, S. E., M. G. Thompson, J. G. Petrie, S. N. Thaker, M. L. Jackson, E. A. Belongia, R. K. Zimmerman, M. Gaglani, L. Lamerato, S. M. Spencer, L. Jackson, J. K. Meece, M. P. Nowalk, J. Song, M. Zervos, P. Y. Cheng, C. R. Rinaldo, L. Clipper, D. K. Shay, P. Piedra, and A. S. Monto. 2014. 'Influenza vaccine effectiveness in the 2011-2012 season: protection against each circulating virus and the effect of prior vaccination on estimates', *Clin Infect Dis*, 58: 319-27.

Okuno, Y., Y. Isegawa, F. Sasao, and S. Ueda. 1993. 'A common neutralizing epitope conserved between the hemagglutinins of influenza A virus H1 and H2 strains', *J Virol*, 67: 2552-8.

Oswald, W. B., T. W. Geisbert, K. J. Davis, J. B. Geisbert, N. J. Sullivan, P. B. Jahrling, P. W. Parren, and D. R. Burton. 2007. 'Neutralizing antibody fails to impact the course of Ebola virus infection in monkeys', *PLoS Pathog*, 3: e9.

Palache, A., V. Oriol-Mathieu, M. Fino, M. Xydia-Charmanta, and force Influenza Vaccine Supply task. 2015. 'Seasonal influenza vaccine dose distribution in 195 countries (2004-2013): Little progress in estimated global vaccination coverage', *Vaccine*, 33: 5598-605.

Palese P., Shaw M.L. 2013. "Orthomyxoviridae: The Viruses and Their Replication." In *Fields Virology*, edited by Bernard N. Fields, David M. Knipe, Peter M. Howley and Ovid Technologies Inc., 1 online resource (2664 p.). Philadelphia: Wolters Kluwer/Lippincott Williams & Wilkins Health,.

Pappas, L., M. Foglierini, L. Piccoli, N. L. Kallewaard, F. Turrini, C. Silacci, B. Fernandez-Rodriguez, G. Agatic, I. Giacchetto-Sasselli, G. Pellicciotta, F. Sallusto, Q. Zhu, E. Vicenzi, D. Corti, and A. Lanzavecchia. 2014. 'Rapid development of broadly influenza neutralizing antibodies through redundant mutations', *Nature*, 516: 418-22.

Parameswaran, P., Y. Liu, K. M. Roskin, K. K. Jackson, V. P. Dixit, J. Y. Lee, K. L. Artiles, S. Zompi, M. J. Vargas, B. B. Simen, B. Hanczaruk, K. R. McGowan, M. A. Tariq, N. Pourmand, D. Koller, A. Balmaseda, S. D. Boyd, E. Harris, and A. Z.

Fire. 2013. 'Convergent antibody signatures in human dengue', *Cell Host Microbe*, 13: 691-700.
Park, M. S., J. I. Kim, S. Park, I. Lee, and M. S. Park. 2016. 'Original Antigenic Sin Response to RNA Viruses and Antiviral Immunity', *Immune Netw*, 16: 261-70.
Parren, P. W., T. W. Geisbert, T. Maruyama, P. B. Jahrling, and D. R. Burton. 2002. 'Pre- and postexposure prophylaxis of Ebola virus infection in an animal model by passive transfer of a neutralizing human antibody', *J Virol*, 76: 6408-12.
Patera, A. C., C. M. Graham, D. B. Thomas, and C. A. Smith. 1995. 'Immunodominance with progenitor B cell diversity in the neutralizing antibody repertoire to influenza infection', *Eur J Immunol*, 25: 1803-9.
Pavri, R., and M. C. Nussenzweig. 2011. 'AID targeting in antibody diversity', *Adv Immunol*, 110: 1-26.
Pettitt, J., L. Zeitlin, D. H. Kim, C. Working, J. C. Johnson, O. Bohorov, B. Bratcher, E. Hiatt, S. D. Hume, A. K. Johnson, J. Morton, M. H. Pauly, K. J. Whaley, M. F. Ingram, A. Zovanyi, M. Heinrich, A. Piper, J. Zelko, and G. G. Olinger. 2013. 'Therapeutic intervention of Ebola virus infection in rhesus macaques with the MB-003 monoclonal antibody cocktail', *Sci Transl Med*, 5: 199ra13.
Popova, L., K. Smith, A. H. West, P. C. Wilson, J. A. James, L. F. Thompson, and G. M. Air. 2012. 'Immunodominance of antigenic site B over site A of hemagglutinin of recent H3N2 influenza viruses', *PLoS One*, 7: e41895.
Powell, T. J., J. D. Silk, J. Sharps, E. Fodor, and A. R. Townsend. 2012. 'Pseudotyped influenza A virus as a vaccine for the induction of heterotypic immunity', *J Virol*, 86: 13397-406.
Powers, D. C., and R. B. Belshe. 1994. 'Vaccine-induced antibodies to heterologous influenza A H1N1 viruses: effects of aging and "original antigenic sin"', *J Infect Dis*, 169: 1125-9.
Prevail Team. 2016. 'A Randomized, Controlled Trial of ZMapp for Ebola Virus Infection', *N Engl J Med*, 375: 1448-56.
Public Health England. 2013. 'Surveillance of influenza and other respiratory viruses, including novel respiratory viruses, in the United Kingdom: Winter 2012/13', Accessed 1 Jan 2017. https://www.gov.uk/government/uploads/system/uploads/attachment_data/file/325217/Annual_flu_report_winter_2012_to_2013.pdf.
Public Health England. 2016. 'Surveillance of influenza and other respiratory viruses in the United Kingdom: Winter 2015 to 2016', Accessed 4 Jan 2017. https://www.gov.uk/government/uploads/system/uploads/attachment_data/file/526405/Flu_Annual_Report_2015_2016.pdf.
Qiu, X., J. Audet, M. Lv, S. He, G. Wong, H. Wei, L. Luo, L. Fernando, A. Kroeker, H. Fausther Bovendo, A. Bello, F. Li, P. Ye, M. Jacobs, G. Ippolito, E. O. Saphire, S. Bi, B. Shen, G. F. Gao, L. Zeitlin, J. Feng, B. Zhang, and G. P. Kobinger. 2016. 'Two-mAb cocktail protects macaques against the Makona variant of Ebola virus', *Sci Transl Med*, 8: 329ra33.
Qiu, X., J. Audet, G. Wong, S. Pillet, A. Bello, T. Cabral, J. E. Strong, F. Plummer, C. R. Corbett, J. B. Alimonti, and G. P. Kobinger. 2012. 'Successful treatment of ebola virus-infected cynomolgus macaques with monoclonal antibodies', *Sci Transl Med*, 4: 138ra81.
Qiu, X., L. Fernando, P. L. Melito, J. Audet, H. Feldmann, G. Kobinger, J. B. Alimonti, and S. M. Jones. 2012. 'Ebola GP-specific monoclonal antibodies protect mice and guinea pigs from lethal Ebola virus infection', *PLoS Negl Trop Dis*, 6: e1575.

Qiu, X., G. Wong, J. Audet, A. Bello, L. Fernando, J. B. Alimonti, H. Fausther-Bovendo, H. Wei, J. Aviles, E. Hiatt, A. Johnson, J. Morton, K. Swope, O. Bohorov, N. Bohorova, C. Goodman, D. Kim, M. H. Pauly, J. Velasco, J. Pettitt, G. G. Olinger, K. Whaley, B. Xu, J. E. Strong, L. Zeitlin, and G. P. Kobinger. 2014. 'Reversion of advanced Ebola virus disease in nonhuman primates with ZMapp', *Nature*, 514: 47-53.

Radic, M. 2008. 'Tracking and trapping somatic mutations in Ig genes', *J Immunol*, 180: 5763-4.

Rhein, B. A., and W. J. Maury. 2015. 'Ebola virus entry into host cells: identifying therapeutic strategies', *Curr Clin Microbiol Rep*, 2: 115-24.

Richardson, E. T., J. D. Kelly, M. B. Barrie, A. W. Mesman, S. Karku, K. Quiwa, R. H. Marsh, S. Koedoyoma, F. Daboh, K. P. Barron, M. Grady, E. Tucker, K. L. Dierberg, G. W. Rutherford, M. Barry, J. H. Jones, M. B. Murray, and P. E. Farmer. 2016. 'Minimally Symptomatic Infection in an Ebola 'Hotspot': A Cross-Sectional Serosurvey', *PLoS Negl Trop Dis*, 10: e0005087.

Rockman, S., L. E. Brown, I. G. Barr, B. Gilbertson, S. Lowther, A. Kachurin, O. Kachurina, J. Klippel, J. Bodle, M. Pearse, and D. Middleton. 2013. 'Neuraminidase-inhibiting antibody is a correlate of cross-protection against lethal H5N1 influenza virus in ferrets immunized with seasonal influenza vaccine', *J Virol*, 87: 3053-61.

Rowe, T., R. A. Abernathy, J. Hu-Primmer, W. W. Thompson, X. Lu, W. Lim, K. Fukuda, N. J. Cox, and J. M. Katz. 1999. 'Detection of antibody to avian influenza A (H5N1) virus in human serum by using a combination of serologic assays', *J Clin Microbiol*, 37: 937-43.

Russell, R. J., L. F. Haire, D. J. Stevens, P. J. Collins, Y. P. Lin, G. M. Blackburn, A. J. Hay, S. J. Gamblin, and J. J. Skehel. 2006. 'The structure of H5N1 avian influenza neuraminidase suggests new opportunities for drug design', *Nature*, 443: 45-9.

Russell, R. J., P. S. Kerry, D. J. Stevens, D. A. Steinhauer, S. R. Martin, S. J. Gamblin, and J. J. Skehel. 2008. 'Structure of influenza hemagglutinin in complex with an inhibitor of membrane fusion', *Proc Natl Acad Sci U S A*, 105: 17736-41.

Saeed, M. F., A. A. Kolokoltsov, T. Albrecht, and R. A. Davey. 2010. 'Cellular entry of ebola virus involves uptake by a macropinocytosis-like mechanism and subsequent trafficking through early and late endosomes', *PLoS Pathog*, 6: e1001110.

Sandbulte, M. R., G. S. Jimenez, A. C. Boon, L. R. Smith, J. J. Treanor, and R. J. Webby. 2007. 'Cross-reactive neuraminidase antibodies afford partial protection against H5N1 in mice and are present in unexposed humans', *PLoS Med*, 4: e59.

Sandbulte, Matthew R., Jin Gao, Timothy M. Straight, and Maryna C. Eichelberger. 2009. 'A miniaturized assay for influenza neuraminidase-inhibiting antibodies utilizing reverse genetics-derived antigens', *Influenza and Other Respiratory Viruses*, 3: 233-40.

Sanjuan, R., M. R. Nebot, N. Chirico, L. M. Mansky, and R. Belshaw. 2010. 'Viral mutation rates', *J Virol*, 84: 9733-48.

Saphire, E. O., and M. J. Aman. 2016. 'Feverish Quest for Ebola Immunotherapy: Straight or Cocktail?', *Trends Microbiol*, 24: 684-6.

Sato, K., T. Morishita, E. Nobusawa, K. Tonegawa, K. Sakae, S. Nakajima, and K. Nakajima. 2004. 'Amino-acid change on the antigenic region B1 of H3 haemagglutinin may be a trigger for the emergence of drift strain of influenza A virus', *Epidemiol Infect*, 132: 399-406.

Schild, G. C. 1969. 'Antibody against influenza A2 virus neuraminidase in human sera', *J Hyg (Lond)*, 67: 353-65.
Schmaljohn, A., and G. K. Lewis. 2016. 'Cell-targeting antibodies in immunity to Ebola', *Pathog Dis*, 74: ftw021.
Schmidt, A. G., M. D. Therkelsen, S. Stewart, T. B. Kepler, H. X. Liao, M. A. Moody, B. F. Haynes, and S. C. Harrison. 2015. 'Viral receptor-binding site antibodies with diverse germline origins', *Cell*, 161: 1026-34.
Schulman, J. L., M. Khakpour, and E. D. Kilbourne. 1968. 'Protective effects of specific immunity to viral neuraminidase on influenza virus infection of mice', *J Virol*, 2: 778-86.
Shedlock, D. J., M. A. Bailey, P. M. Popernack, J. M. Cunningham, D. R. Burton, and N. J. Sullivan. 2010. 'Antibody-mediated neutralization of Ebola virus can occur by two distinct mechanisms', *Virology*, 401: 228-35.
Shirai, M., T. Arichi, M. Chen, T. Masaki, M. Nishioka, K. Ikeda, H. Takahashi, N. Enomoto, T. Saito, M. E. Major, T. Nakazawa, T. Akatsuka, S. M. Feinstone, and J. A. Berzofsky. 1999. 'T cell recognition of hypervariable region-1 from hepatitis C virus envelope protein with multiple class II MHC molecules in mice and humans: preferential help for induction of antibodies to the hypervariable region', *J Immunol*, 162: 568-76.
Shoji, Yoko, Jessica A. Chichester, Gene A. Palmer, Christine E. Farrance, Robert Stevens, Michelle Stewart, Lauren Goldschmidt, Varough Deyde, Larisa Gubareva, Alexander Klimov, Vadim Mett, and Vidadi Yusibov. 2014. 'An influenza N1 neuraminidase-specific monoclonal antibody with broad neuraminidase inhibition activity against H5N1 HPAI viruses', *Human Vaccines*, 7: 199-204.
Shope, R. E. 1931. 'The Etiology of Swine Influenza', *Science*, 73: 214-5.
Shtyrya, Y. A., L. V. Mochalova, and N. V. Bovin. 2009. 'Influenza virus neuraminidase: structure and function', *Acta Naturae*, 1: 26-32.
Si, L., H. Xu, X. Zhou, Z. Zhang, Z. Tian, Y. Wang, Y. Wu, B. Zhang, Z. Niu, C. Zhang, G. Fu, S. Xiao, Q. Xia, L. Zhang, and D. Zhou. 2016. 'Generation of influenza A viruses as live but replication-incompetent virus vaccines', *Science*, 354: 1170-73.
Skehel, J. J., D. J. Stevens, R. S. Daniels, A. R. Douglas, M. Knossow, I. A. Wilson, and D. C. Wiley. 1984. 'A carbohydrate side chain on hemagglutinins of Hong Kong influenza viruses inhibits recognition by a monoclonal antibody', *Proc Natl Acad Sci U S A*, 81: 1779-83.
Skehel, J. J., and D. C. Wiley. 2000. 'Receptor binding and membrane fusion in virus entry: the influenza hemagglutinin', *Annu Rev Biochem*, 69: 531-69.
Skountzou, I., D. G. Koutsonanos, J. H. Kim, R. Powers, L. Satyabhama, F. Masseoud, W. C. Weldon, P. Martin Mdel, R. S. Mittler, R. Compans, and J. Jacob. 2010. 'Immunity to pre-1950 H1N1 influenza viruses confers cross-protection against the pandemic swine-origin 2009 A (H1N1) influenza virus', *J Immunol*, 185: 1642-9.
Skowronski, D., C. Chambers, S. Sabaiduc, G. De Serres, J. Dickinson, A. Winter, K. Fonseca, J. Gubbay, H. Charest, M. Petric, M. Krajden, S. Mahmud, P. Van Caeseele, T. Kwindt, A. Eshaghi, N. Bastien, and Y. Li. 2014. 'Interim estimates of 2013/14 vaccine effectiveness against influenza A(H1N1)pdm09 from Canada s sentinel surveillance network, January 2014', *Euro Surveill*, 19.
Skowronski, D. M., N. Z. Janjua, G. De Serres, S. Sabaiduc, A. Eshaghi, J. A. Dickinson, K. Fonseca, A. L. Winter, J. B. Gubbay, M. Krajden, M. Petric, H. Charest, N. Bastien, T. L. Kwindt, S. M. Mahmud, P. Van Caeseele, and Y. Li. 2014. 'Low

2012-13 influenza vaccine effectiveness associated with mutation in the egg-adapted H3N2 vaccine strain not antigenic drift in circulating viruses', *PLoS One*, 9: e92153.

Smith, K., L. Garman, J. Wrammert, N. Y. Zheng, J. D. Capra, R. Ahmed, and P. C. Wilson. 2009. 'Rapid generation of fully human monoclonal antibodies specific to a vaccinating antigen', *Nat Protoc*, 4: 372-84.

Smith W, Andrewes CH, Laidlaw PP. 1933. ' A virus obtained from influenza patients', *Lancet*, 222: 66-68.

Sok, D., B. Moldt, and D. R. Burton. 2013. 'SnapShot: broadly neutralizing antibodies', *Cell*, 155: 728-28 e1.

Sow, M. S., J. F. Etard, S. Baize, N. Magassouba, O. Faye, P. Msellati, A. I. Toure, I. Savane, M. Barry, E. Delaporte, and Group Postebogui Study. 2016. 'New Evidence of Long-lasting Persistence of Ebola Virus Genetic Material in Semen of Survivors', *J Infect Dis*.

Sridhar, S., S. Begom, A. Bermingham, K. Hoschler, W. Adamson, W. Carman, T. Bean, W. Barclay, J. J. Deeks, and A. Lalvani. 2013. 'Cellular immune correlates of protection against symptomatic pandemic influenza', *Nat Med*, 19: 1305-12.

Srivastava, B., P. Blazejewska, M. Hessmann, D. Bruder, R. Geffers, S. Mauel, A. D. Gruber, and K. Schughart. 2009. 'Host genetic background strongly influences the response to influenza a virus infections', *PLoS One*, 4: e4857.

Staudt, L. M., and W. Gerhard. 1983. 'Generation of antibody diversity in the immune response of BALB/c mice to influenza virus hemagglutinin. I. Significant variation in repertoire expression between individual mice', *J Exp Med*, 157: 687-704.

Su, Y. C., J. Bahl, U. Joseph, K. M. Butt, H. A. Peck, E. S. Koay, L. L. Oon, I. G. Barr, D. Vijaykrishna, and G. J. Smith. 2015. 'Phylodynamics of H1N1/2009 influenza reveals the transition from host adaptation to immune-driven selection', *Nat Commun*, 6: 7952.

Sui, J., W. C. Hwang, S. Perez, G. Wei, D. Aird, L. M. Chen, E. Santelli, B. Stec, G. Cadwell, M. Ali, H. Wan, A. Murakami, A. Yammanuru, T. Han, N. J. Cox, L. A. Bankston, R. O. Donis, R. C. Liddington, and W. A. Marasco. 2009. 'Structural and functional bases for broad-spectrum neutralization of avian and human influenza A viruses', *Nat Struct Mol Biol*, 16: 265-73.

Sullivan, N. J., M. Peterson, Z. Y. Yang, W. P. Kong, H. Duckers, E. Nabel, and G. J. Nabel. 2005. 'Ebola virus glycoprotein toxicity is mediated by a dynamin-dependent protein-trafficking pathway', *J Virol*, 79: 547-53.

Takada, A., H. Ebihara, S. Jones, H. Feldmann, and Y. Kawaoka. 2007. 'Protective efficacy of neutralizing antibodies against Ebola virus infection', *Vaccine*, 25: 993-9.

Tapia, M. D., S. O. Sow, K. E. Lyke, F. C. Haidara, F. Diallo, M. Doumbia, A. Traore, F. Coulibaly, M. Kodio, U. Onwuchekwa, M. B. Sztein, R. Wahid, J. D. Campbell, M. P. Kieny, V. Moorthy, E. B. Imoukhuede, T. Rampling, F. Roman, I. De Ryck, A. R. Bellamy, L. Dally, O. T. Mbaya, A. Ploquin, Y. Zhou, D. A. Stanley, R. Bailer, R. A. Koup, M. Roederer, J. Ledgerwood, A. V. Hill, W. R. Ballou, N. Sullivan, B. Graham, and M. M. Levine. 2016. 'Use of ChAd3-EBO-Z Ebola virus vaccine in Malian and US adults, and boosting of Malian adults with MVA-BN-Filo: a phase 1, single-blind, randomised trial, a phase 1b, open-label and double-blind, dose-escalation trial, and a nested, randomised, double-blind, placebo-controlled trial', *Lancet Infect Dis*, 16: 31-42.

Taubenberger, J. K., and D. M. Morens. 2006. '1918 Influenza: the mother of all pandemics', *Emerg Infect Dis*, 12: 15-22.

Terajima, M., J. Cruz, M. D. Co, J. H. Lee, K. Kaur, J. Wrammert, P. C. Wilson, and F. A. Ennis. 2011. 'Complement-dependent lysis of influenza a virus-infected cells by broadly cross-reactive human monoclonal antibodies', *J Virol*, 85: 13463-7.

The Crick Worldwide Influenza Centre. 2015. 'Report prepared for the WHO annual consultation on the composition of influenza vaccine for the Southern Hemisphere 2016 21st – 23rd September 2015 ', The Francis Crick Institute. https://www.crick.ac.uk/media/273950/crick_sep2015_vcm_report_to_post.pdf.

The Crick Worldwide Influenza Centre. 2016. 'Report prepared for the WHO annual consultation on the composition of influenza vaccine for the Southern Hemisphere 2017 26th – 28th September 2016', The Francis Crick Institute. https://www.crick.ac.uk/media/326439/september_2016_interim_report.pdf.

Thomson, C. A., Y. Wang, L. M. Jackson, M. Olson, W. Wang, A. Liavonchanka, L. Keleta, V. Silva, S. Diederich, R. B. Jones, J. Gubbay, J. Pasick, M. Petric, F. Jean, V. G. Allen, E. G. Brown, J. M. Rini, and J. W. Schrader. 2012. 'Pandemic H1N1 Influenza Infection and Vaccination in Humans Induces Cross-Protective Antibodies that Target the Hemagglutinin Stem', *Front Immunol*, 3: 87.

Thornburg, N. J., H. Zhang, S. Bangaru, G. Sapparapu, N. Kose, R. M. Lampley, R. G. Bombardi, Y. Yu, S. Graham, A. Branchizio, S. M. Yoder, M. T. Rock, C. B. Creech, K. M. Edwards, D. Lee, S. Li, I. A. Wilson, A. Garcia-Sastre, R. A. Albrecht, and J. E. Crowe, Jr. 2016. 'H7N9 influenza virus neutralizing antibodies that possess few somatic mutations', *J Clin Invest*, 126: 1482-94.

Townsend, A., and H. Bodmer. 1989. 'Antigen recognition by class I-restricted T lymphocytes', *Annu Rev Immunol*, 7: 601-24.

Townsend, A. R., F. M. Gotch, and J. Davey. 1985. 'Cytotoxic T cells recognize fragments of the influenza nucleoprotein', *Cell*, 42: 457-67.

Townsend, A. R., and A. J. McMichael. 1985. 'Specificity of cytotoxic T lymphocytes stimulated with influenza virus. Studies in mice and humans', *Prog Allergy*, 36: 10-43.

Tran, E. E., E. A. Nelson, P. Bonagiri, J. A. Simmons, C. J. Shoemaker, C. S. Schmaljohn, G. P. Kobinger, L. Zeitlin, S. Subramaniam, and J. M. White. 2016. 'Mapping of Ebolavirus Neutralization by Monoclonal Antibodies in the ZMapp Cocktail Using Cryo-Electron Tomography and Studies of Cellular Entry', *J Virol*, 90: 7618-27.

Tulip, W. R., J. N. Varghese, A. T. Baker, A. van Donkelaar, W. G. Laver, R. G. Webster, and P. M. Colman. 1991. 'Refined atomic structures of N9 subtype influenza virus neuraminidase and escape mutants', *J Mol Biol*, 221: 487-97.

Tulip, W. R., J. N. Varghese, W. G. Laver, R. G. Webster, and P. M. Colman. 1992. 'Refined crystal structure of the influenza virus N9 neuraminidase-NC41 Fab complex', *J Mol Biol*, 227: 122-48.

Urbanowicz, R. A., C. P. McClure, A. Sakuntabhai, A. A. Sall, G. Kobinger, M. A. Muller, E. C. Holmes, F. A. Rey, E. Simon-Loriere, and J. K. Ball. 2016. 'Human Adaptation of Ebola Virus during the West African Outbreak', *Cell*, 167: 1079-87 e5.

Varghese, J. N., P. M. Colman, A. van Donkelaar, T. J. Blick, A. Sahasrabudhe, and J. L. McKimm-Breschkin. 1997. 'Structural evidence for a second sialic acid binding site in avian influenza virus neuraminidases', *Proc Natl Acad Sci U S A*, 94: 11808-12.

Varghese, J. N., R. G. Webster, W. G. Laver, and P. M. Colman. 1988. 'Structure of an escape mutant of glycoprotein N2 neuraminidase of influenza virus A/Tokyo/3/67 at 3 A', *J Mol Biol*, 200: 201-3.

Venkatramani, L., E. Bochkareva, J. T. Lee, U. Gulati, W. Graeme Laver, A. Bochkarev, and G. M. Air. 2006. 'An epidemiologically significant epitope of a 1998 human influenza virus neuraminidase forms a highly hydrated interface in the NA-antibody complex', *J Mol Biol*, 356: 651-63.

Victora, G. D., and M. C. Nussenzweig. 2012. 'Germinal centers', *Annu Rev Immunol*, 30: 429-57.

Victora, G. D., and P. C. Wilson. 2015. 'Germinal center selection and the antibody response to influenza', *Cell*, 163: 545-8.

Volchkova, V. A., H. Feldmann, H. D. Klenk, and V. E. Volchkov. 1998. 'The nonstructural small glycoprotein sGP of Ebola virus is secreted as an antiparallel-orientated homodimer', *Virology*, 250: 408-14.

Wan, H., J. Gao, K. Xu, H. Chen, L. K. Couzens, K. H. Rivers, J. D. Easterbrook, K. Yang, L. Zhong, M. Rajabi, J. Ye, I. Sultana, X. F. Wan, X. Liu, D. R. Perez, J. K. Taubenberger, and M. C. Eichelberger. 2013. 'Molecular basis for broad neuraminidase immunity: conserved epitopes in seasonal and pandemic H1N1 as well as H5N1 influenza viruses', *J Virol*, 87: 9290-300.

Wan, H., H. Yang, D. A. Shore, R. J. Garten, L. Couzens, J. Gao, L. Jiang, P. J. Carney, J. Villanueva, J. Stevens, and M. C. Eichelberger. 2015. 'Structural characterization of a protective epitope spanning A(H1N1)pdm09 influenza virus neuraminidase monomers', *Nat Commun*, 6: 6114.

Wang, M. L., J. J. Skehel, and D. C. Wiley. 1986. 'Comparative analyses of the specificities of anti-influenza hemagglutinin antibodies in human sera', *J Virol*, 57: 124-8.

Wang, M., J. Qi, Y. Liu, C. J. Vavricka, Y. Wu, Q. Li, and G. F. Gao. 2011. 'Influenza A virus N5 neuraminidase has an extended 150-cavity', *J Virol*, 85: 8431-5.

Wang, W., J. A. Castelan-Vega, A. Jimenez-Alberto, R. Vassell, Z. Ye, and C. D. Weiss. 2010. 'A mutation in the receptor binding site enhances infectivity of 2009 H1N1 influenza hemagglutinin pseudotypes without changing antigenicity', *Virology*, 407: 374-80.

Watanabe, S., T. Watanabe, T. Noda, A. Takada, H. Feldmann, L. D. Jasenosky, and Y. Kawaoka. 2004. 'Production of novel ebola virus-like particles from cDNAs: an alternative to ebola virus generation by reverse genetics', *J Virol*, 78: 999-1005.

Watts, C., A. Antoniou, B. Manoury, E. W. Hewitt, L. M. McKay, L. Grayson, N. F. Fairweather, P. Emsley, N. Isaacs, and P. D. Simitsek. 1998. 'Modulation by epitope-specific antibodies of class II MHC-restricted presentation of the tetanus toxin antigen', *Immunol Rev*, 164: 11-6.

Webster, R. G., G. M. Air, D. W. Metzger, P. M. Colman, J. N. Varghese, A. T. Baker, and W. G. Laver. 1987. 'Antigenic structure and variation in an influenza virus N9 neuraminidase', *J Virol*, 61: 2910-6.

Webster, R. G., V. S. Hinshaw, and W. G. Laver. 1982. 'Selection and analysis of antigenic variants of the neuraminidase of N2 influenza viruses with monoclonal antibodies', *Virology*, 117: 93-104.

Webster, R. G., J. A. Kasel, R. B. Couch, and W. G. Laver. 1976. 'Influenza virus subunit vaccines. II. Immunogenicity and original antigenic sin in humans', *J Infect Dis*, 134: 48-58.

Webster, R. G., and W. G. Laver. 1980. 'Determination of the number of nonoverlapping antigenic areas on Hong Kong (H3N2) influenza virus hemagglutinin with

monoclonal antibodies and the selection of variants with potential epidemiological significance', *Virology*, 104: 139-48.
Webster, R. G., W. G. Laver, G. M. Air, and G. C. Schild. 1982. 'Molecular mechanisms of variation in influenza viruses', *Nature*, 296: 115-21.
Webster, R. G., W. G. Laver, G. M. Air, C. Ward, W. Gerhard, and K. L. van Wyke. 1980. 'The mechanism of antigenic drift in influenza viruses: analysis of Hong Kong (H3N2) variants with monoclonal antibodies to the hemagglutinin molecule', *Ann N Y Acad Sci*, 354: 142-61.
WHO. 1980. *A revised system for nomenclature of influenza viruses*.
WHO. 2012. 'Fact Sheets', Accessed November. http://www.who.int/mediacentre/factsheets/fs211/en/index.html.
WHO 2016. 'Ebola virus disease - Factsheet', WHO. http://www.who.int/mediacentre/factsheets/fs103/en/.
Wiley, D. C., I. A. Wilson, and J. J. Skehel. 1981. 'Structural identification of the antibody-binding sites of Hong Kong influenza haemagglutinin and their involvement in antigenic variation', *Nature*, 289: 373-8.
Wilkinson, T. M., C. K. Li, C. S. Chui, A. K. Huang, M. Perkins, J. C. Liebner, R. Lambkin-Williams, A. Gilbert, J. Oxford, B. Nicholas, K. J. Staples, T. Dong, D. C. Douek, A. J. McMichael, and X. N. Xu. 2012. 'Preexisting influenza-specific CD4+ T cells correlate with disease protection against influenza challenge in humans', *Nat Med*, 18: 274-80.
Wilson, I. A., J. J. Skehel, and D. C. Wiley. 1981. 'Structure of the haemagglutinin membrane glycoprotein of influenza virus at 3 A resolution', *Nature*, 289: 366-73.
Wilson, J. A., M. Hevey, R. Bakken, S. Guest, M. Bray, A. L. Schmaljohn, and M. K. Hart. 2000. 'Epitopes involved in antibody-mediated protection from Ebola virus', *Science*, 287: 1664-6.
Wool-Lewis, R. J., and P. Bates. 1998. 'Characterization of Ebola virus entry by using pseudotyped viruses: identification of receptor-deficient cell lines', *J Virol*, 72: 3155-60.
Wrammert, J., D. Koutsonanos, G. M. Li, S. Edupuganti, J. Sui, M. Morrissey, M. McCausland, I. Skountzou, M. Hornig, W. I. Lipkin, A. Mehta, B. Razavi, C. Del Rio, N. Y. Zheng, J. H. Lee, M. Huang, Z. Ali, K. Kaur, S. Andrews, R. R. Amara, Y. Wang, S. R. Das, C. D. O'Donnell, J. W. Yewdell, K. Subbarao, W. A. Marasco, M. J. Mulligan, R. Compans, R. Ahmed, and P. C. Wilson. 2011. 'Broadly cross-reactive antibodies dominate the human B cell response against 2009 pandemic H1N1 influenza virus infection', *J Exp Med*, 208: 181-93.
Wrammert, J., K. Smith, J. Miller, W. A. Langley, K. Kokko, C. Larsen, N. Y. Zheng, I. Mays, L. Garman, C. Helms, J. James, G. M. Air, J. D. Capra, R. Ahmed, and P. C. Wilson. 2008. 'Rapid cloning of high-affinity human monoclonal antibodies against influenza virus', *Nature*, 453: 667-71.
Wu, Y., M. Cho, D. Shore, M. Song, J. Choi, T. Jiang, Y. Q. Deng, M. Bourgeois, L. Almli, H. Yang, L. M. Chen, Y. Shi, J. Qi, A. Li, K. S. Yi, M. Chang, J. S. Bae, H. Lee, J. Shin, J. Stevens, S. Hong, C. F. Qin, G. F. Gao, S. J. Chang, and R. O. Donis. 2015. 'A potent broad-spectrum protective human monoclonal antibody crosslinking two haemagglutinin monomers of influenza A virus', *Nat Commun*, 6: 7708.
Wu, Y., Y. Wu, B. Tefsen, Y. Shi, and G. F. Gao. 2014. 'Bat-derived influenza-like viruses H17N10 and H18N11', *Trends Microbiol*, 22: 183-91.
Xie, H., X. F. Wan, Z. Ye, E. P. Plant, Y. Zhao, Y. Xu, X. Li, C. Finch, N. Zhao, T. Kawano, O. Zoueva, M. J. Chiang, X. Jing, Z. Lin, A. Zhang, and Y. Zhu. 2015.

'H3N2 Mismatch of 2014-15 Northern Hemisphere Influenza Vaccines and Head-to-head Comparison between Human and Ferret Antisera derived Antigenic Maps', *Sci Rep*, 5: 15279.

Xu, R., D. C. Ekiert, J. C. Krause, R. Hai, J. E. Crowe, Jr., and I. A. Wilson. 2010. 'Structural basis of preexisting immunity to the 2009 H1N1 pandemic influenza virus', *Science*, 328: 357-60.

Ye, L., J. Lin, Y. Sun, S. Bennouna, M. Lo, Q. Wu, Z. Bu, B. Pulendran, R. W. Compans, and C. Yang. 2006. 'Ebola virus-like particles produced in insect cells exhibit dendritic cell stimulating activity and induce neutralizing antibodies', *Virology*, 351: 260-70.

Yen, H. L., E. Hoffmann, G. Taylor, C. Scholtissek, A. S. Monto, R. G. Webster, and E. A. Govorkova. 2006. 'Importance of neuraminidase active-site residues to the neuraminidase inhibitor resistance of influenza viruses', *J Virol*, 80: 8787-95.

Yewdell, J. W., A. J. Caton, and W. Gerhard. 1986. 'Selection of influenza A virus adsorptive mutants by growth in the presence of a mixture of monoclonal antihemagglutinin antibodies', *J Virol*, 57: 623-8.

Yewdell, J. W., and W. Gerhard. 1981. 'Antigenic characterization of viruses by monoclonal antibodies', *Annu Rev Microbiol*, 35: 185-206.

Yewdell, J. W., E. Reits, and J. Neefjes. 2003. 'Making sense of mass destruction: quantitating MHC class I antigen presentation', *Nat Rev Immunol*, 3: 952-61.

Yewdell, J. W., R. G. Webster, and W. U. Gerhard. 1979. 'Antigenic variation in three distinct determinants of an influenza type A haemagglutinin molecule', *Nature*, 279: 246-8.

Yonezawa, A., M. Cavrois, and W. C. Greene. 2005. 'Studies of ebola virus glycoprotein-mediated entry and fusion by using pseudotyped human immunodeficiency virus type 1 virions: involvement of cytoskeletal proteins and enhancement by tumor necrosis factor alpha', *J Virol*, 79: 918-26.

Zanin, M., S. Duan, S. S. Wong, G. Kumar, P. Baviskar, E. Collin, C. Russell, S. Barman, B. Hause, and R. Webby. 2016. 'An amino acid in the stalk domain of N1 neuraminidase is critical for enzymatic activity', *J Virol*.

Zeitlin, L., J. Pettitt, C. Scully, N. Bohorova, D. Kim, M. Pauly, A. Hiatt, L. Ngo, H. Steinkellner, K. J. Whaley, and G. G. Olinger. 2011. 'Enhanced potency of a fucose-free monoclonal antibody being developed as an Ebola virus immunoprotectant', *Proc Natl Acad Sci U S A*, 108: 20690-4.

Downloaded from http://www.jci.org on September 16, 2016. http://dx.doi.org/10.1172/JCI81104

Focused antibody response to influenza linked to antigenic drift

Kuan-Ying A. Huang,[1] Pramila Rijal,[2] Lisa Schimanski,[2] Timothy J. Powell,[2] Tzou-Yien Lin,[1,3] John W. McCauley,[4] Rodney S. Daniels,[4] and Alain R. Townsend[2]

[1]Division of Pediatric Infectious Diseases, Department of Pediatrics, Chang Gung Children's Hospital, Taoyuan City, Taiwan. [2]Human Immunology Unit, Weatherall Institute of Molecular Medicine, University of Oxford, John Radcliffe Hospital, Oxford, United Kingdom. [3]College of Medicine, Chang Gung University, Taoyuan City, Taiwan. [4]Crick Worldwide Influenza Centre, The Francis Crick Institute, Mill Hill Laboratory, The Ridgeway, Mill Hill, London, United Kingdom.

The selective pressure that drives antigenic changes in influenza viruses is thought to originate from the human immune response. Here, we have characterized the B cell repertoire from a previously vaccinated donor whose serum had reduced neutralizing activity against the recently evolved clade 6B H1N1pdm09 viruses. While the response was markedly polyclonal, 88% of clones failed to recognize clade 6B viruses; however, the ability to neutralize A/USSR/90/1977 influenza, to which the donor would have been exposed in childhood, was retained. In vitro selection of virus variants with representative monoclonal antibodies revealed that a single amino acid replacement at residue K163 in the Sa antigenic site, which is characteristic of the clade 6B viruses, was responsible for resistance to neutralization by multiple monoclonal antibodies and the donor serum. The K163 residue lies in a part of a conserved surface that is common to the hemagglutinins of the 1977 and 2009 H1N1 viruses. Vaccination with the 2009 hemagglutinin induced an antibody response tightly focused on this common surface that is capable of selecting current antigenic drift variants in H1N1pdm09 influenza viruses. Moreover, amino acid replacement at K163 was not highlighted by standard ferret antisera. Human monoclonal antibodies may be a useful adjunct to ferret antisera for detecting antigenic drift in influenza viruses.

Introduction

Influenza viruses circulating in humans mutate and change their antigenicity at a rate that necessitates frequent updating of subunit vaccines. This process of antigenic drift requires a global collaboration, organized through the WHO, to monitor the antigenic relatedness of new viruses and select the most appropriate for inclusion in vaccines that are updated regularly (1). The selective force driving the evolution of influenza in humans is thought to be the neutralizing antibody response. However, this raises a paradox, as the antibody response is polyclonal and in principle is capable of neutralizing the virus at multiple sites on the hemagglutinin glycoprotein (HA). As many as 12 sequential mutations in the hemagglutinin may be required to completely abrogate neutralization by a strong immune serum (2). This would require mutation at multiple positions in HA simultaneously for the virus to escape in nature, which should be a very rare event.

Two alternative mechanisms have been suggested to resolve the paradox. Adsorptive amino acid substitutions have been described that can globally reduce the neutralizing power of a serum (3). It is thought that this is mediated through the substitutions causing an increase in the binding affinity of hemagglutinin for its receptor sialic acid (4). Selection of virus variants of this type has been demonstrated in an animal model of influenza infection (4, 5) and also defined with neutralization-resistant variants selected in vitro with certain monoclonal antibodies (3, 6). However, a recent analysis of the evolution of H3N2 viruses has demonstrated that the binding affinity of H3 hemagglutinin has significantly decreased since the appearance of H3N2 viruses in humans in 1968, which suggests additional mechanisms may be at work (7).

The second possibility is that, in some humans, the antibody response can be focused on a subregion of the hemagglutinin to such an extent that it becomes functionally monoclonal and can select viruses with point mutations. Early evidence for this came from finding reduced neutralization of viruses with single-point mutations (8–12) and selective inhibition by sera of binding by characterized hemagglutinin-specific monoclonal antibody Fab fragments (13). A recent paper has identified a single amino acid substitution (K163Q in our numbering) to be responsible for reduced serologic reactivity with 2013–2014 H1N1pdm09 viruses in up to 42% of middle-aged adults born between 1965 and 1979, who would have been exposed to the H1N1 viruses that reemerged in 1977 (14).

These studies did not address the clonal basis for the focused antibody responses in humans or show that the antibodies in the sera were able to select antigenic variants of influenza viruses. We have addressed this by analysis of 157 monoclonal antibodies isolated from a donor with reduced serological reactivity to the recently evolved clade 6B H1N1pdm09 influenza viruses. We show that the response was markedly polyclonal and displayed varying cross-reactivity for recent seasonal H1N1 viruses. However, 88% of the isolated antibodies failed to recognize the clade 6B viruses, while all of these clones neutralized A/USSR/90/1977

Authorship note: Kuan-Ying A. Huang and Pramila Rijal contributed equally to this work.
Conflict of interest: The authors have declared that no conflict of interest exists.
Submitted: January 22, 2015; **Accepted:** April 16, 2015.
Reference information: *J Clin Invest*. 2015;125(7):2631–2645. doi:10.1172/JCI81104.

Downloaded from http://www.jci.org on September 16, 2016. http://dx.doi.org/10.1172/JCI81104

Table 1. Vaccination history and vaccine content

Date	Vaccine composition
November 11, 2008	A/Brisbane/59/2007 H1N1-like virus
	A/Brisbane/10/2007 H3N2-like virus
	B/Florida/4/2006-like virus
November 26, 2009	A/Brisbane/59/2007 H1N1-like virus
	A/Brisbane/10/2007 H3N2-like virus
	B/Brisbane/60/2008-like virus
November 10, 2011	A/California/07/2009 H1N1-like virus
	A/Perth/16/2009 H3N2-like virus
	B/Brisbane/60/2008-like virus

(H1N1), which circulated during the donor's childhood. Resistant viruses isolated in vitro with representative monoclonal antibodies selected amino acid substitutions at HA K163 that matched a defining substitution in the recently evolved 6B clade. Viruses with this single substitution in HA were resistant to neutralization by multiple monoclonal antibodies from the donor and the donor's serum.

Lysine 163 lies in a localized, conserved patch of surface residues in the Sa antigenic site that are common to the 1977 H1N1 viruses circulating in the donor's childhood and the H1N1pdm09 virus (15). This suggests that antibodies primed by this common patch of surface may have been selectively recalled and expanded by exposure to the H1N1pdm09 hemagglutinin to form a focused antibody response, capable of selecting antigenic variants with substitutions at K163. Our results match the focused antibody response in a subset of humans with the recent evolution of the clade 6B H1N1pdm09 influenza viruses. They also show that selection of virus variants with human monoclonal antibodies isolated from vaccinated or infected individuals may be able to predict the sites of future antigenic drift in influenza A viruses. Finally, the K163 substitutions in the clade 6B H1N1pdm09 viruses were not flagged as significant antigenic drift by standard ferret antisera. Panels of human monoclonal antibodies may be a useful adjunct to ferret antisera in detection of antigenic drift and in the selection of viruses for inclusion in influenza vaccines.

Results

Influenza virus–specific antibody response after vaccination. A healthy adult volunteer (referred to as donor H) had received trivalent inactivated influenza vaccine 3 times since 2008. The vaccines contained the antigens shown in Table 1.

Figure 1 shows the neutralization titers recovered from donor H for former seasonal H1, H3, pandemic H1N1 2009, and H5 viruses. Before the first vaccination in November 2008, plasma contained low-titer antibodies to all influenza A subtypes screened. Six months after the first dose of vaccine, a response was seen to former seasonal H1 (A/Brisbane/59/2007) and H3 (A/Victoria/361/2011) viruses that did not cross-neutralize H1N1pdm09 or H5. This pattern of reactivity was maintained 2 years after the second vaccination. The third vaccination on November 10, 2011, contained H1N1pdm09 HA for the first time. One day after the third vaccination a low-level response to H1N1pdm09 virus was detected. This may have reflected an earlier exposure or a very early response to vaccination. Twelve days after vaccination a very strong response to H1N1pdm09 influenza was detected, which was associated with a small-titer increase to H3 viruses and no change in the titer to seasonal H1. The titer to an H5-pseudotyped influenza, albeit low, was boosted by the H1pdm09 virus as compared with levels before vaccination.

This serum was next tested on a selection of the recently evolved clade 6B H1N1pdm09 viruses. We found a substantial reduction in the neutralization titer of between 4- and 8-fold on the clade 6B viruses. To analyze the clonal basis for this reduced titer, we isolated monoclonal antibodies from the donor's plasmablasts taken 7 days after vaccination.

Identification of HA-specific B cells. We have previously confirmed that influenza virus–specific plasmablasts are induced transiently in large number in the peripheral blood during the first week after vaccination with inactivated former seasonal H1N1 and H1N1pdm09 viruses and the frequency of influenza virus–specific plasmablasts significantly correlated with the level of neutralizing antibody response (16–18). At day 7 after vaccination of donor H, flow cytometry surface marker analysis revealed a distinct population of plasmablasts (defined as $CD3^-CD20^{lo}CD20^-CD19^+CD27^{hi}CD38^{hi}$ cells), which accounted for 0.9% of total peripheral lymphocytes. We next detected hemagglutinin-specific cells by ex vivo B cell ELISpot with purified hemagglutinin and measured frequencies of H1N1pdm09 (A/California/07/2009) HA-specific and Eng195 (A/England/195/2009) HA-specific IgG plasmablasts at 425 and 315 per million peripheral blood mononuclear cells.

Binding of recombinant HA to transmembrane Ig G1. In these experiments, the HA molecules did not have any mutations to abolish sialic acid binding, as described by Whittle et al. (19). In contrast to Whittle's method, in which the trimeric HA was combined in excess with streptavidin to form oligomers prior to staining, we stained sequentially with hemagglutinin followed by ExtrAvidin. For specificity this method relies on the high affinity of membrane-bound antibody for HA, compared with the low affinity of single HA trimers for sialic acid.

We first established that our preparations of recombinant soluble HA could detect specific transmembrane Ig expressed at the cell surface. As shown in Supplemental Figure 1A, row 4 (supplemental material available online with this article; doi:10.1172/JCI81104DS1), all of the cells transfected with the reconstructed transmembrane Ig G1 (TMIgG1) clones were stained with an anti-IgG reagent. The cells were then stained with biotin-labeled recombinant H3 (A/Victoria/361/2011; Supplemental Figure 1A, row 2), H1N1pdm09 (A/England/195/2009; Supplemental Figure 1A, row 1), H5 (A/Vietnam/1203/2004; Supplemental Figure 1A, row 3), and H7 (A/Anhui/1/2013; Supplemental Figure 1A, row 5) HAs. The H3 HA stained specifically the anti-H3–transfected cells (Supplemental Figure 1A, column 4); H1N1pdm09 HA stained cells expressing TMIgG1 to epitopes in the head and stem of H1 HA (Supplemental Figure 1A, columns 1–3); and the H5 protein stained only the cells expressing TMIgG1 specific for the stem of H1N1pdm09 HA (Supplemental Figure 1A, column 3) that cross-reacted with the H5 HA. The H7 HA

Downloaded from http://www.jci.org on September 16, 2016. http://dx.doi.org/10.1172/JCI81104

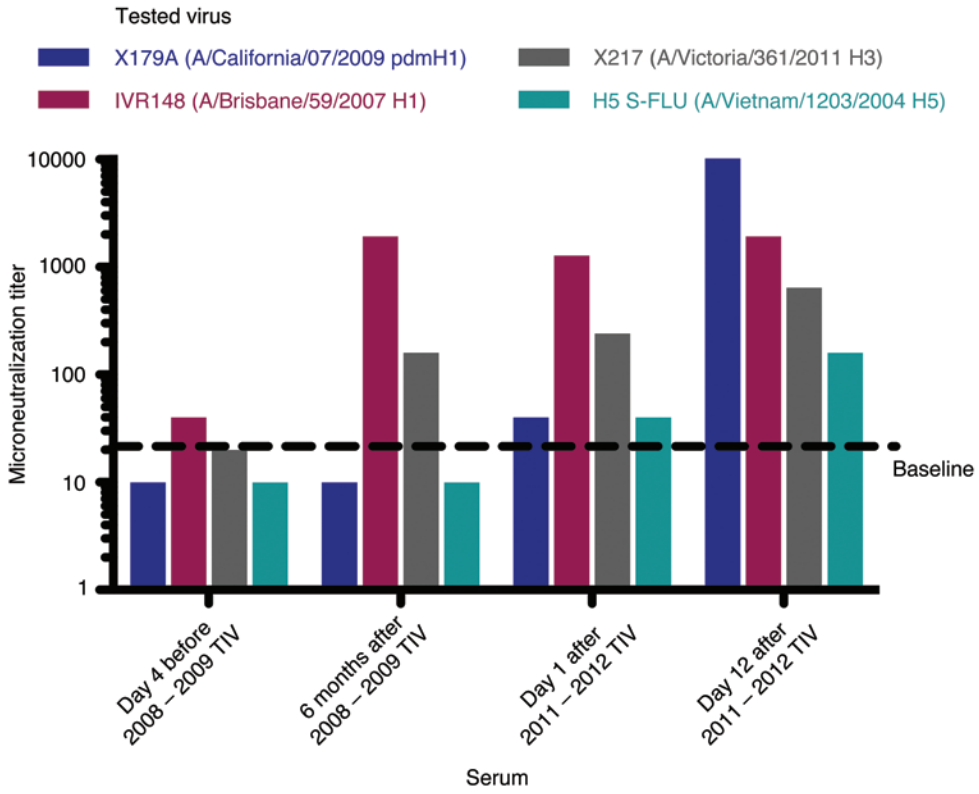

Figure 1. The serological neutralization titers for former seasonal H1, H3, H1pdm09, and H5-pseudotyped influenza viruses in donor H before and after trivalent seasonal influenza vaccination. Donor H received the 2008–2009, 2009–2010, and 2011–2012 influenza vaccines, which contain antigens from the viruses listed in Table 1. The assay was performed in duplicate and means are shown. Pseudotyped influenza viruses are more sensitive to stem antibodies than wild-type viruses. TIV, trivalent seasonal influenza.

failed to stain any of the TMIgG1-transfected cells and acted as a negative control (Supplemental Figure 1A, row 5). Similar results were obtained with HA specifically labeled on the C-terminus or randomly chemically labeled with biotin. These results established that our preparations of soluble HA contained typical head and stem epitopes and could be used to stain cells expressing HA-specific IgG1 in the plasma membrane.

Antigen-specific sorting of plasmablasts. The biotinylated HA of A/England/195/2009 stained approximately 26% of the plasmablasts at day 7 after the vaccination of donor H during the 2011–2012 influenza season (Supplemental Figure 1B). A total of 288 cells stained with the HA were sorted singly, and 167 cells were found to be PCR positive for the heavy and light chains of Ig. These 167 cells were used to produce human monoclonal antibodies (20). Of the 167 antibodies, 157 were shown to bind HA by one or more of the following: staining of HA-transfected cells, ELISA, hemagglutination inhibition (HAI), specific neutralization, or binding in Western blots. Each of the 157 antibodies had a unique sequence, which was identified as a productive sequence by the International Immunogenetics Information System (21).

Table 2. Set of 157 HA-binding and productive sequences

Specificity	V_H gene usage	No. of antibodies	No. of clones[A]	Size of the largest clone	Characteristics of the largest clone			
					HCDR3 length	V_H	D_H	J_H
Head S	3-7	88	6	73	18	3-7*01	3-16*01	6*02
	3-33	12	2	10	17	3-33*01 or 05 or 06	1-26*01	6*02
	1-18	20	5	15	17	1-18*01	2-21*02	6*02
Head CR	3-15	18	3	16	17	3-15*01 or 02	3-22*01	4*02
Stem CR	1-69	8	4	5	13	1-69*01 or 1-69D*01	2-2*02	6*03
	3-23	4	3	2	17	3-23*01 or 3-23D*01	3-22*01	4*02
	4-39	1						
Undetermined	3-30	3						
	4-59	1						
	3-21	1						
	3-9	1						

[A]Each of the V_H-related sets were defined by their specific VDJ rearrangements. HCDR3, heavy chain complementarity-determining region 3; D_H, heavy chain diversity region; J_H, heavy chain joining region; Head S, head specific; Head CR, head cross reactive; Stem CR, stem cross reactive.

Downloaded from http://www.jci.org on September 16, 2016. http://dx.doi.org/10.1172/JCI81104

Table 3. MN of natural variants and in vitro antibody-selected variant viruses[A]

			H1N1 viruses								Clade 6B viruses				Antibody-selected mutants		
Antibody	V_H	Specificity	A/USSR/90/1977	A/Bayern/7/1995	A/Beijing/262/1995	A/New Caledonia/20/1999	A/Brisbane/59/2007	IVR148 (A/Brisbane/59/2007)	A/Bayern/69/2009 (G155E)	X179A (A/California/07/2009)	A/Malta/MV14319/2013 (K163Q)	A/Belgium/14G0500/2014 (K163Q)	A/Serbia/NS-601/2014 (NQS 161-163)	A/England/621/2013 (NNS 162-164)	T2-6A ΔX179A (K163E)	T3-4B ΔX179A (K163Q)	2-12C ΔX179A (K130E)
	Donor H day 12 serum[B]									1:10,240							
	Donor H day 7 serum		1:320							1:2,560	1:640	1:640	1:480	1:480	–	–	1:2,560
T2-9A	3-7*01	Head S		–	–	–	–	–	++++	++++					–	–	
T2-6A	3-7*01	Head S	++++	–	–	–	–	–	++++	++++	–	–	–	–	–	–	++++
T2-7D	3-7*01	Head S	++++	-	–	–	–	–	++++	++++	–	–	–	–	–	–	++++
T2-8A	3-33*01	Head S	+++	–	–	–	–	–		+++	–	–	–	–	–	–	+++
T2-11C	1-18*01	Head S	+++	–	–	–	–	–		++	–	–	–	–	–	–	+++
T2-5D	3-15*01	Head CR	+++	+++	+++	+++	+++	+++	++	+++	–	–	–	–	–	–	+++
T3-4B	3-15*01	Head CR	+++	++	++	+++	+++	+++	+++	+++	–	–	–	–	–	–	+++
T1-9B	3-15*01	Head CR	+++	+++	–	+++	+++	+++	++	+++	–	–	–	–	–	–	+++
T2-12A	3-15*01	Head CR		+++	++			+++		++					–	–	++
T3-3C	3-15*01	Head CR	+++	+++	–			+++		+++	–	–	–	–	–	–	+++
T3-1A	3-15*01	Head CR		+++	–			+++		+++					–	–	+++
Controls																	
2-12C	5-51*01	Head S	–	–	–	–	–	–	++	++++	++++	++++	++++	++++	++++	++++	–
Q11A6	3-21*01	Head S	–					–		+++	++	++	+	+	++	++	-
15-2A06	1-2	Head CR	++					++		++	–	–	–	–	–	–	+++
19-4G05	3-74*01	Head CR	+					++		++	–	–	–	–	–	–	++
T1-3B	1-69*01	Stem CR	–	–	–	+	++	+	+	++	++	++	+	+			
FI6v3	3-30*18	Stem CR	–							++	++	++	+	++			

[A]MN EC_{50} values: –, negative; +, 2~20 μg/ml; ++, 0.2~2 μg/ml; +++, 20~200 ng/ml; ++++, 0~20 ng/ml. [B]Sera were obtained on day 7 and 12 after 2011–2012 influenza vaccination.

The 157 unique sequences of HA-binding antibodies could be divided into 11 sets defined by their use of particular heavy chain variable region (V_H) genes (Table 2); 150 of 157 sequences (96%) were derived from the 6 largest V_H sets (Figure 2A and Table 2). Each V_H set was composed of several clones defined by specific VDJ rearrangements (Figure 2A and Table 2) in the heavy chain, and each clone was further diversified by a unique pattern and frequency of somatic mutations. In each V_H-related set, one clone tended to dominate (Table 2). For example, within the V_H 3-7 set, 73 of 88 antibodies belong to one clone, which diversified by somatic mutation (Supplemental Figure 2). These clones are defined by the unique identity of their VDJ segments and their reading frames. Selections of clones from each of the 6 largest V_H-related sets were expanded, and their antibodies were purified and tested in a quantitative assay (see Methods) for neutralization of a variety of viruses (Figure 2).

Several different neutralization assays are described in the literature, so quantitative comparisons between data sets are difficult. For direct comparison, we have included samples of 7 published antibodies (Figure 2B) (see Methods and Acknowledgments for details). Two antibodies reacted broadly to the H1 head, 15-2A06 and 19-4G05 (22), and five antibodies were reactive to the stem of the HA, V3-2G6 (23), FI6v3 (24), SF70-1F02 (25), and 05-2G02 and 09-3A01 (22). The antibodies from donor H neutralized influenza in our quantitative assay at comparable concentrations to the reference antibodies and showed similar patterns of activities to the various virus isolates. Six percent of clones (10 of 157) were definitely defined as reacting with the HA stem on the basis of competition for binding with the canonical stem-reactive antibody C179 (26, 27), inability to block red cell agglutination, and broad neutralization, including our example of a V_H 3-23 antibody (T3-5D) that recognized seasonal and pandemic H1, H5, and recent H3 HAs (Figure 2B). Three further antibodies were very closely related in sequence to definite stem antibodies and have been classified as "stem" in Table 2. Eighty-eight percent of antibodies (138 of 157) were able to inhibit hemagglutination and showed less broad reactivity, consistent with binding to the globular head domain of HA. The sequences of all antibodies named in Figure 2B are deposited in the GenBank database (accessions KP231608–KP231649).

Downloaded from http://www.jci.org on September 16, 2016. http://dx.doi.org/10.1172/JCI81104

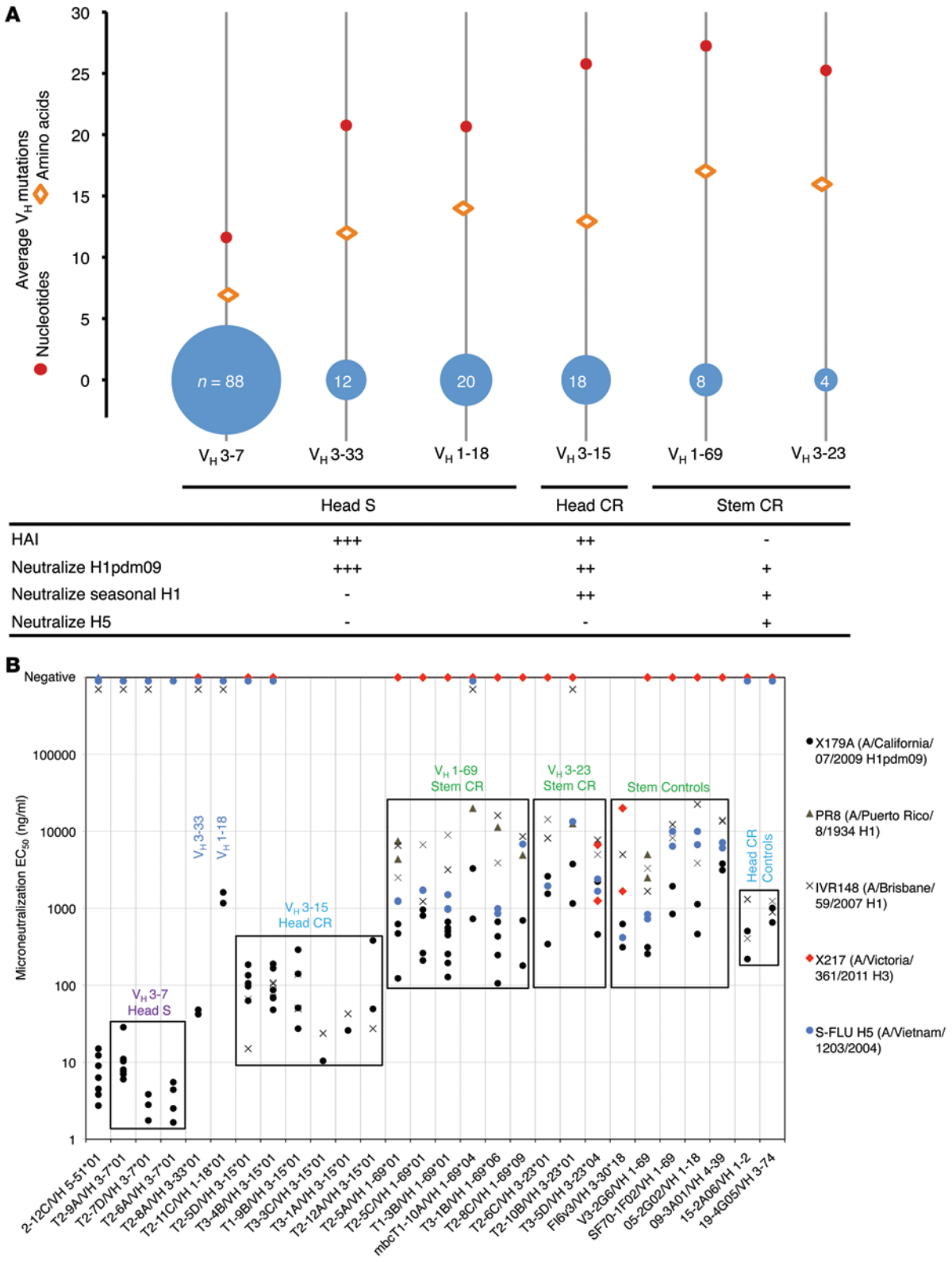

Figure 2. The 6 largest V_H-related sets of HA-binding antibodies derived from day 7 Eng195 HA-specific B cells. (**A**) The average number of V_H nucleotide and amino acid replacements in the 6 largest sets of HA-binding antibodies. The representative HAI and MN results of head-specific (Head S), head cross-reactive (Head CR), and stem cross-reactive (Stem CR) antibodies are summarized in the figure. –, negative; +, EC_{50} ~366 ng/ml; ++, EC_{50} ~70 ng/ml; +++, EC_{50} ~7 ng/ml for neutralization of X179A virus (A/California/07/2009 H1pdm09). (**B**) Neutralization titers of head-specific, head cross-reactive, and stem cross-reactive antibodies for former H1, H3, H1pdm09, and H5 viruses. Two H1 head-specific, 15-2A06 and 19-4G05 (22), and 5 stem-reactive, FI6v3 (24), V3-2G6 (23), SF70-1F02 (25), and 05-2G02 and 09-3A01 (22), reference antibodies were included. Each symbol represents an independent measurement. Some measurements overlap. MN titers were assayed at least twice for each antibody. The mean EC_{50} for neutralization for the 6 largest sets of HA-binding antibodies in the MN assay was analyzed by 1-way ANOVA, and a *P* value less than 0.05 was considered significant.

Downloaded from http://www.jci.org on September 16, 2016. http://dx.doi.org/10.1172/JCI81104

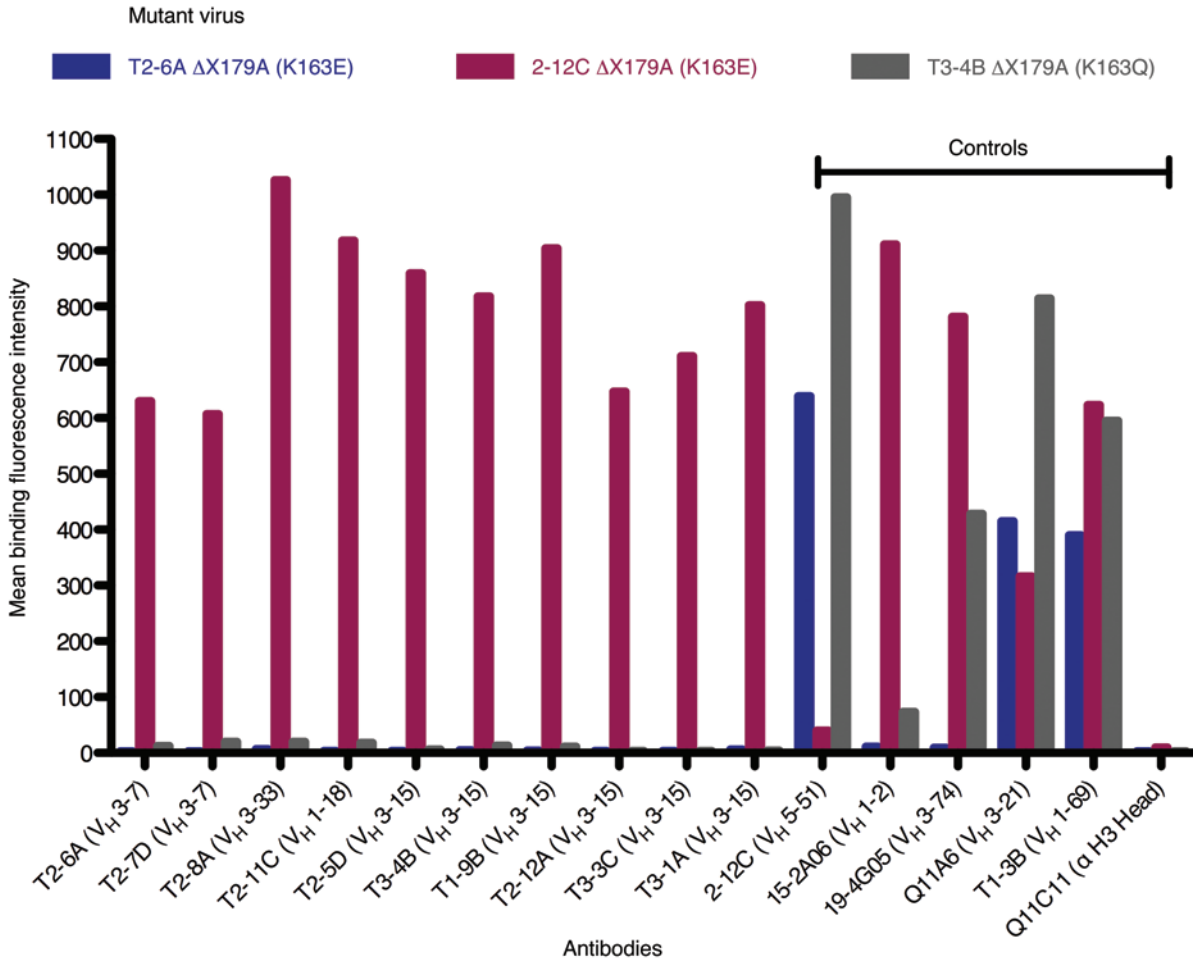

Figure 3. Binding activity of HA head-specific and head cross-reactive antibodies on cells infected with the variant viruses. A selection of head-specific (V_H 3-7, 3-33, 1-18) and head cross-reactive (V_H 3-15) antibodies and controls, including the stem cross-reactive antibody T1-3B (V_H 1-69), were tested for binding to MDCK-SIAT1 cells infected with variant viruses selected with monoclonal antibody T2-6A (V_H 3-7) that selected the K163E substitution, T3-4B (V_H 3-15) that selected K163Q, and the control 2-12C (V_H 5-51) that selected (K130E/G170R). The assay was done twice with equivalent results.

H1N1pdm09 HA–specific clones that do not recognize recent seasonal H1N1 viruses. Fifty-six percent (88 of 157) of the sequences were derived from a dominant V_H-related set, in which the Ig variable region was encoded by V_H 3-7, associated most frequently with J_H 6*02/D_H 3-16*01 and V_λ 1-40*01/J_λ 2*01 (Table 2 and Supplemental Figure 2). At least 6 clones could be identified within this set based on their unique VDJ heavy chain gene rearrangements, all of which resulted in a CDR3 length of 18 amino acids (Table 2). One dominant clone made up 73 of 88 sequences. An amino acid sequence dendrogram of the VDJ regions (Supplemental Figure 2) revealed the diversity in these sequences generated by V region somatic mutations (which induced an average of 7–amino acid changes per sequence) and clonal D-J combinations. This result is very similar to findings by Krause et al. (28) and Jackson et al. (29), who identified very similar sets of clones based on V_H 3-7/J_H 6 rearrangements in individuals responding to the Sa site of H1N1pdm09 HA and discussed the evidence for intraclonal divergence and interclonal convergence of these sequences.

Initial screening showed that clones from the V_H 3-7 set inhibited hemagglutination by H1N1pdm09 (X179A A/California/07/2009) virus. Three examples were expanded, and purified IgG1 was titrated against various viruses in HAI and microneutralization (MN) assays. The antibodies from these clones were the most potent of all those isolated, with an EC_{50} for neutralizing H1N1pdm09 virus at concentrations of approximately 7 ng/ml (~5×10^{-11} M), but they failed to react by HAI or MN with recent seasonal H1 viruses (Figure 2 and Table 3).

To identify the site recognized by these V_H 3-7*01 clones, variants of the vaccine virus X179A (containing A/California/07/2009 HA) were selected with the V_H 3-7*01 antibody T2-6A (see Methods). We found a single mutation encoding the K163E substitution in the HA in the Sa antigenic site to be associated with loss of neutralization and binding by this antibody and related members of the V_H 3-7 set (Figure 3 and Table 3). The K163E substitution corresponds to K166E isolated by Krause et al. (28), with their V_H 3-7*01 clone 4K8 in the context of A/California/04/2009 HA (our sequence numbering is as used in the WHO annual reports) (30).

Two further V_H-related sets of sequences characterized by rearrangements of V_H 3-33 (12 of 157) and V_H 1-18 (20 of 157) had similar properties to the V_H 3-7 family. They also were polyclonal (Table 2) and specific for H1N1pdm09 (Figure 2A) but tended to require higher concentrations of antibody for neutralization (Fig-

Downloaded from http://www.jci.org on September 16, 2016. http://dx.doi.org/10.1172/JCI81104

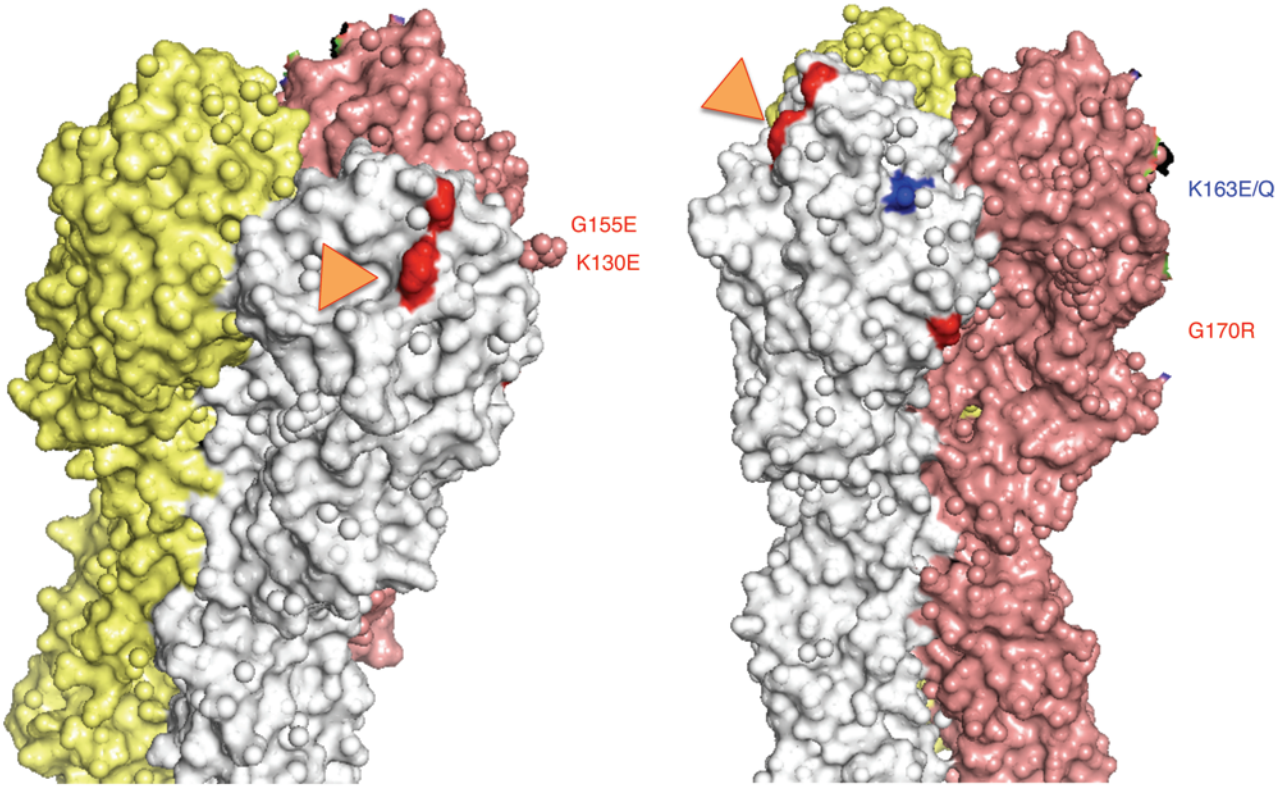

Figure 4. Mapping of K163E/Q substitutions selected by head-specific T2-6A (V_H 3-7) and head cross-reactive T3-4B (V_H 3-15) antibodies. K130E, G155E, and G170R (shown in red) resulted in loss of binding by the 2-12C control antibody. The G170R amino acid substitution, coselected by the control antibody 2-12C, is thought to be coincidentally associated with K130E. The orange triangle indicates the position of the sialic acid–binding site. K163E/Q is shown in blue. Mutations were mapped with PYMOL version 1.7 onto PDB:3LZG (15).

ure 2B) and contained more somatic mutations (Figure 2A; 21 ± 2 mutations for V_H 3-33 and 20 ± 3 mutations for V_H 1-18). Remarkably, neutralization and binding by representatives of both sets of antibodies were lost for the same K163E variant, selected by the V_H 3-7*01 clone (Figure 3 and Table 3).

Antibodies to H1 HA head that cross-react on former seasonal H1N1 strains. A fourth dominant set of clones (18 of 157, 11%) (Table 2), which cross-reacted almost equally between seasonal (A/Brisbane/59/2007) and H1N1pdm09 (A/California/07/2009) viruses in HAI and MN tests, was characterized by rearrangements of V_H 3-15 (Figure 2 and Table 3). Further analysis revealed neutralization of a broad range of former seasonal H1N1 viruses isolated between 1995 and 2007 (Table 3). All of the V_H 3-15 clones inhibited hemagglutination and were not able to compete for binding by stem-specific antibody C179 (26). This suggests that the V_H 3-15 antibodies bind to an epitope in the head of H1 HAs conserved between recent former seasonal and H1N1pdm09 viruses (27). The mean EC_{50} for neutralization for a selection of these V_H 3-15 antibodies in the MN assay was approximately 70 ng/ml for X179A (Figure 2B), significantly higher than that for the V_H 3-7 family (ANOVA, $P < 0.001$). The average number of somatic mutations in the 18 V_H 3-15 sequences was 25 ± 4 (Figure 2A), which was also significantly higher than that for the V_H 3-7 H1N1pdm09-specific clones (ANOVA, $P < 0.001$).

To identify the site recognized by these more broadly reactive antibodies, we selected mutants of X179A with a representative V_H 3-15*01 antibody, T3-4B. It selected a mutation at exactly the same position, K163Q, as the V_H 3-7*01 clone T2-6A, which selected K163E.

Antibodies to the globular head focused on K163. We then tested a selection of antibodies from the 4 V_H-related sets, representing 138 of 157 of the antibodies isolated from donor H, for binding and neutralization of viruses that contained K163E and K163Q substitutions (Figure 3 and Table 3 summarize the results). The K163E and K163Q substitutions abolished neutralization (Table 3) and binding (Figure 3) by all 4 antibody sets (V_H 3-7, 3-33, 1-18, and 3-15) recognizing the globular head. Both mutations also prevented neutralization by the 2 broadly reactive control antibodies recognizing the globular head, 15-2A06 and 19-4G05 (22), which are encoded by different V_H genes (V_H 1-2 and 3-74, respectively), implying that these 2 antibodies bind to closely related epitopes. The K163Q substitution only partially inhibited binding by the 19-4G05 control antibody, but this was sufficient to prevent neutralization (Figure 3 and Table 3).

By contrast, a clone from a different individual, 2-12C (V_H 5-51), was not affected by the substitutions at K163E/Q in neutralization or binding assays (Figure 3 and Table 3). The 2-12C antibody selected a variant virus with HA substitutions K130E and G170R. This variant resulted in loss of neutralization and binding by the selecting antibody but was still susceptible to antibodies from donor H that were sensitive to changes at K163, showing that the binding sites of the 2 antibodies were functionally independent. Subsequently,

Downloaded from http://www.jci.org on September 16, 2016. http://dx.doi.org/10.1172/JCI81104

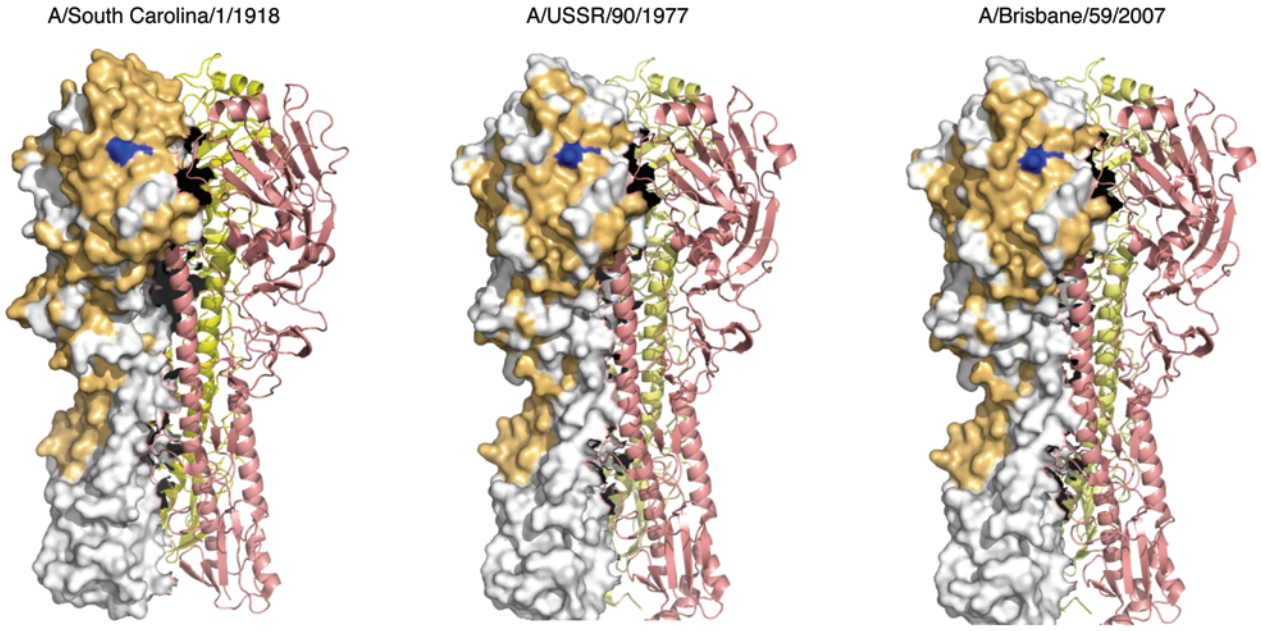

Figure 5. Mapping of the HA1 K163 residue in former H1N1 viruses. Conserved HA1 residue HA1 K163 (shown in blue), which was selected for substitution by the V_H 3-7*01 and 3-15*01 antibodies, is situated in a patch (colored gold) of surface conserved among A/California/07/2009, A/Brisbane/59/2007, A/USSR/90/1977, and A/South Carolina/1/1918 HAs. Conserved residues were mapped with PYMOL version 1.7 onto PDB:3LZG (15).

we found that an antigenic variant (A/Bayern/69/2009) with a single HA1 G155E substitution (WHO Influenza Centre February 2010 report; ref. 30) showed greatly reduced recognition by 2-12C antibody but was susceptible to antibodies from donor H (Table 3). The substitutions K130E and G170R also prevented neutralization by another control antibody, Q11A6 (V_H 3-21) from a different donor, with a pattern of reactivity similar that of to 2-12C (Table 3). Binding of 2-12C to cells infected with K163E/Q variant viruses was retained in full (Figure 3) but was abolished for cells infected with its own K130E/G170R variant. Binding by Q11A6 was reduced on the K130E/G170R variant (Figure 3), but this was associated with complete loss of neutralization (Table 3). As an additional positive control, a typical V_H 1-69 HA stem-reactive antibody produced by donor H reacted with all of the selected variant viruses in the infected cell–binding assays (Figure 3).

Mapping the substitutions onto a HA 3D structure (15) showed that positions 130 and 155, recognized by clone 2-12C, lie close together, bordering the sialic acid–binding site (shown in red in Figure 4). By contrast, K163, recognized by representatives of the 4 V_H-related sets of receptor-blocking antibodies from donor H, and the 2 broadly reactive control antibodies, 15-2A06 and 19-4G05 (21), map into the Sa antigenic site on the far side of the globular head domain but in reasonable proximity to the receptor-binding site (shown in blue in Figure 4). This physical separation is consistent with independent binding sites for the respective antibodies. The G170R amino acid substitution coselected by the control antibody 2-12C is likely to be coincidentally associated with K130E, as it is widely separated from K130 in the structure and was absent in the antigenic drift variant A/Bayern/69/2009, which also showed reduced neutralization by 2-12C.

As shown in Table 3, within the set of V_H 3-15 sequences were members sharing identical VDJ rearrangements and differing only in somatic mutations that could distinguish between drifted viruses of former seasonal H1 viruses in the MN assay. For example, 3 of 6 V_H 3-15 antibodies lost reactivity to A/Beijing/262/1995, while retaining reactivity with A/Bayern/7/1995. These two viruses differ at several positions, including K163N.

Reactivity with natural antigenic drift variants of H1N1pdm09 virus. Since 2009, the H1N1pdm09 viruses isolated in various centers around the globe have acquired a significant number of mutations, leading to HA amino acid substitutions, but have not undergone major antigenic drift, as determined by ferret antisera after infection in the HAI assay (WHO Influenza Centre February 2015 report; refs. 30, 31). It was of interest to assess the reactivity of the antibodies from donor H with recent H1N1pdm09 viruses.

The most informative comparisons are shown in Table 3. The EC_{50} for neutralization by the donor H serum harvested 7 days after 2011–2012 influenza vaccination was reduced from 1:2,560 on X179A to 1:480–1:640 on a selection of clade 6B viruses isolated in 2013 to 2014. Consistent with this, the head-specific monoclonal antibodies derived from the 4 most abundant V_H-related sets (V_H 3-7, 3-33, 1-18, and 3-15), representing 138 of 157 (88%) of the clone sequences from donor H, lost the ability to neutralize clade 6B viruses (Table 3). HA K163Q is one of the substitutions that defines the 6B clade, but it is absent in A/California/07/2009 (WHO Influenza Centre September 2014 report; ref. 30).

By contrast, antisera from ferrets infected with A/California/07/2009 are known to focus on the Sa site around positions 153–155, which is conserved in the clade 6B viruses (32). The control antibody from a different donor, 2-12C, which mapped to positions 130 and 155, like the ferret antisera, retained the capacity to neutralize clade 6B viruses at <10 ng/ml, similar to its activity on the A/California/07/2009 virus (Table 3). The amino acid sequence between 128 and 159 is identical for A/California/07/2009 and

Downloaded from http://www.jci.org on September 16, 2016. http://dx.doi.org/10.1172/JCI81104

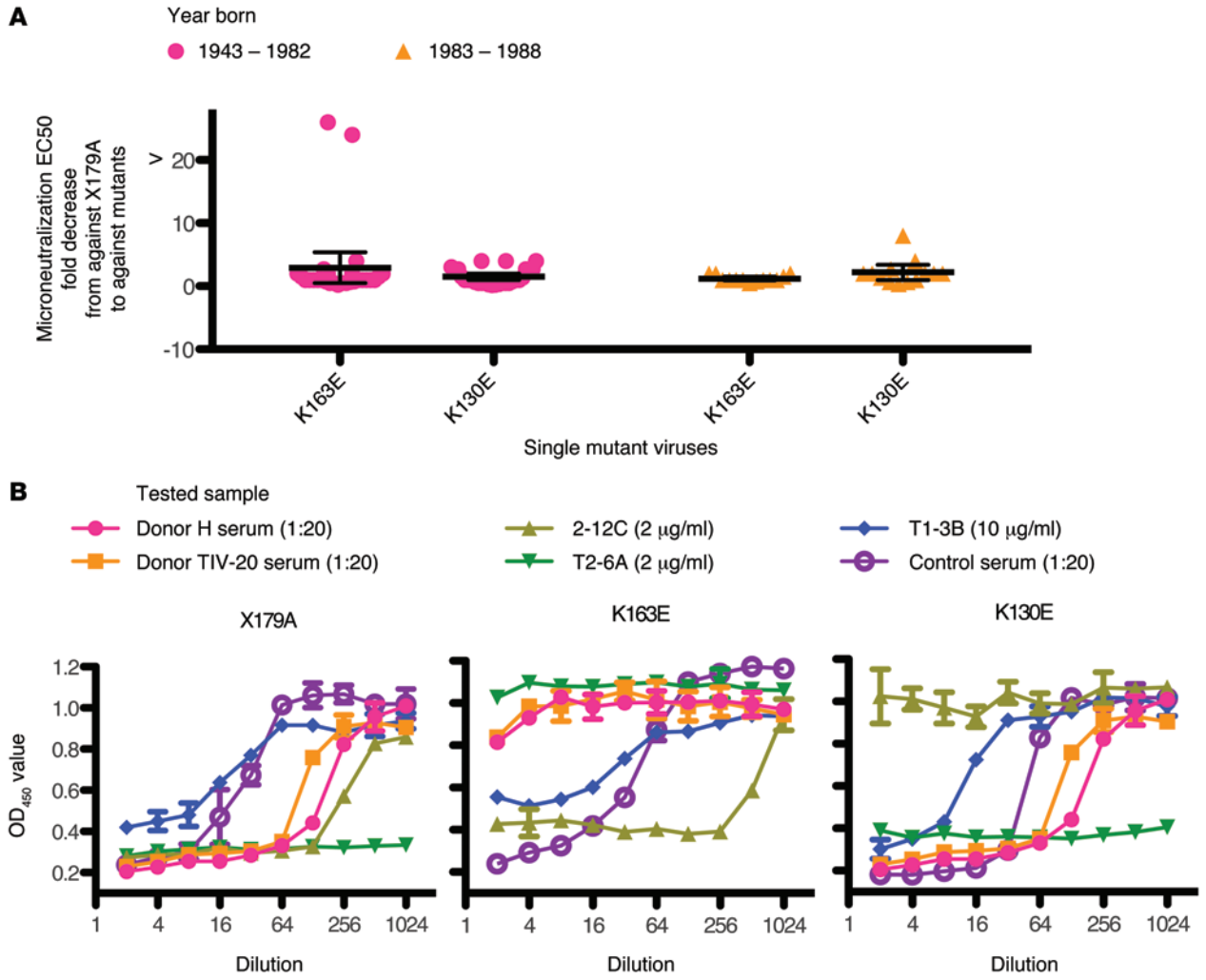

Figure 6. Neutralizing activities by sera and monoclonal antibodies from vaccinated individuals against the variant viruses. (**A**) Sera from recently vaccinated individuals born between 1943 and 1982 (n = 28) and 1983 and 1988 (n = 13) were tested for neutralization of X179A and HA variants carrying single amino acid substitutions. Sera from two individuals (donor H and TIV-20) failed to neutralize the K163E variant of X179A, and their response was focused on the Sa site. Sera from two individuals born between 1983 and 1988 were focused on K130 (Ca2 site). Mean and 95% confidence interval are shown. (**B**) Serum after vaccination and the V_H 3-7 antibody T2-6A from donor H, together with serum after vaccination from another donor (TIV-20), neutralized X179A strongly but failed to neutralize the K163E virus variant. Their neutralizing activity was unaffected by the K130E substitution. T1-3B and control serum had similar neutralization titers to all the viruses. In our MN assays, the OD_{450} readout was dependent on NP expression following viral entry (65). The MN assays were performed in duplicate.

the clade 6B viruses, which is consistent with retention of the binding sites for the standard ferret antisera and antibody 2-12C. The Q11A6 control showed similar recognition to 2-12C and also retained neutralization of clade 6B viruses.

Cross-inhibition by antibodies to H1N1pdm09 HA. We looked for cross-inhibition of binding to purified HA by the various sets of antibodies isolated from donor H that are sensitive to K163E/Q substitution and compared them to both the receptor-blocking antibody 2-12C (V_H 5-51*01 recognizing K130/G155) isolated from a different donor and a typical V_H 1-69 stem-reactive antibody. We tested 3 sets of receptor-blocking antibodies from donor H based on V_H 3-7*01, 1-18*01, and 3-15*01 and found they were all able to cross-inhibit each other in an ELISA but were not inhibited by the typical V_H 1-69 stem-reactive antibody (Supplemental Figure 3). By contrast, none of these antibodies from donor H could compete for binding with the H1N1pdm09 HA–specific antibody 2-12C, which was mapped adjacent to the receptor-binding site by the substitutions K130E and G155E. As shown by Supplemental Figure 3, the 2-12C antibody could inhibit the binding of the V_H 3-15 antibody, T3-4B. This unidirectional competition suggests overlap in the binding footprints of these two antibodies.

The antibody response from donor H is focused. Taken together, these results suggest that approximately 88% of HA-reactive monoclonal antibodies derived from day 7 plasmablasts produced by donor H in response to vaccination with H1N1pdm09 HA from A/California/07/2009 were focused on a limited region of the HA head domain and shared an overlapping footprint that included position K163, which was substituted in the clade 6B viruses that have evolved since 2013 (WHO Influenza Centre September 2014 report; ref. 30).

Downloaded from http://www.jci.org on September 16, 2016. http://dx.doi.org/10.1172/JCI81104

Reactivity with A/USSR/90/1977. The high frequency of somatic mutations in the 4 sets of monoclonal antibodies from donor H that recognize K163 suggested that they may have been selected from the memory B cell pool (33). It is well known that the first exposure to influenza virus induces a repertoire of B cells that remain for life, from which subsequent exposures to influenza can select, if cross-reactive (34–37). The H1N1 viruses related to A/USSR/90/1977 reappeared in humans in 1977 after being absent since 1957. As donor H was a child in 1977, it is highly likely that the first exposure to H1N1 viruses was to a virus related to A/USSR/90/1977.

A selection of monoclonal antibodies from the 4 V_H-related sets (3-7, 1-18, 3-33, and 3-15), which were dependent on residue K163, were tested for neutralization of A/USSR/90/1977. All of these antibodies neutralized the 1977 virus strongly, suggesting that they may have been primed by this virus (Table 3). The amino acid residues surrounding K163, when mapped onto the HA structure, form a patch of conserved surface shared between the 1977 and 2009 HAs, consistent with the cross-reactivity shown by these antibodies (Figure 5).

A second donor with a similar pattern of reactivity to that of donor H. To assess the frequency of individuals that can make a highly focused antibody response to the region around K163, we compared sera for reactivity with A/California/07/2009 and variant viruses carrying substitutions at K163. Of the 41 sera samples screened after vaccination (MN titer >1:40), we found a second example in which the sera lost the ability to neutralize H1N1 viruses with K163 substitutions (Figure 6). These findings with sera are consistent with those of the survey of Linderman et al. (14), who found up to 42% of sera from donors born before 1979 showed reduced reactivity with clade 6B H1N1pdm09 isolates. Both our sera were from donors born before 1982 (2 of 28).

Broadly reactive antibodies to the H1 HA stem. Not all of the antibodies isolated from the day 7 plasmablasts from donor H were dependent on K163. We identified 10 of 157 (6%) definite stem-reactive antibodies (and 3 additional closely related sequences) by a combination of 4 assays: inhibition of C179 antibody binding to purified HA in ELISA (26, 27), broad neutralization (Figure 2), lack of HAI activity, and lack of reactivity in Western blots (data not shown). Six antibodies were encoded by V_H 1-69, 3 by V_H 3-23, and 1 by V_H 4-39 (Figure 2B and Table 2). These antibodies required a significantly higher concentration (mean 366 ng/ml for the V_H 1-69 clones; ANOVA, $P < 0.001$) to achieve neutralization of X179A compared with typical receptor-blocking antibodies in our MN assays, in which the readout was nucleoprotein (NP) expression following virus entry (Figure 2B). The V_H 1-69 and V_H 3-23 stem-reactive antibodies were able to cross-neutralize an H5-pseudotyped influenza virus (EC_{50} ~1 μg/ml) that was coated in HA from A/Vietnam/1203/2004 (Figure 2B). This proportion of stem-reactive antibodies is consistent with the low level of neutralization of the H5-pseudotyped influenza by 12 days after vaccination in serum from donor H (Figure 1).

Therapeutic potential. To determine whether representatives of the 3 major sets of antibodies isolated from donor H, studied in detail here, were protective in vivo, we treated DBA/2 mice 24 hours after intrapulmonary infection with X179A virus (that contained HA from A/California/07/2009) with a single dose of 10 mg/kg of each antibody. The DBA/2 mouse strain is extremely sensitive to influenza infection (38), and we used an inoculum of virus approximately 150 times that required to cause 20% weight loss in at least 50% of the recipients. As shown in Supplemental Figure 4, antibodies with the 3 major specificities (head-specific V_H 3-7, head cross-reactive V_H 3-15, and stem cross-reactive V_H 1-69) were able to reverse weight loss after a 24- to 48-hour delay. By contrast, animals treated with PBS, or an H3 HA–specific antibody, failed to respond.

Discussion

Our study has confirmed that staining and sorting peripheral B cells with soluble HA can greatly enrich for virus HA-specific clones (19, 23). This enabled us to analyze a large sample of monoclonal antibodies from a single individual, for which heavy and light chains and function could be assigned. However, we acknowledge that this method may not sample the complete repertoire of B cells specific for HA. Plasmablasts that have lost expression of surface Ig would be missed, and the PCR strategy used selects for IgG-expressing clones. In addition, the plasmablasts taken at day 7 may not sample the complete hemagglutinin-reactive B cell repertoire present in the pool of memory B cells.

Sequence analysis of the 157 HA-reactive antibodies clearly showed that the B cell response in donor H was dominated by relatively few V_H and $V_{\lambda/\kappa}$ genes and was focused around residue K163 (Table 2 and Supplemental Table 1). This selection was unlikely to have been an artifact of the sorting procedure with HA because (a) we established that our HA preparation presented epitopes from head and stem to membrane-bound Ig (Supplemental Figure 1A); (b) in ELISA (data not shown), our HA preparation was bound by H1 HA–specific antibodies recognizing multiple epitopes in the head and stem (antibodies were from our own laboratory and the laboratories of Ahmed, Schrader, and Lanzavecchia); (c) the same method of production has been used to obtain crystals of correctly folded protein (39); and (d) the dominant effect of K163 on antibody binding was seen in the polyclonal sera as well as the selected monoclonal antibodies (Figure 6 and Table 3), as expected from the high proportion of the monoclonal antibodies that recognized this residue.

Eleven V_H gene-related sets, diversified by variations in J and D rearrangements, accounted for the 157 unique antibody sequences isolated. Six of the ten V_H-related sets provided 96% of the antibody sequences, and the majority of these sets, while polyclonal, were dominated by a single expanded clone, defined by a unique pattern of gene rearrangements in heavy and light chains (Table 2). Each V_H set was further diversified by extensive somatic mutation, such that each of the 157 sequences was unique. The frequency of somatic mutations in each set is shown in Figure 2A. The high level of neutralization and accumulation of somatic mutations indicated that they may have been derived from preexisting memory B cells (16, 23, 27, 33, 40).

The limited V_H gene usage we have found in donor H is similar in extent to the response detected to vaccination by Moody et al. (41), with up to 12 V_H-related sets in any one individual; however, our data contrast with data from Okada et al. (42, 43), who isolated 221 unique V_H sequences that reacted with H3 HA by phage display from a single individual, who, unlike our donor,

Downloaded from http://www.jci.org on September 16, 2016. http://dx.doi.org/10.1172/JCI81104

was hyperimmunized by multiple exposures and vaccinations. V_H gene usage was considerably more diverse in their collection, and antibodies to all 5 antigenic sites in H3 HA were identified. Similarly, the majority of serum samples obtained after infection in 1978, 10 years after the introduction of H3 viruses into humans, contained antibodies to more than one site on the HA (13). However, of samples obtained within 3 years of H3 introduction, 1969–1971, 17% recognized a single site (13). This suggests that multiple exposures to influenza may induce a broader range of antibodies encoded by a larger selection of V_H genes than we have detected in donor H, who had probably been exposed to H1N1pdm09 for the first time (44).

Of the 157 clones from donor H, 138 (88%) were derived from 4 V_H-related sets of antibodies targeting the globular head of HA that cross-reacted between A/USSR/90/1977 and the recent H1N1pdm09 virus. At least 10 antibodies (6%) from 3 V_H-related sets were specific for the HA stem. In addition, within the HA head-specific antibodies, a subgroup of 18 antibodies encoded by V_H 3-15 were broadly reactive against former seasonal H1 viruses, whereas the others did not recognize those viruses isolated from at least 1995 to 2007. These patterns and degrees of cross-reactivity between various A viruses and human monoclonal antibodies generated against influenza HA are comparable those found by others (22, 23, 25, 27, 28, 45, 46).

The dominance of HA head-specific V_H 3-7*01/J_H 6*02 sequences that we found in the largest V_H-related set has been seen in other individual responses following exposure to H1N1pdm09 (28, 29). For example, the V_H 3-7/J_H 6 antibodies rearranged with a different group of 4 D segments (3-16*02, 3-22*01, 6-13*01, and 4-17*01) from those from our donor (3-16*01, 3-3*01 in reading frame 2 and 3, and 3-3*02) (28). However, all of these D segments are closely related and share an amino acid sequence motif, DTY, at the D-J junction. In addition an antibody from a representative of our V_H 3-7*01 clones selected the identical K163E substitution as clone 4K8 isolated by Krause et al. (28). This result suggests that both sets of V_H 3-7*01 clones bind the same site on the HA. Krause et al. also showed that their antibodies, while failing to cross-react with recent former seasonal H1 viruses (including A/Brisbane/59/2007), recognized the HAs from A/USSR/92/1977 and A/South Carolina/1/1918 (28).

In addition, in a deep-sequencing study of H1N1pdm09-vaccinated subjects, Jackson et al. (29) noted that clonal lineages using V_H 3-7/J_H 6 were overrepresented, with the majority forming a CDR3 of 18 amino acids, as we have found in our donor (Table 2). This combination formed a signature for the antibody response to the 2009 H1 hemagglutinin.

In a V_H amino acid sequence dendrogram (Supplemental Figure 2), the V_H 3-7 clones defined by their unique VDJ rearrangements do not separate into clone-defined branches. Krause et al. (28) and Jackson et al. (29) discuss this phenomenon in detail and provide evidence for interclonal convergence and intraclonal divergence in the sequences of their V_H 3-7 sets, suggesting that the structural requirements for binding to the H1N1pdm09 HA had been solved independently in clones that used V_H 3-7*01 by different combinations of particular VDJ rearrangements and convergent somatic mutations (28, 29). We came to the same conclusion for our set of 6 V_H 3-7 clones.

The other 3 major V_H sets of receptor-blocking antibodies and 2 V_H sets of stem-specific antibodies from donor H also showed evidence for polyclonality (Table 2), emphasizing the richness of the repertoire available for binding to particular HA epitopes within an individual. In addition, within each clone defined by its VDJ rearrangements, there was extensive somatic mutation, which in general increased with increasing breadth of cross-reactivity (Figure 2A). This would be consistent with repeated rounds of selection in the germinal center with each influenza exposure for the more cross-reactive clones and would be expected to contribute to the phenomena of "antigen seniority" (47) and the stability of "antibody landscapes" (44) observed in serological surveys of human populations over time.

In the case of the V_H 3-15 set, point mutations gave rise to changes in fine specificity for circulating influenza variants isolated in 1995 (Table 3). For example, clones T2-5D and T1-9B share the same gene rearrangements in H and L chains but differ in somatic mutations, and this is associated with a difference in their ability to neutralize A/Beijing/262/1995 (Table 3). This reactivity of naturally produced human monoclonal antibodies to HA selected through natural antigenic drift mirrors the classic studies on clonal antibody specificity in individual BALB/c mice, tested for binding variant viruses selected in vitro, which demonstrated a similar restricted V gene usage with polyclonality (48) and a clearly defined role for somatic mutation influencing the fine specificity for the HA Sb site (49, 50).

Both V_H 3-7 and broadly reactive V_H 3-15 antibodies to the globular head as well as a V_H 1-69 clone specific for the HA stem were therapeutic in DBA/2 mice at a dose of 10 mg/kg (Supplemental Figure 4), despite their widely differing neutralization titers in vitro (Figure 2B), as seen for murine monoclonal antibodies (51). These results emphasize that the antibodies we have studied are functional. It is noteworthy that, although the V_H 3-15 antibodies would now be redundant as therapeutic agents because of the recent expansion of the clade 6B viruses, they would have been useful for at least 14 years (1995–2009), during which their neutralizing epitope was conserved.

In view of our evidence for diversity and redundancy in the human antibody response to individual antigenic sites on the HA, it is surprising that all 4 receptor-blocking V_H-related sets of antibodies from donor H, representing 138 of 157 (88%) of the total rescued clones, focus on a limited overlapping region on the HA head, involving residue K163. The site recognized was shown to be distinct from the site occupied by the 2-12C receptor-blocking antibody from another individual (Figure 4 and Table 3) and reference ferret antisera after H1N1pdm09 virus infection, which do not detect a major change in antigenicity in the clade 6B viruses (WHO Influenza Centre September 2014 report; ref. 30). This conclusion was based on loss of neutralization of the recently evolved clade 6B viruses (that all contain mutations at K163) by all 4 sets of antibodies (Table 3), selection of substitutions at the same site (K163) by V_H 3-7*01 and V_H 3-15*01 clones, loss of recognition of K163E/Q variant viruses by all 4 sets (Figure 3), and cross-inhibition between the 4 sets of antibodies for binding to HA (Supplemental Figure 3).

Focusing of the polyclonal antibody response in donor H was confirmed by the loss of neutralizing activity for viruses selected for

Downloaded from http://www.jci.org on September 16, 2016. http://dx.doi.org/10.1172/JCI81104

the K163E/Q substitution, compared with A/California/07/2009, in the sera obtained 12 days after vaccination (Table 3). In addition, a screen of 41 immune sera revealed a second vaccinated donor whose serum was unable to neutralize viruses with the K163E/Q substitutions (Figure 6), and two of the control human antibodies that cross-react between former seasonal and H1N1pdm09 viruses described previously (22), provided by Li et al., also recognized K163 (Table 3).

The results of our detailed clonal analysis extend two recent serological studies of the human antibody response to the H1N1pdm09 virus (14, 37). Li et al. have shown that human individuals born between 1983 and 1996 (after donor H), who were exposed in early life to former seasonal H1 viruses that retained K130, narrowly focused their antibody response on this region on exposure to H1N1pdm09 (37). This is similar to the site defined by our antibody, 2-12C, derived from a control individual, which selected for the K130E substitution, and we also detected 2 sera after vaccination with reduced neutralization of viruses carrying the K130 substitution (Figure 6A), confirming the observations of Li et al. However, mutations at K130 have not as yet appeared as new variant hemagglutinins isolated from infected humans (WHO Influenza Centre September 2014 report; ref. 30).

Linderman et al. noted that severe influenza infection was occurring with higher frequency in middle-aged individuals in the 2013–2014 season that was related to the appearance of clade 6B H1N1pdm09 viruses and showed that, in the cohort born between 1965 and 1979 (which would have included our donor), 42% of serum samples had reduced titer in HAI and MN assays on viruses with K166E/Q substitutions (K163 in our HA numbering) (14). Our paper extends these results by showing that multiple monoclonal antibodies from such individuals can select substitutions at this same site, which suggests that selection is occurring in nature. This link between the focused antibody response in humans and selection of substitutions in the HA from influenza viruses found in nature has long been suspected but not directly demonstrated (4, 5, 8–13, 48, 52–55).

The mechanism by which this focusing of the antibody response occurs is not clear from these data, but three possibilities include (a) a limited response in the first exposure to a new virus (13), (b) selection of cross-reacting B cells from the available repertoire induced by earlier exposure to related influenza viruses (15, 16, 25, 34–37, 41, 44, 47, 56, 57), or (c) the selection and expansion of B cells making antibodies that influence antigen processing and presentation to T cells in such a way that optimizes T cell help, "T-B reciprocity" (33, 58–62). These mechanisms are not mutually exclusive and could act together.

The region of the H1 HA surface that immediately surrounds residue K163 substitutions, which were selected for by the V_H 3-7*01 and 3-15*01 antibodies, is to a large extent conserved among A/California/07/2009, A/Brisbane/59/2007, A/USSR/90/1977, and A/South Carolina/1/1918 (Figure 5 and refs. 15, 56). Antibodies cloned from survivors of the 1918 pandemic also select variants with amino acid substitutions at this site (15, 56). This concurs with the very broad reactivity of the V_H 3-15 antibodies and the more restricted pattern of recognition by V_H 3-7 antibodies that cross-react with the HAs from 1918, 1977, and 2009 but not 2007 (ref. 28 and this paper). Donor H was born between the emergence of the H2 viruses in 1957 and the reappearance of former seasonal H1 influenza in 1977, so it is possible that exposure to A/USSR/90/1977 was the stimulus that primed the B cells, which reemerged as the dominant and focused response to the H1N1pdm09 virus.

Together, these results suggest that the highly focused antibody responses made by some individuals is a "partial anamnestic response" to epitopes shared between a virus infecting them in early life and the current challenge virus, as demonstrated by de St. Groth and Webster in an animal model in 1966 (35), as conceived originally by Thomas Francis as "original antigenic sin" (34), and as elaborated and refined in recent surveys (44, 47, 57).

Our evidence suggests that the great majority of antibodies generated by donor H share an overlapping footprint on the HA receptor-binding domain that includes residue K163. Substitutions at this site have recently become common in clade 6B H1N1pdm09 viruses collected in 2013–2014 (WHO Influenza Centre September 2014 report; ref. 30). This implies that antibodies similar to the dominant sets in donor H may be actively involved in selecting variants of currently circulating viruses in regions of sequence that were previously conserved in H1 HAs (Figure 5). In principle, this process of selecting virus variants by a focused antibody response to patches of conserved sequence could occur sequentially, as long as a sufficient pool of susceptible individuals were available in the population to expand new variants and transmit them to additional individuals with different antigen exposure histories that focused the antibody response on new sites. This concept could be tested by extension of the work we have described here. Our results suggest that dominant families of antibodies identified by deep sequencing after vaccination (29) may be excellent candidates for making recombinant monoclonal antibodies for selection of influenza variants in vitro that could predict future antigenic drift.

The clade 6B variants are considered to be A/California/07/2009-like antigenically by the WHO. Antigenic similarity has been ascribed based on HAI reactivity with panels of primary ferret antisera after infection raised against a range of H1N1pdm09 viruses, including A/California/07/2009 (WHO Influenza Centre February 2015 report; ref. 30). Mutagenesis studies have shown that the ferret HAI response to A/California/07/2009 is tightly focused on residues 153–155 in the Sa antigenic site (32). The single HA G155E substitution in A/Bayern/69/2009 defines this, and, with K130, G155 helps form the epitope recognized by our antibody 2-12C. The amino acid sequence between 126 and 159, which incorporates all of these residues, is identical in A/California/07/2009 and the clade 6B viruses; this sequence overlap is compatible with preservation of the ferret HAI and MN response and the MN titers with antibody 2-12C that do not distinguish between the two.

In contrast to the ferret antisera, the greater part of the monoclonal antibody responses that we have detected, and 42% of serological responses of individuals born between 1965 and 1979 (14), do distinguish these two sets of viruses. These observations show that individual humans can focus their antibodies differently from ferrets and that the patterns of antigenic relatedness between virus isolates determined by ferret antisera may not always predict the specificity of human antibody responses

Downloaded from http://www.jci.org on September 16, 2016. http://dx.doi.org/10.1172/JCI81104

(14, 37). The importance of this distinction lies in the fact that the 2013–2014 H1N1 viruses, which were not detected as drifted in the standard analysis with ferret sera, have been associated with severe infections in middle-aged and elderly humans previously shown to be relatively protected (63).

Our detailed clonal analysis extends the serological survey from Linderman et al. (14) and the deep-sequencing study of Jackson et al. after vaccination (29) by showing that the antibodies detected in these studies can select virus variants in vitro that match the dominant natural clade 6B variants that have arisen since 2013. Our results show that assessing antigenic relatedness of evolving influenza viruses with panels of defined, renewable, and human monoclonal antibodies could be a very useful supplement to traditional ferret antisera and may also be used to predict antigenic drift. In addition, the production of therapeutic monoclonal antibodies should be considered as part of national planning for pandemic influenza. This is particularly relevant to the H7N9 threat, for which virus isolates with the NA-R292K substitution show resistance to the neuraminidase inhibitors but retain their virulence and transmissibility (64).

Methods

Secreted HA of influenza A/England/195/2009 virus. cDNA corresponding to codons 1 to 520 of the ectodomain of HA from influenza A/England/195/2009 virus was amplified and purified as previously described (39, 65). Briefly, the construct incorporated at the C-terminus included a thrombin cleavage site, a trimerization sequence, a histidine-tag region for protein purification, and the BirA recognition sequence LNDIFEAQKIEW for site-specific biotinylation. The cDNA sequence was codon optimized for eukaryotic expression in 293T cells. Biotinylation was performed with BirA enzyme from Avidity.

Staining and sorting of plasmablasts. The identification of plasmablasts by flow cytometry was based on the methods of Smith et al. (20) with minor modifications. A week after vaccination, fresh peripheral blood mononuclear cells were suspended in staining buffer. A mix of surface antibodies, including Pacific Blue anti-CD3 (BD; catalog 558117), FITC anti-CD19 (BD; catalog 555412), Allophycocyanin-H7 anti-CD20 (BD; catalog 641396), PE-Cyanine 7 anti-CD27 (BD; catalog 560609), and PE-Cyanine 5 anti-CD38 (BD; catalog 555461), were added to the aliquot of peripheral blood mononuclear cells with 10 μg/ml biotinylated Eng195 HA and incubated for 30 minutes on ice. After washing with staining buffer, cells were further incubated with ExtrAvidin-PE (Sigma-Aldrich) for 30 minutes on ice. Cells were washed and resuspended in PBS and passed through a cell strainer. The MoFlo cell sorter (DakoCytomation) was used for sorting. After applying a gate on $CD3^{-}CD20^{-}CD20^{lo}CD19^{+}CD27^{hi}CD38^{hi}Biotin^{+}$ cells, single plasmablasts were sorted into 96-well plates containing 10 μl RNase-inhibiting RT-PCR catch buffer (20).

Generation of monoclonal antibodies. Human monoclonal antibody was produced from single B cells as described previously (20). In brief, single B cells were sorted directly to RT-PCR buffer, and the variable region genes from each cell were amplified in a One-Step RT-PCR reaction (Qiagen), using a cocktail of primers specific for the leader region and antisense primers to the Cγ constant region for heavy chain and Cκ and Cλ for light chain as described previously (20). The RT-PCR products were amplified in separate PCR reactions for the individual heavy and light chain gene families using nested primers to incorporate restriction sites at the ends of the variable gene as described previously (20). These variable genes were then cloned into expression vectors for the heavy and light chains as described previously (20). Plasmids were transfected into the 293T cell line for expression of recombinant human monoclonal antibodies.

Construction of transmembrane forms of human monoclonal antibodies. The transmembrane-spanning domain of human IgG1 (66) (GenBank X52847.1) was cloned from sorted human plasmablasts between unique SmaI and HindIII sites, with the oligonucleotides 5′ GCCCCCATCCCGGGATGAGCTG and ATGGTCAAGCTTACTAGGCCCCCTGTCCGATCATG. Full-length TMIgG1 cDNAs encoding antibodies that we isolated and characterized were reconstructed by replacing the sequence between the unique SmaI and HindIII sites in the IgG1 expression vector of Smith et al. (20) (GenBank FJ517647) and transfected into 293T cells for staining with preparations of labeled recombinant HAs. Three antibodies were converted to the TM form: one specific for the head of seasonal H3 HA (N2B10, V_H 4-61*01) as well as one for the head (T2-9A, V_H 3-7*01) and one for the stem (T1-3B, V_H 1-69*01) of H1N1pdm09 and H5 HAs.

Enzyme-linked immunosorbent, indirect immunofluorescent, virus titration, HAI, and MN assays. Assays were performed using standard procedures as described previously (65). The ELISA or MN titers were expressed as half maximal effective concentrations (EC_{50}: midpoint between negative and plateau positive controls) derived by linear interpolation from neighboring points in the titration curve. The MN assay detects inhibition of virus entry into MDCK-SIAT-1 cells in the absence of trypsin (67), with antibody present throughout the assay (23). MN assays with clade 6B viruses incorporated a replication step in the presence of trypsin for 48 hours, which gave lower background staining with the developing antibody to NP AA5H (65). Serum and plasma samples were heat inactivated at 56°C without RDE treatment, and monoclonal antibodies were untreated. Serum and plasma samples from donor H taken on the same day did not give significantly different titers in the MN assay. Seven published antibodies were included: 15-2A06, 19-4G05, 05-2G02, and 09-3A01 (22) as well as SF70-1F02 (25) were gifts from Rafi Ahmed (Emory University, Atlanta, Georgia, USA); V3-2G6 (23) was a gift from John Schrader (University of British Columbia, Vancouver, British Columbia, Canada); and FI6v3 (24) was a gift from Antonio Lanzavecchia (Institute for Research in Biomedicine, Bellinzona, Switzerland). Antibody competition was assessed by ELISAs performed with biotin-labeled antibodies in the presence of excess unlabeled blocking antibodies. Detection was performed with HRP-labeled ExtrAvidin (Sigma-Aldrich).

Animal studies. DBA/2 (DBA/2^{OlaHsd}) $H2^{d}$ mice were purchased from Harlan and housed in individually vented cages. X179A vaccine virus (provided by the National Institute for Biological Standards and Control, South Mimms, United Kingdom) had a minimum dose which caused at least 20% weight loss in 50% of the mice (MD_{50}) of 32 tissue culture 50% infectious dose ($TCID_{50}$). Mice were anesthetized with isoflurane (Abbot) and were intranasally infected with 4.6×10^3 $TCID_{50}$ X179A (~150× MD_{50}), followed 24 hours later by i.p. transfer of 500 μl antibody at a dose of 10 mg/kg into anesthetized animals. Mice were weighed and scored according to previously described criteria (65), and mice with 20% weight loss or morbid clinical scores were humanely killed.

Downloaded from http://www.jci.org on September 16, 2016. http://dx.doi.org/10.1172/JCI81104

Selection of influenza variants with monoclonal antibodies. Approximately 10^7 $TCID_{50}$ X179A virus was mixed with antibody at 20 μg/ml and incubated at 37°C for 1 hour. The mixture was then diluted to 10 ml (~2–4 μg/ml antibody) with viral growth medium (DMEM, 0.1% BSA, 10 mM HEPES, pH 7.0, penicillin and streptomycin) (65), and 100 μl was added to 80 wells of a flat-bottomed 96-well microtiter plate containing confluent monolayers of MDCK-SIAT-1 cells (68) plated the previous day. The remaining wells contained medium without virus for comparison. The mix was incubated for a further hour at 37°C, and then 100 μl viral growth medium was added, containing trypsin at 2 μg/ml. The mix was incubated at 37°C for 48 hours and then the medium from each well was removed and stored. The monolayers were stained for NP expression as described previously (65), and viruses from wells showing replication in the presence of antibody were cloned by limiting dilution in the presence of antibody at a final concentration of 1 μg/ml (or a known saturating concentration). Viruses from single clones were expanded in 3-ml cultures for extraction of RNA, PCR amplification of HA and neuraminidase, and sequencing of the PCR products.

Hemagglutinin sequence numbering. Sequence numbering throughout the manuscript refers to the mature H1 HA polypeptide, i.e., with the signal sequence removed, as used in annual and interim reports from the WHO Collaborating Centre for Reference and Research on Influenza, the Crick Worldwide Influenza Centre, and summaries of the WHO Vaccine Composition Meetings (1, 30).

Statistics. Graphs were generated using GraphPad Prism software (version 5) and Microsoft Excel 2010. Statistical analysis was done by GraphPad Prism and SPSS. *P* values of less than 0.05 were considered significant.

Study approval. This study was performed in accordance with the Declaration of Helsinki and Good Clinical Practice guidelines. Protocols and informed consent were reviewed and approved by the Oxford Tropical Research Ethics Committee and the Weatherall Institute of Molecular Medicine. Signed informed consent was obtained from each individual donor who supplied a blood sample. All animal procedures were approved by an internal University of Oxford Ethics Committee and the United Kingdom Home Office.

Acknowledgments

We are grateful to the Ahmed, Lanzavecchia, and Schrader laboratories for providing reference antibodies 15-2A06, 19-4G05, 05-2G02, and 09-3A01 (22) as well as SF70-1F02 (25); FI6v3 (24); and V3-2G6 (23), respectively, for the comparisons in the tables and figures. We also thank Simon Davis, Davide Corti, and Antonio Lanzavecchia for their helpful comments on the manuscript. These studies were funded by the Townsend-Jeantet Charitable Trust (registered charity no. 1011770), The Human Immunology Unit (MRC), Oxford University, Chang Gung Medical Research Program grant (CMRPG4B0041-3), and Taiwan Ministry of Science and Technology grant (MOST 104-2320-B-182A-002-MY2). J.W. McCauley and R.S. Daniels are supported by MRC programme no. U117512723.

Address correspondence to: Alain R. Townsend, Weatherall Institute of Molecular Medicine, John Radcliffe Hospital, Headington, Oxford, OX3 9DS, United Kingdom. Phone: 44.1865.222328; E-mail: alain.townsend@imm.ox.ac.uk.

1. Barr IG, et al. WHO recommendations for the viruses used in the 2013–2014 Northern Hemisphere influenza vaccine: epidemiology, antigenic and genetic characteristics of influenza A(H1N1)pdm09, A(H3N2) and B influenza viruses collected from October 2012 to January 2013. *Vaccine*. 2014;32(37):4713–4725.
2. Das SR, et al. Defining influenza A virus hemagglutinin antigenic drift by sequential monoclonal antibody selection. *Cell Host Microbe*. 2013;13(3):314–323.
3. Yewdell JW, Caton AJ, Gerhard W. Selection of influenza A virus adsorptive mutants by growth in the presence of a mixture of monoclonal antihemagglutinin antibodies. *J Virol*. 1986;57(2):623–628.
4. Hensley SE, et al. Hemagglutinin receptor binding avidity drives influenza A virus antigenic drift. *Science*. 2009;326(5953):734–736.
5. Gerber P, Loosli CG, Hambre D. Antigenic variants of influenza A virus, PR8 strain. I. Their development during serial passage in the lungs of partially immune mice. *J Exp Med*. 1955;101(6):627–638.
6. Daniels RS, et al. The receptor-binding and membrane-fusion properties of influenza virus variants selected using anti-haemagglutinin monoclonal antibodies. *EMBO J*. 1987;6(5):1459–1465.
7. Lin YP, et al. Evolution of the receptor binding properties of the influenza A(H3N2) hemagglutinin. *Proc Natl Acad Sci U S A*. 2012;109(52):21474–21479.
8. Haaheim LR. Haemagglutination-inhibition antibodies in human sera to an antigenic mutant of influenza A/Texas/1/77 (H3N2) virus obtained in vitro. *Acta Pathol Microbiol Scand B*. 1980;88(6):351–353.
9. Oxford JS, Haaheim LR, Slepushkin A, Werner J, Kuwert E, Schild GC. Strain specificity of serum antibody to the haemagglutinin of influenza A (H3N2) viruses in children following immunization or natural infection. *J Hyg (Lond)*. 1981;86(1):17–26.
10. Natali A, Oxford JS, Schild GC. Frequency of naturally occurring antibody to influenza virus antigenic variants selected in vitro with monoclonal antibody. *J Hyg (Lond)*. 1981;87(2):185–190.
11. Lambkin R, McLain L, Jones SE, Aldridge SL, Dimmock NJ. Neutralization escape mutants of type A influenza virus are readily selected by antisera from mice immunized with whole virus: a possible mechanism for antigenic drift. *J Gen Virol*. 1994;75(pt 12):3493–3502.
12. Popova L, et al. Immunodominance of antigenic site B over site A of hemagglutinin of recent H3N2 influenza viruses. *PLoS One*. 2012;7(7):e41895.
13. Wang ML, Skehel JJ, Wiley DC. Comparative analyses of the specificities of anti-influenza hemagglutinin antibodies in human sera. *J Virol*. 1986;57(1):124–128.
14. Linderman SL, et al. Potential antigenic explanation for atypical H1N1 infections among middle-aged adults during the 2013-2014 influenza season. *Proc Natl Acad Sci U S A*. 2014;111(44):15798–15803.
15. Xu R, Ekiert DC, Krause JC, Hai R, Crowe JE Jr, Wilson IA. Structural basis of preexisting immunity to the 2009 H1N1 pandemic influenza virus. *Science*. 2010;328(5976):357–360.
16. Wrammert J, et al. Rapid cloning of high-affinity human monoclonal antibodies against influenza virus. *Nature*. 2008;453(7195):667–671.
17. Halliley JL, et al. Peak frequencies of circulating human influenza-specific antibody secreting cells correlate with serum antibody response after immunization. *Vaccine*. 2010;28(20):3582–3587.
18. Wu J, et al. Optimal vaccination strategies for 2009 pandemic H1N1 and seasonal influenza vaccines in humans. *Vaccine*. 2011;29(5):1009–1016.
19. Whittle JR, et al. Flow cytometry reveals that H5N1 vaccination elicits cross-reactive stem-directed antibodies from multiple Ig heavy-chain lineages. *J Virol*. 2014;88(8):4047–4057.
20. Smith K, et al. Rapid generation of fully human monoclonal antibodies specific to a vaccinating antigen. *Nat Protoc*. 2009;4(3):372–384.
21. International ImMunoGeneTics Information System. The global reference in immunogenetics and immunoinformatics. IMGT Web site. http://www.imgt.org. Updated March 05, 2015. Accessed April 17, 2015.
22. Li GM, et al. Pandemic H1N1 influenza vaccine induces a recall response in humans that favors broadly cross-reactive memory B cells. *Proc Natl Acad Sci U S A*. 2012;109(23):9047–9052.

Downloaded from http://www.jci.org on September 16, 2016. http://dx.doi.org/10.1172/JCI81104

23. Thomson CA, et al. Pandemic H1N1 influenza infection and vaccination in humans induces cross-protective antibodies that target the hemagglutinin stem. *Front Immunol*. 2012;3:87.
24. Corti D, et al. A neutralizing antibody selected from plasma cells that binds to group 1 and group 2 influenza A hemagglutinins. *Science*. 2011;333(6044):850–856.
25. Wrammert J, et al. Broadly cross-reactive antibodies dominate the human B cell response against 2009 pandemic H1N1 influenza virus infection. *J Exp Med*. 2011;208(1):181–193.
26. Okuno Y, Isegawa Y, Sasao F, Ueda S. A common neutralizing epitope conserved between the hemagglutinins of influenza A virus H1 and H2 strains. *J Virol*. 1993;67(5):2552–2558.
27. Corti D, et al. Heterosubtypic neutralizing antibodies are produced by individuals immunized with a seasonal influenza vaccine. *J Clin Invest*. 2010;120(5):1663–1673.
28. Krause JC, et al. Epitope-specific human influenza antibody repertoires diversify by B cell intraclonal sequence divergence and interclonal convergence. *J Immunol*. 2011;187(7):3704–3711.
29. Jackson KJ, et al. Human responses to influenza vaccination show seroconversion signatures and convergent antibody rearrangements. *Cell Host Microbe*. 2014;16(1):105–114.
30. Worldwide Influenza Centre: Annual and interim reports. The Francis Crick Institute Web site. http://crick.ac.uk/research/worldwide-influenza-centre/annual-and-interim-reports. Updated February 25, 2015. Accessed April 17, 2015.
31. Barr IG, et al. A new pandemic influenza A(H1N1) genetic variant predominated in the winter 2010 influenza season in Australia, New Zealand and Singapore. *Euro Surveill*. 2010;15(42):19692.
32. Chen Z, et al. Generation of live attenuated novel influenza virus A/California/7/09 (H1N1) vaccines with high yield in embryonated chicken eggs. *J Virol*. 2010;84(1):44–51.
33. Gitlin AD, Shulman Z, Nussenzweig MC. Clonal selection in the germinal centre by regulated proliferation and hypermutation. *Nature*. 2014;509(7502):637–640.
34. Francis T. On The doctrine of original antigenic sin. *P Am Philos Soc*. 1960;104(6):572–578.
35. de St Groth F, Webster RG. Disquisitions of original antigenic sin. I. Evidence in man. *J Exp Med*. 1966;124(3):331–345.
36. Morens DM, Burke DS, Halstead SB. The wages of original antigenic sin. *Emerg Infect Dis*. 2010;16(6):1023–1024.
37. Li Y, et al. Immune history shapes specificity of pandemic H1N1 influenza antibody responses. *J Exp Med*. 2013;210(8):1493–1500.
38. Srivastava B, et al. Host genetic background strongly influences the response to influenza a virus infections. *PLoS One*. 2009;4(3):e4857.
39. Stevens J, Corper AL, Basler CF, Taubenberger JK, Palese P, Wilson IA. Structure of the uncleaved human H1 hemagglutinin from the extinct 1918 influenza virus. *Science*. 2004;303(5665):1866–1870.
40. Frolich D, et al. Secondary immunization generates clonally related antigen-specific plasma cells and memory B cells. *J Immunol*. 2010;185(5):3103–3110.
41. Moody MA, et al. H3N2 influenza infection elicits more cross-reactive and less clonally expanded anti-hemagglutinin antibodies than influenza vaccination. *PLoS One*. 2011;6(10):e25797.
42. Okada J, et al. Monoclonal antibodies in man that neutralized H3N2 influenza viruses were classified into three groups with distinct strain specificity: 1968–1973, 1977–1993, and 1997–2003. *Virology*. 2010;397(2):322–330.
43. Okada J, et al. Localization of epitopes recognized by monoclonal antibodies that neutralized the H3N2 influenza viruses in man. *J Gen Virol*. 2011;92(pt 2):326–335.
44. Fonville JM, et al. Antibody landscapes after influenza virus infection or vaccination. *Science*. 2014;346(6212):996–1000.
45. Whittle JR, et al. Broadly neutralizing human antibody that recognizes the receptor-binding pocket of influenza virus hemagglutinin. *Proc Natl Acad Sci U S A*. 2011;108(34):14216–14221.
46. Hong M, et al. Antibody recognition of the pandemic H1N1 Influenza virus hemagglutinin receptor binding site. *J Virol*. 2013;87(22):12471–12480.
47. Lessler J, et al. Evidence for antigenic seniority in influenza A (H3N2) antibody responses in southern China. *PLoS Pathog*. 2012;8(7):e1002802.
48. Staudt LM, Gerhard W. Generation of antibody diversity in the immune response of BALB/c mice to influenza virus hemagglutinin. I. Significant variation in repertoire expression between individual mice. *J Exp Med*. 1983;157(2):687–704.
49. Clarke SH, Huppi K, Ruezinsky D, Staudt L, Gerhard W, Weigert M. Inter- and intraclonal diversity in the antibody response to influenza hemagglutinin. *J Exp Med*. 1985;161(4):687–704.
50. Radic M. Tracking and trapping somatic mutations in Ig genes. *J Immunol*. 2008;180(9):5763–5764.
51. Mozdzanowska K, Furchner M, Washko G, Mozdzanowski J, Gerhard W. A pulmonary influenza virus infection in SCID mice can be cured by treatment with hemagglutinin-specific antibodies that display very low virus-neutralizing activity in vitro. *J Virol*. 1997;71(6):4347–4355.
52. Smith CA, Barnett BC, Thomas DB, Temoltz-in-Palacios F. Structural assignment of novel and immunodominant antigenic sites in the neutralizing antibody response of CBA/Ca mice to influenza hemagglutinin. *J Exp Med*. 1991;173(4):953–959.
53. Nakajima S, Nobusawa E, Nakajima K. Variation in response among individuals to antigenic sites on the HA protein of human influenza virus may be responsible for the emergence of drift strains in the human population. *Virology*. 2000;274(1):220–231.
54. Skehel JJ, Wiley DC. Receptor binding and membrane fusion in virus entry: the influenza hemagglutinin. *Annu Rev Biochem*. 2000;69:531–569.
55. Haaheim LR, Tomasov CC, Barr IG, Hampson AW, Komadina N. Identification of genetic diversity by cultivating influenza A(H3N2) virus in vitro in the presence of post-infection sera from small children. *Vaccine*. 2006;24(44–46):6708–6711.
56. Yu X, et al. Neutralizing antibodies derived from the B cells of 1918 influenza pandemic survivors. *Nature*. 2008;455(7212):532–536.
57. Miller MS, et al. antibodies against previously encountered influenza virus strains increase over time: a longitudinal analysis. *Sci Transl Med*. 2013;5(198):198ra107.
58. Manca F, Kunkl A, Fenoglio D, Fowler A, Sercarz E, Celada F. Constraints in T-B cooperation related to epitope topology on E. coli beta-galactosidase. I. The fine specificity of T cells dictates the fine specificity of antibodies directed to conformation-dependent determinants. *Eur J Immunol*. 1985;15(4):345–350.
59. Barnett BC, Graham CM, Burt DS, Skehel JJ, Thomas DB. The immune response of BALB/c mice to influenza hemagglutinin: commonality of the B cell and T cell repertoires and their relevance to antigenic drift. *Eur J Immunol*. 1989;19(3):515–521.
60. Watts C, et al. Modulation by epitope-specific antibodies of class II MHC-restricted presentation of the tetanus toxin antigen. *Immunol Rev*. 1998;164:11–16.
61. Shirai M, et al. T cell recognition of hypervariable region-1 from hepatitis C virus envelope protein with multiple class II MHC molecules in mice and humans: preferential help for induction of antibodies to the hypervariable region. *J Immunol*. 1999;162(1):568–576.
62. Moss CX, Tree TI, Watts C. Reconstruction of a pathway of antigen processing and class II MHC peptide capture. *EMBO J*. 2007;26(8):2137–2147.
63. Davila JG, Chowell G, Borja-Aburto VH, Viboud C, Grajales Muniz C, Miller M. Substantial morbidity and mortality associated with pandemic A/H1N1 influenza in Mexico, Winter 2013–2014: gradual age shift and severity. *PLoS Curr*. 2014;6:ecurrents.outbreaks.a855a92f19db1d-90ca955f5e908d6631.
64. Hai R, et al. Influenza A(H7N9) virus gains neuraminidase inhibitor resistance without loss of in vivo virulence or transmissibility. *Nat Commun*. 2013;4:2854.
65. Powell TJ, Silk JD, Sharps J, Fodor E, Townsend AR. Pseudotyped influenza A virus as a vaccine for the induction of heterotypic immunity. *J Virol*. 2012;86(24):13397–13406.
66. Kinoshita K, Shimizu A, Honjo T. The membrane exons of the pseudo-γ-chain gene of the human immunoglobulin are apparently functional and highly homologous to those of the γ 1 gene. *Immunol Lett*. 1991;27(2):151–155.
67. Rowe T, et al. Detection of antibody to avian influenza A (H5N1) virus in human serum by using a combination of serologic assays. *J Clin Microbiol*. 1999;37(4):937–943.
68. Matrosovich M, Matrosovich T, Carr J, Roberts NA, Klenk HD. Overexpression of the α-2,6-sialyltransferase in MDCK cells increases influenza virus sensitivity to neuraminidase inhibitors. *J Virol*. 2003;77(15):8418–8425.